THE BIOLOGY OF THE MALE GAMETES OF TWO PARASITIC NEMATODES : *NIPPOSTRONGYLUS BRASILIENSIS* AND *NEMATOSPIROIDES DUBIUS*

ELIZABETH JANE WRIGHT
B.Sc.(Hons.) (Adelaide)

Department of Zoology
The University of Adelaide

A thesis submitted to the University of Adelaide in fulfilment of the requirements for the degree of Doctor of Philosophy.

NOVEMBER 1982

CONTENTS

SUMMARY

Nippostrongylus brasiliensis and *Nematospiroides dubius* are common strongylid parasites of rodents, which have been extensively used as models in experimental parasitology. This thesis first compares and contrasts spermatogenesis and sperm maturation in the two species. It then examines the spermatozoa of *N. brasiliensis* more closely, in particular investigating their membranes and the nature of their surface coat.

In both *N. brasiliensis* and *N. dubius*, the testis is a long tubular organ which can be divided into four developmental zones. From anterior to posterior, these are the zones of mitosis, growth, meiosis and maturation. The major difference between the two species is that in *N. dubius* the testis and the spermatogenic cells are twice the size of those in *N. brasiliensis*. Other morphological features of the testes are, however, similar in the two species. The higher resolving power of the TEM revealed further similarities in spermatogenesis and sperm maturation. The major sperm organelles not only shared a close resemblance in the two species, but were shown to have identical origins. Moreover, the mature sperm, although different in detailed morphology, have the same general form; each can be divided into three regions - a small amoeboid anterior, an organelle-containing cytoplasmic region and, at the posterior, a highly condensed tail-like nucleus. After insemination, the sperm of both species undergo a dramatic morphological change termed 'activation'. The amoeboid anterior enlarges considerably, while the cytoplasmic region shrinks. The movement of activated sperm of *N. brasiliensis* was described and compared with a published account of locomotion in the sperm of *N. dubius*.

The membrane and the surface coat of the sperm of *N. brasiliensis* was examined using freeze-fracture and specific molecular probes. FITC-conjugated lectins revealed some regionalization of the sperm surface, as well as minor changes associated with activation. Staining with ruthenium red was weak and, since it was not significantly reduced by neuraminidase, it was attributed to negatively charged phospholipids rather than sialic acid. Comparison of the surface labelling characteristics of unfertilized oocytes and sperm allowed speculation about sperm-egg interactions in this species. Freeze-fracture revealed a uniform density of particles on the nuclear and cytoplasmic regions of sperm from males of *N. brasiliensis*. After insemination, regionalization became apparent and there was a significant increase in particle density on all but one of the membrane faces. Measurements of particle size showed that while some of the new particles were $\leqslant$10nm, the greater proportion belonged to the 11 - 11.6nm and 13nm size classes. A less extensive, qualitative study of the sperm membranes in *N. dubius* showed similar trends in particle density. Specialized particle arrays were also noted and their possible functions discussed.

Spermatogenesis and sperm maturation were found to be very similar in *N. brasiliensis* and *N. dubius*. Indeed, the spermatogenic cells were so similar that if the two species were used for different aspects of a broader investigation, the results could still be related in a meaningful way. Together the two species constitute a 'model system' which, when used instead of a single species, could greatly increase the scope of an investigation. The type of experiments which may prove suitable and the extent to which a model of this kind may contribute to the broader field of cell biology is discussed.

DECLARATION

This thesis contains no material which has been accepted for the award of any other degree or diploma in any university and, to the best of my knowledge and belief, contains no material previously published or written by another person, except where due reference is made in the text.

ACKNOWLEDGEMENTS

I would like to thank my supervisor, Dr R.I. Sommerville, for his encouragement, advice and criticism during the course of this study. Discussions with Dr Guy Cox, E.M. Unit, University of Sydney, concerning freeze-fracture and its interpretation were greatly appreciated. Dr Sam Ward, Carnegie Institution of Washington, Maryland, U.S.A., kindly sent me unpublished data and offered helpful comments.

Some aspects of the project required equipment which was not available in the Zoology Department and I am grateful for access to facilities in other departments and institutions. Dr D.J.H. Cockayne, E.M. Unit, University of Sydney, kindly allowed me access to the Balzars freeze-etch machine and Dr Guy Cox instructed me in its use. Many other facilities of the Unit were also made available to me during my visits and I am most grateful for this assistance. Dr Alan Bird, C.S.I.R.O., Division of Horticulture and the Department of Microbiology, University of Adelaide, allowed me the use of their equipment for fluorescent microscopy. Time-lapse cinematography equipment was kindly loaned by Professor P.G. Martin, Botany Department, University of Adelaide. The use of the JEOL 100 cx electron microscope at the Waite Agricultural Research Institute, Glen Osmond, for part of this study was much appreciated.

The plates for this thesis were produced with the assistance of Mr. Philip Kempster and Ms. Suzanne James, Zoology Department, University of Adelaide. Thanks are also due to Lesley Hurley, Bob Inns and Craig Proctor for their comments, criticisms and encouragement; Craig, in particular, showed great patience and understanding during the final stages of this study.

THIS THESIS IS DEDICATED TO MY FATHER:

HIS ENCOURAGEMENT AND SUPPORT WAS A VITAL STIMULUS

THROUGHOUT MY EDUCATION

SECTION 1

CHAPTER I. INTRODUCTION AND LITERATURE REVIEW

I.I Introduction

Spermatozoa were first observed in I677 by the Dutch microscopist, Antony van Leeuwenhock. Although he recognised their importance as seeds from which new organisms could arise, many of his contempories dismissed them as parasites or inert bodies. This controversy lasted until the middle of the I9th century. By this time sperm penetration of the egg had been described and it had been conclusively demonstrated that sperm were formed by proliferation of testis tissue.

It is now recognised that spermatozoa are highly differentiated cells which are specialized to perform a number of functions associated with fertilization. For example, the long mitochondrion, coiled around the midpiece of the flagellum, is clearly involved in providing energy for sperm motility. The large acrosomal vesicle at the anterior of the sperm head contains lytic enzymes which aid penetration of the egg investments. In invertebrates, the newly exposed acrosomal membrane makes first contact and fuses with the oolemma. Because of these clearly defined functional specializations and their availability in large numbers, often as a synchronized population, sperm have become important models in cell biology. In particular, they have been extensively used in the study of membranes and their regionalization, the cell surface, cell-cell recognition and cell fusion. Furthermore, investigations of sperm metabolism, physiology and longevity have more practical applications in either promoting or reducing fertility in domestic animals, parasites and *Homo sapiens*.

Historically, nematodes have also been important in shaping our ideas about cell biology. In the late I9th century, studies of spermatozoa, eggs and embryos of the common horse roundworm, *Parascaris equorum (Ascaris megalocephala)*, generated some of the fundamental principles of cytology, including the significance of meiosis and fertilization (Van Beneden, I883), the nature of polar bodies (Hertwig, I890) and the principle of cell lineage (Zur Strassen, I896). Because of their unusual form and lack of flagellum and acrosome, nematode sperm aroused the curiosity of cytologists and became a popular subject of study in the late I9th and early 20th centuries. Recently, renewed interest has been shown in these highly modified sperm.

Descriptions of sperm locomotion (Wright and Sommerville, I977) and fertilization (Foor, I968) have demonstrated that nematode sperm have evolved novel solutions to the problems of motility and egg penetration. The amoeboid anterior is both the organ of locomotion and serves to make first contact with the egg. Furthermore, investigations of sperm motility illustrate that studies of these unusual sperm may have significance to the wider field of cell biology. Thus, although nematode sperm move in a similar way to many other cells, including white blood cells (Wright and Sommerville, I977), the mechanism by which they generate motility may prove to be unique (Roberts and Ward, I982a).

The potential of nematode sperm to add to our understanding of cell biology and reproduction remains largely unexploited. Experimental studies have been confined to the better known species, e.g. *C. elegans* and *A. suum*, and although the literature contains descriptions of sperm from over 30 other species, this represents only a small fraction of the group. The majority of studies have

concentrated on the Secernentea, in particular, the orders Ascaridida, Rhabditida and Tylenchida. The orders Spirurida and Strongylida as well as the subclass Adenophorea have not been thoroughly examined.

The present study originated as an investigation of spermatogenesis and sperm maturation in a parasitic nematode. The species to be investigated was chosen from the Strongylida, which is believed to have originated as a separate branch of the Secernentea (Chabaud,I974). Thus, it was anticipated that the study would not only extend our knowledge of nematode sperm in general, but would also provide a broader basis for comparisons and generalizations within the subclass.

Within the order Strongylida, *Nippostrongylus brasiliensis* has been used extensively as a laboratory model for a wide range of physiological experiments. Models are important in the study of parasitic nematodes, as often the disease-causing organism, itself, is unsuitable for laboratory studies, either because of its physiology or host specificity.

Experiments by Phillipson (I969, I970, I973) have provided data on aspects of reproduction in *N. brasiliensis*, including factors affecting copulation, the reproductive potential of male and female worms and the ability of females to store and use sperm. Jamuar (I966) produced one of the earliest descriptions of the ultrastructure of spermiogenesis in nematodes using this species. In I969, Lee extended our understanding of reproduction in nematodes by demonstrating, again with *N. brasiliensis*, that immune hosts can interfere with sperm production in their parasites. Since little was known about nematode sperm at that time, there was virtually no scope for comparisons with other species. Moreover, a number of questions raised by these studies could not be answered

at the time, but are now amenable to investigation using modern techniques.

With this background in mind, it was decided to undertake a thorough study of spermatogenesis and sperm maturation in *N. brasiliensis*. However, rather than simply provide another ultrastructure description of sperm, two other facets were added to the study. One of these consisted of constructing a 'two-species model' for the study of nematode sperm. The rationale for this is as follows. No one species is suitable for every kind of experimental manipulation. This is illustrated in current work on mammalian sperm, where the particular species under study is often chosen to suit the methodology rather than for its intrinsic interest (see Koehler and Kinsey, I977, p 332 'Discussion with Reviewers'). The biggest problem of adopting this approach is the lack of complementarity of the results. One way to overcome this is to select two species which are closely related and, before proceeding further, to ensure that the general form of the sperm and the major events of spermatogenesis are similar. This investigation constitutes Section II.

Nematospiroides dubius was chosen as the second species for a number of reasons. It belongs to the same family as *N. brasiliensis* and preliminary observations of its sperm (Wright and Sommerville, I977) suggested that they resemble those of *N. brasiliensis*. Furthermore, *N. dubius* has been used extensively as a laboratory model and can be maintained *in vitro* (Sommerville and Weinstein, I964).

The third facet of this study constitutes Section III. It entails an exploration of two aspects of the cell biology of the sperm of *N. brasiliensis*, namely its membrane and its surface coat.

The reason for this choice was twofold. First, the sperm surface, i.e. the membrane and the cell coat, is central to a number of very important functions of the sperm, including locomotion, adhesion, recognition and ultimately fertilization. Second, it was considered likely that activation, i.e. the morphological changes which nematode sperm are known to undergo after insemination, would be accompanied by changes to the sperm surface. This was predicted because capacitation, the functional equivalent of activation in mammals, involves modifications of the sperm surface. Since these modifications in mammalian sperm can be revealed by surface labelling and freeze-fracture, these two techniques were chosen to explore surface changes in the sperm of *N. brasiliensis* during activation.

I.2 Spermatogenesis in nematodes: theme and variation.

The following review summarizes the modern ultrastructural descriptions of spermatogenesis in nematodes. Although this generalized account of development is representative of the majority of species examined to date, exceptions are noted and described. Such exceptions, although often ignored in reviews, may provide clues to the functions of specialised organelles within the mature spermatozoa. Spermatozoon morphology has also been compared, both between and within the major taxonomic groups, and is considered in the light of the evolutionary relationships within the Nematoda.

The review also demonstrates the scope and extent of fine structural investigations of nematode sperm. The more recent experimental work on *C. elegans* and *A. suum* will be only briefly summarized here as specific details concerning sperm activation and motility will be discussed in later chapters where appropriate.

TABLE 1.1

SPECIES	SUPERFAMILY	STAGE EXAMINED				AUTHORS
		Spermato-gonia	Spermato-cytes	Sperm in Males	Sperm in Females	
Subclass Secernentea						
Aphelenchoides blastophthorus	Aphelenchoidea	✓	✓	✓	✓	Shepherd & Clark (1976)
Ancylostoma caninum	Ancylostomatoidea			✓	✓	Foor (1970)
"	"	*✓	*✓	*✓		Ugwanna & Foor (1977)
					✓	Foor (1968)
Ascaris lumbricoides	Ascaridoidea					
"	"		✓	✓	✓	Foor (1970)
	"			✓	✓	Clark, Moretti & Thomson (1967, 1972)
A. suum	"		*✓	*✓		McMahon & Foor (1977)
"	"		✓	✓	✓	Goldstein (1977)
"	"	✓	✓	✓	✓	Favard (1961)
Parascaris equorum	"				✓	Foor (1970)
Polydelphis sp	"			✓	✓	Foor (1974): Burghardt & Foor (1975)
Brugia pahangi	Filarioidea			✓	✓	Foor, Johnson & Beaver (1971)
Dipetalonema viteae	"	✓	✓	✓	✓	McLaren (1973a)
"	"	✓	✓	✓		Maeda, Harada, Nakashima, Sadakata, Ando, Yonamine, Otsuji & Sato (1970)
Dirofilaria immitis	"				✓	Harada, Maeda, Nakashima, Sadakata, Ando, Yonamine, Otsuji & Sato (1970)
"	"				✓	Foor (1970)
Gnathostoma sp	Gnathostomatoidea	✓	✓	✓	✓	Lee (1971)
Heterakis gallinarum	Heterakoidea		✓	✓	✓	Foor (1970)
Angiostrongylus cantonensis	Metastrongyloidea	✓	✓	✓		Lee & Anya (1967)
Aspiculuris tetraptera	Oxyuroidea		✓		✓	Foor (1970)
Physaloptera sp	Physalopteroidea	✓	✓	✓		Wolf, Hirsh & McIntosh (1978)
Caenorhabditis elegans	Rhabditoidea				✓	Ward & Carrel (1979)
"	"		✓	✓		Pasternak & Samoiloff (1972)
Panagellus silusiae	"	*✓	*✓	*✓		Shepherd & Clark (1977)
Rhabditis oxycerca	"	✓	✓	✓	✓	Beams & Sekhon (1972)
R. pellio	"	✓	✓	✓	✓	Martin & Lee (1980a)
Nematodirus battus	Trichostrongyloidea		✓	✓	✓	Jamuar (1966)
Nippostrongylus brasiliensis	"	✓	✓	✓	✓	Shepherd, Clark & Kempton (1974)
Globodera rostochiensis	Tylenchoidea	✓	✓	✓		"
Heterodera schachtii	"	✓	✓	✓		Goldstein & Triantaphyllou (1980)
Meloidogyne hapla	"	*✓	*✓	*✓		Shepherd & Clark (1979)
M. incognita	"					
Subclass Adenophorea						
Dioctophyma renale	Dioctophymatoidea		✓	✓	✓	Foor (1970)
Longidorus macrosoma	Dorylaimoidea			*✓		Shepherd & Clark (1980)
Xiphinema index	"			*✓		"
Deontostoma californicum	Enoploidea				✓	Wright, Hope & Jones (1973)
"	"	✓	✓	✓		Hope (1974)
Capillaria hepatica	Trichuroidea	✓	✓	✓	✓	Neill & Wright (1973)

List of species for which ultrastructural descriptions of spermatogenesis exist in the literature.
✓ denotes which stages were examined and * signifies papers presented as abstracts only.

Table I.I lists the original studies from which this summary has been synthesized. No specific reference will be made to these papers unless the species which they describe differ significantly from the general pattern of spermatogenesis. Studies on members of the Secernentea will be summarised first. This will be followed by a discussion of the Adenophorea.

Subclass Secernentea. The spermatogonia of secernentean nematodes are characterized by numerous free ribosomes and large nuclei, with one or more nucleoli. They also contain mitochondria, a small amount of rough endoplasmic reticulum (RER) and a few Golgi complexes. In addition, the spermatogonia of *Parascaris equorum* contain lipid globules. Mitotic divisions of the spermatogonia produce spermatocytes. They are larger than the spermatogonia and contain a large nucleus, prominent nucleolus, mitochondria, Golgi bodies, many ribosomes and more extensive RER.

Spermatocytes are characterized by the appearance of a system of membranes, associated with a bundle of fibres. They have been called $\propto$ bodies (Lee, I97I), membrane specializations (Foor, I968), fibrillar bodies (Shepherd and Clark, I976), C- bodies (Pasternak and Samoiloff, I972), ovoid bodies (Maeda et al, I970), batonnet granules (Favard, I96I), special membrane structures (Wolf et al, I978), mitochondrionlike inclusions (Jamuar, I966) and membranous organelles (McLaren, I973a). This profusion of names has arisen because the different appearance of these organelles at different stages of spermatogenesis has obscured their homology. McLaren (I973a) argued that their name should be specific enough for immediate identification, but should not specify an as yet unproven function. Since their membranes are a persistant and common feature, she elected to call them membranous organelles. This name has gained acceptance recently (Burghardt and Foor, I978; Nelson and

Ward, I980) and will be used here.

For a time, there was also confusion over the origin of these organelles. Jamuar (I966) called them mitochondrionlike inclusions. Consequently, after having described their formation from modified mitochondria in *A. lumbricoides* and *Angiostrongylus cantonensis*, Foor (I970) proposed that they originate from mitochondria in all ascarids and strongylids. Some authors rejected this notion (Clark et al, I972; McLaren, I973a) in view of their own observations and an earlier study by Favard (I96I) which clearly showed their Golgi origin in *P. equorum*. Later, in a brief report on *A. suum*, Foor and McMahon (I977) described an association of dense bodies and Golgi membranes, which gave rise to a bundle of microfilaments. They did not name the membranous components, but presumably these were membranous organelles. This abstract suggests that Foor has re-examined the formation of the membranous organelles in *A. suum* and recognized their Golgi origin.

There is now a consensus that the membranous organelles originate as dilated saccules of Golgi complexes which obtain osmiophilic material from nearby RER. These three structures remain in close association throughout the first phase of their development. In *D. viteae* numerous other Golgi vesicles fuse to form a hollow cylinder, closed at both ends. Into this a fibrous material is secreted. In *R. pellio* and *H. gallinarum*, the original dilated saccules become flattened, then bent into hemispherical cups. A fibrous material is secreted within these cups. The original osmiophilic material remains in a swelling of the otherwise closely applied membranes.

In *C. elegans*, a so-called 'special vesicle' first appears as a bulbous enlargement of a Golgi vesicle, bounded on one side by a cisterna of RER. On the opposite side, part of the vesicle is

constricted by a collar of electron-dense material. Fibrous bodies, surrounded by a double membrane, also form in the cytoplasm at this stage. The authors were unable to determine whether these originate from the Golgi or RER. Later, finger-like projections on one side of the special vesicles fuse with the membrane of the fibrous bodies and form typical membranous organelles.

During the development of the spermatocytes of *P. silusiae*, ovoid crystalline bodies, consisting of a double membrane wrapped around a bundle of fibres, form from Golgi complexes. The intra-membrane space may be enlarged in one place and here an electron-dense material accumulates. A total and selective degradation of these C-bodies follows their formation and at the same time vesicular bodies appear in the cytoplasm. The membrane over most of this organelle forms deep, tubular invaginations, but in one area it is differentiated into a small knob. This knob fuses with the plasma membrane as sperm pass through the ejaculatory duct. Although the authors noted a similarity between their V-bodies and the membranous organelles in the sperm of other nematodes, they did not recognize any relationship between C-bodies and previously described cytoplasmic organelles. In my opinion, the C-bodies closely resemble the early stages of fibrous body formation within the membranous organelles of other species. Moreover, since Pasternak and Samoiloff (I972) do not describe the synthesis of the V-bodies, I propose that they are derived from the C-bodies. Thus the V- and C- bodies of *P. silusiae* probably represent two stages in the formation of typical membranous organelles.

In *P. equorum* the initial synthesis of these organelles is more complex. Dense lipid globules in the cytoplasm of the spermatocyte become surrounded by concentric rings of RER. When about five layers

are built up, the lipid disappears and is replaced by a granule of the protein, ascaridine. As this enlarges the layers of RER peel off. Each ascaridine granule then becomes associated with small Golgi complexes of 4-5 saccules. The terminal saccule, which is dilated with an electron-dense material, adheres to the ascaridine granule and a fibrillar material forms between the two. Thus there are four components in the developing membranous organelles of *P. equorum*, compared with just three in other species.

Maeda et al (I970) found that membranous organelles, or ovoid bodies as they called them, develop in spermatocytes of *Dirofilaria immitis* from vacuoles near Golgi complexes and SER. They describe their contents as particulate, but their micrographs suggest that the material is fibrillar and that the organelles resemble those of *D. viteae*.

Aphelenchoides blastophthorus is the one exception in which there is no obvious association between the membranous organelles and Golgi complexes. As they consist of double membranes, wrapped around a fibrillar material, they resemble typical membranous organelles. The authors were puzzled by the lack of Golgi bodies in the spermatocytes and suggested that this may have been an artifact of fixation.

In summary, the membranous organelles of nematode spermatocytes are generally formed from Golgi membranes, in association with RER. The vesicles become compressed, causing the membranes to lie close to one another, except in one region which is swollen and contains an electron-dense material. When this structure bends into a crescent, a bundle of parallel fibres is deposited in the hollow.

Similar bundles of parallel fibres form in the spermatocytes of *Meloidogyne hapla* and *M. incognita*, unassociated with membranes. Golgi bodies are rarely encountered in the spermatocytes and although some RER is present, the majority of ribosomes are free in the cytoplasm. Very similar fibrous bodies appear after meiosis in the cyst nematodes, *Globodera rostochiensis* and *Heterodera schachtii*. Membranous organelles do not occur in any of these species, all of which belong to the super-family Tylenchoidea. It appears that an association with membranous components is not essential for synthesis of the fibrous bodies.

Late spermatocytes contain a large nucleus, ribosomes, mitochondria, Golgi bodies, SER, RER and membranous organelles. As they approach meiosis, the chromosomes condense and the nuclear envelope breaks down. The centrioles contain nine tubular elements, which are connected by a dense ring in *A. suum*. In the spermatid of *Nippostrongylus brasiliensis* the two centrioles are parallel and are reported to consist of I8 tubules (for discussion of this see Chapter 7.2). After division in *H. gallinarum*, active Golgi complexes produce membranes which form the walls dividing the spermatids from each other.

Early spermatids are usually round with a central mass of condensed chromatin, not bounded by a nuclear envelope. Mitochondria are clustered around the chromatin and the RER, ribosomes, Golgi bodies and membranous organelles fill the peripheral cytoplasm. The spermatids now enter a period of differentiation called spermiogenesis, in which major changes are made to the cytoplasm and its organelles.

Although nuclear modification is not a common feature of spermiogenesis in nematodes, it does occur in some species. In *Nematodirus battus*, *Ancylostoma caninum* and *N.brasiliensis* the DNA condenses into a tail-like structure after meiosis. The

chromatin first condenses into filaments. As these twist into a spiral, the material elongates and ultimately evaginates. The centrioles are located immediately anterior of the chromatin. The nuclear material of *G. rostochiensis* and *G. virginiae* is also modified after meiosis. First, it condenses into a central mass, surrounded by microtubules. Then, in the late spermatid, it breaks up into smaller clumps, becoming like 'small beads connected by fine strands'. Upon entry of the sperm into the spermatheca of females, the nuclear material reverts back to a dense central mass, but soon it breaks up into dense strands, interconnected in a three-dimensional network. Attached to this are several electron-dense 'spongy-looking spherical bodies'. In other members of the Heteroderidae, i.e. *H.schachti* and *H.avenae*, the chromatin remains unchanged after meiosis.

Both the chromatin and the cytoplasm of *Aspiculuris tetraptera* undergo extensive changes during spermiogenesis. The nuclear material, with its two centrioles and associated microtubules, forms an arc around the mitochondria. The latter fuse and finally form a single, large mitochondrion which then elongates. The microtubule-chromatin complex becomes bounded by an electron-dense sheath and forms two distinct bundles, one on each side of the mitochondrion. At this stage, there is a sharp reduction for DNA staining with Feulgen and acridine orange. As the mitochondrion and microtubule-chromatin complex elongate, they form a protruberance which becomes the long filamentous tail of the mature spermatozoon. The head contains abundant cytoplasm and is capable of extending long pseudopodia. Although the DNA is

difficult to localize, the authors suggest that it is likely to be found in the microtubule complex. At no stage are membranous organelles observed in the spermatogenic cells of *A. tetraptera*.

Excess cytoplasm, consisting of ribosomes, RER, and Golgi complexes, is discarded from the spermatids in a residual body. In *P.equorum*, *D. viteae*, *C.elegans* and *A. blastophthorus*, this residual body forms close to the bridges which connect the groups of two or four spermatids. In *R. pellio*, *D. immitus* and *H. gallinarum*, however, it is extruded after the spermatids have separated. The contents of the residual bodies are not lost from the animal, they are phagocytosed by epithelial cells lining the vas efferens (McLaren, I973a; Shepherd et al, I974).

After casting out the residual body, the major organelles remaining in the cytoplasm are mitochondria and membranous organelles. *A. blastophthorus* also contains electron-lucent vesicles and microtubular elements which persist in the spermatozoon. At this stage, the membranous organelles consist of a double membrane, forming an incomplete envelope around the fibrous body. In *C. elegans*, the fibres measure 4.8 $\pm$ I.I nm, whereas in *P. silusiae* they were found to be 5.7nm thick and 5nm apart. The double membrane is still swollen in one place by an electron-dense granule. In *D. viteae*, one part of the granule contains 6-8 membrane bound tubules and another area is crystalline.

Just after meiosis, the membranes separate from the fibrous body. They fold into spherical bodies, with many deep, microvillous-like invaginations. The secretion vesicle, with its characteristic crystalloid in *D. viteae* and *D. immitis*, is still recognizable, but the electron-dense granule may disappear. In *P. equorum*, the ascaridine granules detach from the membranes and fuse to form 4-5 large pools of lipid-like droplets. These ultimately coalesce to become the characteristic refringent cone. In general, the fibrous

bodies gradually disassemble and are no longer visible in the mature spermatozoon. An exception is *A. blastophthorus*, where scattered bundles may remain. The fibrous bodies of the immature sperm of *B.pahangi* and *D. viteae* come together and lengthen into rod-like structures and the sperm become long and narrow to accomodate them. This form of the fibrous body is short-lived in *D. viteae*, but still present in the mature sperm of *B. pahangi*.

Mature spermatozoa in the seminal vesicles of males are generally round or ovoid. The chromatin is central, either in discrete chromosomes or a dense single mass. Often, it is surrounded by a dense halo, which cytochemical tests have shown to be RNA (Clark et al, I972; Goldstein and Triantaphyllou, 1980; Ward, Argon and Nelson, I98I). Mitochondria aggregate around the DNA. Membranous organelles may be scattered throughout the cytoplasm, but more often they lie close to the plasma membrane.

In the few members of the Strongylida examined to date, the cytoplasmic region is ovoid or elongate. Membranous organelles line the periphery and mitochondria fill the central region. The chromatin occurs in the tail-like part except in *A. cantonensis*, where it is a central mass as in *A. suum* and *C. elegans*.

Limited areas of the anterior cytoplasm of mature sperm may be capable of producing pseudopodia, e.g. in *H. gallinarum*, *D. viteae*, but in many cases sperm in the seminal vesicle of males are not amoeboid. The sperm of the plant-parasitic nematodes differ in this respect. Here, the sperm cells are amoeboid before meiosis and the surface of spermatids and spermatozoa is elaborated into numerous needle-like filopodia. Moreover, except in *A. blastophthorus*, these cells have a complex outer membrane which is lined by a single layer of microtubules. These lie in a parallel

array beneath the entire surface. In tangential section, they sweep around in curves and bends such that they resemble a fingerprint.

After insemination into the female reproductive tract, the spermatozoa of almost all species change morphologically. This has been called activation (Foor and McMahon, I973). Here, a comment should be made regarding terminology. In several recent publications, a number of authors refer to mature sperm cells in males as spermatids and they call those which have been activated, spermatozoa (Burghardt and Foor, I978; Nelson and Ward, I980; Ward et al, I98I). Clark et al (I967) also described sperm in this way. Many other authors (Lee and Anya, I967; Lee, I97I; Shepherd and Clark, I976) consider that the mature cells in the seminal vesicles of males are spermatozoa. Shepherd (I98I) has stressed that agreement and conformity in the use of such terminology is important. In mammals, the question is straightforward as the end of spermiogenesis is signaled by the release of the independent spermatozoon from the seminiferous epithelium (Setchell, I978). However, no such convenient marker exists in nematodes. In these cases, Roosen-Runge (I977) defines the end of spermiogenesis as, "the time at which the spermatid has come to appear like a 'mature' spermatozoon". Shepherd (I98I) advocates that extrusion of the residual body should mark the end of spermiogenesis. Since the latter definition is more precise and is less open to errors of interpretation, it will be used here. Maturation of spermatozoa in the female reproductive tract of mammals is called capacitation (Austin, I952). Although nematode sperm also undergo changes after insemination, this process is not analagous to capacitation as, at least in *A. suum*, the stimulus for change originates in the male (Foor, I973). The term "activation" (Foor and McMahon, I973), is an appropriate description of this

process.

During activation, the organelles migrate to one pole and the remaining cytoplasm becomes amoeboid. Foor (I968) designated this amoeboid region the anterior, because it enters the oocyte first during fertilization. Moreover, this area consistently leads during locomotion in both *C. elegans* (Nelson, Roberts and Ward, I982) and *N. dubius* (Wright and Sommerville, I977). Activation also involves the fusion of the membranous organelles with the plasma membrane and, in the ascarids, the fusion of ascaridine granules to form a large refringent body.

After activation in some species, tubules appear both in the posterior cytoplasm and in parallel rows beneath the plasma membrane. They have been called microtubules in *R.pellio* and SER in *B. pahangi* and *D. viteae* (Foor et al, I97I). McLaren (I973a) does not describe them in her study of *D. viteae*. Although these structures resemble each other and the subplasmalemmal microtubules in the spermatids and spermatozoa of the heteroderids, their true homologies are not known. A system of laminar membranes forms at the junction of the cell body and pseudopod of *C. elegans* after activation. These are distinctly membranous rather than tubular and their possible function will be discussed later in relation to spermatozoon motility (Chapter 7.2).

In summary, activation causes a rearrangement of the sperm cytoplasm. The chromatin, mitochondria and membranous organelles migrate to the posterior which is hemispherical or ovoid. The anterior half of the sperm is filled with a granular or amorphous material and is amoeboid. The membranous organelles fuse with the plasma membrane and remain there, attached by permanent pores.

Those species in which the chromatin is condensed into a tail-like region undergo a similar bipolarization. Similarly, in *A. caninum* where there is a mixing of nuclear and cytoplasmic regions, the anterior of the sperm is amoeboid.

Subclass Adenophorea

Neill and Wright's study of *Capillaria hepatica* is the only thorough description of spermatogenesis in an adenophorean. Other workers (Table I.I) have generally described only the mature sperm. Thus the following is not a comprehensive summary but it does represent our current knowledge of spermatogenesis in the group.

The testis of *C. hepatica* is hologonic. Spermatogonia are located at the periphery of the testis, close to the basal lamina and surrounded by sustentacular cells. The spermatogenic cells move inwards as they mature and the central lumen contains spermatids and spermatozoa. Thus this hologonic testis resembles a single seminiferous tubule in a mammalian testis. In *Deontostoma californicum*, the gonad is telegonic and spermatogonia undergoing mitosis are found only in the distal end.

The early germ cells of *C. hepatica* are like those described for the Secernentea. The spermatogonia have large nuclei, numerous free ribosomes, Golgi bodies, mitochondria, RER and lipid droplets. Spermatocytes are similar, but slightly larger. Their plasma membrane develops out-foldings which may form multiple membrane stacks. The perinuclear cisternae are continuous with the RER and widen as the spermatocytes develop. The spermatids remain connected by intercellular bridges after meiosis. The residual cytoplasm, consisting of Golgi bodies, RER, vesicles and mitochondria, is pinched off near these interconnections.

Although the characteristic membrane stacks does not reappear after division, a unique sequence of events during spermiogenesis leads to the formation of membranous inclusions in the cytoplasm. These inclusions are unlike the membranous organelles of other species. They first appear after the extrusion of the residual body as thick tubules, 85-I25nm in diameter. Each collapses into a concave vesicle, then fuses with a neighbouring vesicle to form a double membrane loop, enclosing a portion of cytoplasm. Later, fine filaments approximately I0nm thick, differentiate between the concentric membranes. After the nucleus has condensed into a trilobed body, the spermatozoa elongate. A constriction separates the pointed tail from the blunt head. The membranous inclusions are packed tightly around the periphery of the tail, while mitochondria and β glycogen occur centrally. Much of the cytoplasm of the head also contains β glycogen, in addition to the chromatin, mitochondria and an anastomosing network of tubules. The authors describe these tubules as unusual SER or a fixation pattern of glycogen. They are similar to the tubular networks in some secernentean sperm. Pseudopodia are produced from both the head and the tail, but are more common around the head. No movement was detected in sperm dissected into physiological saline. Sperm in the uterus of females resembled those of males.

In a report on reproduction in marine nematodes, Hope (I974) gave a brief description of the mature sperm of *D. californicum*. They are spindle-shaped cells, measuring 8 by 18µm, with a central nuclear mass I5 µm long and 3 µm across. A more detailed description of sperm in the uterus of females was given by Wright et al (I973). The nucleus consists of Feulgen-positive fibres

oriented longitudinally within a less-dense filamentous material. Membranous organelles, with deep, microvillous-like invaginations, fill the peripheral cytoplasm. Some were connected to the plasma membrane by narrow necks, reinforced by a dense collar; others had not discharged their contents.

The mature sperm of *Longidorus macrosoma* and *Xiphinema index* share some characters with *D. californicum*, but in other ways resemble the sperm of the Heteroderidae and Meloidogynidae. For example, while their chromatin is condensed into a network of filaments, their outer membrane is lined by parallel arrays of microtubules. They do not contain membranous organelles, but fibrous bundles occur in the cytoplasm.

The sperm of *Dioctophyma renale* are bizarre (Foor, I970) and resemble no other known forms. In the male they are rod-shaped and bounded by a double membrane. A dense material, with a beaded appearance, lies between these two membranes. The rest of the cytoplasm contains only centrioles, dense chromatin and laminar membranes. Other spermatozoa, interpreted as being more mature, are round and largely occupied by chromatin. The inner membrane has folded into tortuous channels which open to the outside and are associated with the laminar membranes. After insemination the sperm produce pseudopodia but otherwise are unchanged.

An overview.

In I970, Foor postulated that the spermatozoa of nematodes can be divided into at least four groups. He designated these the ascaroid, strongyloid, oxyuroid and dioctophymoid types. Anya (I976) has criticised this grouping on the grounds that differences within types are often as great as differences between them.

For example, *Angiostrongylus cantonensis* was placed in the strongyloid group although, as Foor himself recognised, its sperm morphology is unlike others of this type. Similarly, not all members of the ascaroid group have sperm with a refringent cone. Moreover, the scheme has proved insufficient to cover some of the species examined since 1970.

Anya (1976) proposed a "hypothetical scheme of evolution of sperm morphology in the Nematoda". He chose the sperm of *Rhabditis pellio* to represent the least specialized form. Derived from this are three basic types, represented by *Globodera rostochiensis (Heterodera rostochiensis)*, *Trichinella spiralis* and *Heterakis gallinarum*. It is suggested that these in turn produced all other types. As well as containing a number of factual errors (the paper by Neill and Wright, 1973, contains no mention of the sperm of *T. spiralis*), the scheme oversimplifies sperm morphology by ignoring some important features. Thus, when Anya described *R. pellio* sperm as like those of *G. rostochiensis*, he overlooked the amoeboid form of early stages, the modified chromatin and the lack of membraneous organelles in the latter. Similarly, he suggested that the sperm of *Aspiculuris tetraptera* were the end product of modifications to this line, but it is difficult to envisage the subplasmalemmal microtubule system of *G. rostochiensis* as the forerunner of the microtubule-chromatin complex of *A. tetraptera*. More importantly, the author has ignored the phylogenetic relationships established for the Nematoda using other criteria. In this way, similarities which arise from convergent evolution, have been mistaken for relatedness. Thus, while he proposed that the strongylid sperm-type was derived from the heterakid form, the current belief is

that the strongylids and heterakids are only distantly related (Chabaud, I974). A more useful approach is to group species according to their sperm morphology and their phylogenetic relationships. At present it is too early to attempt this exercise with the Nematoda. Because important organelles are beyond the resolution of the light microscope, ultrastructural descriptions of sperm are essential. At present, however, we have adquate descriptions of only 40 or 50 species. Furthermore, a number of suborders remain unexamined. The degree of variation within the taxonomic groups must also be determined. A brief report on spermatozoa of the Rhigonematidae (Oxyurida) illustrates that sperm diversity may be great, even within a single family (Wirth, I974). Although all sperm examined lacked a nuclear envelope and flagellum, the chromatin occurred in several forms, either as a single mass, separate chromosomes, an elongate strand or fine filaments dispersed throughout the sperm. The shape and size of the sperm also varied markedly. Characters which show such great variation within a family are unlikely to be useful indicators of phylogenetic relationships. Further ultrastructural studies will be needed to determine which characters may be useful in this regard. While it is important to consider the evolution of sperm morphology in the light of established phylogenetic groupings, studies of sperm morphology may challenge previously accepted relationships. Comparisons of sperm structure in Australian native rodents (Breed and Sarafis, 1979) and marsupials (Hughes, I965; Harding, Carrick and Shorey, I98I) have suggested relationships which passed unnoticed in phylogenetic studies based on morphological data alone. In nematodes, the separation of *Heterodera* and *Globodera* into distinct genera relied partly on differences in sperm morphology (Shepherd and Clark, I979).

Similarly sperm structure is one character which suggests that the Tylenchina are closer to the Dorilaimida than the Aphelenchina (Shepherd and Clark, I980). Spermatozoon morphology is a good taxonomic character because sperm are regarded as evolutionary stable cells (Afzelius, I979). It should be remembered, however, that they are only one character and must be considered together with all available evidence.

Experimental studies using nematodes sperm.

There are two major groups conducting experimental studies on nematode sperm. One group in Carnegie, led by Sam Ward, is examining the molecular genetics of the sperm of *C. elegans*. They are attempting to establish the function of individual gene products by genetic cloning and the identification of mutant individuals defective in the synthesis of particular molecules. Background and preliminary studies have provided information on sperm activation (Nelson and Ward, 1980), movement (Nelson, Roberts and Ward, 1982; Roberts and Ward, 1982a) the sperm surface (Roberts and Ward, 1982b) and fertilization (Ward and Carrell, 1979). Another group, with W.E. Foor at Wayne State, Detroit, aims to dissect the sequence of steps occurring during sperm-egg interaction in nematodes, by studying *in vitro* fertilization in *A. suum* (Grevengood, Lande and Foor, 1981). Once again preliminary studies have produced data on sperm activation (Foor and McMahon, 1973; Abbas and Cain, 1979), surface proteins and glycoproteins (Abbas and Cain, 1980) secretions of the reproductive tracts (Abbas and Foor, 1978; Fitzgerald and Foor, 1979) and egg maturation (Wu and Foor, 1980).

CHAPTER 2. THE EXPERIMENTAL ANIMALS AND THEIR MAINTENANCE.

2.I Background

2.I.I *Nippostrongylus brasiliensis*.

Nippostrongylus brasiliensis is common and widely distributed in its natural host the Norway rat, *Rattus norvegicus*. A variety of other rodents, including the laboratory rat, the golden hamster, the rabbit and the mouse, can be experimentally infected with this parasite (Haley, I96I).

N.brasiliensis is pathogenic to its host. A very heavy infection may cause death, primarily from pneumonia brought about by the migration of larvae through the lungs (Porter, I935). Adults in the intestine also cause local tissue damage. The villi become short, irregularly shaped and fused; associated with this is an increase in epithelial cell number and turnover (Symons, I965). Much of this damage is caused because the parasite feeds on host tissue rather than gut contents (Rogers and Lazarus, I949). The precise way in which *N. brasiliensis* feeds is not known. Lee (I969b) suggests that as the worms move they press their longitudinal cuticular ridges into the mucosa and abrade it. If they then released digestive enzymes, some perhaps from the excretory pore, the lesions would enlarge and the resultant cell debris could be ingested by the worm.

As the tissue damage caused by *N. brasiliensis* resembles the pathology of other conditions, such as ulcerative colitis and niacin deficiency (Symons, I965; Ogilvie and Jones, I97I), this species is considered useful as a model for studying

intestinal disease (Symons, I965). More recently, it has become an important model in the study of immunity to metazoan parasites. It provides many advantages for investigations in this field, since it is highly immunogenic, it has a short prepatent period and both the worm and its host are readily maintained in the laboratory. The mechanism underlying the immunological control of *N. brasiliensis* in rats has proved more complicated than anticipated (Ogilvie and Love, I974). Further work is required to determine if it is typical of the immune response of hosts to their helminth parasites.

N. brasiliensis has been utilized as a model in a number of other areas of study. In the field of behavioural ecology the following have been examined: migration and site selection by larvae (Croll and Ma, I978), location of adults in the host intestine (Brambell, I965), the influence of host feeding and diet on worm distribution (Croll, I976), and the role of pheromones in adult behaviour (Bone, Gaston and Reed, I980; Glassburg, Zalisko and Bone, I98I). In addition, the availability of techniques for *in vitro* culture of *N. brasiliensis* (Weinstein and Jones, I957; Sommerville and Weinstein, I967) has enabled a range of biochemical and physiological experiments to be performed on this parasite. Examples include studies of gene control during development (Bolla, Bonner and Weinstein, I972) and enzyme activity during development and ageing (Bolla and Weinstein, I980)

2.I.2 *Nematospiroides dubius*

N. dubius lives in a number of common murid and cricetid rodents and occurs in both North America and Europe. Feral *Mus musculus* are commonly infected (Forrester, I97I), but worm burdens are light ($\bar{\chi}$ =5.8, range I-30; Forrester, I97I).

Infections of I50-300 worms can be readily maintained in laboratory mice, where they are found to have a long period of patency ($\bar{x}$ = 8.7 months, range 4-II months; Cross, I960).

Sublethal doses may cause considerable damage to host tissue, particularly when the larvae wander through the gastric mucosa and encyst within the wall of the small intestine. If the larvae pierce the intestinal wall, peritonitis with subsequent death ensues (Spurlock, I943; Baker, I954). The ingestion of host tissue by adults (Panter, I969) causes anaemia and damage to the intestinal epithelium (Baker, I954).

N. dubius has been extensively studied and is often used as a laboratory model. Like *N. brasiliensis*, it is easily maintained in the laboratory and has a short prepatent period. Moreover, it has the advantage of a long period of patency and since worms will copulate *in vitro* (Sommerville and Weinstein, I964) this species can be grown from egg to egg *in vitro*. As well as being the subject of studies on moulting and exsheathment (Sommerville and Bailey, I973), *N. dubius* has been used as a model for intestinal disease. The gastric lesions produced by the larvae resemble those caused by *Ostertagia ostertagia* (Liu, I965a) and different species of *Oesophagostomum* in humans, cattle, sheep and pigs (Liu, I965b). Furthermore, some of the characteristics of repeated infections resemble those of human hookworm (Bartlett and Ball, I972).

Although the long patent period suggests that there is little resistance in mice to *N. dubius*, two or three inoculations of larvae can induce immunity (Panter, I969). Recently, immunologists have turned their attention to this species. They have shown that immunity is both initiated by and against the L3, following their penetration of the intestinal wall (Chaicumpa, Prowse, Ey

and Jenkin, I977). Further work on the mechanisms involved in the expulsion of worms has continued (Dobson and Owen, I978; Prowse, Ey and Jenkin, I978; Dobson, I982) and could possibly lead to the development of a vaccine against nematodes.

2.2 Classification.

2.2.I Historical Perspective

N. brasiliensis

This species was first described by Travassos in I9I4, having been found in the small intestine of the Norway rat, *Rattus norvegicus*, in Rio de Janeiro, Brazil. It was placed in the genus *Heligmosomum* and given the specific name *brasiliense*. In I920, Yokogawa described a similar, but to him, distinct species in *Rattus norvegicus* from Baltimore, Maryland. He named this *Heligmosomum muris*. Lane (I923) relocated this species to a new genus, *Nippostrongylus*, and named *N.muris* as the type. He considered that the assymmetrical bursa in the male and bell-shaped posterior in the female precluded it from the genus *Heligmosomum*. Lane apparently overlooked Travassos' I9I4 description of *H. braziliense*. It has since been claimed (Haley I96I), and is generally accepted, that *N. muris* and *N. braziliense* are identical. Subsequently, Travassos (I937, cited by Haley, I96I) changed the spelling of the specific name to *brasiliensis*. Thus it is now known as *Nippostrongylus brasiliensis* and *N. muris* remains a commonly used synonym.

N. dubius

This species has also undergone a number of reclassifications. In I926, Schulz (reported by Skrjabin, I952) described a nematode from *Apodemus sylvaticus* and named it *Heligmosomoides skrjabini*. In the same year, Baylis founded a new genus, *Nematospiroides*, with the type species, *N. dubius*, also from *A. sylvaticus*. He made the absence of a dorsal ray on the bursa diagnostic of the genus. When

the presence of a reduced dorsal ray was later recognized, *N. dubius* was recorded as a synonym for *H. skrjabini*. Later, Travassos and Darriba (I929) united *Heligmosomoides*, Hall, I9I6 and *Heligmosomum* Railliet and Henry, I909. Thus Skrjabin (I952) named both *N. dubius* and *Heligmosomoides skrjabini* as synonyms for *Heligmosomum skrjabini*. Chabaud (I965) concorded with this.

In I968 the name of this nematode was reassessed once more (Durette-Desset, I968). Examination of original drawings revealed that it was described by Dujardin in I845 and named *Strongylus polygyrus*. Since this species was transferred to the newly formed genus *Heligmosomum* by Railliet and Henry (I909), the correct name is *Heligmosomum polygyrum*. As *Nematospiroides dubius* is still commonly used, especially in the fields of physiology and reproduction, this name will be used here.

2.2.2 Taxonomic Characters

The most obvious external feature of *N. brasiliensis* and *N. dubius* is the large copulatory bursa of the male, which is characteristic of the order Strongylida. This order includes many important parasites of domestic animals such as the lung worms, the swine kidney worm, *Stephanurus dentatus*, the stomach worm, *Haemonchus contortus*, and the hookworms, Ancylostomatidae. *N. brasiliensis* and *N. dubius* are distinguished as members of the super-family Trichostrongyloidea by their meromyarial musculature and their small buccal capsule, lacking sclerotized walls. The single uterus places both species in the family Heligmosomatidae.

N. brasiliensis is characterized by a cuticular fold which overhangs the vulva of the female and by an assymetrical bursa in the male. It is a small worm, the female measuring 4-5mm and

the male 3-4mm (Yokogawa, I920; Haley and Parker, I96I). *N. dubius* is larger, females being I8-2Imm and males 8-I0mm (Ehrenford, I954; Forrester, I97I). The spine on the tail of the female and the bifurcate spicules of the male distinguish *Nematospiroides* and *Nippostrongylus*. The two species used in this study conformed to the description in the literature.

2.3 Life cycle

N. brasiliensis

In I936 Lucker undertook a thorough study of the life cycle of *N. brasiliensis*. He showed that it follows a common pattern of 2 preparasitic and 2 parasitic moults. Until then, it was believed that this species moulted only once in the free-living state (Yokogawa, I920; Schwartz and Alicata, I935). Haley (I962) has summarized previous studies of the life cycle and the following account is drawn largely from his review.

When eggs are passed in the host's faeces, they are in the 4-I6 cell stage. After 20-24h they hatch into rhabditiform larvae (LI) and, in charcoal faecal cultures, the LI moult between 36-48 hours after hatching. They moult again after 3 days and within a few hours of reaching this infective stage, the majority exsheathe.

Rodents can become infected by ingesting infective 3rd stage larvae, but the usual mode of entry is via the skin. Once in the host, the parasites move to the lungs, through the blood, or occasionally via the lymphatics. The majority have completed this migration by I5h post-infection. They remain in the lungs for 35-50h, during which time they feed and grow. The 3rd moult occurs in the lungs at about 32h. The resultant L4 migrate up the trachea, down the oesophagus and through the stomach to the small intestine. Here they feed and grow and then undergo their final moult at 90-I08h.

Adults begin to become sexually mature after I30h and by I37h most females contain both sperm and fertilized eggs. In general, eggs can be found in the host's faeces on the 6th day of infection.

N. dubius

In I973, Bryant provided a detailed description of the life history of *N. dubius*. This work was important, as although there were some previous accounts of the life cycle (Spurlock, I943; Ehrenford, I945; Fahmy, I956; Cross, I960) the majority were incomplete and there were discrepancies between them. The following account is based on Bryant's work with some additional details from Liu (I965a) and Sommerville and Weinstein (I964).

Eggs hatch into LI 36-37h after passage in the host's faeces. The moult to L2 takes place 28-29h after hatching. I7-20h later, they undergo a partial moult to form the ensheathed infective larvae. The normal route of infection is by ingestion, but larvae administered intravenously, subcutaneously and intraperitonealy can migrate successfully to the small intestine (Chaicumpa et al, I977). Exsheathment of the larvae occurs in the stomach within 5 min of inoculation. Although some larvae quickly move through the stomach to the small intestine, about one third penetrate the gastric mucosa of the fundic region. Liu (I965a) gives a detailed account of this migration.

By 36h, all larvae have moved into small intestine where they burrow down to the muscularis and encyst. The 3rd moult occurs inside the cyst at about 90-96h post-infection. Some males may undergo their final (4th) moult in the mucosa as early as I44h,

while others emerge as 4th stage larvae and moult in the lumen of the intestine. In general, males both emerge and moult before females. Although some females were *in copula* and had eggs in the uterus at 192h, it was not until 216h that the majority were producing fertile eggs. Eggs can be detected in the host's faeces after 240h and the total time from egg to egg is 13.5 days

2.4 Maintenance in the laboratory

N. brasiliensis

Adult populations of *N. brasiliensis* were obtained from the small intestines of rats, previously inoculated with infective larvae. Stocks of these larvae were kept in shallow tap water in 15cm diameter petri dishes and stored in the dark at 20°C. They remained viable for about 2 months, after which time they were replenished in the following way.

Seven days after inoculation with infective larvae, rats were placed in wire cages and their faeces collected in trays lined with damp paper. Each day, the faeces were transferred to 10cm glass petri dishes, previously filled to a depth of 0.5cm with a paste made from animal charcoal (H.B. Selby and Co. Ltd.) and water. This paste kept the faeces moist during incubation and acted a substrate across which larvae could migrate. After 7 days' incubation at 20°C, in the dark, most of the larvae had moved across the charcoal and up onto the lid of the dish. They were washed off with tap water and stored as described previously.

Rats were injected when 6-8 weeks old. They were anaethetized lightly with chloroform and the larvae, suspended in 0.5ml of water, were injected subcutaneously. Larvae were counted according to the

method of Downey and Connolly (I963) and the dosage ranged from I,000 - 2,000 depending on their age and condition.

To obtain adult worms, rats were killed with chloroform 7-I0 days post-infection. The first 40-50cm of small intestine was excised and opened under 0.85% NaCl. Male and female worms were removed from the intestinal wall and transferred into fresh saline using a fine hooked needle.

For one aspect of the study, I required recently inseminated females with sperm in the vagina,ovejector or lower uterus. I attempted to obtain females after their first mating, when there were few eggs in the uterus and ovejector. This was important for two reasons. First, it was easier to see sperm in the vagina if eggs were not present. Second, it is difficult to cut good sections of the reproductive tract when fertilized eggs, with their relatively hard egg shells, are present. An examination of worms at II7, I20, I23, I26, I29 and I32h after infection showed that at I32h a high proportion of females had recently mated, yet few contained fertilized eggs. Thus when these specific conditions were required, rats which had been infected I32h previously were used.

N. dubius

Populations of adult *N. dubius* were obtained by inoculating uninfected mice, weighing 25-30gm, with I50-200 infective larvae. The larvae were suspended in 0.05ml of water and administered orally. They were obtained as follows.

Faeces from infected mice were collected overnight on damp paper, then mashed into a paste with a little water. This paste was spread across moist filter paper in plastic petri dishes. After incubation at 20°C for 7 days, the larvae were harvested from the

base of the dishes. They were stored at 4°C under shallow water and used within 3 months.

Adult *N. dubius* were obtained from infected mice 9 or more days after inoculation. Mice were killed with chloroform and the first 10cm of small intestine removed and opened under 0.85% NaCl. Male and female worms sometimes *in copula*, were found coiled around the villi of the intestine. They were quickly removed and placed in fresh saline.

CHAPTER 3. MATERIALS AND METHODS

3.I Preparation of tissue for light and transmission electron microscopy.

3.I.I Dissection of worms prior to fixation.

Since fixatives penetrate nematode cuticle only slowly, the reproductive organs of both males and females were dissected out of worms prior to fixation.

To obtain testes, males were placed in 2-3 drops of 0.IM Sorenson's phosphate (Glauert, I974), pH 7.2-7.4, on a clean glass microscope slide and cut just posterior to the junction of the vas deferens and seminal vesicle. Once the cuticle was ruptured, the high body pressure forced the internal organs out of the worm and after a short time the testis became free and could be transferred into fixative. Uteri were removed from females in a similar way. When worms were cut in the region of the ovejector, the uterus, along with a short length of posterior ovary, could be separated from the rest of the reproductive tract and placed in fixative. This procedure often caused minor damage to the ovejector or vagina. To obtain these regions undamaged, it was necessary to cut females in the vicinity of the anterior uterus and to fix the posterior reproductive tract within the cuticle. Fixation of intact worms for 5 min prior to dissection prevented major disruption of the organs during this procedure.

3.I.2. Schedule for fixing and embedding tissue.

This schedule of fixation follows methods which have previously given good results in ultrastructure studies of nematode spermatozoa (Foor, I968; Beams and Sekhon, I972). Minor modifications are from Glauert (I974).

The tissue was fixed in cold (4°C) 3% glutaraldehyde in 0.IM Sorenson's phosphate buffer, pH 7.2 - 7.4, for I.5 - 2h, then rinsed in three changes of cold phosphate buffer for I0 min each. The tissue was post-fixed in I% osmium tetroxide in 0.IM Sorenson's phosphate for Ih at 4°C, then quickly washed in two changes of buffer. For some specimens, a tertiary fixation, consisting of *en bloc* staining with uranyl acetate, was used to improve section contrast (Locke, Krishnan and McMahon, I97I). In this case, the tissue was placed in 2% aqueous uranyl acetate for 24h at 60°C, then briefly washed with two changes of water before dehydration.

All material was dehydrated with ethanol as follows - 30%, 50%, 70%, 90%, 96% for I0 min each, then I00%, three changes of I0 min each. The tissue was infiltrated with Spurr low viscosity embedding medium (Polysciences Inc.) at room temperature and under vaccum. I00% ethanol and Spurr in equal proportions was used for the first I8h, followed by fresh Spurr for a further 8h. Finally, specimens were orientated in flat embedding moulds, covered with fresh Spurr and polymerized at 68°C for 48-96h.

3.I.3 Cutting and staining sections for light microscopy.

Before commencement of the ultrastructural studies, the reproductive tracts of both *N. dubius* and *N. brasiliensis* were examined with the light microscope using Iμm "thick" sections. Suitable blocks were chosen and testes were sectioned from the anterior end, along their whole length. The Iμm thick transverse sections were cut on a Reichert OM3 ultramicrotome with glass knives. Initially, each section was collected, but it was soon found that every tenth one was sufficient. Longitudinal sections of various areas of the testis were also cut. For this, lengths of testis were

orientated across the top of the embedding mould prior to polymerization and then carefully alligned before sectioning.

In all cases, sections were transferred to drops of water on clean glass slides. They were dried on a hotplate at 85°C, then stained for 2 min with I% toluidine blue in I% borax (Meek, I970). After rinsing in water, the sections were differentiated in 50% ethanol, dried, cleared in xylene and mounted with DPX (BDH Chemicals Ltd.)

Sections were viewed and photographed with a Zeiss Photomicroscope III or Wild M20, using Kodak high contrast copy film (64ASA) or Ilford FP4(I25ASA).

3.I.4 Cutting and staining sections for transmission electron microscopy.

Tissue to be examined in the electron microscope was surveyed with Iμm thick sections, stained as described previously. When suitable areas of tissue had been located, the block was retrimmed and "silver" ultrathin sections were cut on the Reichert OM3 ultramicrotome using glass knives. If the block was retrimmed at any stage, more thick sections were cut before ultra-thin sectioning was resumed. Thus, since each section examined in the electron microscope had a corresponding thick section, the ultrastructural detail of the testis could be compared with its general morphology.

Ultrathin sections were transferred onto copper grids which were either uncoated or coated with formvar and carbon. They were stained at 45°C with 5% aqueous uranyl acetate for periods of 2-30min depending on the nature of the tissue. After rinsing and drying, the sections were counter-stained with Reynolds' lead citrate (Reynolds, I963) for 2 min. Sections cut from specimens stained *en bloc* with uranyl acetate were stained with lead only.

Some material was viewed and photographed in a Siemens Elmiskop I. Later a JEOL JEM IOOCX and a JEOL IOOS were used.

3.2 Schedule for labelling sperm and oocytes with ruthenum red.

In the first attempt to stain sperm and oocytes with ruthenium red (RR), whole testes and uteri were immersed in fixative containing 0.I% RR. Examination of unstained sections of this material showed that the RR was unable to penetrate either the testis of uterine epithelium. In an effort to overcome this, the tissue was cut into segments of approximately 0.5mm before fixation. Unfortunately this only increased penetration for IO-20μm at the cut ends; deeper in the tissue sperm remained unstained. The final modification of the RR labelling technique involved removing sperm from the reproductive tracts before staining.

Sperm were dissected from uteri and seminal vesicles by gently teasing the tissue in I-2 drops of buffer on the base of a small (5.5cm diameter) plastic petri dish. Sperm are sticky and the majority adhered to the plastic when the dish was flooded with fixative, 3% buffered glutaraldehyde containing 0.I% RR. As phosphate buffers are not compatable with RR (Luft, I97Ia), 0.IM sodium cacodylate, pH 7.2, was used. After 3 x IO min washes, the tissue was post-fixed for 3h in cacodylate buffered, I% osmium tetroxide containing 0.I% RR. To reduce the reaction between RR and osmium, this solution was made just prior to use and specimens were kept in the dark during fixation. After several quick rinses in buffer, the tissue was dehydrated and embedded by pouring epon into the petri dish and polymerizing in the usual way. When the resin was hard, it could be easily separated from the dish. In this regard it was important to use polyethylene petri dishes as polystyrene and

glass bond to Spurr.

To examine RR staining of unfertilized oocytes, the region of the ovary just anterior to the oviduct was excised. Here, the eggs have separated from the rachis and are ready for fertilization. After removal from the uterine epithelium, the oocytes stuck to polyethylene petri dishes and could therefore be processed in the same way as the sperm.

The affinity of oocytes and sperm for RR was evaluated with the aid of two controls. Some specimens were treated as before, except that RR was omitted from both the glutaraldehyde and the osmium. Alternatively, the tissue was stained after incubation in neuraminidase (Gress and Lumsden, I976). In this procedure, sperm or eggs were dissected into petri dishes and fixed in buffered glutaraldehyde for I.5 - 2h. After a brief rinse, they were incubated at 37^{o}C for 3h in I0 units/ml neuraminidase (Type VI purified from *Clostridium perfringens*, Sigma Chemical Co.) in acetate buffer, pH 5.4. Specimens were then rinsed in acetate buffer, followed by cacodylate buffer and post-fixed in I% osmium tetroxide in cacodylate buffer containing 0.I% RR. Dehydration and embedding was as described previously.

3.3 Schedule for staining spermatozoa with tannic acid.

Tannic acid is a complex mixture of polyphenolic materials, all of which have a galloylated glucose structure. It acts as a mordant between osmicated structures and lead and as such induces high contrast both within the tissue and at the surface of cells (Simionescu and Simionescu, I976; Suzuki and Nagano, I980). It also enhances preservation of some subcellular structures such as microfilaments and microtubules (Burton, Hinkley and Pierson, I975; Begg and Rebhun, I978). Its exact mode of action in this regard is

unknown, but it is believed to coat these structures and prevent their disruption during osmication and dehydration.

In this study, tannic acid was used to enhance the surface coat of sperm and to preserve cytoplasmic filaments during processing for electron microscopy. Although Simionescu and Simionescu (1976) recommend staining after osmication, tannic acid must be added to the primary fixative to preserve microfilaments. Since tannic acid was unable to penetrate the epithelial cells of the uterus and testis, it was necessary to dissect sperm onto the base of petri dishes as for RR staining (Chapter 3.2). The primary fixative was 3% glutaraldehyde in 0.1M Sorenson's phosphate pH 7.2, containing 0.2% or 1.0% tannic acid (Mallinckrodt Inc., code No. 1764). Subsequent processing followed the routine procedure described in Chapter 3.1.2.

3.4 Specimen preparation and staining with fluorescein-conjugated lectins.

In the majority of studies where cells are labelled with lectins conjugated to fluorescein isothiocyanate (FITC), the cells are stained while in suspension and the reagents removed by centrifugation. This technique is particularly suitable for spermatozoa, since large numbers of sperm can be collected in suspension (Schwarz and Koehler, 1979). The small quantity of sperm available from *N. brasiliensis*, precluded the use of this technique here. Instead, advantage was taken of the stickiness of sperm. They were allowed to settle onto glass coverslips and were transferred through the appropriate solutions while stuck to this substrate.

The protocol described here was adapted from the methods used by Schwarz and Koehler (1979) for guinea pig sperm. Initially only prefixed sperm were labelled, but experiments with unfixed sperm were planned to follow if the technique was successful. For each

treatment, sperm from the reproductive tracts of 5-6 individuals were dissected onto a single glass coverslip. The area was then flooded with 2.5% paraformaldehyde in 0.IM Sorenson's phosphate, pH 7.2 - 7.4, and the sperm fixed for 0.5 - 2h. After a quick rinse in buffer, the specimens were incubated in 0.2M glycine in buffer for 60 min (changed at least three times), to block unreacted aldehyde groups (Schwarz and Koehler, I979). Sperm were then washed for 5 min with buffer, labelled with 200µg/ml lectin in buffer for 30 min at room temperature and rinsed with buffer. Controls were incubated in a mixture of lectin and sugar inhibitor. These had been made up 30 min previously to ensure that all receptor sites on the lectin were filled by the sugar. In addition, the control samples were rinsed with buffer containing inhibitor. The lectins used, their source and their specific inhibitors are listed in Table 3.I. After labelling, all preparations were stored in the dark to prevent extinction of fluorescence with stray UV light.

Specimens were examined with epi-illumination in a Zeiss Photomicroscope I, equipped with FITC filters. Sperm were photographed with Kodak Tri-X pan film (400 ASA) using exposures of 2.5-3 min.

To test both the materials and the technique, '' positive" controls were included. These consisted of samples of rodent sperm with known lectin-binding patterns (Koehler, I98I). The epididymides of adult male guinea pigs and mice were excised immediately after death and minced in 0.9% saline with scissors. After incubation at 37^{o}C for 5-I5 min, the sperm had swum free of the tissue and could be washed by centrifugation at 2,000rpm for 5 min. When sperm had been washed twice and resuspended in fresh saline, 2-3 drops of suspension were placed on clean coverslips. Once the sperm

TABLE 3.1

Lectin	Conjugant	Source	Inhibitor	Concentration Used	Source
Concanavalin A	FITC	Sigma Chem. Co.	∝ methyl-D-mannoside	0.1M	Sigma Chem. Co.
Wheat germ agglutinin	FITC	"	ovomucoid, Type III-O	5mg/ml	"
Soy bean agglutinin	FITC	"	N-acetyl-D-galactosamine	0.1M	"
Ricinus communis agglutinin (Type II M.W. 60,000)	FITC	"	lactose	0.1M	British Drug Houses Ltd.

The lectins used to label sperm, their source and their specific inhibitors.

had settled and adhered to the glass, they were flooded with fixative. The procedure was then the same as for nematode sperm.

The lectin binding properties of the surface of unfertilized oocytes of *N. brasiliensis* were also examined. Oocytes were obtained from the posterior ovary as previously described (Chapter 3.2) and since they stuck to glass coverslips they were handled in the same way as spermatozoa.

3.5 Freeze-fracture.

3.5.I Specimen preparation.

Reproductive tracts from both males and females of *N. brasiliensis* and *N. dubius* were freeze-fractured after fixation and glycerination according to the following schedule.

Testes and uteri were removed from worms as described previously. They were fixed in 3% glutaraldehyde in 0.IM Sorenson's phosphate, pH 7.2 -7.4, for I-2 h at 20°C, then rinsed in three changes of buffer for I0 min each. The tissue was then infiltrated with I5% glycerol in buffer for 30 min and finally transferred into 30% glycerol, where it was stored until required. Specimens to be kept for more than one day were stored at 4°C.

To render the tissue clearly visible amongst ice and frozen glycerol, it was lightly stained in a toluidine blue-glycerol mixture: 3-5 drops of I% toluidine blue in 5-I0 drops of buffered 30% glycerol. After staining for 5 min, specimens were rinsed in fresh glycerol, loaded into specimen holders and frozen. A standard Balzars 3mm gold specimen holder, with a central well Imm in diameter was used. To ensure that the knife could reach the tissue during fracturing, specimens had to be raised above the lip of the well on one or two small pieces of filter paper. Filter paper was chosen as it would not significantly alter the freezing rate, unlike a support

which was impenetrable to glycerol. Once mounted, the tissue was frozen firstly in liquid freon 22, cooled by liquid N_2, then in liquid N_2 alone.

Specimens were fractured at -II0°C in a Balzars freeze-etch machine and etched for one minute at -I00°C. The fracture face was then shadowed at 45° with platinum and backed with carbon. The resultant replica was floated in distilled water and the tissue removed in 25% and 50% chromic acid. Occasionally, 75% acid was used for rapid removal of tissue. When replicas were clean, they were washed in two changes of double distilled (dd) H_2O, mounted on 400 or 300 mesh, uncoated copper grids and examined in a Phillips EM 400.

Several uteri from females of *N. dubius* were fractured without prior fixation and glycerination. This was done for two reasons. First to assess the effects of these two procedures on particle distribution in the membranes and second to allow deep-etching and hence exposure of the true surface of the membranes. Immediately after removal from worms, unstained uteri were placed in a drop of buffer on the specimen holder. They were frozen as described for fixed tissue. Etching was carried out for I-2 min at -I00°C. Replicas were produced in the usual way and examined in a JEOL I00S microscope.

3.5.2. Measurement of particle size and density

When replicas are viewed in the transmission electron microscope, membranes appear as flat faces, bearing particles measuring approx. I0nm in diameter. Since freeze-fracture reveals the interior of the membrane (Chapter 9.I), these particles are called intramembranous particles or IMPs. Particle size and density were measured on the different membrane faces in the following way.

Suitable regions of the replicas were photographed at magnifications ranging from 20,500 to 27,000 X. The specimen height was set and the magnification calibrated using a grating replica. The negatives were enlarged to I55,000 x and regions of the membrane face were printed. Poorly shadowed areas and regions judged from stereo pairs to be steeply sloping were excluded. Particle size was measured from the positives to the nearest 0.Imm, using a Polaron measuring eyepiece.

The density of particles was initially measured as IMPs/cm^2 using a Icm-square grid on the photographic print. This value was subsequently converted to IMPs/μm^2. When graphing the results, the density in each size class was derived from the fraction of particles in that class multiplied by the overall density of particles on that fracture-face.

3.6 Techniques used to record and analyse movement of the sperm of *N. brasiliensis*.

Spermatozoon motility was studied by direct observation and by time-lapse cinematography. Seminal vesicles or uteri were dissected in a drop of either 0.85% NaCl or sperm medium, on a glass slide coated with egg albumin. Sperm medium (Nelson and Ward, I980) consisted of the following: 50mM HEPES (N-2-hydroxy-ethylpiperazine N'-2-ethanesulfonic acid, Calbiochem-Behring Corp.) titrated to pH 7.0 with NaOH, 50mM NaCl, 25mM KCl, 5mM $CaCl_2$, ImM $MgSO_4$ and Img/ml bovine serum albumin (Commonwealth Serum Laboratories). To prevent dessication, the coverslip was sealed over the preparation with hot paraffin wax.

Sperm were examined at 37^{o}C with phase contrast and photographed at intervals of 0.5s on I6mm film (Kodak Tri-X reversal, I60 ASA), using a Bolex HI6M camera in conjunction with Olympus ACM-3 cine-

photography equipment. Analysis were made from outlines, drawn from enlargements of individual frames of the film and were aligned with the aid of a reference grid.

The effect of cytochalasin B on the movement of sperm was tested as follows. Preparations containing translocating sperm were perfused with cytochalaisin by drawing the solution across an unsealed chamber using filter paper. Cytochalasin B (Imperial Chemical Industries Limited) was stored as a stock solution in dimethyl sulphoxide (DMSO) and diluted with sperm medium or saline. It was used at concentrations of I0-I00 μM, with the concentration of DMSO never exceeding I%. Leukocytes were used to test the effectiveness of cytochalasin on other cells. A drop of heparinized rat or mouse blood was spread on a clean slide, incubated at $37^{o}C$ for 5-I0 mins, then rinsed with saline. The red and white blood cells could be separated in this way, as the latter generally adhered to the glass but the former did not. Preparations of translocating leukocytes were perfused with cytochalasin B in the same way as sperm. All experiments included controls in which the cytochalasin had been omitted from the perfusate.

SECTION II

A COMPARISON OF SPERM DEVELOPMENT AND MATURATION IN *N. BRASILIENSIS* AND *N. DUBIUS*

CHAPTER 4. INTRODUCTION TO SECTION III.

4.I Objectives

It is often difficult to choose an experimental organism which is entirely suitable for a particular study. Yet, if several species are used to explore different aspects of a broader question, one may be confronted by problems of interspecific variation and the lack of complementarity of the results. These problems will be minimized, however, if two related species can be found in which all of the fundamentals and some of the details of the system under study are similar. There must also be enough variation between the two species such that each will be advantageous for particular facets of the overall investigation. The following section is an attempt to produce such a system for the study of nematode sperm using *Nippostrongylus brasiliensis* and *Nematospiroides dubius*. The question of complementarity has been approached in the following way. First, the gross morphology of the testes of the two species was examined and compared at the level of the light microscope. The fine structure of spermatogenesis and spermatozoon maturation was then explored with the electron microscope. Finally, sperm motility in *N. brasiliensis* was examined. This enabled a comparison to be made with locomotion in the sperm of *N. dubius* (Wright and Sommerville, 1977). The descriptions and observations for the two species are presented separately in Chapters 5 and 6. Some freeze-fracture micrographs obtained during a later study of the membranes of the sperm have been included as they illustrate the three-dimensional nature of the cellular organelles and their relationships with one another. Chapter 7 constitutes a general discussion, in which the

descriptions of the sperm of the two species are compared and contrasted and discussed in relation to the sperm of nematodes generally, other invertebrates and mammals.

In order to provide an overview of reproduction in the two species under study, the remainder of Chapter 4 contains a brief summary of the gross anatomy of both the male and female reproductive tracts.

4.2 The female reproductive tract of *N. brasiliensis* and *N.dubius.*

The female reproductive tract of nematodes can be divided into ovary, uterus, ovejector and vagina (Chitwood and Chitwood, I950). Unlike in most nematodes, the ovaries and uteri of *N. brasiliensis* and *N. dubius* are unpaired (Figures 4.I A,B). In both species, the ovary is nearly as long as the worm and contains oogonia and oocytes. It sometimes lies as far anterior as the base of the oesophagus and usually bends to form a loop in this region (Yokogawa, I920). The developing oocytes are joined to one another by a central axial rachis. As they approach the uterus, they separate from the rachis, become more spherical and then leave the ovary via a narrow constriction called the oviduct. Since most of the spermatozoa congregate in the anterior uterus, it is called the seminal receptacle. Fertilization is thought to occur here (Phillipson, I969). The epithelium is thick in this region, but more distally it becomes thinner. The uterus empties into the ovejector, a thick-walled, muscular region, which is thought to control egg movements into the vagina (Bird, I97I). The vagina is also thick walled and is lined with cuticle. It terminates in the ventral vulva, which is situated just anterior to the anus. The form and shape of the female reproductive tracts of *N. brasiliensis* and *N. dubius* are very similar, but the latter is larger (Figure 4.I A,B). For example, the uterus is 0.85-0.95mm long and about 0.Imm

FIGURE 4.1 : A,B. Female reproductive tracts of *N. dubius* (A) and *N. brasiliensis*. Note the relative sizes in the two species; the seminal receptacle is disproportionately long in *N. dubius*.

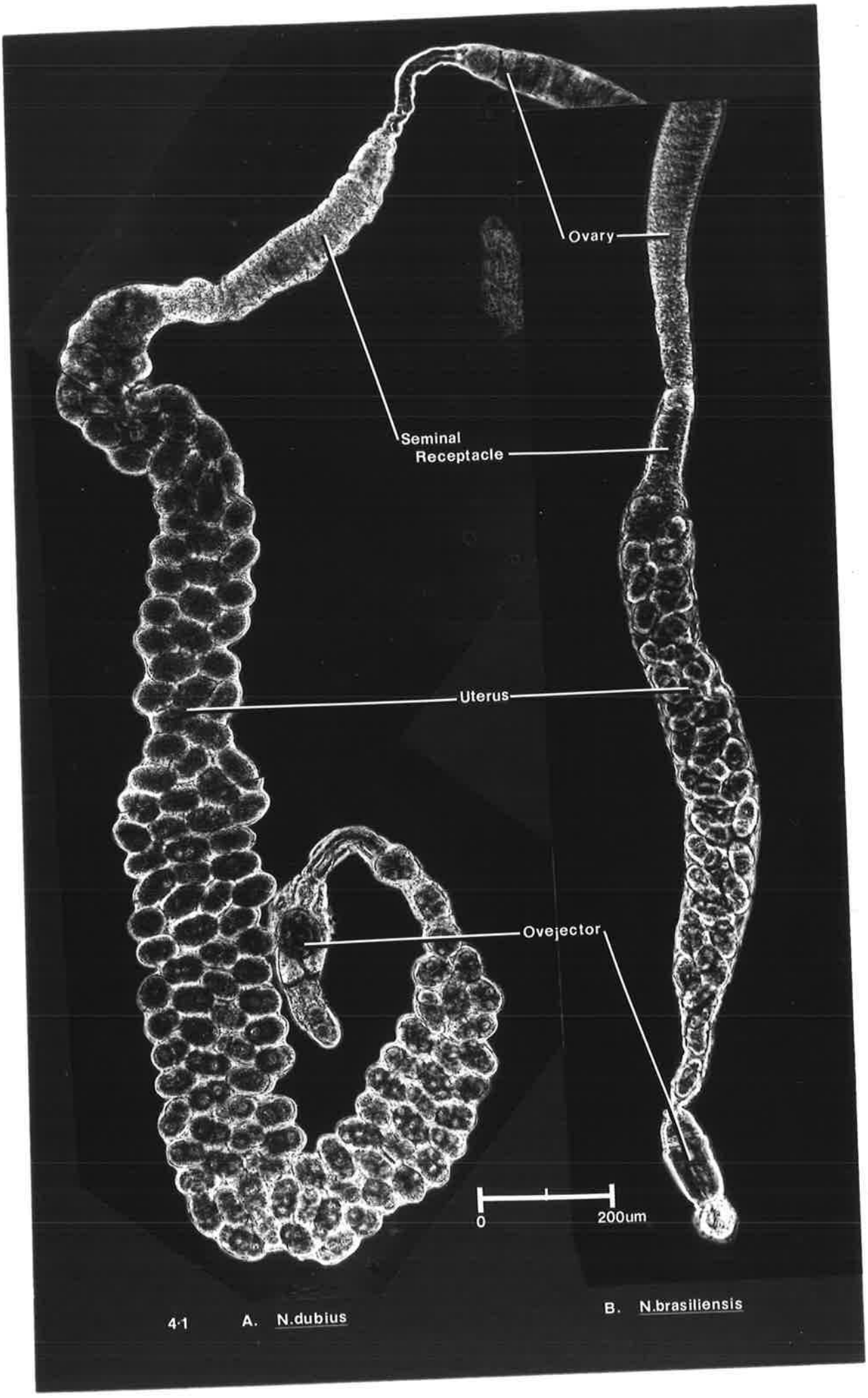

4·1 A. N.dubius B. N.brasiliensis

across in *N. brasiliensis* but 2.5-2.7mm long and 0.I-0.2mm in diameter in *N. dubius*. Consequently the uterus of *N.brasiliensis* contains far fewer eggs than *N. dubius* (approx. 30 and I80 respectively). These eggs are also smaller, being 55µm long and 3Iµm across (Haley, I96I) compared with 78µm x 47µm in *N. dubius* (Forrester, I97I). Moreoever, the seminal receptacle of *N. dubius* has a greater capacity to store sperm as it is disproportionately long (0.5mm compared with 0.Imm in *N. brasiliensis;* compare SR Figures 4.I, A,B). This, together with the longer ovary and larger uterus, would provide *N. dubius* with a greater egg-bearing capacity than *N. brasiliensis*.

4.3 The male reproductive tract of *N. brasiliensis* and *N.dubius*.

The reproductive tract of male nematodes consists of three parts: the testis, the seminal vesicle, and the vas deferens (Figure 4.2). Like the majority of nematodes, *N. brasiliensis* and *N. dubius* have a single tube-like testis, covered by a thin epithelium. Spermatogonia are proliferated from the anterior end and as they develop, they move back along the testis in a synchronous progression. This is a telegonic pattern of organization. It contrasts with the hologonic form, where the germinal area occurs along the outer margin of the testis and sperm cells move in towards the lumen as they mature. The rate of movement of cells along the telegonic testis is assumed to be constant, as development is continuous and no gaps occur between different stages. Given this, the distance along the testis travelled by the sperm cells during each stage of differentiation will be a reflection of the time required to complete each of these developmental stages. That is, rapid changes will occur within a

FIGURE 4.2 : A young male of *N. brasiliensis* showing the major organs of the reproductive system.

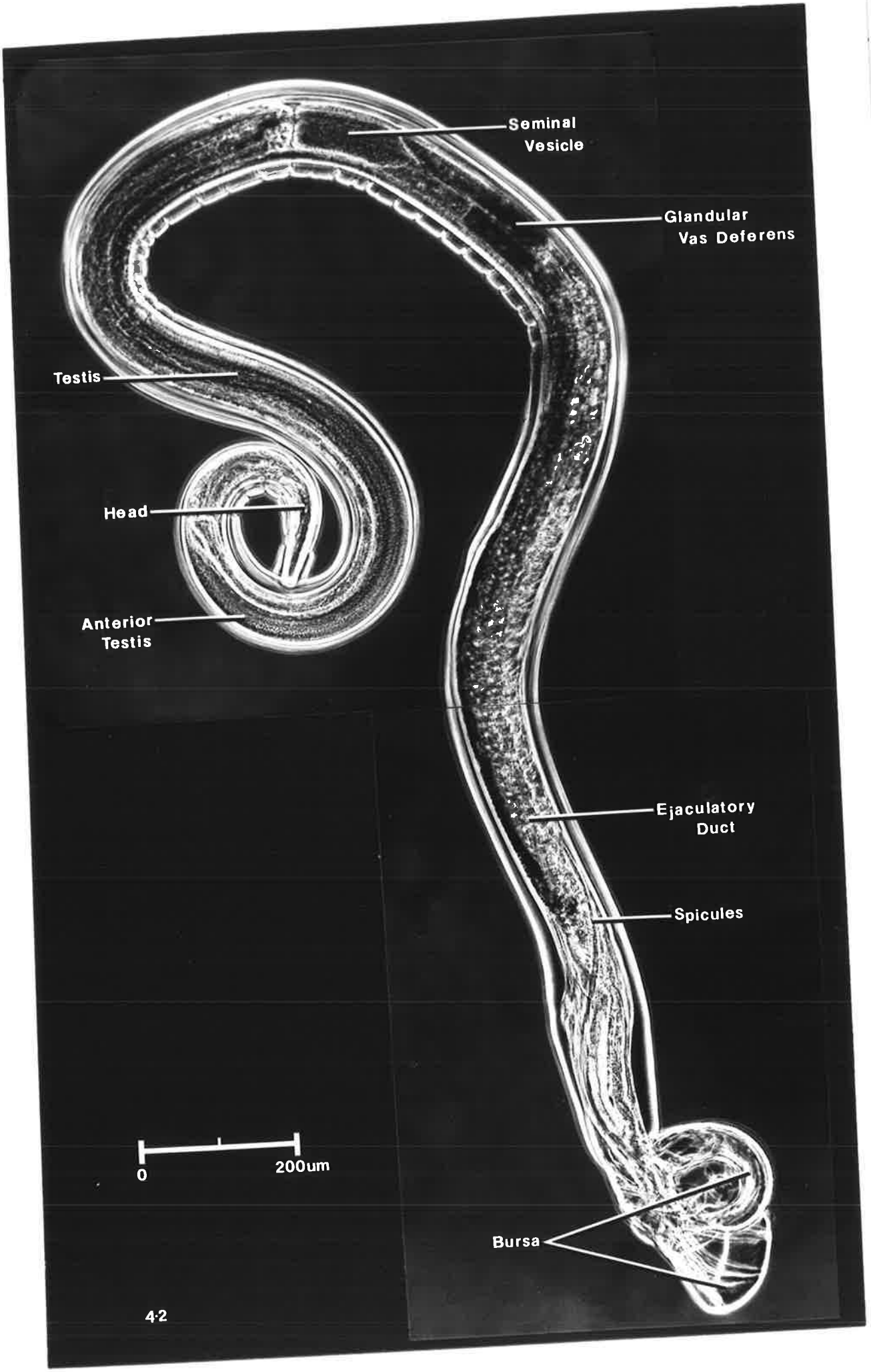
Seminal
Vesicle
Glandular
Vas Deferens
Testis
Head
Anterior
Testis
Ejaculatory
Duct
Spicules
0
200um
Bursa

4·2

restricted region of the testis, whereas slow changes will take place gradually over a greater distance. In this way, although I have not determined the absolute time required for differentiation of spermatozoa, the time taken for each developmental stage relative to one another has been estimated.

The proximal region of the testis of both *N. brasiliensis* and *N. dubius* lies near the base of the oesophagus and is often folded back to form a loop (Yokogawa, I920; Jamuar, I966). The seminal vesicle is separated from the testis by four cuboidal epithelial cells which form a narrow duct, usually referred to as the vas efferens (Chitwood and Chitwood, I950). When mature, spermatozoa pass through this duct into the seminal vesicle, where they remain until mating. Immediately adjacent to the seminal vesicle is the vas deferens. The anterior region contains high columnar cells with granular cytoplasm, suggesting a glandular function. In contrast, the posterior part is muscular and is often called the ejaculatory duct.

The vas deferens opens into the cloaca at the posterior end of the worm. Around the cloaca is a prominent cuticular expansion, the bursa, consisting of both lateral and dorsal lobes. It is used by the male to clasp the female during copulation (Sommerville and Weinstein, I964), but it may also be important during initial contact with the female as it contains sensory nerves (Croll and Wright, I976). A pair of spicules lie dorsal to the posterior vas deferens. Contraction of the spicular muscles pushes them out through the cloaca and inserts them into the female during mating (Bird, I97I; Lee, I973). They serve to dilate the vulva, allowing the male to deposit spermatozoa into the vagina (Phillipson, I969). As the spicules are innervated (Lee, I973;

Dick and Wright, I974), they are also likely to act as sensitive probes which detect the vaginal opening. This would facilitate the positioning of the male prior to copulation and would prevent internal damage to the female during their insertion (Lee, I973; Dick and Wright, I974).

As was the case in females, the general form of the male reproductive tracts of *N. brasiliensis* and *N. dubius* is very similar. Again there is a considerable difference in size, with the testis of *N. brasiliensis* measuring I.8 - 2mm and that of *N. dubius* being close to 4mm. Other minor differences in testis morphology will be described in Chapter 6.I.

Chapter 5. Spermatogenesis and spermatozoan maturation in *N. brasiliensis.*

5.I Morphology of the testis.

The following description is based on observations of thick sections and whole mounts of the testis. It is included to give perspective to the more detailed account of spermatogenesis which follows.

A single cell, often called the " cap cell" (McLaren, I973a; Chitwood and Chitwood, I950), occupies the anterior tip of the testis, where it is continuous with the testis epithelium (Figure 5.I). It is ovoid, measures 7-I0μm, and has a large nucleus and prominent nucleolus. The lumen of the anterior testis is filled with spermatogonia, occasionally dividing by mitosis. Their shape is variable, but could generally be described as ovoid. They are 6-7μm long and 5μm across. Like the cap cell, they have a large nucleus and one or two prominent nucleoli.

Fine threads of cytoplasm extend from the apices of the spermatogonia to the centre of the testis, where they join with a core of cytoplasm called the rachis. This rachis extends from the anterior of the testis to the region of meiosis (Figure 5.2). Its growth and differentiation can be traced in a series of transverse sections cut at intervals along the testis (Figure 5.3). Close to the cap cell it is small and measures only I x 3μm (Figure 5.3A). It rapidly expands in one dimension to 8μm, but remains only Iμm wide (Figures 5.3 B,C). It therefore resembles a plate or band of cytoplasm running through the centre of testis and linking the spermatogonia. 300-350μm from the cap cell it contracts into a central core of cytoplasm, which is initially only 3μm across (Figure 5.3F), but gradually enlarges to I0μm (Figures 2, 5.3 G). It remains in this form throughout the rest of its length.

FIGURE 5.1 : Longitudinal section of the anterior testis of *N. brasiliensis*. The flat, plate-like rachis can be seen in the lower part of the figure. Dotted lines show the positions of transverse sections seen in Figure 5.3A,B.

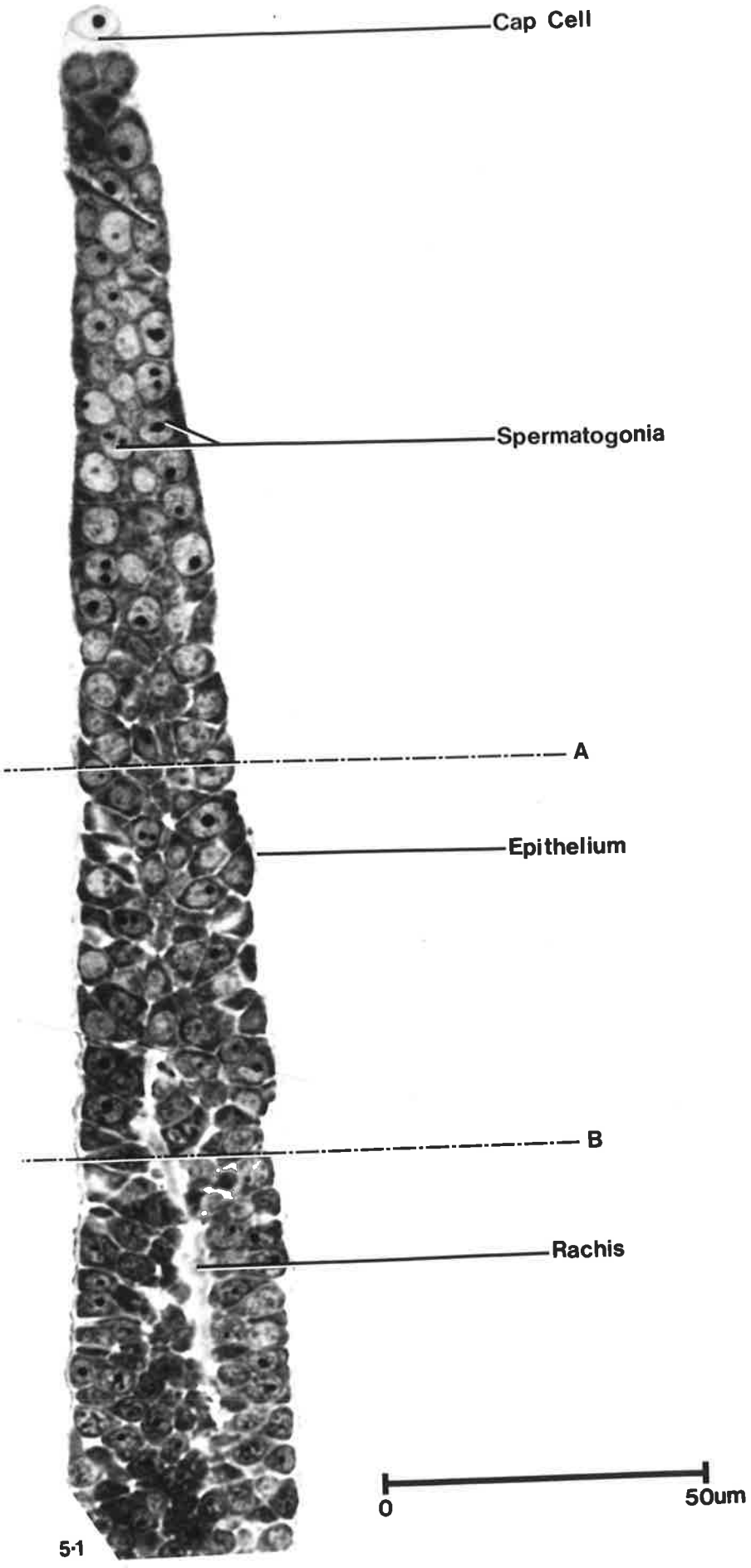

5-1

FIGURE 5.2 : Phase contrast montage of the testis and seminal vesicle (SV). Near the anterior are spermatogonia (Sg), which differentiate into spermatocytes (Sc) at 250µm from the cap cell. After meiosis the spermatids (St) mature into spermatozoa (Sz). The rachis (Ra) is small at the anterior but rapidly enlarges, it shrinks back to fine threads in the zone of meiosis.

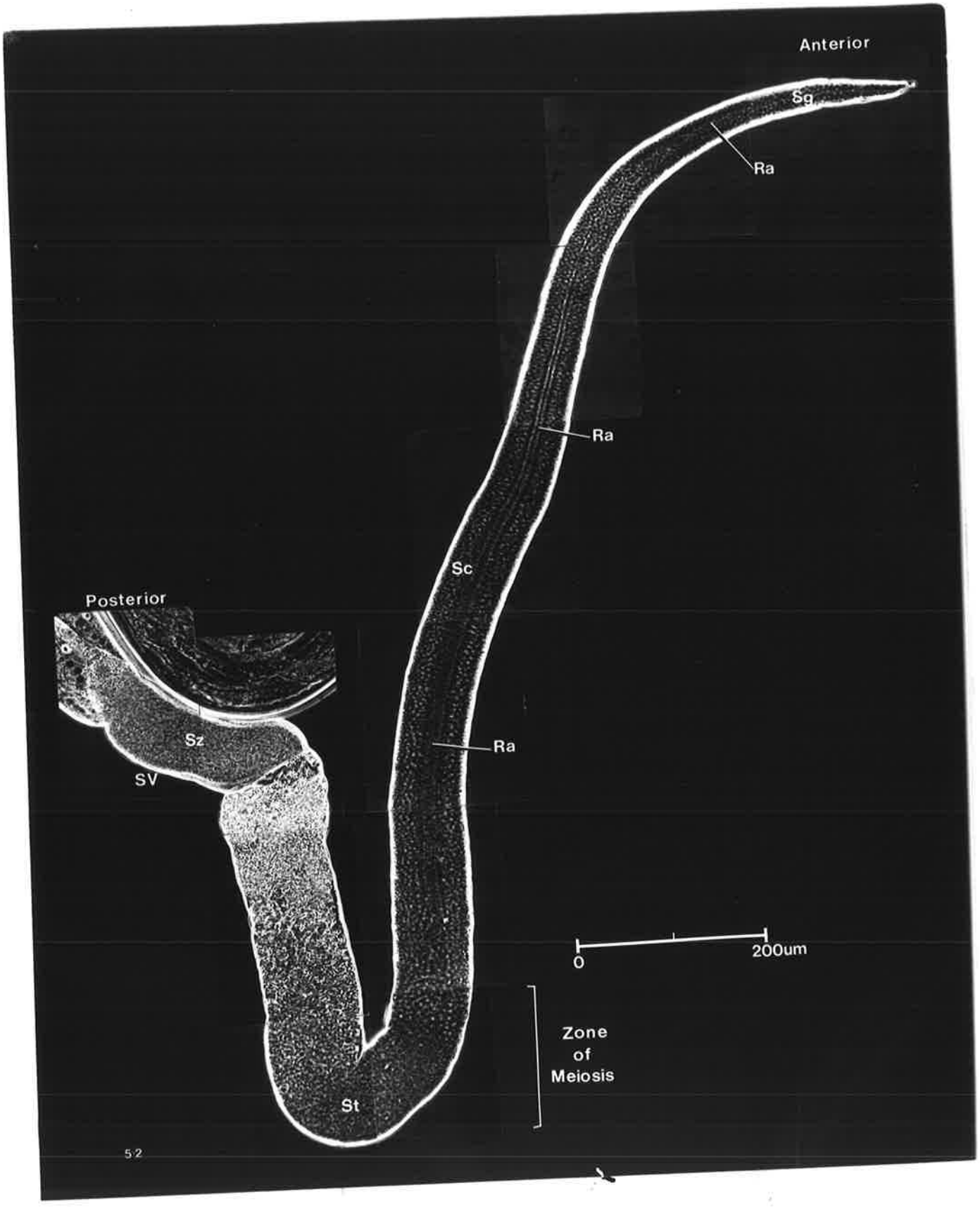
Anterior
Sg
Ra
Ra
Sc
Posterior
Sz
SV
Ra
0
200um
Zone
of
Meiosis
St

FIGURE 5.3 : Series of transverse sections of the testis cut from anterior to posterior. A,B,C,D show spermatogonia (SG), joined by fine threads of rachis (R). In E the spermatocytes (SC) have large, homogeneous nuclei and in F, the rachis has become a central core. The granularity within the spermatocytes in G and H is due to the formation of membranous organelles in the cytoplasm; the rachis has begun to shrink in H.

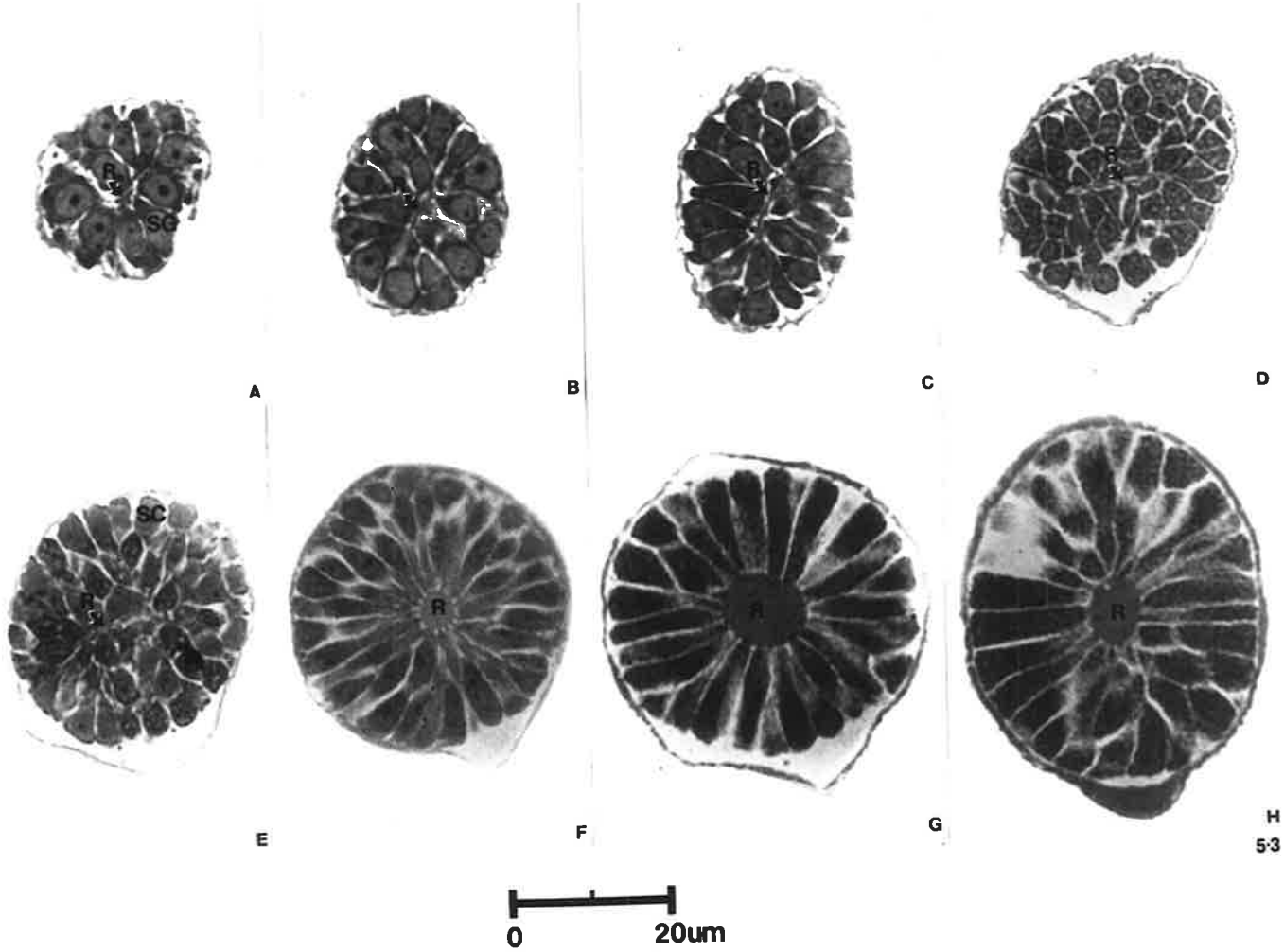

5·3

At 200-250μm from the anterior of the testis, the spermatogonia undergo a final mitotic division. Although few cells contain mitotic figures,they become noticeably smaller (3.0 x 5.5 μm) and more numerous (Figures 5.3 D,E). The chromatin at this stage is patchy and condensed, but within the next 50μm the cells regain the large nuclei which characterized the spermatozogonia (Figure 5.3 E). Since they now embark upon a course of growth and differentiation, they are considered to be spermatocytes.

When the rachis contracts into a central core, the spermatocytes become arranged around it in a rosette (Figure 5.3F). Consequently they become longer and thinner and now measure 2.5 x I0μm. In a region 400μm from the cap cell, their cytoplasm becomes granular (Figure 5.3F). This granularity persists and soon discrete densly-stained inclusions can be resolved (Figure 5.3G). Later, it becomes evident that these are precursors of the membranous organelles of the mature spermatozoa.

The spermatocytes now enter a period of growth which extends for 600μm along the testis. During this time they become wedge-shaped, with a maximum width of 4μm at the perimeter of the testis and a length of I4μm. Their cytoplasmic connections to the rachis thicken (Figure 5.3G), but few other changes can be detected with the light microscope.

The rachis reaches its maximum size of I2-I5μm at 900-I000μm from the cap cell. For the next I00μm it narrows (Figure 5.3H) then it forks and branches until the spermatocytes are joined only by fine threads of cytoplasm (Figure 5.3I). As their chromosomes condense in preparation for meiosis, the spermatocytes become round. Secondary spermatocytes (SS, Figure 5.3J) are round or ovoid and

FIGURE 5.3 : As the spermatocytes (SC) approach meiosis in I, the rachis (R) branches. Secondary spermatocytes (SS) shown in J are bigger than spermatids (ST) in K. Excess cytoplasm is discarded from the spermatids after meiosis and fuses to form the large residual bodies (RB) visible in L and M. The spermatozoa (SZ) are elongate in L and have formed tails in M and N. The latter also show how the testis epithelium (E) thickens after engulfing the residual bodies.

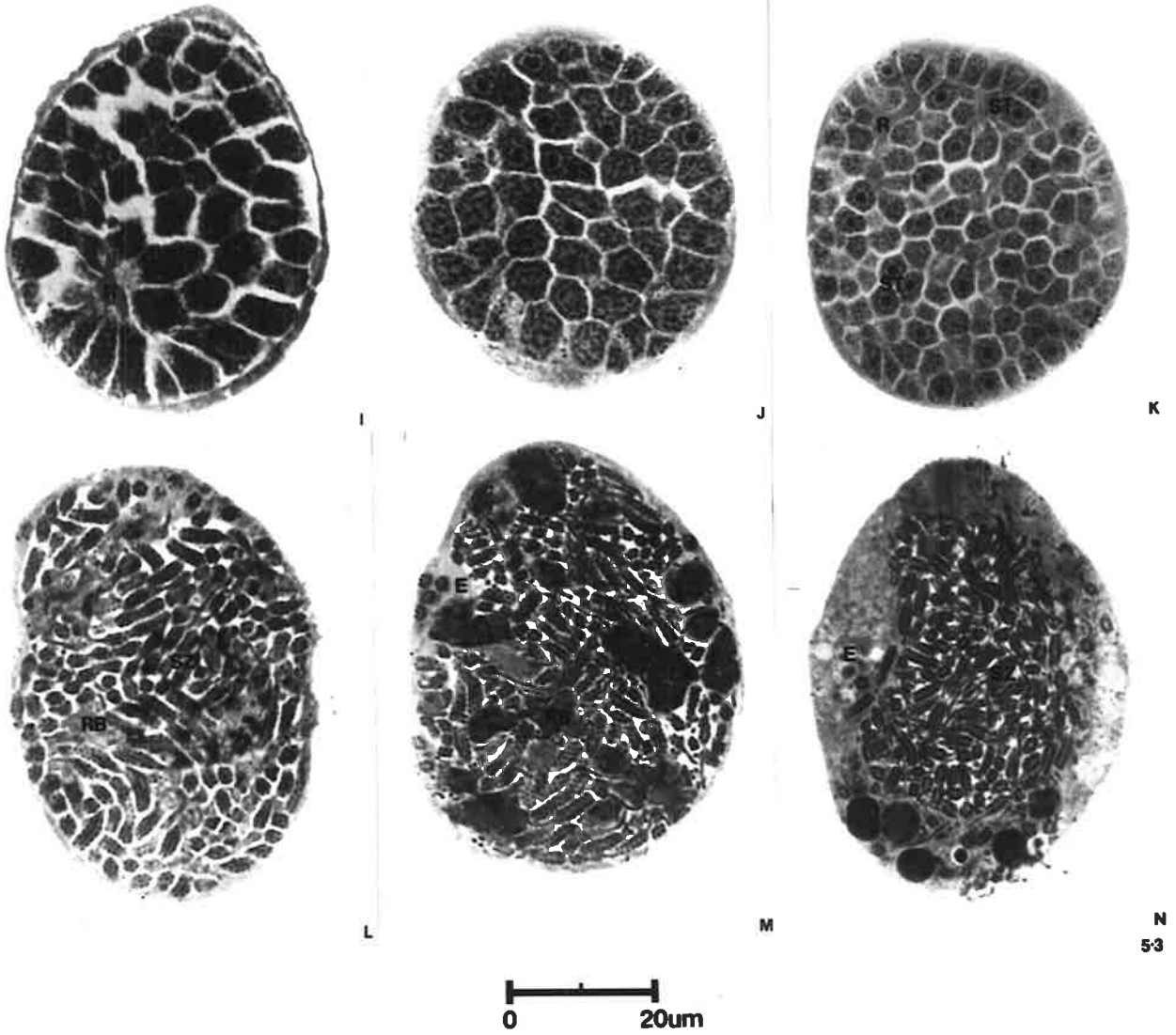

5·3

6.7μm in diameter. Their chromatin is a dense central mass. The second division appears to follow rapidly and at a distance of I350-I400μm along the testis, all divisions have been completed. The membranous organelles are equally distributed amongs the spermatids during division.

Initially, the spermatids (Figure 5.3 K) resemble the secondary spermatocytes, although they are smaller (4μm in diameter). Within a short time, both the chromatin and the spermatids elongate and a bulge of excess cytoplasm, forms at one end (Figure 5.3L). When the spermatids are 6-7μm long, the chromatin continues to elongate, but the rest of the cell does not. Thus the nuclear material is extruded in a tail-like structure (Figure 5.3M, 5.4). At the same time, the excess cytoplasm is discarded. These residual bodies of cytoplasm fuse together to form large heterogeneous masses up to I5μm across (Figure 5.3M, 5.4), which are later absorbed and broken down by the testis epithelium (Figures 5.3N, 5.4).

Mature spermatozoa occur in the posterior testis and seminal vesicle (Figure 5.4). They have a cytoplasmic part designated the anterior (see Chapter I.2)and a nuclear tail of IIμm (Figure 5.5). The cytoplasmic region is cylindrical and measures 2 x 7μm. The membranous organelles are arranged in rows along the length of the sperm and favourable sections show that there are 6 such rows with 6 or 7 organelles in each. No other details can be resolved with the light microscope.

FIGURE 5.4 : Longitudinal section through the testis and seminal vesicle showing their junction at the vas efferens. At the anterior are spermatids (St) which later develop into spermatozoa (Sz). Where the epithelium (E) absorbs the refringent bodies (RB) it is noticeably thicker. The positions of the transverse sections in Figure 5.3L,M and N are shown by the dotted lines.

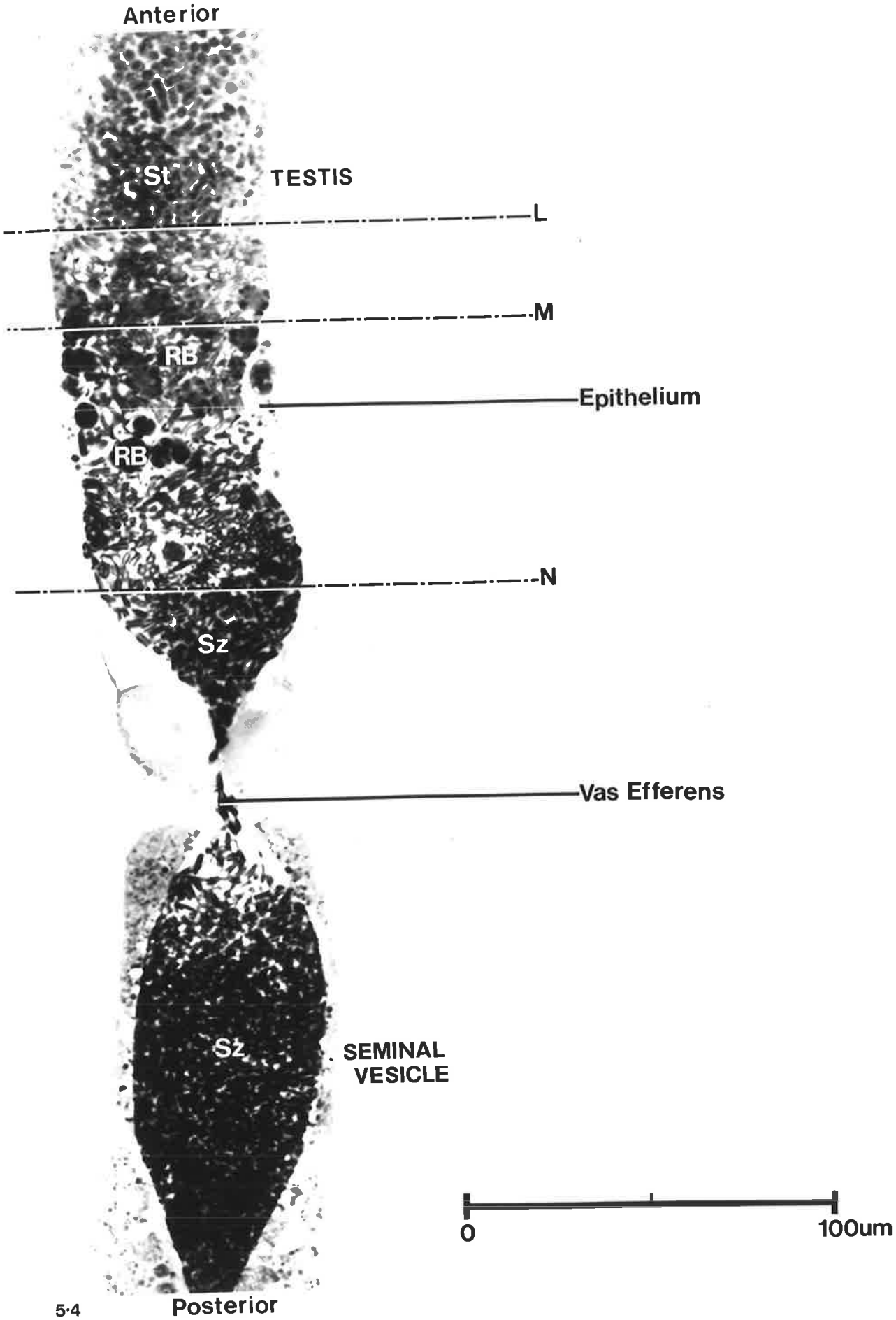
Anterior
St
TESTIS
L
M
RB
Epithelium
RB
N
Sz
Vas Efferens
Sz
SEMINAL
VESICLE
0
100um
Posterior

5·4

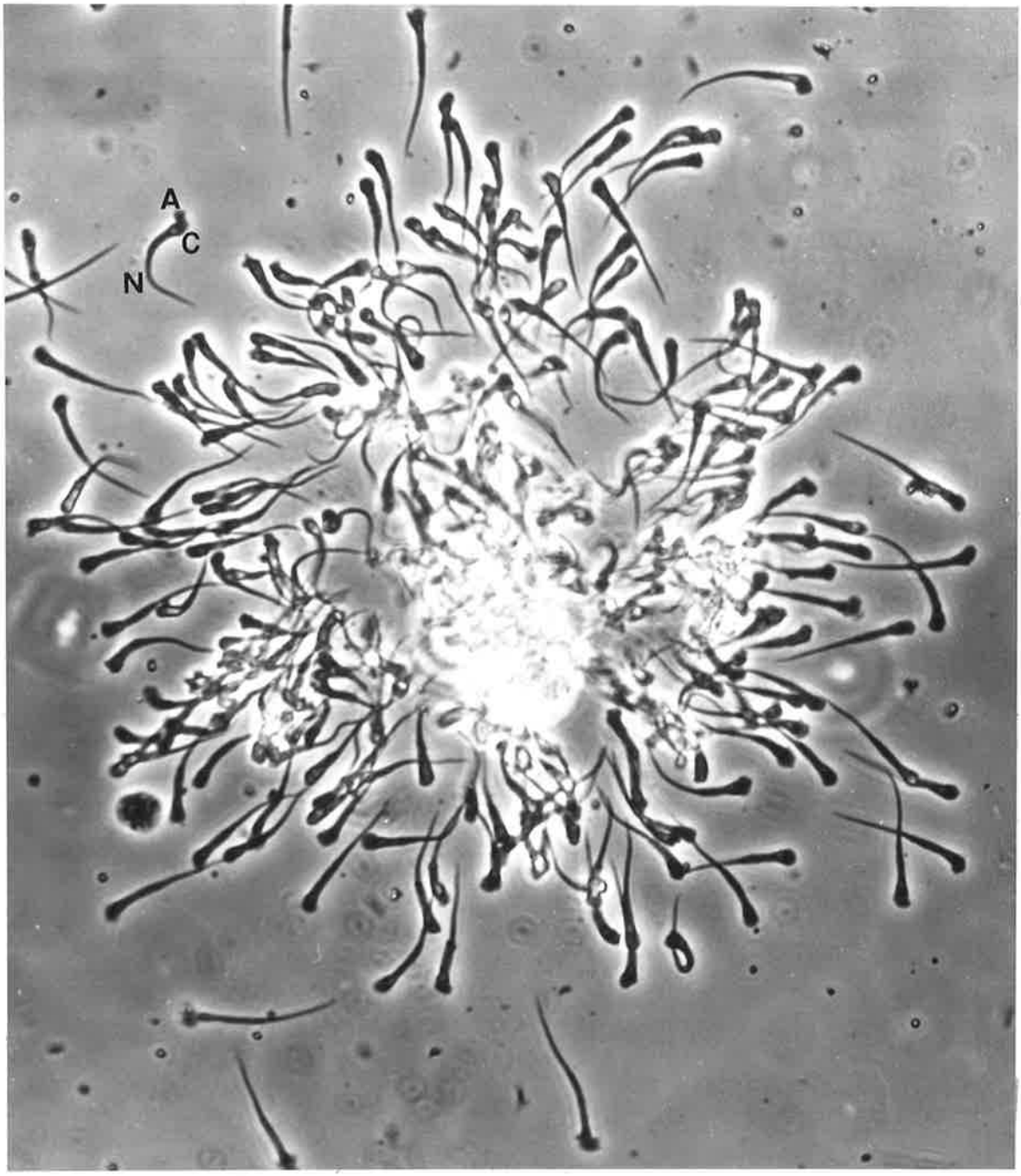

FIGURE 5.5 : Mature sperm dissected from the seminal vesicle of a male. They have a cytoplasmic region, designated the anterior and a nuclear tail; some are producing pseudopodia at the anterior.

SYMBOLS

used to mark electron micrographs in Chapters 5 and 6

A	amoeboid anterior	N	nucleus
Af	filamentous amoeboid region	NE	nuclear envelope
Ag	granular amoeboid region	NP	nuclear pore
C	centriole	Nu	nucleolus
Ch	chromosome	P	pore
Cr	chromatin	PF	protoplasmic face
DB	dense body	Pr	protrusion of nucleus
DI	dense inclusion	R	rachis
DS	dense sphere	RB	refringent body
E	epithelium	RER	rough endoplasmic reticulum
EF	exoplasmic face	S	stack of RER
F	fibril	SC	spermatocyte
FB	fibrous body	SG	spermatogonium
Fi	filaments	Sp	spindle fibres
G	Golgi body	ST	spermatid
GB	granular body	Sy	synaptonemal complex
I	inclusion	SZ	spermatozoon
In	invagination	T	tubular elements
K	knob	TA	tubular aggregations
M	mitochondrion	V	vesicle
MO	membranous organelle		

5.2 Ultrastructure of the testis - spermatogenesis.

Spermatogonia.

The spermatogonia (Figure 5.6) have large granular nuclei, containing I or 2 prominent nucleoli. The outer leaflet of their nuclear envelope is studded with ribosomes and it is frequently traversed by pores. The cytoplasm contains mitochondria, cisternae of rough endoplasmic reticulum (RER), numerous microtubules and abundant ribosomes. The mitochondria are round or ovoid, measure 0.3 - 0.6μm, and have an electron-lucent matrix. The cristae are few and generally plate-like. It is interesting that mitochondria in the testis epithelium are quite different from those of the spermatogonia. They are larger and have more numerous cristae and a denser matrix (see Figure 5.I2). Microtubules, measuring 2I-22nm in diameter occur throughout the cytoplasm of the spermatogonia, but are more abdundant near the nucleus and beneath the plasma membrane (Figure 5.6). This latter arrangement is particularly well illustrated by tangential sections (see Figure 5.I2).

The cytoplasm of the spermatogonia also contains dense bodies (DB), granular bodies (GB), and large aggregations of anastomosing tubules (TA; Figures 5.6, 5.7, 5.8, 5.9). It is clear from the examination of many sections that these structures are associated with one another. The tubular aggregations are interpreted to be cisternae of RER because the membranes are studded with particles the same size and density as the ribosomes seen in the cytoplasm (Figure 5.7) Between these cisternae is a granular matrix. This material is elaborated into a granular body (GB; Figure 5.6) at the edge of the tubular aggregations. One or

FIGURE 5.6 : Spermatogonia at the anterior end of the testis have large, clear nuclei and prominent nucleoli. They contain many free ribosomes, mitochondria, dense bodies, granular bodies, tubular aggregations and dense vesicles. At the bottom of the figure is a small part of the rachis (R) which is thread-like at this time. Arrows indicate microtubules beneath the plasmalemma.

FIGURE 5.7 : A large tubular aggregation and adjacent dense body in the cytoplasm of a spermatogonium.

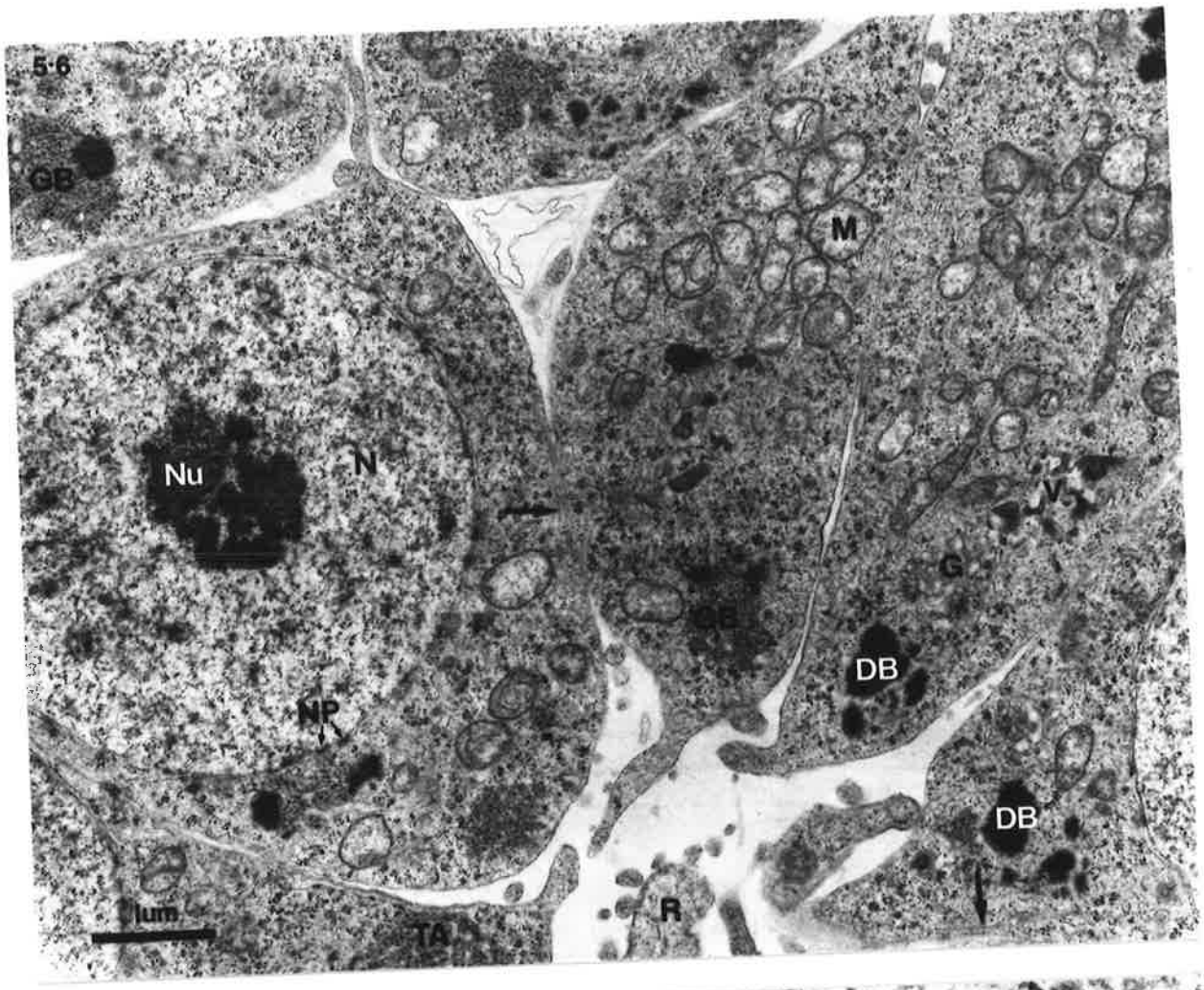
5·6
GB
M
Nu
N
V
G
DB
NP
DB
1um
TA
R

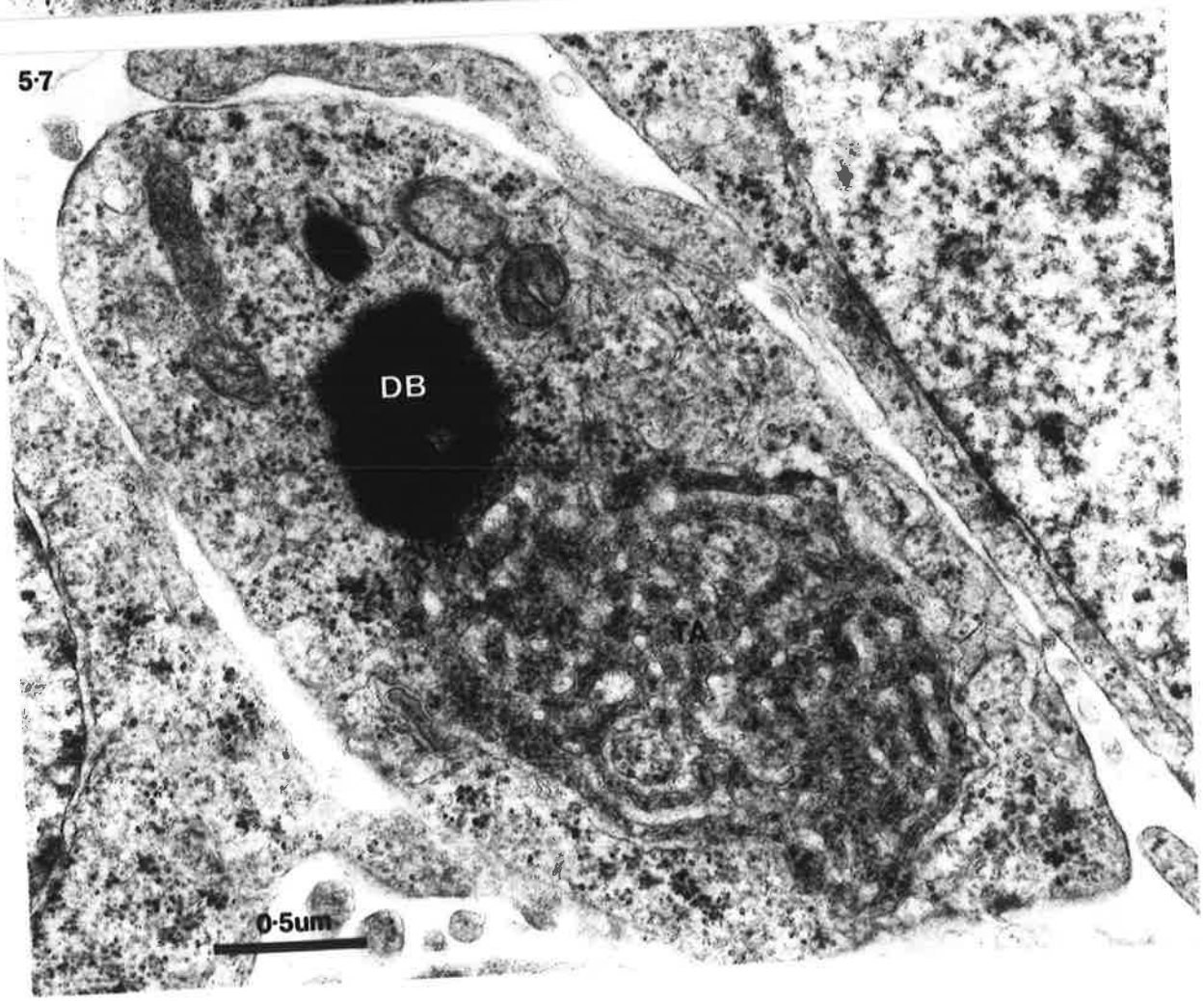
5·7
DB
TA
0·5um

two dense bodies, 0.5-Iμm across, are associated with either this granular body (DB, GB; Figure 5.6), or the tubular aggregations (DB, TA; Figure 5.7). Favourable sections show that one side of the granular body is bounded by a long tubule of RER which extends into the adjacent cytoplasm (GB, RER, Figure 5.8). It curves around into a crescent and encloses a Golgi body (G; Figure 5.9). Secretion vesicles from this RER contribute to the forming face of the Golgi stack. On the side opposite the granular body are clusters of larger membrane-bound vesicles (V, Figure 5.6). These are very distinctive as they are triangular in shape and bear electron-dense contents. It seems likely that they are secretion products of the Golgi body. Figure 5.I0 summarizes the relationships between these structures.

Longitudinal sections taken at about I50μm from the anterior end of the testis illustrate both the enlargement and differentiation of the rachis at this stage (Figures 5.8, 5.9). Whereas previously, it was simply a continuation of the cytoplasm of the spermatogonia (R, Figure 5.6), now it has a distinctive appearance. It contains fewer mitochondria and ribosomes, but more RER than the spermatogonia. Golgi bodies may be associated with the RER (RER, G; Figure 5.8). An electron-dense flocculent material, often in the form of fibrils, gives the cytoplasm a distinctive appearance (arrows, Figure 5.8). This material also accumulates beneath the plasma membrane, especially where the rachis joins to the spermatogonia (arrows, Figure 5.9).

At about this stage, the chromatin of the spermatogonia condenses in preparation for its final mitotic division (Figure 5.II). A pair of centrioles can be seen close to the nuclear

FIGURE 5.8 : In this section, a granular body is associated with a long cisterna of RER which is producing secretion vesicles (*). Within the nearby rachis, RER is associated with a Golgi body. Flocculent material (arrows) is beginning to accumulate in the rachis.

FIGURE 5.9 : Longitudinal section cut at about 150µm from the anterior of the testis, showing spermatogonia attached to the narrow band of rachis. The flocculent material in the rachis may form fibrils and also accumulate beneath the plasmalemma (arrows). The association between granular body, RER and Golgi is clearly illustrated in one spermatogonium.

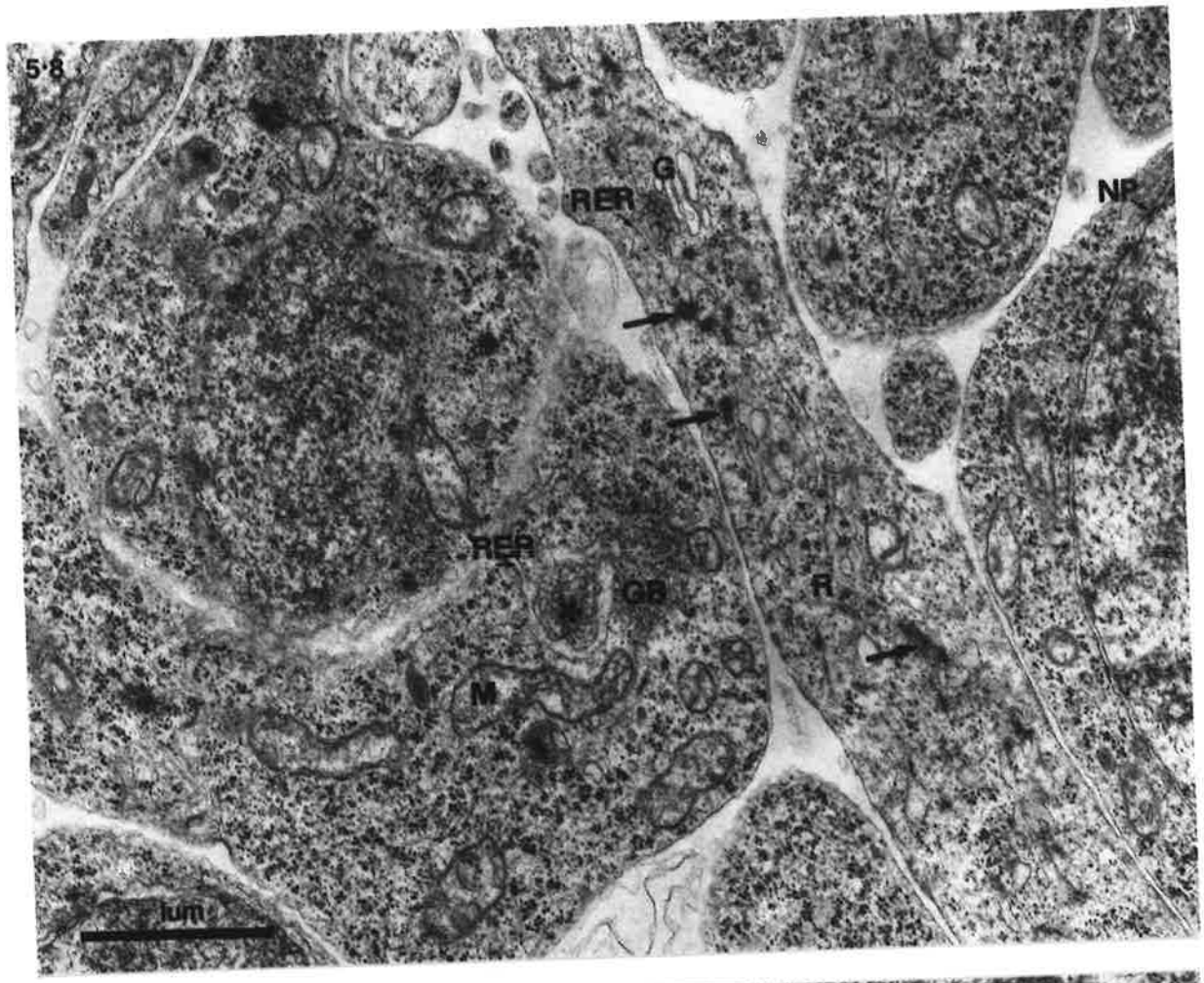
5·8
RER
G
NP
RER
GB
R
M
lum

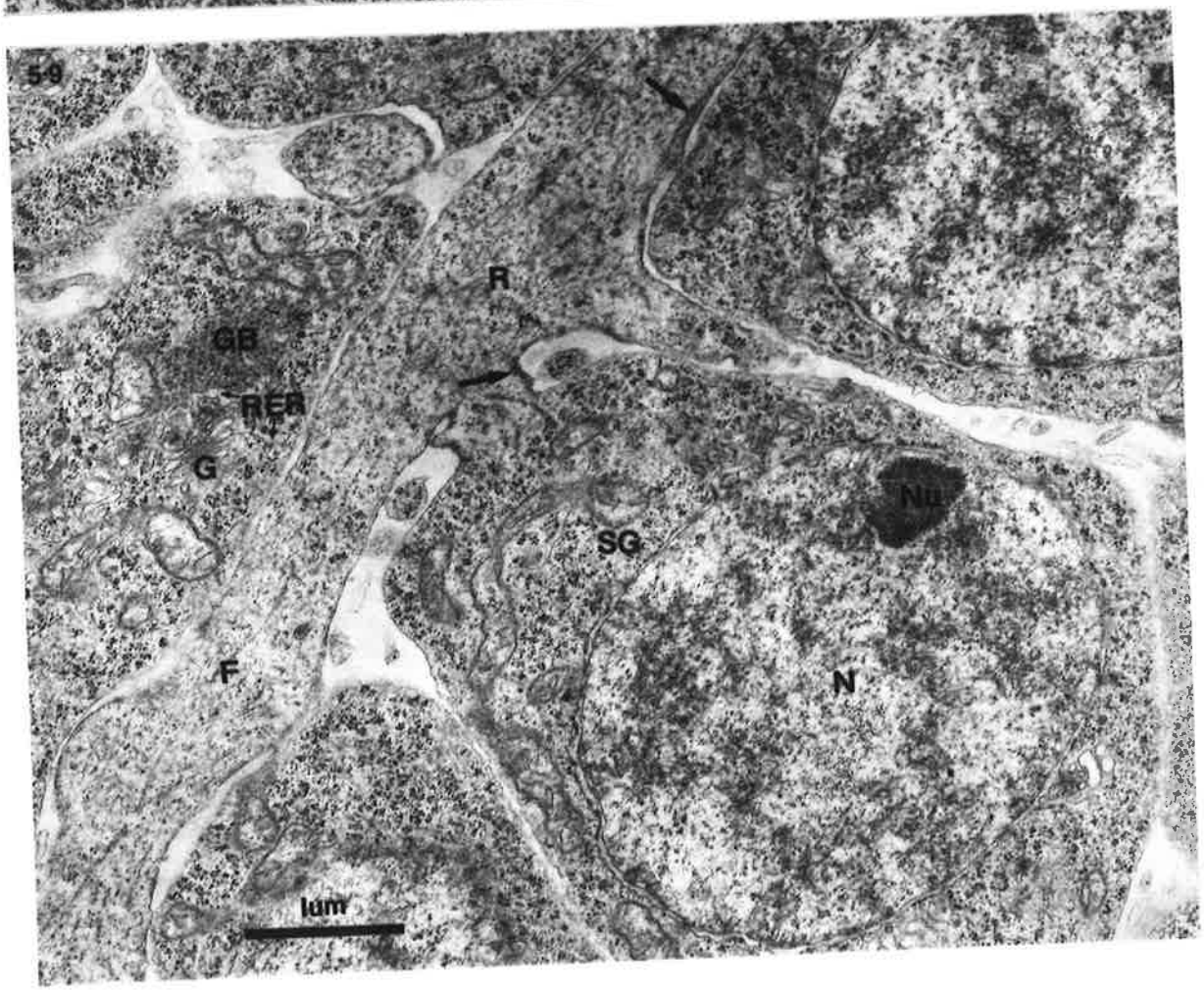
5·9
R
GB
RER
G
Nu
SG
F
N
lum

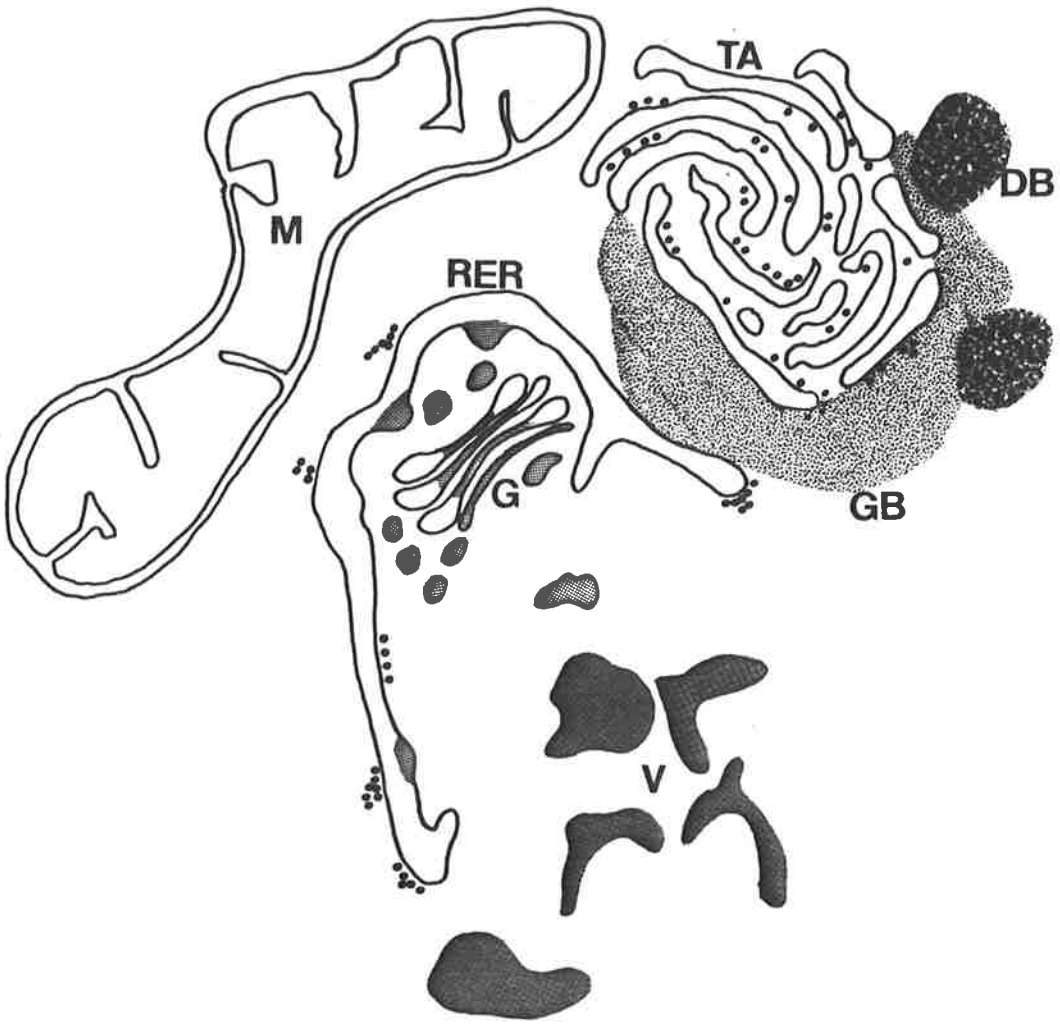

FIGURE 5.10 : Summary of relationship between dense bodies (DB), granular bodies (GB) and tubular aggregations (TA). Adjacent to the granular body is a cisterna of RER which is contributing material to an adjacent Golgi body (G). The three-sided dense vesicles (V) seem to be formed from Golgi secretions. A mitochondrion (M) is closeby.

envelope. They consist of a pale core 550nm across, surrounded by a dense band 130nm wide, adjacent to which is a ring of 9 microtubules (inset, Figure 5.II). The granular bodies, with their associated RER and Golgi complexes, are still visible in the cytoplasm (Figure 5.I2). In some places the outer leaflet of the nuclear envelope blebs out to form wide perinuclear cisternae (arrows, Figures 5.II, 5.I3). These may be extended into tubules of RER, which are sometimes associated with Golgi bodies.

Spermatocytes.

Very early spermatocytes are recognised by their clear, homogeneous nuclei, contrasting with the extreme heterochromatin of the late spermatogonia (compare Sg, Sc, Figure 5.I3). Soon, the chromatin begins to condense around synaptonemal complexes (Sy, Figures 5.I4, 5.I5) signifying the pachytene stage of meiosis. The nucleus becomes irregular in shape, often extending protrusions into the cytoplasm (Pr, Figure 5.I4). Elsewhere long sheets of ER lie alongside the nuclear envelope. They form stacks of 2-3 cisternae which vary in length from 0.8-2μm (S, Figure 5.I4). In regions without such stacks, connections between portions of enlarged perinuclear cisternae and RER are common (arrow heads, Figures 5.I4, 5.I5). Golgi bodies are numerous, but the granular and dense bodies of the spermatogonia have disappeared. Microtubules are still common in the cytoplasm, especially adjacent to the plasma membrane (arrows, Figure 5.I4). By this stage, the rachis has differentiated further (Figures 5.I6, 5.I7). It is now a chord of cytoplasm running through the centre of the testis and measuring 4.5μm in diameter. The spermatocytes are arranged around it in a rosette and connected to it by narrow bridges of cytoplasm.

FIGURE 5.11 : While the chromatin condenses, the nuclear envelope blebs out (arrows) often joining with RER which may be associated with Golgi bodies. Pairs of centrioles lie near the nucleus; their nine tubules are clearly shown in the inset.

(Inset: 67,000 X)

FIGURE 5.12 : Granular bodies, associated with RER and Golgi bodies are still common in the spermatogonia. A tangential cut through the nucleus (top) reveals numerous nuclear pores. Arrows indicate microtubules close to the plasma membrane. Note that mitochondria in the testis epithelium are more dense than those in the spermatogonia.

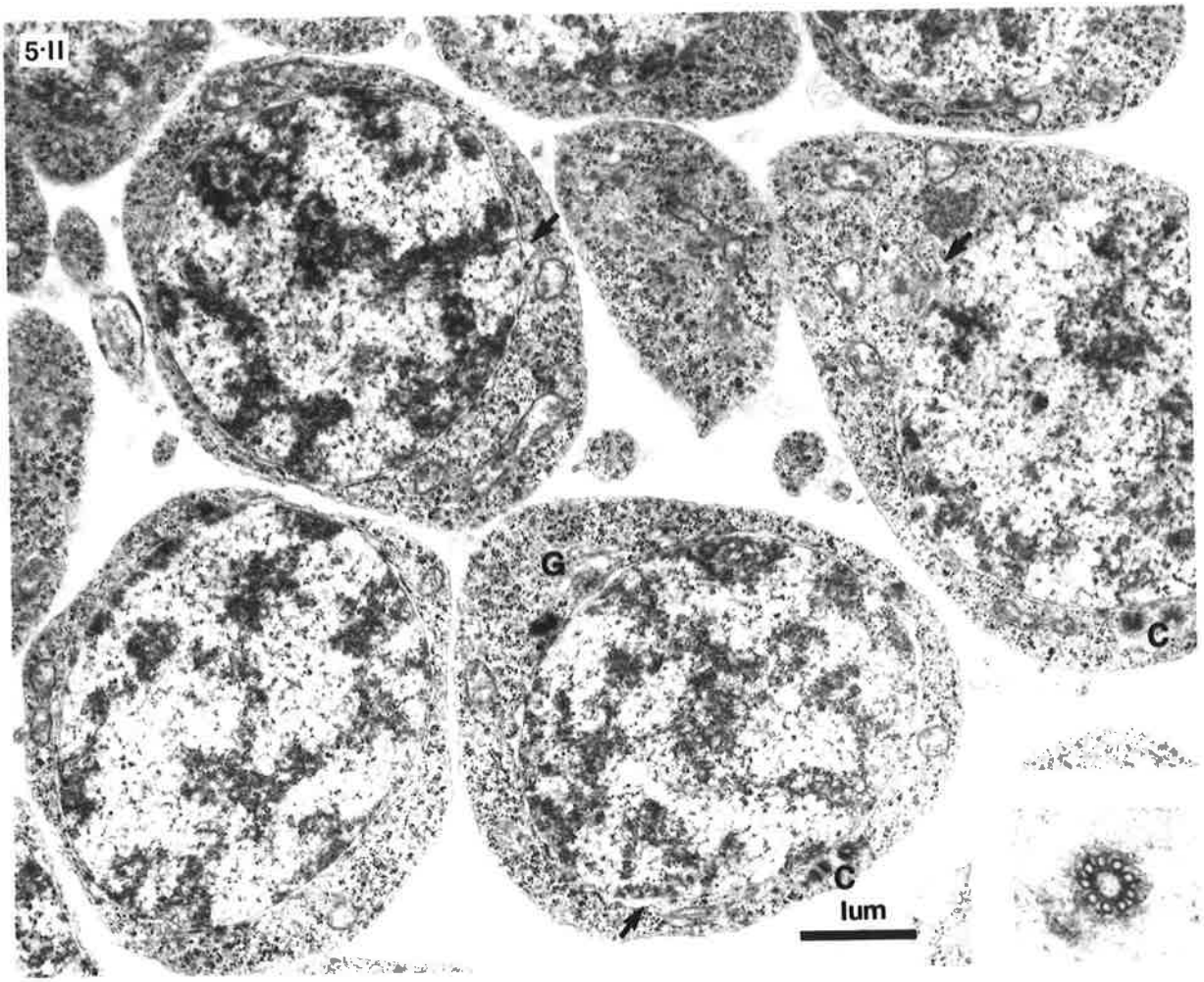
5·11
G
C
C
lum

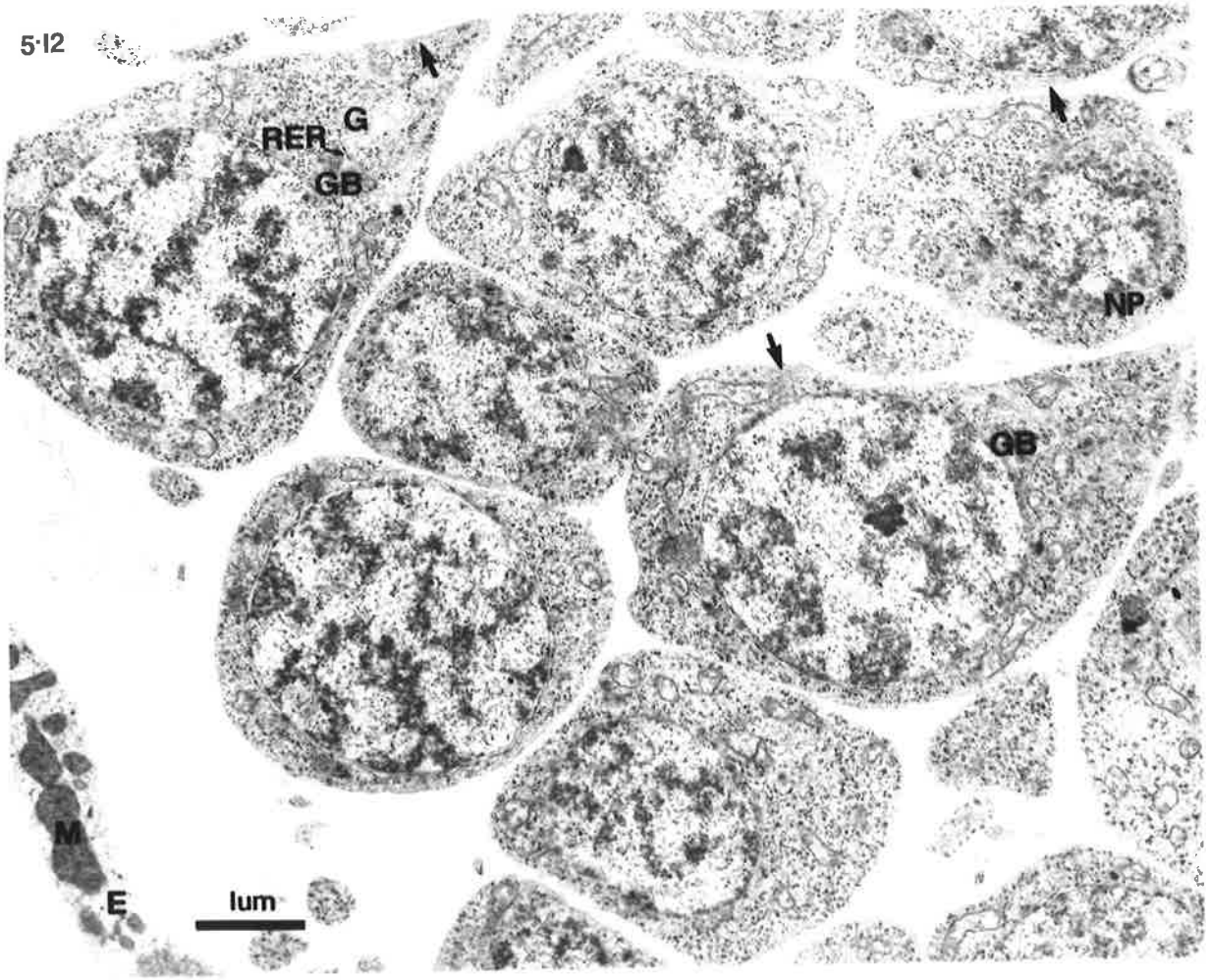
5·12
RER
G
GB
NP
GB
M
E
lum

FIGURE 5.13 : The clear nucleus of a spermatocyte contrasts with the heterochromatin of a spermatogonium. The perinuclear cisternae are enlarged in places (arrows).

FIGURE 5.14 : The nuclei of these spermatocytes contain synaptonemal complexes and extend protrusions out into the cytoplasm. Stacks of RER lie next to the nuclear envelope, which blebs out to join the RER in places (arrow heads). Golgi bodies are more common in the cytoplasm now. Microtubules are shown by arrows.

5·13

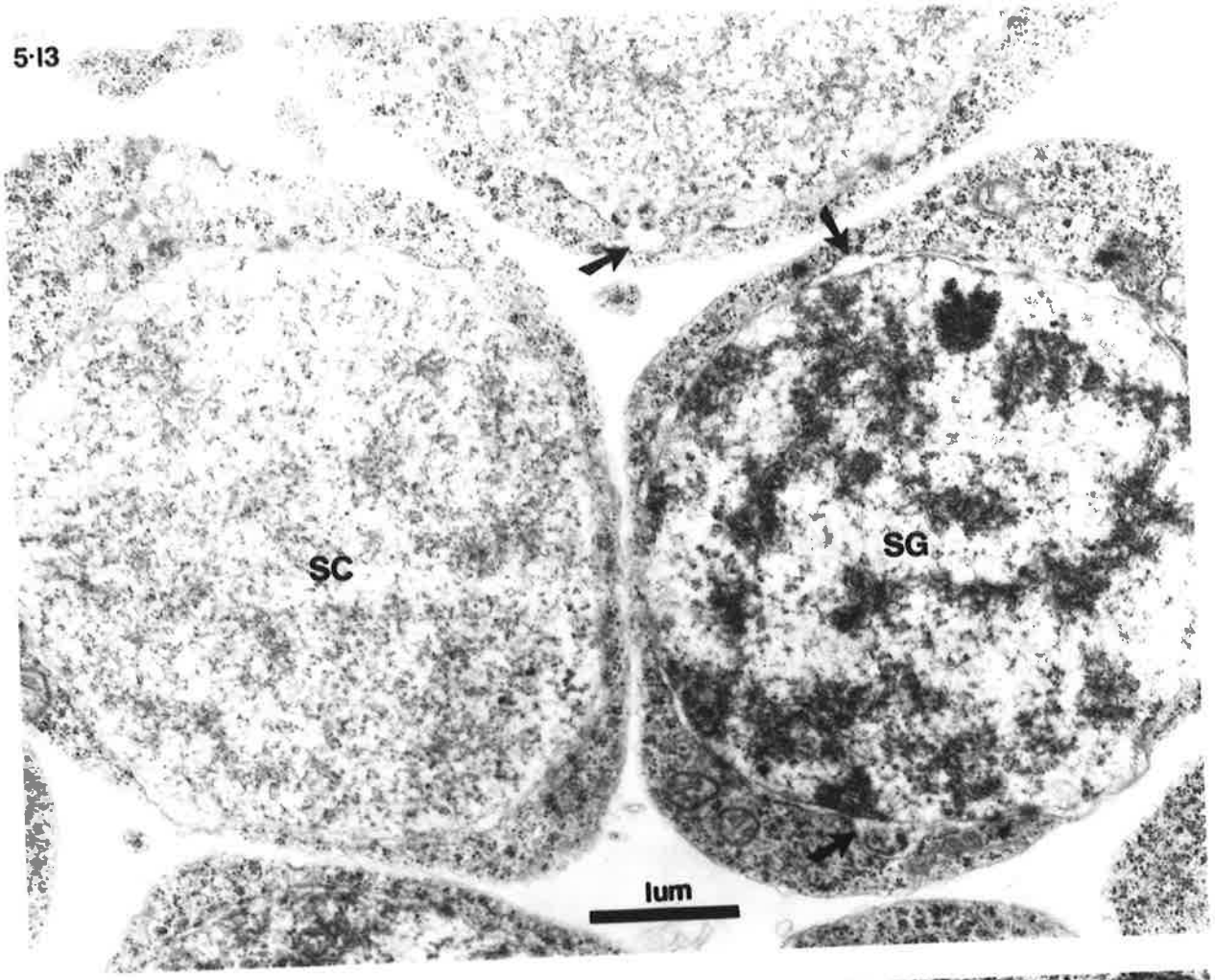

5·14

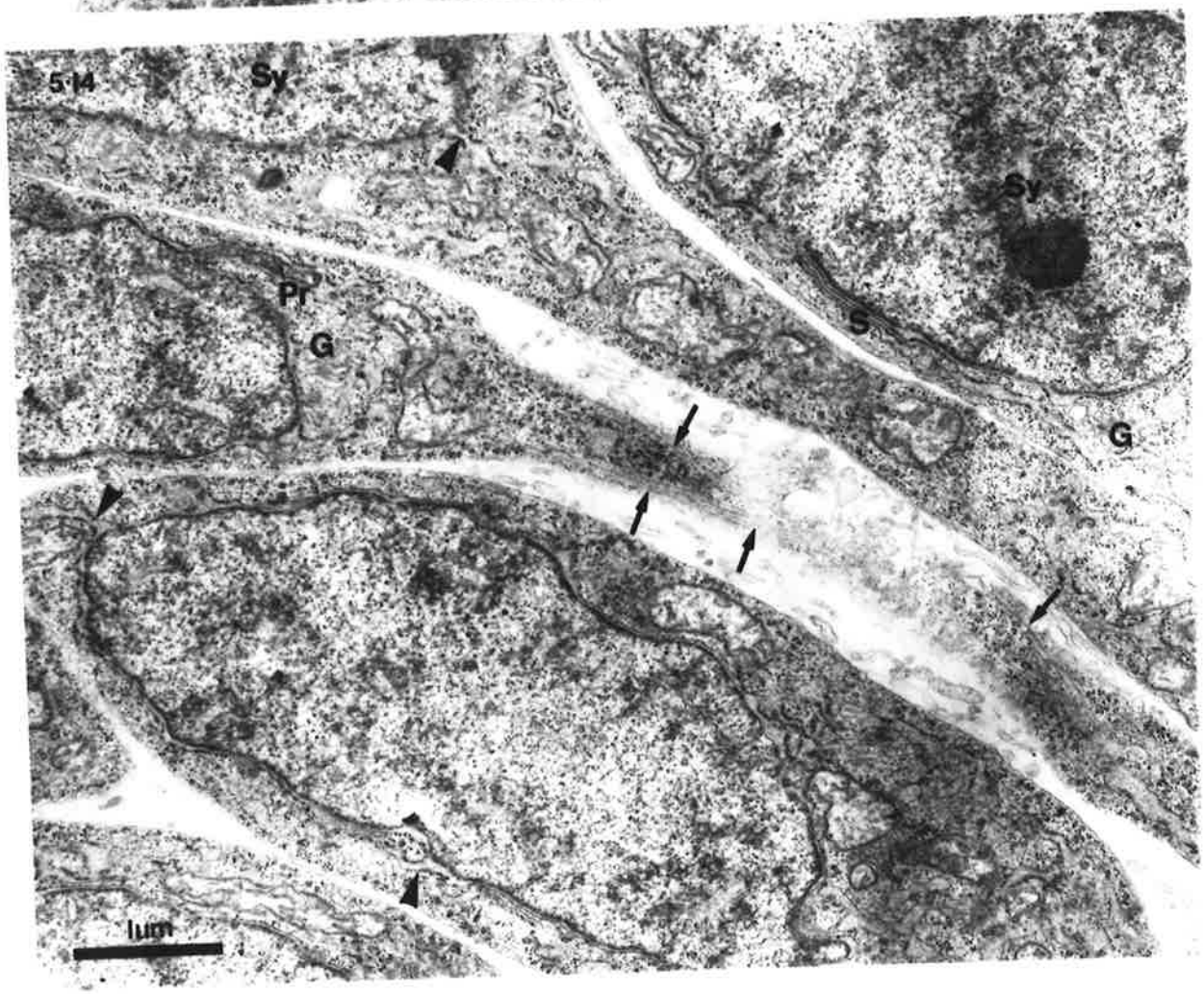

FIGURE 5.15 : In these spermatocytes the perinuclear cisternae are wide and associated with RER (arrows). Synaptonemal complexes are still visible and Golgi bodies are very common.

FIGURE 5.16 : This section shows the edge of the rachis which is now a central core of cytoplasm containing mitochondria, ribosomes, RER, microtubules (arrows) and fibrillar material. Within the spermatocytes, the membranous organelles (MO) are being synthesized from the Golgi in association with RER.

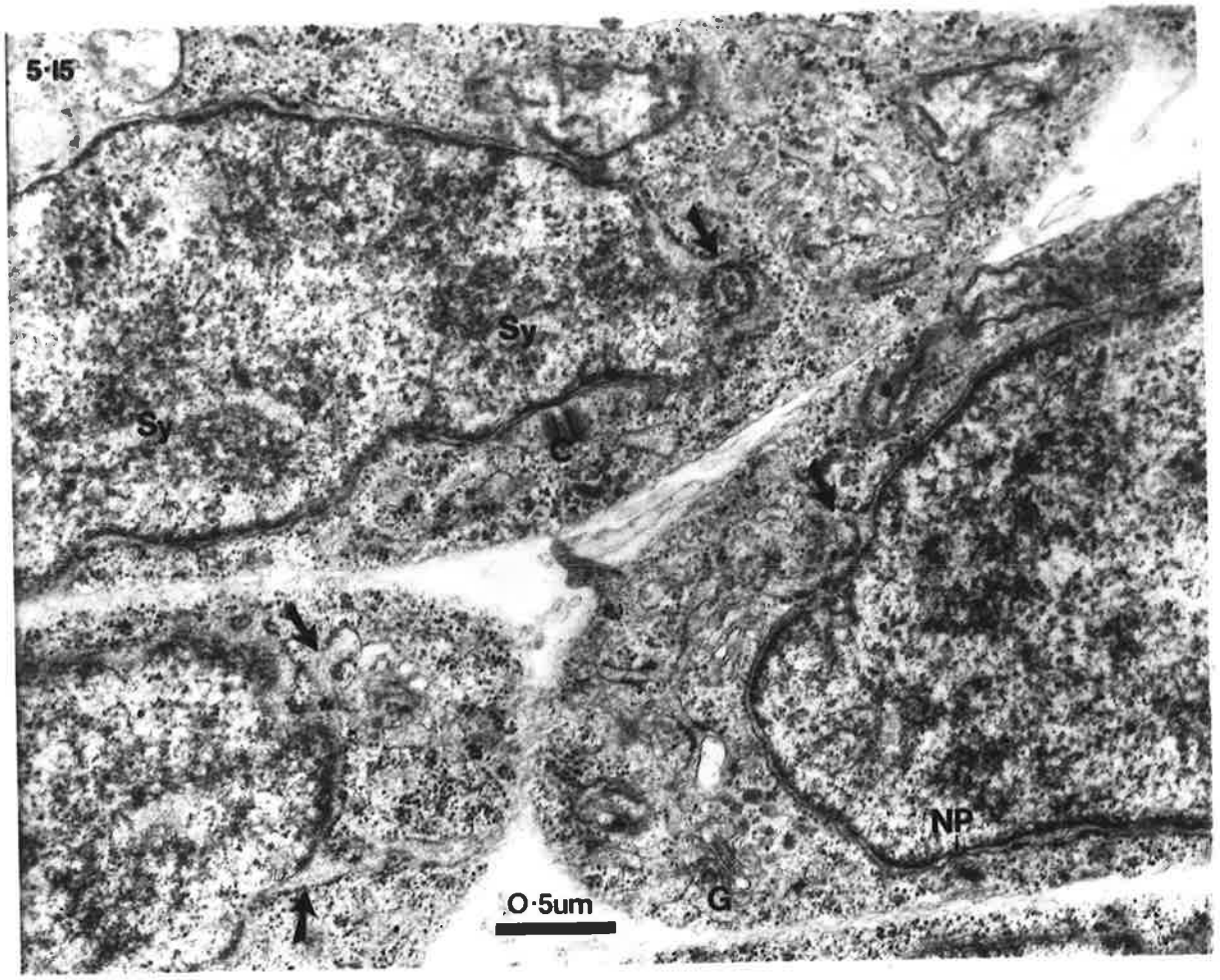
5·15
Sy
Sy
NP
0·5um
G

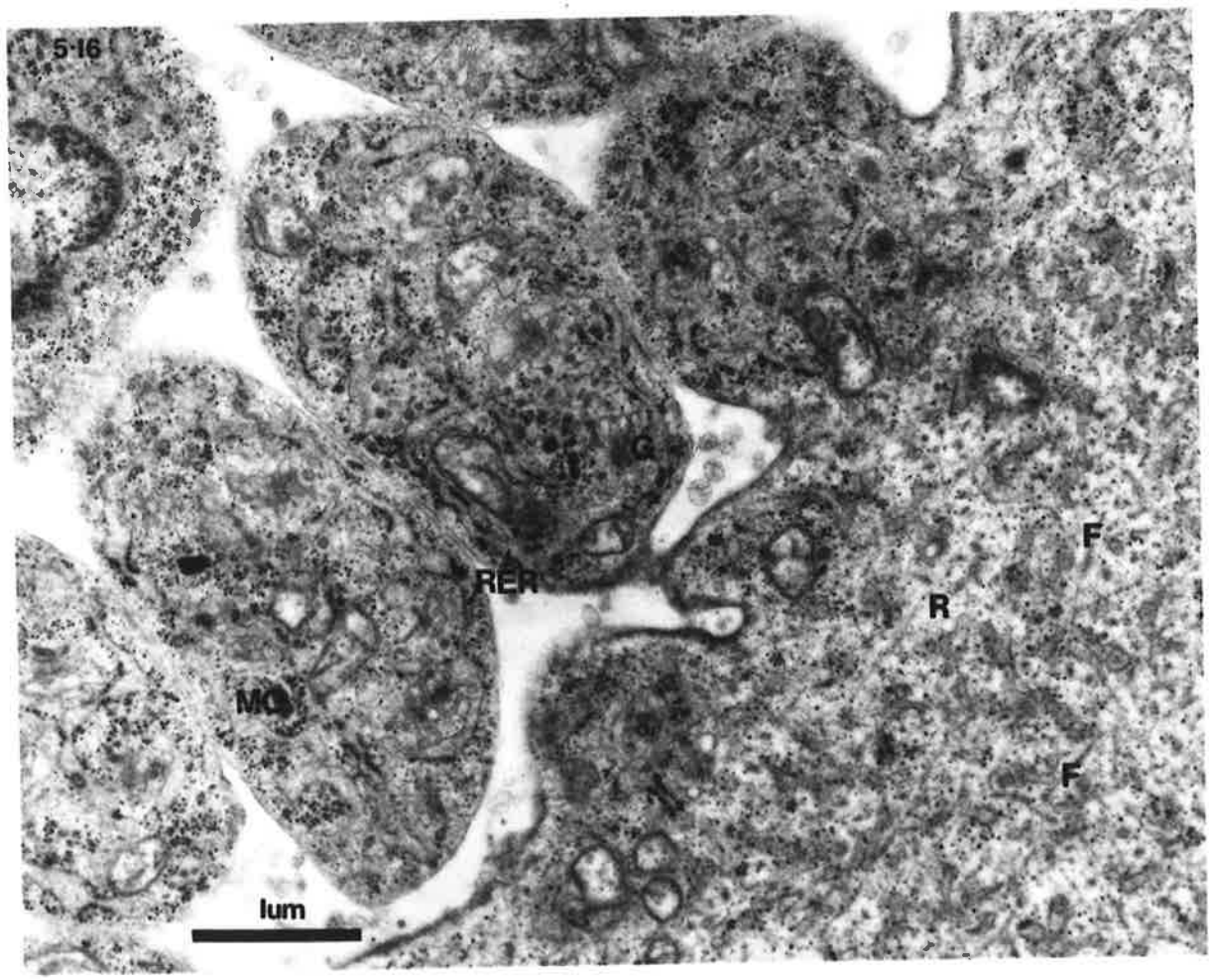
5·16
G
RER
F
R
F
MC
lum

It contains microtubules, RER, ribosomes, some mitochondria and a few Golgi bodies. The groundplasm has retained its fibrillar appearance and the dense deposit beneath its plasma membrane is pronounced.

In the next stage of their development, the spermatocytes synthesize membranous organelles. These organelles differentiate from an enlargement of the terminal saccules of Golgi bodies, into which an electron dense material has been secreted (MO, Figure 5.I6). Initially, they are only 60nm across, but they rapidly enlarge. A classical pattern of secretion is shown in Figures 5.I7 and 5.I8. Material of moderate electron density is transferred from the RER to the proximal saccule of an adjacent Golgi body (G). This saccule is large and electron-lucent, but more distal cisternae have a dense central core and pale bulbous ends. The terminal saccule is uniformly dense. The vesicles which bud off from it fuse with the adjacent membranous organelle. Mitochondria are usually closeby.

Figure 5.I8 shows that the rachis has not changed substantially at this stage. The cisternae of RER, have expanded a little and are now associated with Golgi bodies and membranous organelles. The latter are common, having appeared in the rachis a little later than in the spermatocytes. Microtubules, which occur throughout the rachis and spermatocytes, are alligned along the cytoplasmic bridges between the two (arrows Figure 5.I8).

Figure 5.I9 is the freeze-fracture counterpart of Figure 5.I8 (for explanation of freeze-facture terminology, see Chapter 9.I). It shows the EF-faces of two spermatocytes near their junction with the rachis. The rachis has been cross-fractured and the three-dimensional nature of its extensive RER is particularly well illustrated. Pores (denoted by arrows), 70nm in diameter, can be

FIGURE 5.17 : Within these two spermatocytes, which are joined to the rachis, many MOs are being synthesized. Tubular profiles of RER are common in the rachis; this figure clearly shows the flocculent material which lines its plasmalemma.

FIGURE 5.18 : At the stage shown here, MOs are found in the rachis as well as the spermatocytes. An indentation has formed in one side (arrows) and a bundle of fibres is being deposited there. Microtubules (arrow heads) run along the bridges which join the spermatocytes to the rachis.

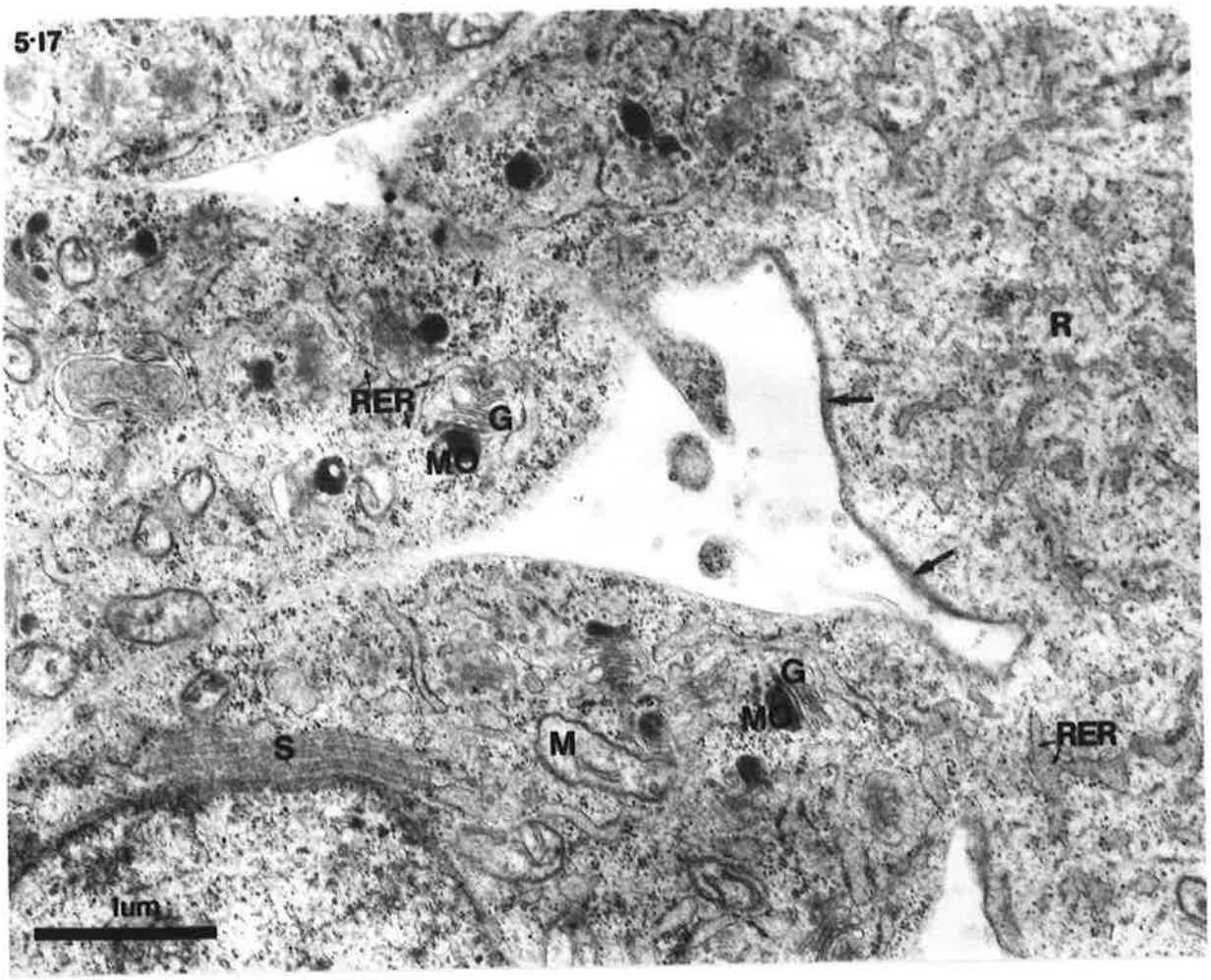
5·17
R
RER
G
MO
G
MO
S
M
RER
1um

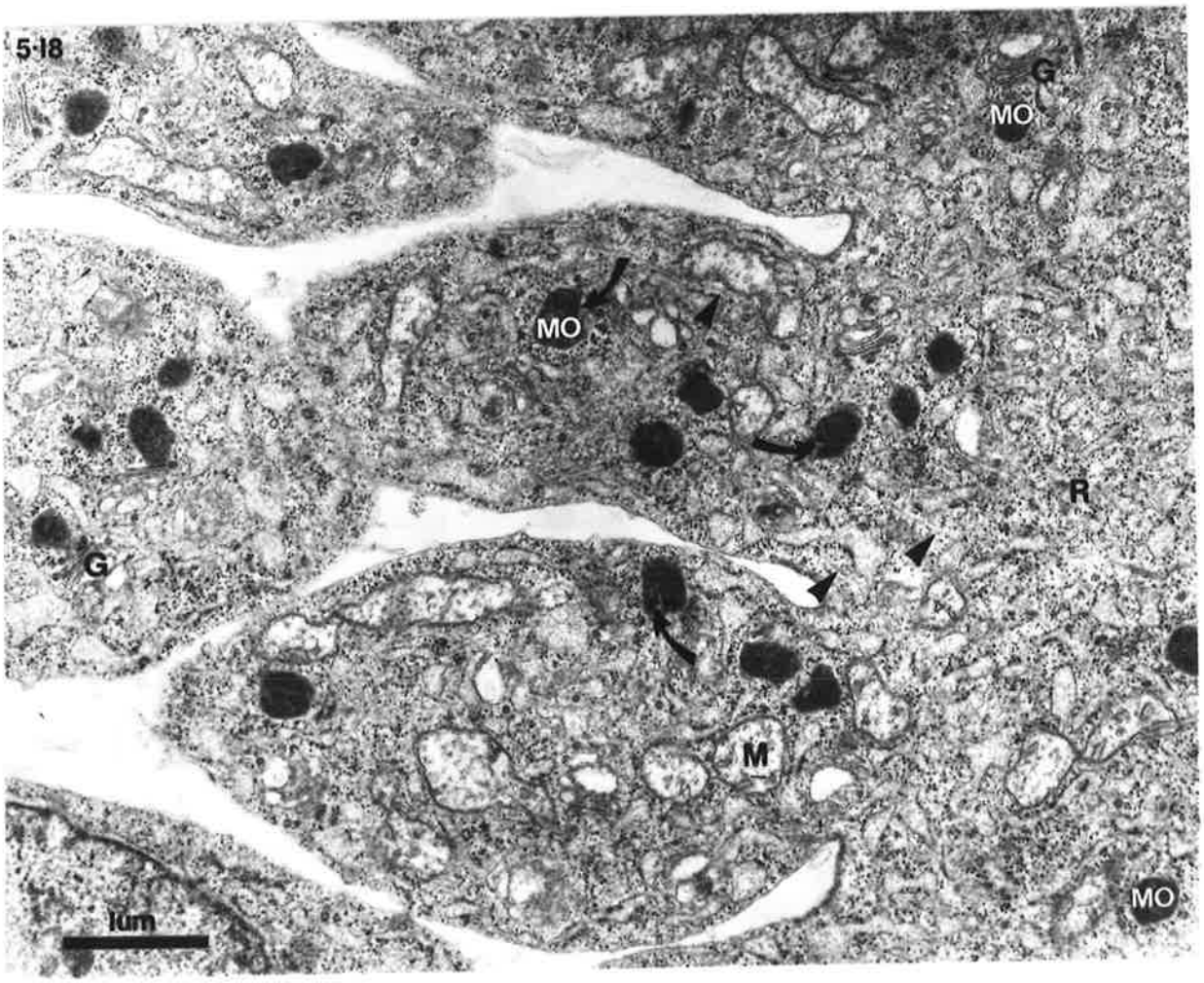
5·18
G
MO
MO
R
G
M
MO
1um

FIGURE 5.19 : This freeze-fracture counterpart of Figure 5.18 confirms the relationship between RER, Golgi and MOs. Pores (arrows) can be seen traversing the cisternae of RER in the rachis. The fracture has passed around the spermatocytes exposing the EF-faces of their membranes.

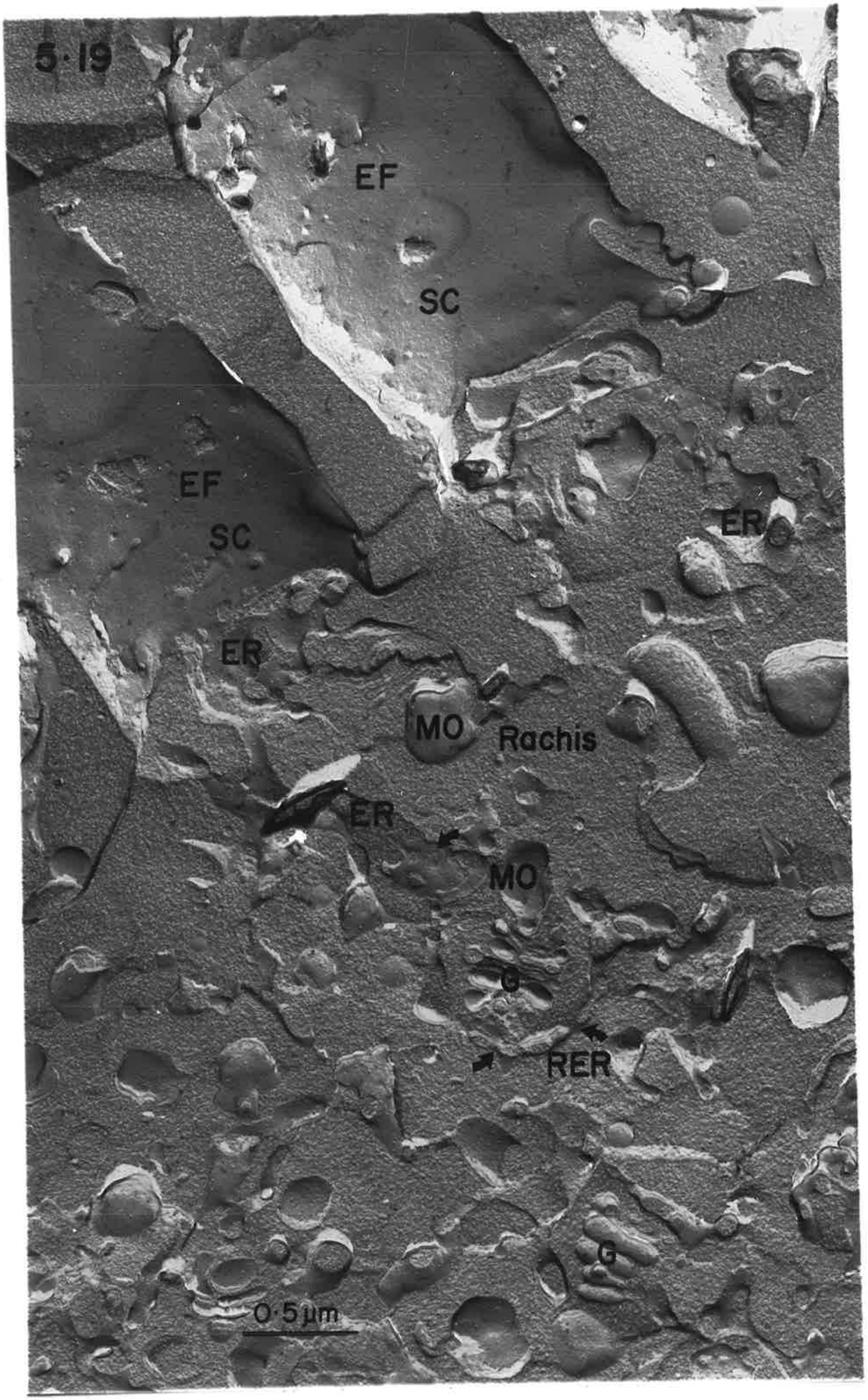
5·19
EF
SC
EF
SC
ER
ER
MO
Rachis
ER
MO
G
RER
G
0·5 µm

seen traversing the tubular and sheet-like cisternae. These become obvious in thin sections only later (see Figure 5.25). The fracture has also revealed both EF- and PF- faces of the membranous organelles. Particles are scattered randomly across both faces, but are more dense on the PF-face. The association between RER, Golgi and membranous organelles, noted previously in thin sections, is confirmed in this freeze-fracture micrograph.

When the membranous organelles measure 400nm in diameter, a number of parallel fibres is deposited in a small depression on one side (arrows, Figure 5.I8). These fibres elongate and increase in number until they occupy almost one third of the organelle, which by now measures 600nm (Figure 5.20A). Each fibre is I0nm across and surrounded by 6 others in a hexagonal arrangement (Figure 5.20B). This fibrous body is not bounded by a membrane on its cytoplasmic side, thus, since the outermost fibres sometimes appear incomplete, the cytoplasm may be contributing directly to their synthesis. Other differentiations of the membranous organelles have occurred. Their contents are no longer uniformly electron-dense, but are patchy. Moreover, within each one is a small region measuring 50 x 250-300μm, which is less dense than the remaining contents (I, Figure 5.20A). This inclusion first appeared when the fibrous body was formed. Figure 5.2IA is a cross-fracture of a spermatocyte. It matches Figure 5.20A in both its position adjacent to the testis epithelium and its developmental stage. The fracture has crossed the cytoplasm of the spermatocyte and passed around the outer leaflet of the nuclear envelope (N), exposing clusters of nuclear pores (NP). Such pores are occasionally visible in thin sectioned material (arrows, Figure 5.20A). The extensive system of tubular RER at the periphery of the spermatocytes is clearly depicted by freeze-fracture. At this stage, the testis epithelium (E) is thin and contains only mitochondria. Particles

FIGURE 5.20A : Spermatocytes close to the testis epithelium at the stage when pale inclusions have formed in the MOs and the fibrous bodies occupy 1/3 of their volume; Golgi bodies are still contributing to their growth.
Nuclear pores traverse the nuclear envelope which is studded with ribosomes.
Note the difference between the mitochondria in the spermatocytes and those of the epithelium.

FIGURE 5.20B : Transverse section through a fibrous body showing the hexagonal arrangement and spacing of the fibres.

5·20A

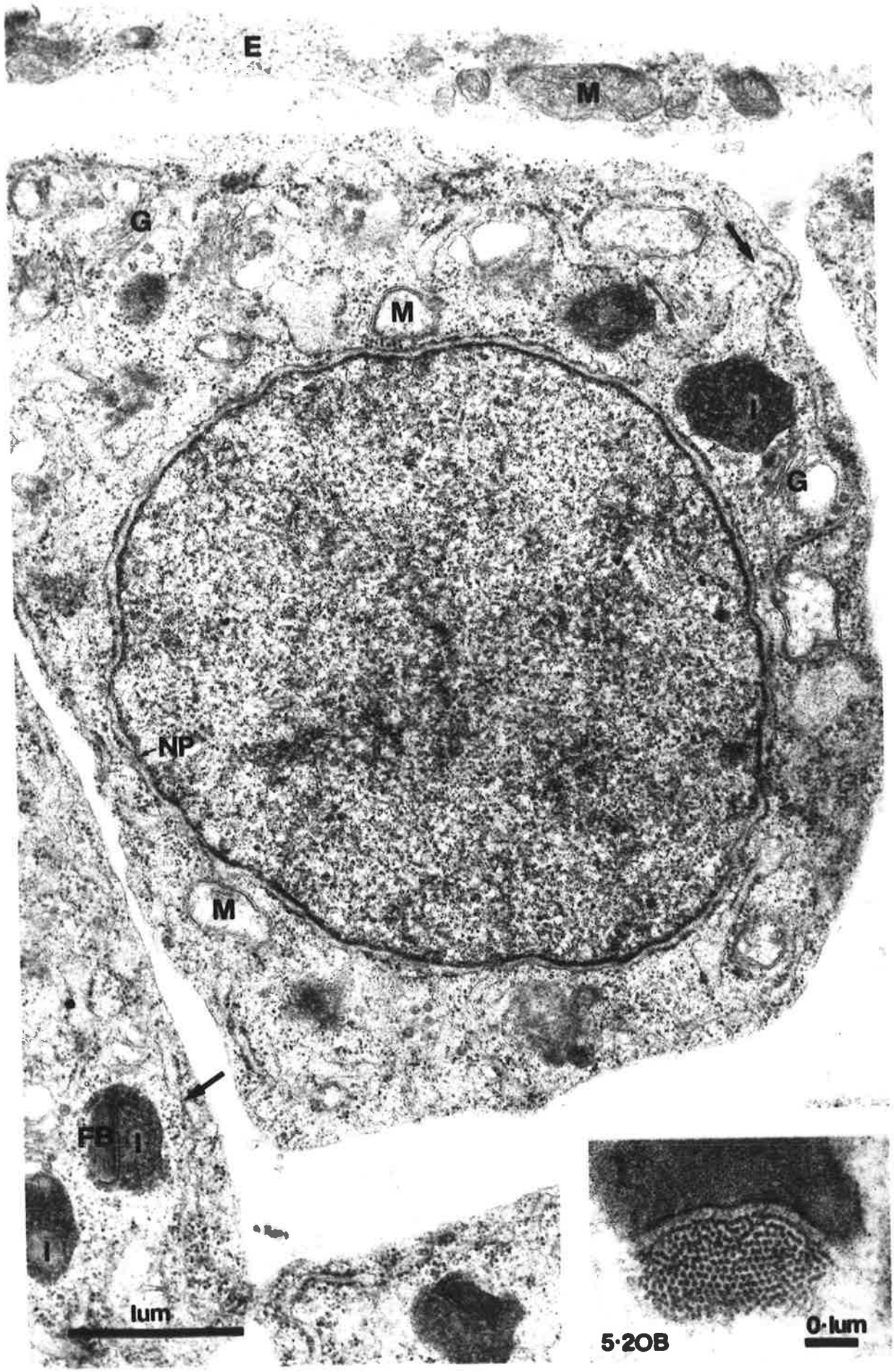

5·20B

FIGURE 5.21A : Freeze-fracture micrograph matching the thin section shown in Figure 5.20A. IMPs occur on both PF- and EF-faces of the membranes of the MOs. RER and Golgi bodies are close to the MOs. In the epithelium are vesicles and mitochondria.

FIGURE 5.21B : The fracture has pulled the fibrous body out of this MO leaving a particle-lined hollow.

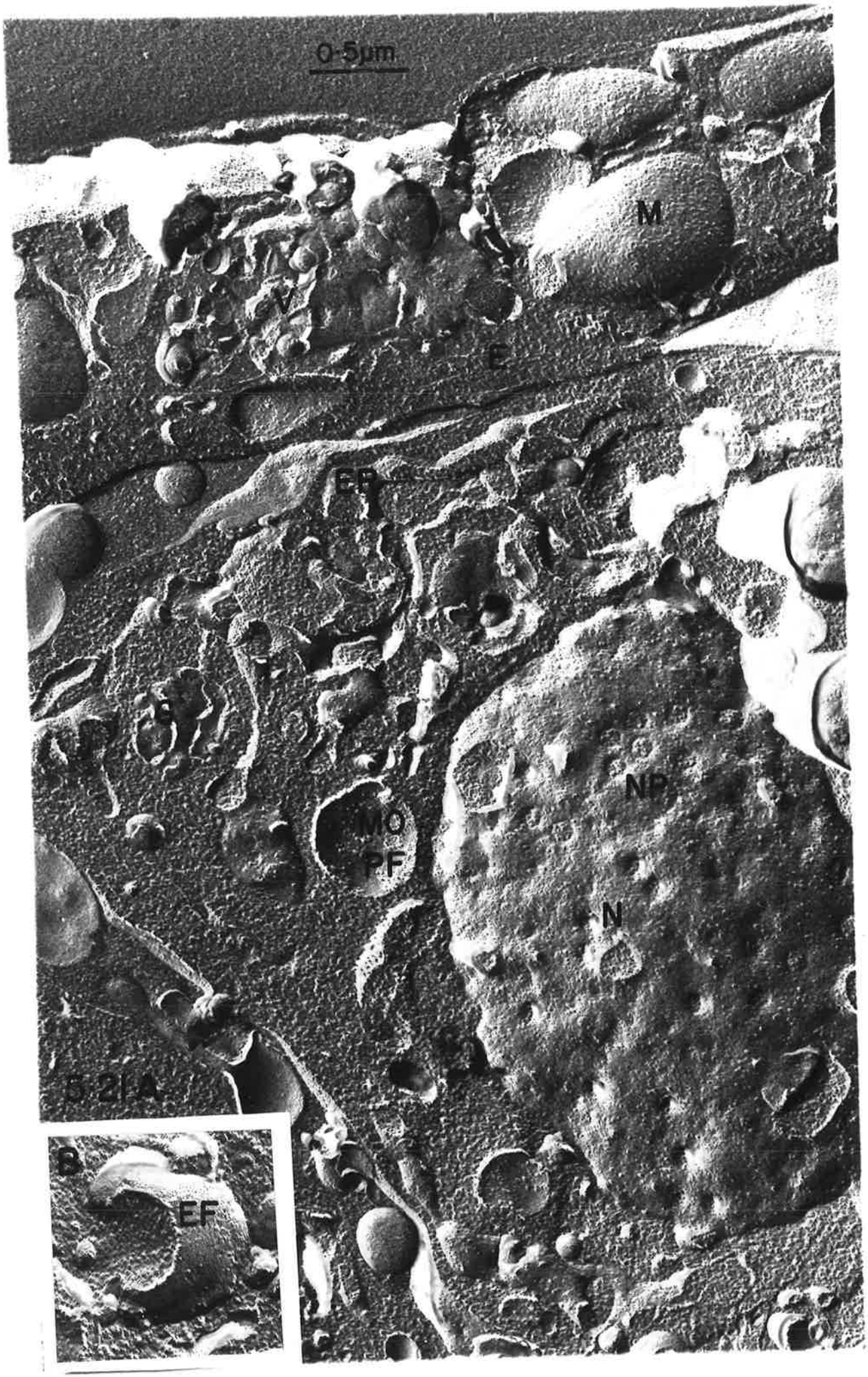

B 21 A

on the EF-face of the membranous organelles are still randomly distributed, whereas those on the PF-face are clustered. A particle-lined hollow remains in one membranous organelle, after fracturing has plucked out its fibrous body (Figure 5.2IB).

The rachis reaches its maximum diameter I,000μm from the anterior end of the testis. Subsequently, it narrows and within I00μm it forks and branches. At the same time, the spermatocytes become rounded, their chromatin condenses, and the nuclear envelope breaks down (Figure 5.22). By now, the membranous organelles have left the rachis and returned to the spermatocytes. They measure 800-850μm across and have lost their pale inclusions, but remain associated with RER and Golgi bodies at the edge of the spermatocytes. Ribosomes are also confined to this outer perimeter, while the central region contains only chromosomes (Ch) and spindle elements (Sp). The mitochondria are more spherical and electron-dense than previously (compare M, Figures 5.20A, 5.22).

Spermatids

Meiosis occurs within a short region of the testis. The nuclear envelope does not reform after division and the DNA becomes a central granular mass, 2 μm across. Two centrioles sit in a small indentation on one side (In, Figure 5.23A). Their position ultimately determines the anterior of the mature spermatozoon. Each centriole is surrounded by a ring of dense material. The two rings meet and fuse in the region between the centrioles (Figure 5.23B). Microtubules occur both inside and outside these rings. The centrioles themselves resemble those of the spermatocytes.

FIGURE 5.22 : In this spermatocyte, the chromosomes are condensing and the nuclear envelope has broken down; spindle fibres are common. At the perimeter are the cytoplasmic organelles including the MOs which have now lost their pale inclusions. The mitochondria are denser and more rounded than previously.

FIGURE 5.23A : After meiosis, the centrioles remain in a hollow on one side of the chromatin; the latter is not bounded by a nuclear envelope.

FIGURE 5.23B : The two centrioles are surrounded by rings of dense material and microtubules; they are parallel, not perpendicular to each other.

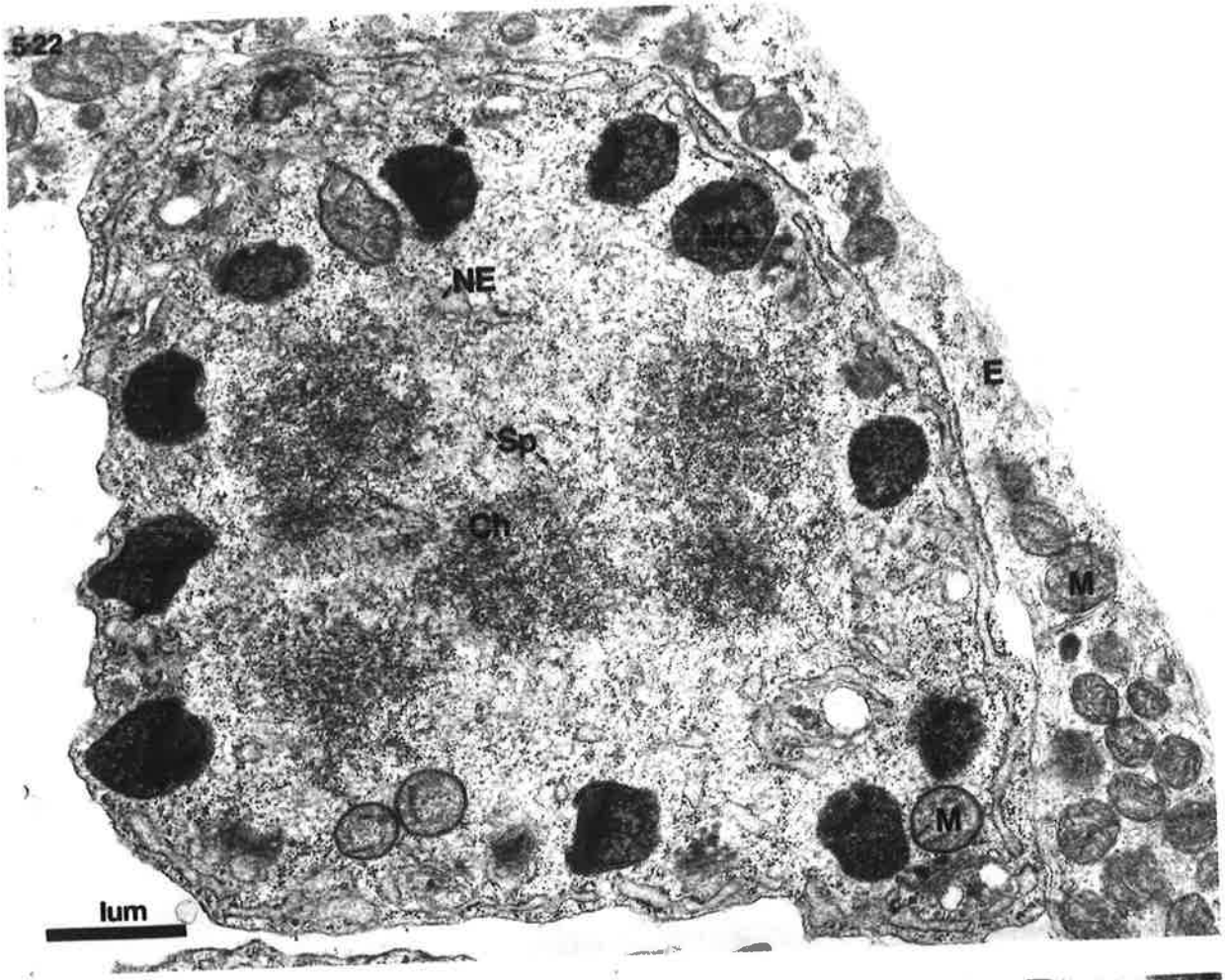
5-22
NE
E
Sp
Ch
M
M
lum

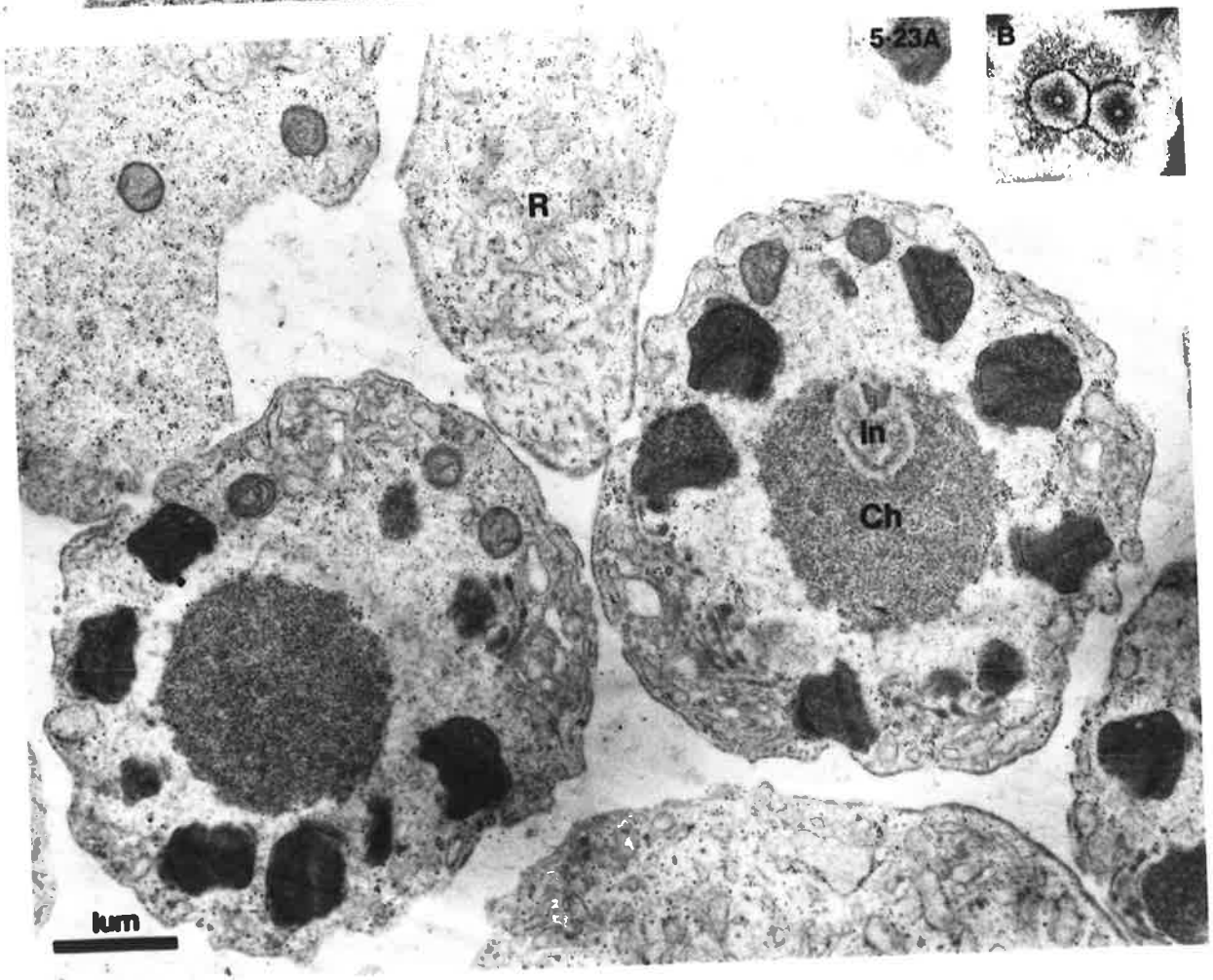
5-23A
B
R
In
Ch
lum

After meiosis, the spermatocytes do not separate entirely. They remain in groups of four, often attached to remnants of the rachis (Figure 5.24). In these areas of the rachis, cisternae of RER are often swollen into pools up to Iμm across. Many contain interesting paracrystalline inclusions, consisting of dense particles in a hexagonal array (PI). Pores, previously seen traversing the RER in freeze-fracture micrographs (Figure 5.19) are also common (P, Figure 5.24).

Shortly after division, the nuclear material condenses into fine filaments which wind into a spiral (Figure 5.25). At the same time, the sphere of chromatin narrows and lengthens, while the hollow which accomodates the centrioles enlarges. As the chromatin continues to elongate it comes to resemble a cone, with the pair of centrioles in a conical indentation at its base. A ring of microtubules ensheathes the outer perimeter of the chromatin (arrows, Figure 5.24) and another set runs from the centrioles up into the indentation (arrows, Figures 5.25, 5.26). The spermatids elongate with the chromatin and the membranous organelles become arranged in rows along their length (Figures 5.25, 5.26). On the outer side of these organelles, the membrane has invaginated into a series of tiny pockets (arrows). The RER, Golgi bodies and ribosomes aggregate near the tip of the nucleus (Figures 5.24, 5.25) and are cast out of the spermatid. Many of these cytoplasmic masses, or residual bodies as they are called, fuse together to form large pools of cytoplasm up to I5μm across (Figure 5.26). These areas are broken down and eventually absorbed by the testis epithelium. Initially, they contain RER and Golgi bodies. These produce large numbers of secretory vesicles which probably contain lysosomal enzymes. It is not

FIGURE 5.24 : After division, the spermatids remain joined by threads of rachis; here, the RER is swollen into large pools containing pores and paracrystalline inclusions. As the chromatin begins to condense, it is surrounded by a ring of microtubules (arrows).

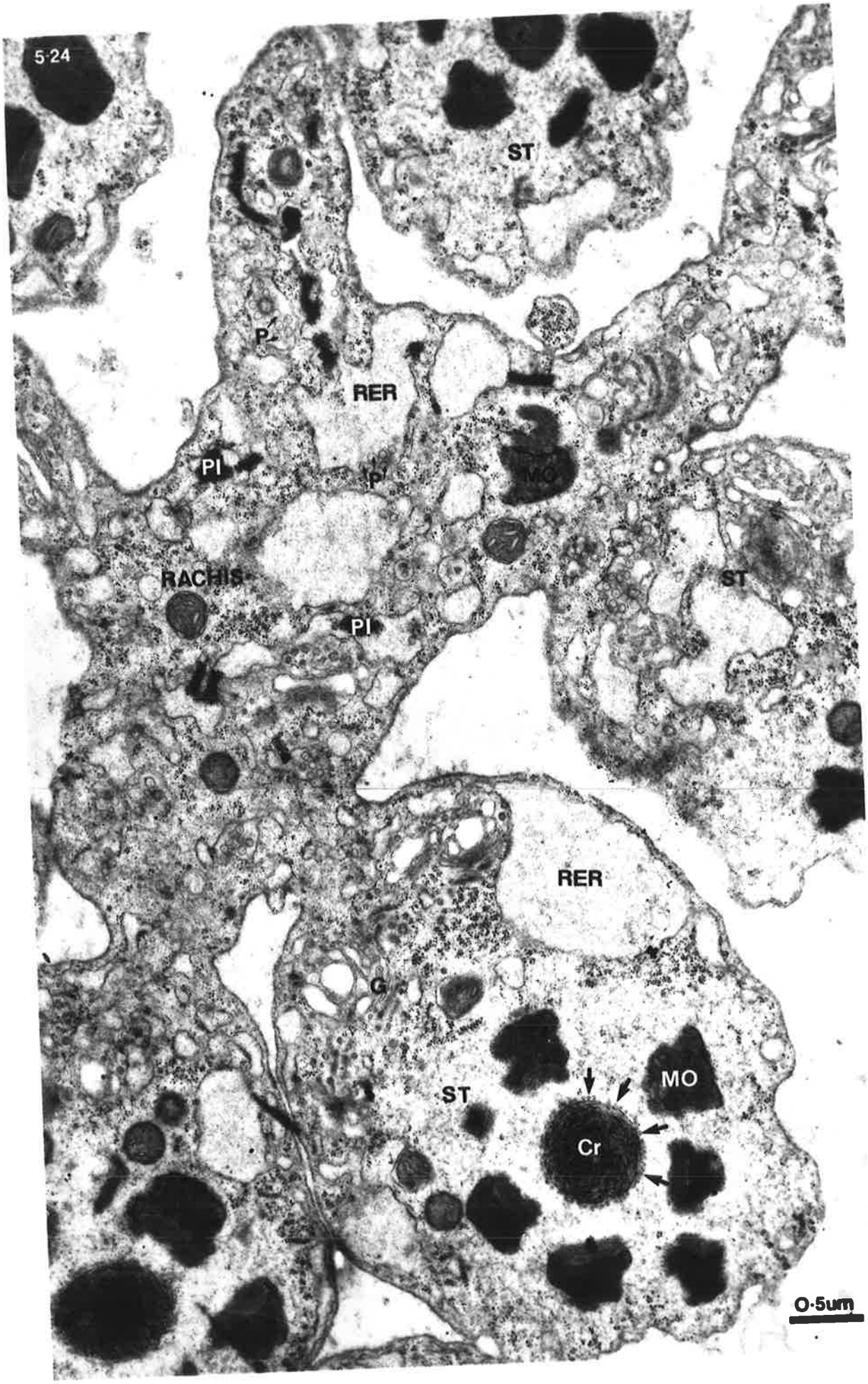
5·24
ST
P
RER
PI
P
MO
RACHIS
PI
ST
RER
G
ST
MO
Cr
0·5um

FIGURE 5.25 : This section shows the chromatin of spermatids winding into a spiral and elongating. Microtubules run back from the centrioles into the centre of the cone of DNA and along its outer edge (short arrows). Small indentations (long arrows) have formed on the outer side of the MOs. Most of the other organelles now move to the end of the spermatid (RB) which is still attached to remnants of the rachis.

FIGURE 5.26 : At the bottom of the figure is a large mass of residual cytoplasm in which RER and Golgi are producing many secretion vesicles. In the sperm above, the chromatin has been extruded; microtubules (arrows) run from the anterior to the posterior of the sperm.

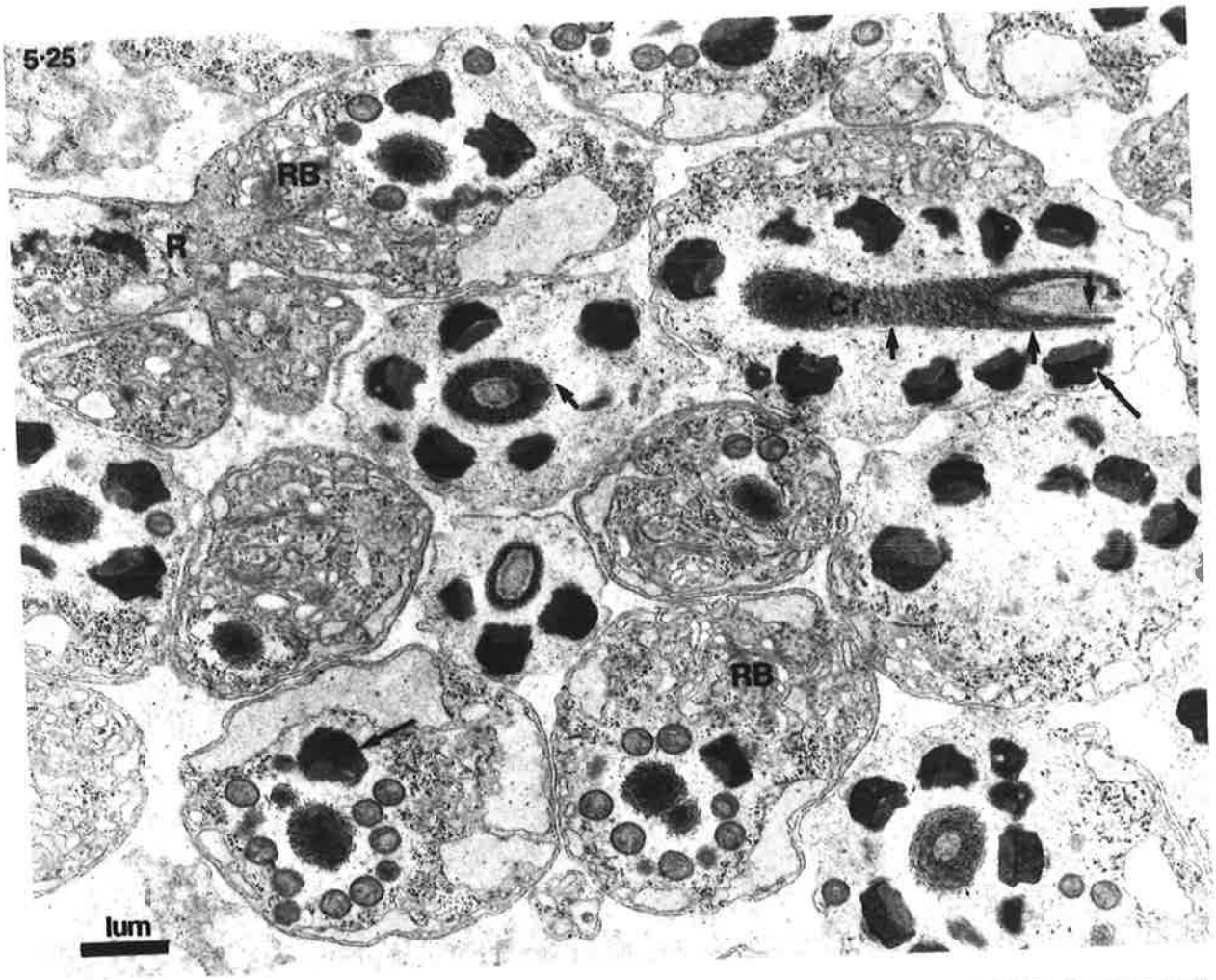
5·25
RB
R
Cr
RB
lum

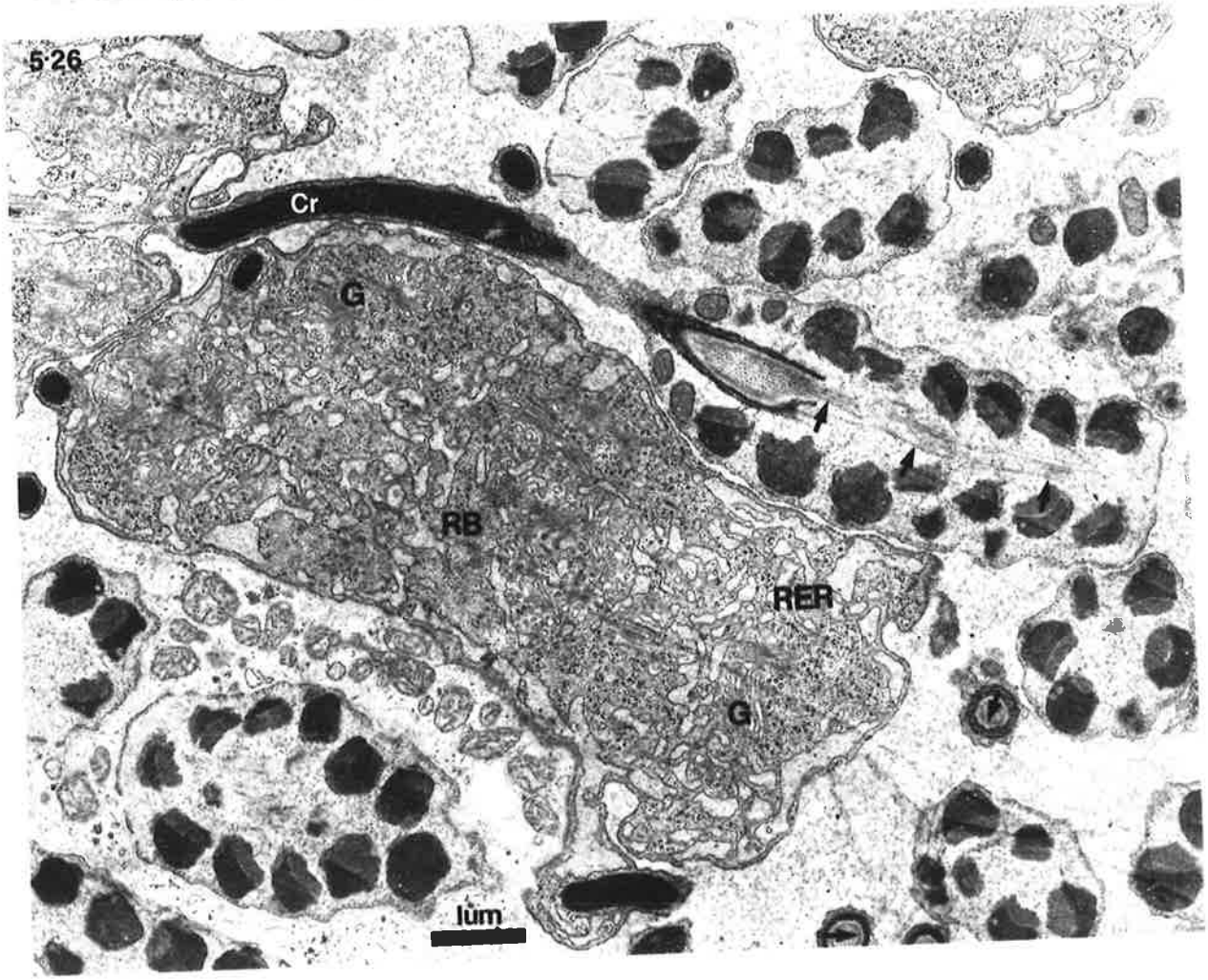
5·26
Cr
G
RB
RER
G
lum

uncommon to find spermatids amongst these vesicles (Cr, Figure 5.27). The uptake and degredation of spermatids by these masses of residual cytoplasm seems an efficient mechanism for removing cells which are defective in some way. The clusters of mitochondria within the cytoplasmic masses (M, Figures 5.26, 5.27) are probably providing energy for the degredative pathways. As the breakdown of material proceeds, there is a general disorganization of the organelles (Figure 5.28). Large electron-lucent vesicles are common and areas which were previously filled by ribosomes, are now empty. Figure 5.29 shows the final form of the residual cytoplasm before it is absorbed by the epithelium. Except for the mitochondria, which are presumably still functional, the organelles are unrecognizable. Two spermatozoa (Sz) which are trapped within the body appear to be undergoing degredation.

Spermatozoa

The extrusion of the residual body marks the transition of the spermatid to the spermatozoon (see Chapter I.2). Elongation continues until they measure 6-7μm, then the whole nuclear complex moves back along the cell and evaginates to form a tail (Figure 5.26). The sheath of microtubules which encircled the chromatin has disappeared and has been replaced by a coarse granular material (arrows, Figure 5.27)

The final maturation of the spermatozoa occurs in the seminal vesicle. The fibrous bodies of the membranous organelles slowly disappear, apparently dissolving into the cytoplasm (F, Figure 5.29). A small deposit precipitates near the membranous organelles (arrows, Figures 5.29, 5.30A) and forms small dense masses in the sperm cytoplasm. The membranous organelles themselves become spherical and more tightly packed (Figure 5.30B). Favourable sections show a

FIGURE 5.27 : A large mass of residual cytoplasm containing RER, Golgi bodies, mitochondria and degenerating sperm nuclei. In nearby sperm, note dense chromatin surrounded by a granular material and MOs bearing knobs.

FIGURE 5.28 : At the top of the figure is a large mass of residual cytoplasm containing degenerating RER and Golgi bodies. Maturing sperm lie below.

5·27

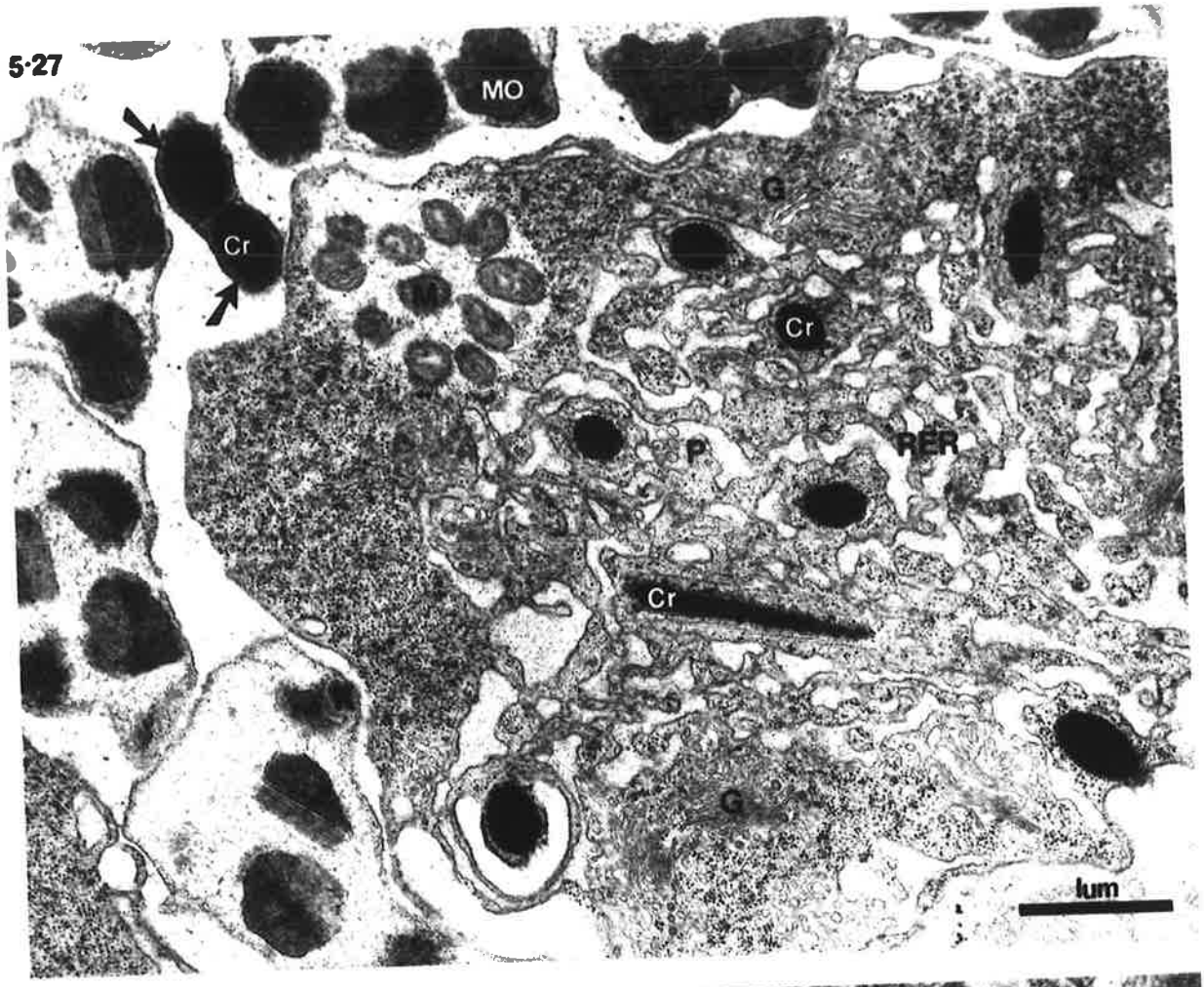

5·28

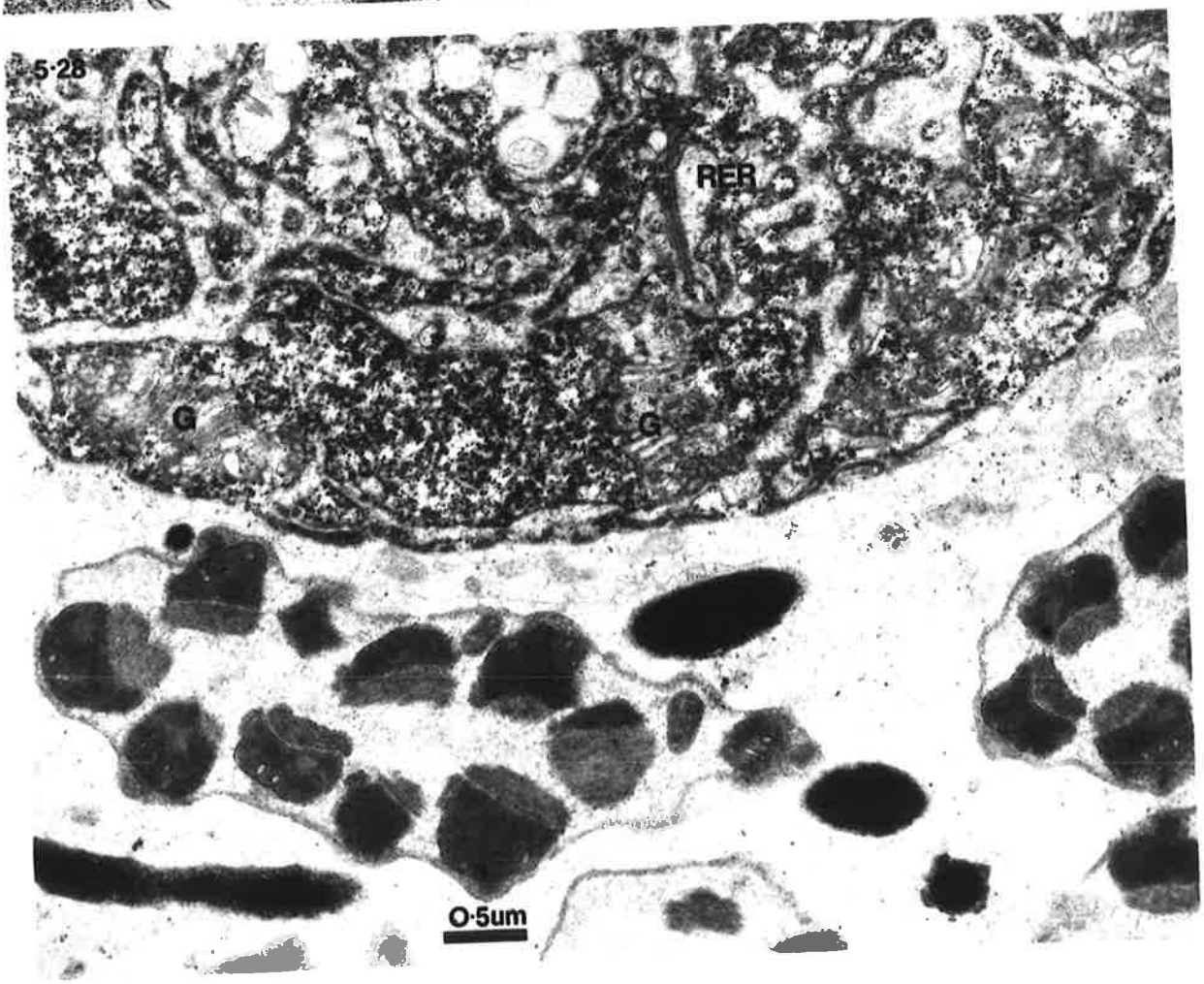

FIGURE 5.29 : Section near the testis epithelium showing a large mass of residual cytoplasm just before it is absorbed; only the mitochondria can be recognized. Two sperm are also undergoing degredation. In other sperm the fibrous bodies are disassembling and a dense material (arrows) has accumulated outside the MOs.

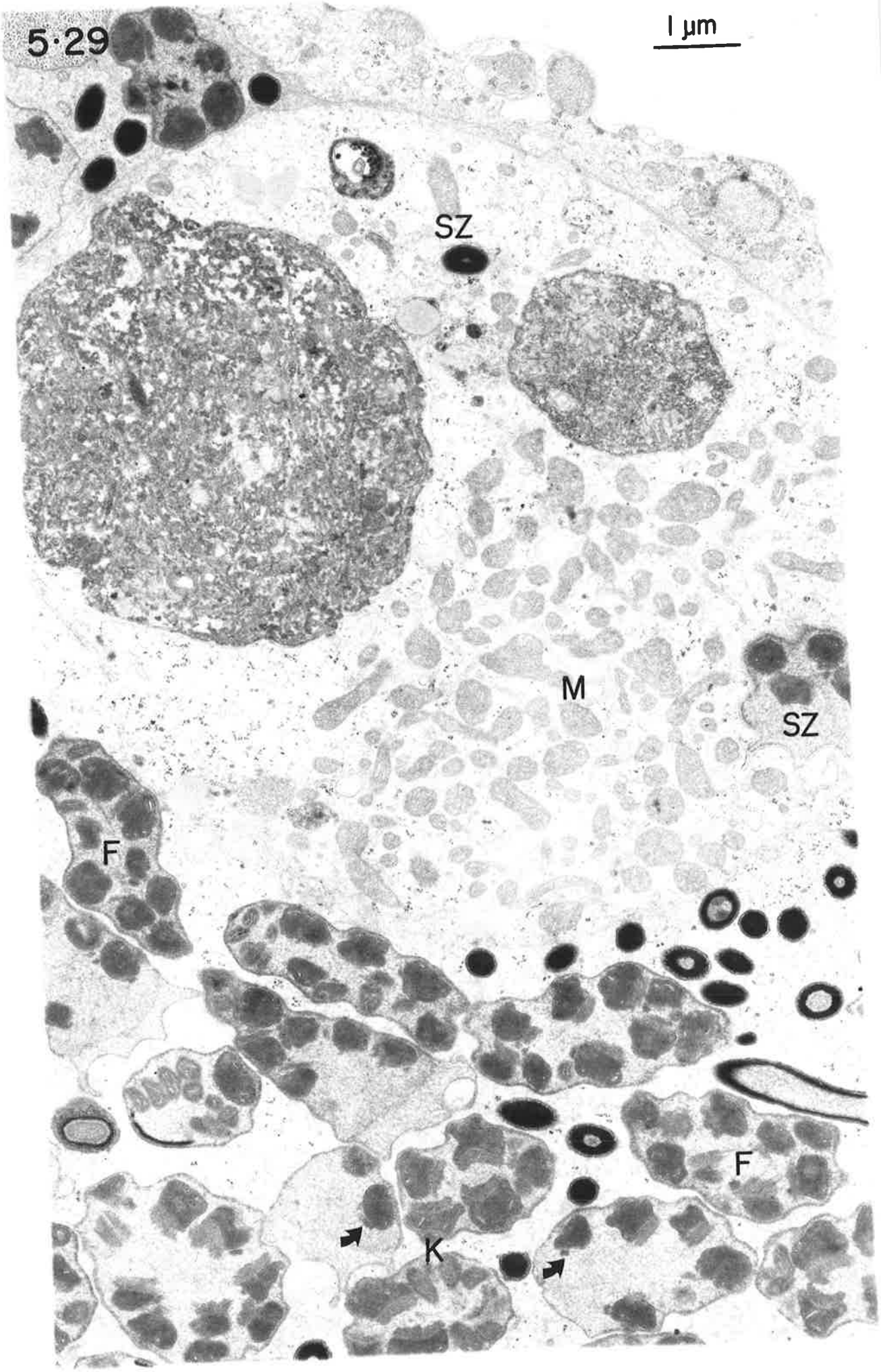
5·29
1 µm
SZ
M
SZ
F
F
K

knob on their outer side (K). Freeze-fracture reveals that these knobs are encircled by a ring of indentations (arrows, Figure 5.3IA,B). These were noted previously in thin sections (Figure 5.25, 5.26). The non-random distribution of particles, seen on the PF-face of the membranous organelles at an earlier stage, is more accentuated now. The EF-face has few particles and a bumpy uneven surface (Figure 5.3IC). A small region at the anterior of the spermatozoon becomes capable of producing pseudopodia and is therefore described as amoeboid (A, Figures 5.30A,B). It is devoid of organelles and contains material which has no consistent organization; at times it looks filamentous but elsewhere it appears granular. A dense layer of material lines the plasma membrane of the sperm except in the amoeboid region (Figures 5.29, 5.30A).

When the chromatin finishes elongating and evaginating, it loses its filamentous texture and becomes very electron-dense (Figure 5.30A,B). The nature of the bonds maintaining this form was explored using the ionic detergent, sodium dodecyl sulphate, SDS (Sigma Chemical Co.) and dithiothreitol, DTT (Sigma Chemical Co.), a reducing agent. Sperm were dissected onto glass slides, then viewed during perfusion with 1% SDS or 0.IM DTT, in 0.IM sodium borate, pH 9.0. Specimens were re-examined at intervals for up to an hour later. Sodium borate alone and DTT had no effect, but after a few seconds' exposure to SDS, the sperm disintegrated in a manner resembling an explosion. This demonstrates that ionic and not covalent bonds are responsible for maintaining the characteristic form of the DNA.

FIGURE 5.30A,B : Spermatozoa undergoing their final maturation; the MOs move closer together, the chromatin becomes very dense and loses its filamentous texture and a small region at the anterior becomes amoeboid. Mitochondria tend to aggregate at the posterior and often fill the hollow part of the chromatin. Dense material lies beneath the plasmalemma, except in the amoeboid region.

FIGURE 5.31A,B : PF-face (A) and EF-face (B) of the membrane of an MO, showing a ring of indentations (arrows) around the knob.

5.31C : Particles are scarce on the EF-face but more numerous and clumped on the PF-face of the MOs.

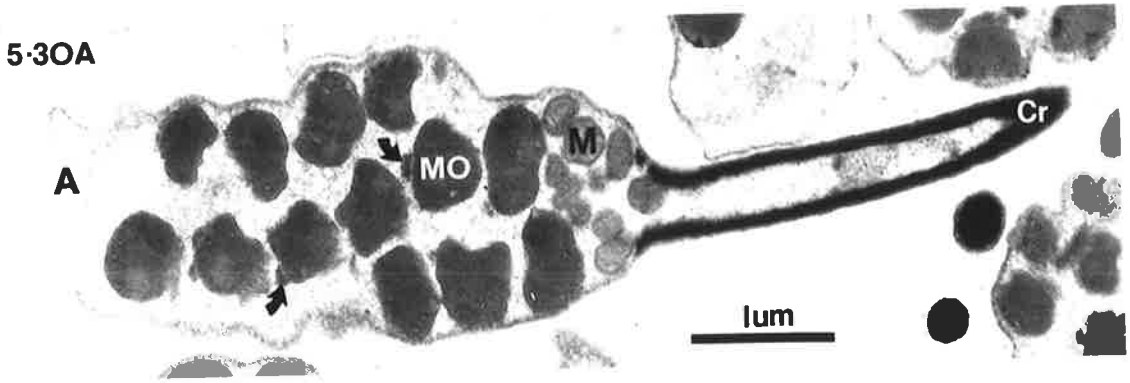
5·3OA
A
MO
M
Cr
lum


5·3OB
A
MO
M
lum


5·3IA
K
O·lum


B
EF
K
O·lum

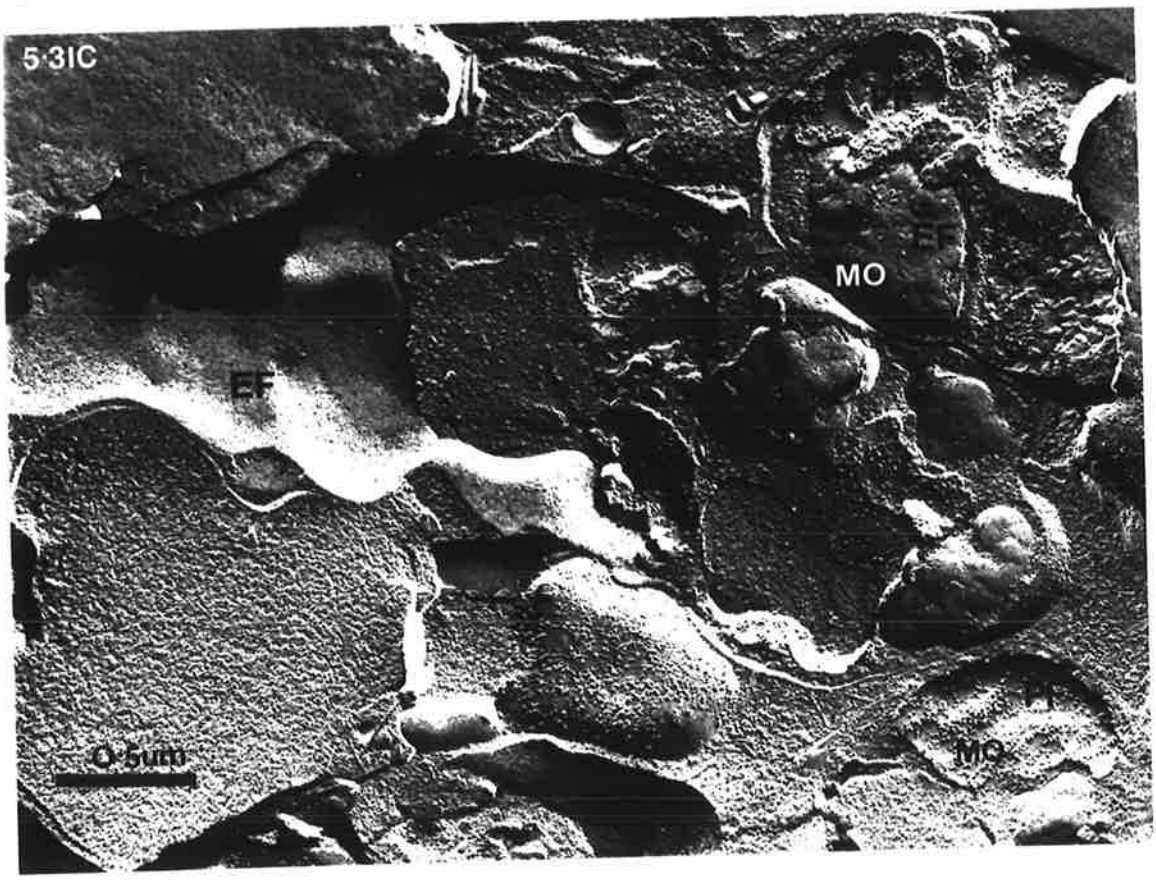
5·3IC
EF
MO
EF
O·5um
MO

The chromatin remains tubular at its base, but both the microtubules and the centrioles within it disappear. Instead, the hollow is filled with mitochondria (Figure 5.30B). The granular material, which lay between the chromatin and the plasma membrane, also disappears and is replaced by a substance of medium electron density (Figure 5.30B).

Spermatozoa in the seminal vesicle are surrounded by a flocculent material. (Figures 5.29, 5.30A). Its significance is not known, although it could be a kind seminal fluid which bathes the spermatozoa during insemination.

5.3 Maturation of spermatozoa after insemination.

During copulation, spermatozoa are inseminated into the vagina of females. They quickly move up through the ovejector and into the uterus. When dissected into saline and examined with the light microscope, these spermatozoa are different from those removed from the seminal vesicles of males (compare Figures 5.32 and 5.5). The most striking change is the enlargement of the amoeboid anterior (A, Figure 5.32), which can now be extended to lengths of 5µm. It is an effective locomotory organ, as sperm can readily translocate across glass at 37°C (see Chapter 5.4).

The region between the amoeboid anterior and the nuclear tail (N) contains the cytoplasmic organelles (C). Now it is half it's former size (3µm long, Iµm across). The electron microscope reveals that the membranous organelles have fused with the plasma membrane and released their contents (Figures 5.33, 5.34). In doing so, they have shrunk to half their former size. This sequence of events can be followed in longitudinal sections of the posterior reproductive tract of females (Figure 5.33). Initially the

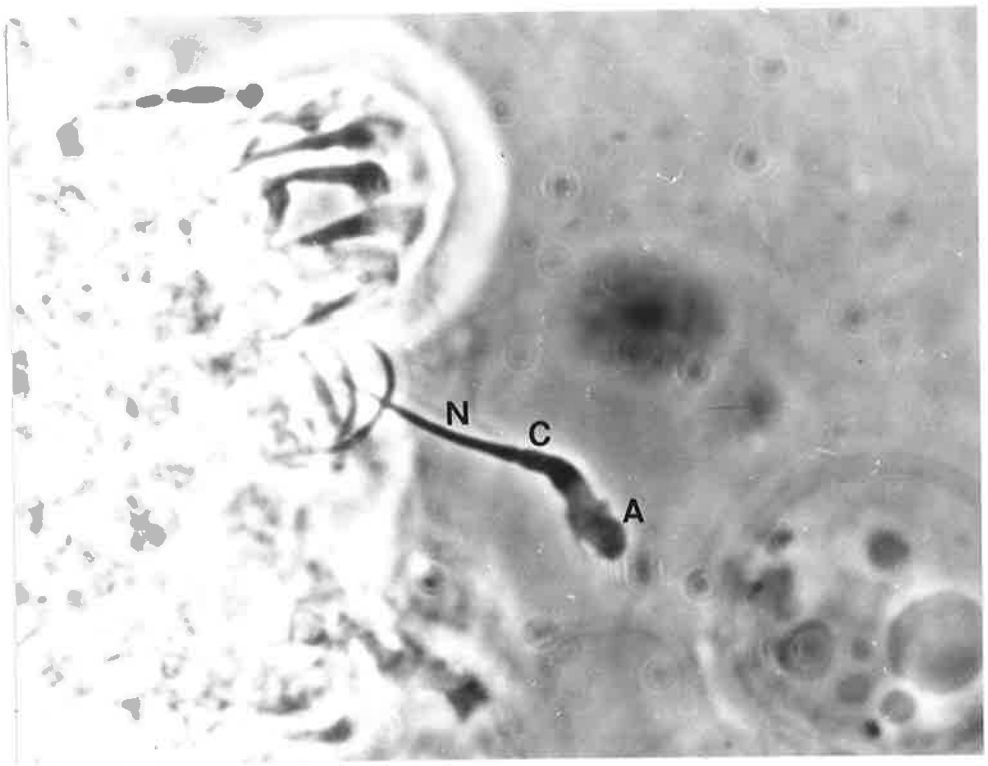

FIGURE 5.32 : Phase contrast micrograph of an activated sperm from the uterus of a female; it has a large amoeboid anterior and a smaller cytoplasmic region, but the nucleus is unchanged.

FIGURE 5.33 : Longitudinal section of the posterior reproductive tract of a female; in some sperm the MOs are releasing their contents. Five stages are evident ranging from those which resemble the MOs in unactivated sperm (1) to those which are pale and have deep microvillous-like invaginations (5). Dense material (arrows) remains near to some of the MOs and mitochondria are still found at the base of the tail of chromatin. Sometimes the material in the amoeboid region appears filamentous and elsewhere it is granular.


5·33
3
M
5
5
5
4
1
M
Cr
Ag
2
1
Af
1 µm

FIGURE 5.34 : Transverse section of activated sperm in the upper uterus of a female. The chromatin is dense and, near its junction with the cytoplasm, it surrounds the mitochondria. The MOs have released their contents and their membranes bear a fuzzy coat on one side (arrow heads) and are thickened on the other (arrows). The amoeboid region contains mitochondria close to the plasmalemma, vesicles, tubular elements and filaments.

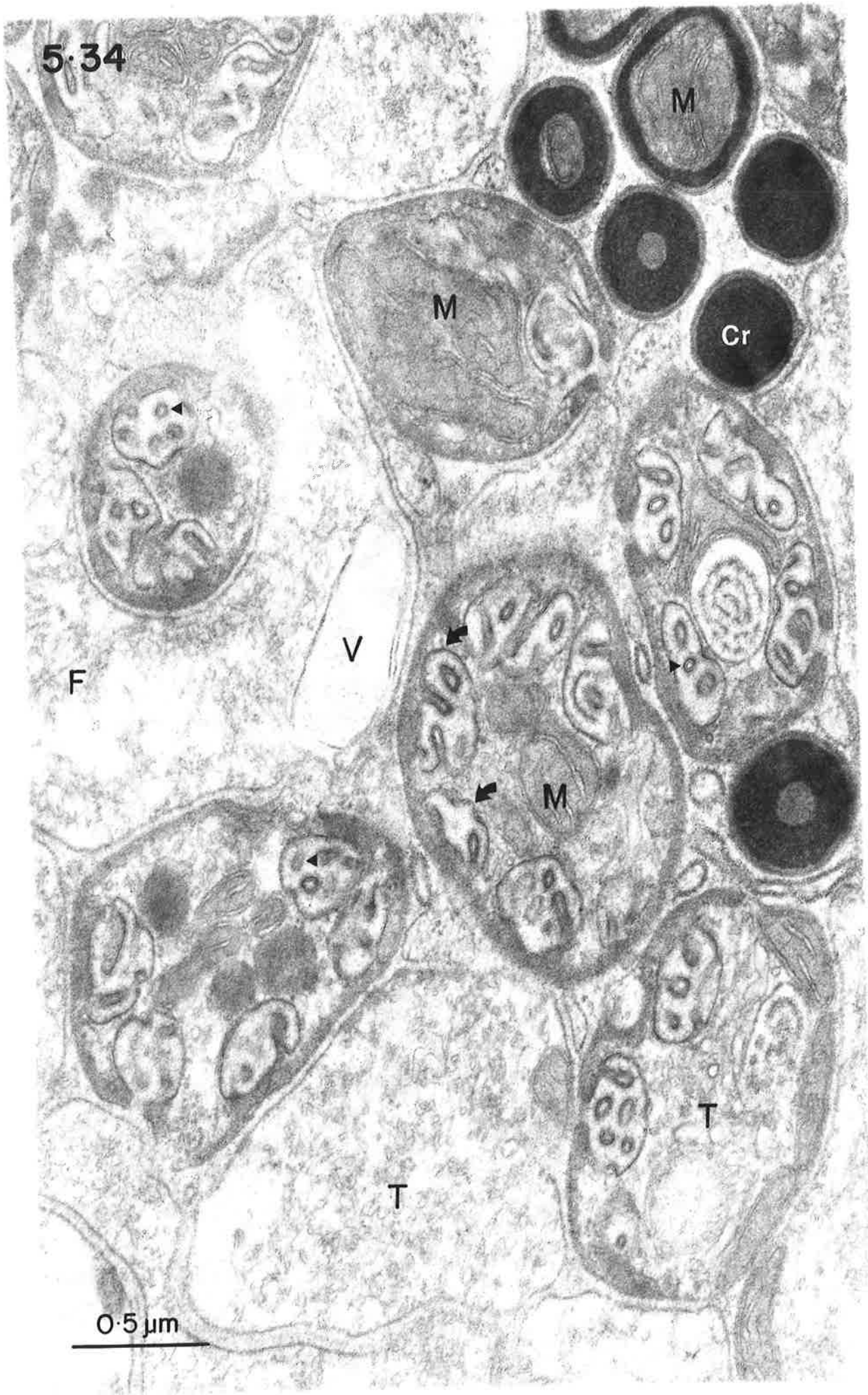
5·34
M
M
Cr
V
F
M
T
T
0·5 µm

membranous organelles are the same size and density as in spermatozoa from males (Stage I). For a short time after releasing their contents, they are large electron-lucent vesicles (Stages 2 and 3), then the invaginations in their membranes deepen and become tube-like (Stages 4 and 5). Figure 5.34 shows their final structure. The cytoplasmic side of their membrane is thickened (arrows) and the outer leaflet bears a fuzzy coat (arrow heads).

Freeze-fracture demonstrates that a dense random distribution of particles has replaced the clumping seen previously on the PF-face of the membranous organelles (Figure 5.35). There are few particles on the EF-face. The pores joining the membranous organelles to the plasma membrane are striking in freeze-fracture (P, Figure 5.36). Thin sections reveal that each pore is surrounded by a collar of material (P, Figure 5.37), which is slightly more dense than the amorphous layer lining the plasma membrane of the cytoplasmic region (Figure 5.37).

The small dense deposits which were secreted into the cytoplasm of the sperm when they reached maturity in the male, persist in the spermatozoa after insemination (arrows Figure 5.33). In sperm in the seminal receptacle, they have fused to form a single dense mass. This dense sphere lies at the anterior or the cytoplasmic area, close to its junction with the amoeboid region (arrows, Figure 5.37).

The chromatin appears unchanged after insemination. Using the same technique as described previously (Chapter 5.2), it was found that SDS, but not DTT or borate buffer alone, disrupts the nuclear tail of the sperm. Thus the nature of the bonds maintaining the form of the DNA is unchanged after insemination.

FIGURE 5.35 : Cross-fracture of sperm in the uterus of a female. After the MOs have released their contents, the PF-faces of their membranes bear a dense random distribution of particles; even the invaginations are covered with particles, but the EF-face is almost bare.

FIGURE 5.36 : Here, the fracture passes around the spermatozoa and reveals pores (arrows) joining the MOs to the plasmalemma.

5·35

5·36

A narrow band of medium electron-density remains in the gap between the chromatin and the plasma membrane (Figure 3.34).

The amoeboid anterior begins to enlarge as soon as the spermatozoa enter the female, but it does not reach its maximum size until sperm reach the uterus. During this time there is a transformation in the substance of this region. Initially, it is dense and granular (Ag, Figure 3.33), but then it becomes filamentous (Af). The filaments do not fill the entire region. Instead they form clumps and chains, which are sometimes attached to the plasma membrane (Figure 5.37). It was possible that this configuration of filaments was an artifact of fixation with osmium tetroxide (Pollard and Maupin, I978). Tannic acid was therefore added to the primary fixative in order to stabilize filaments during subsequent processing (Begg, Rodewald and Rebhun, I978). Although this treatment increased the contrast of the sections, the arrangement of filaments was unchanged (Figure 5.38). The amoeboid region also contains mitochondria, usually closely associated with the plasma membrane, (M, Figures 5.37, 5.38) as well as vesicles, ranging in size from 0.2 - Iμm (V, Figure 5.34). Membrane profiles of smaller diameter, often with a tubular appearance (T, Figure 5.34, 5.37), occur at the junction of the amoeboid and cytoplasmic regions. Figure 5.37 shows the sperm intimately associated with the uterine epithelium (E). This suggests that as well as being the organ of locomotion, the amoeboid anterior acts as a holdfast which enables the sperm to maintain their position in the anterior uterus.

Although fertilization was not studied at the ultrastructure level, oocytes were dissected from the upper uterus in an attempt

FIGURE 5.37 : Longitudinal section of sperm in the seminal receptacle of a female. In particular note the chains of fibrils in the amoeboid region, the tubular elements between this part and the cytoplasmic area, and the dense collars around the pores which join the MOs to the cell membrane. The dense material originating from the MOs has coalesced into dense spheres (arrows). On the left of the figure, the sperm are intimately associated with the uterine epithelium.

FIGURE 5.38 : In sperm stained with tannic acid to preserve microfilaments, the appearance of the amoeboid region is unchanged. Note the mitochondria and microfilaments associated with the membrane.

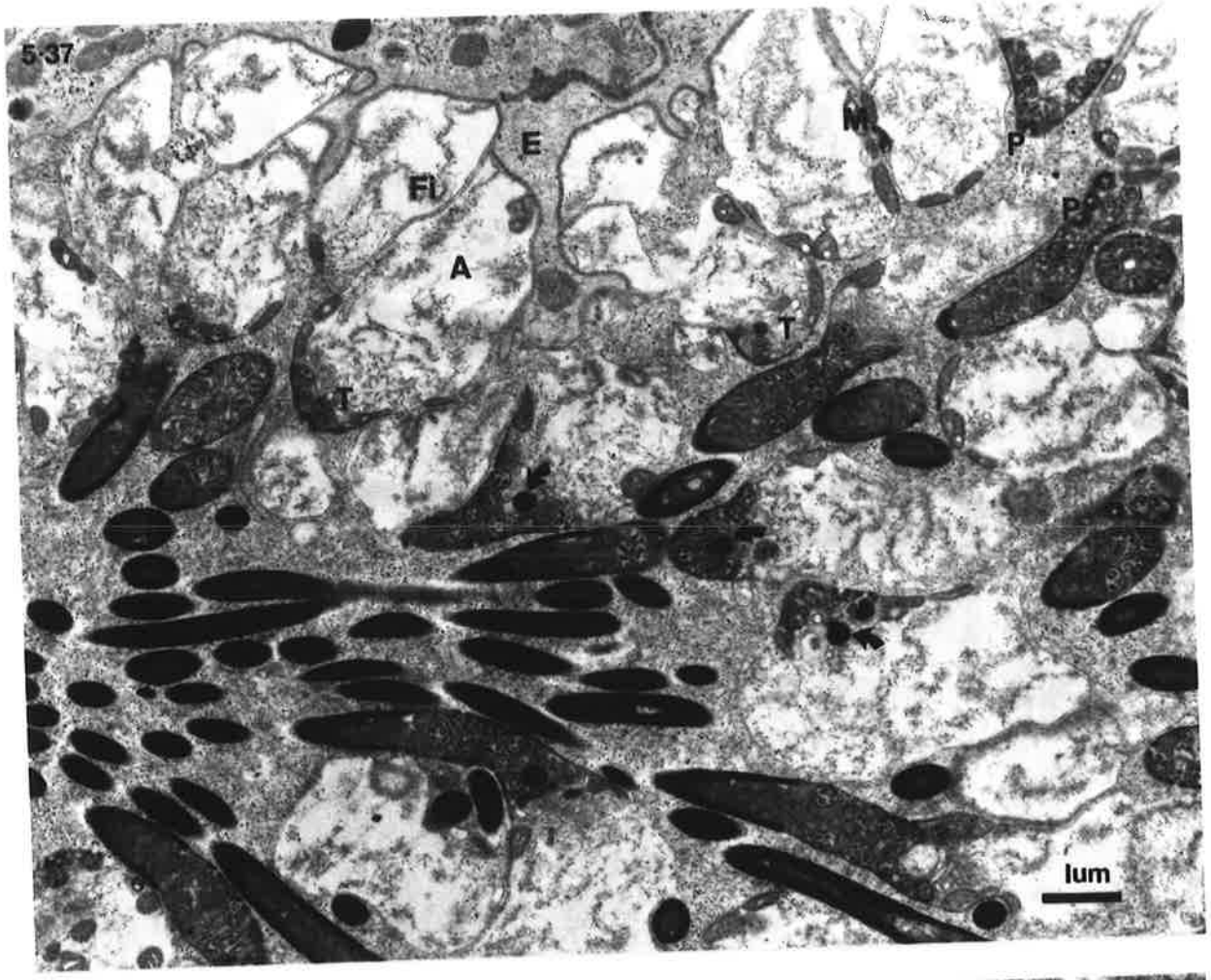
5·37
E
Fl
A
T
T
M
P
P
lum

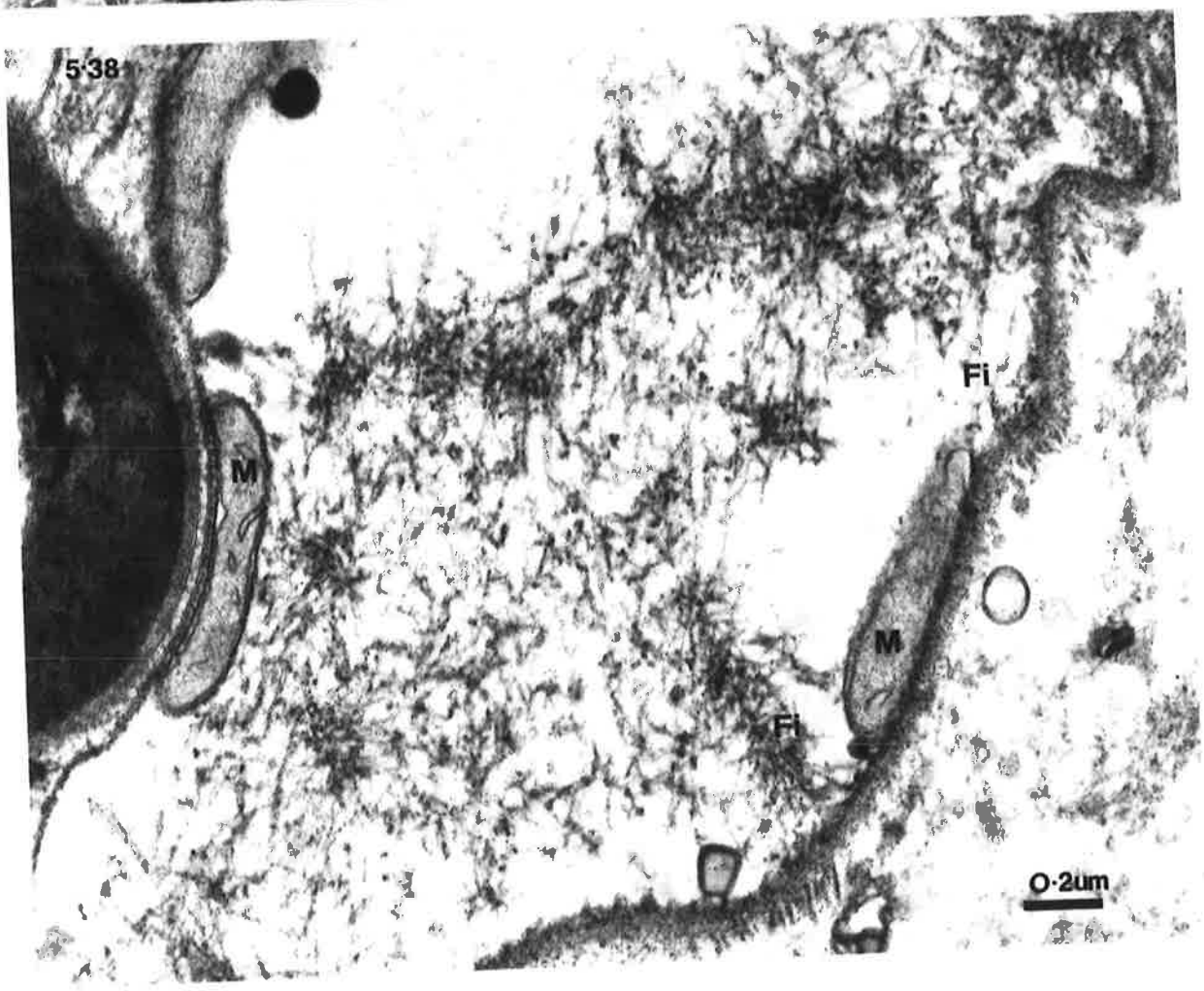
5·38
M
Fi
M
Fi
0·2um

to witness this event with the light microscope. Unfertilized oocytes can be recognized by their kidney-shape. Many such oocytes were examined, but only two were found to have sperm attached. On both occasions, a single sperm was tightly adherent to the oocyte by its anterior amoeboid end. These sperm defied all attempts at removal, including gentle pressure on the coverslip and perfusion with saline. It appears, therefore, that fertilization was occurring and that in *N. brasiliensis*, it is the amoeboid anterior of the sperm which unites with the oocyte during fusion of the gametes.

5.4 Sperm motility *in vitro* and *in vivo*.

5.4.I Spermatozoa from females.

When spermatozoa were dissected from the seminal receptacle of female worms and observed at 37°C, some attached to and crawled across the surface of glass slides. The behaviour of translocating sperm was recorded using time-lapse cinematography and films were analysed from outlines, drawn from enlargements of individual frames of the film.

During translocation, the amoeboid anterior adheres to the surface, while the rest of the sperm is dragged passively behind. A cycle of events, depicted in Figures 3.39, 3.40, occurs at the leading edge. First, a small protrusion is extended (Figure 5.40A; hatched area, Figure 5.39). A constriction forms at its base (arrows), then the protrusion swells (black area, Figure 5.39), until it is as wide as the rest of the sperm (Figure 5.40 C,D). The formation of another small protrusion at the new leading edge (Figure 5.40E), completes the cycle of events which takes 6-8 seconds. The mean speed of 20 sperm, translocating over a glass surface, was I2.3µm/min (S.D. 4.3µm/min).

The black arrows in Figure 5.40 represent the position of the constriction rings in a translocating sperm. Although they remain stationary relative to the substrate (denoted by grid), they move back along the sperm and subside on reaching the cytoplasmic region at the rear. This region appears rigid and does not change shape during locomotion. Before a constriction ring is halfway along the sperm, a new pseudopodium forms at the leading edge. Thus, up to three constriction rings may occur across

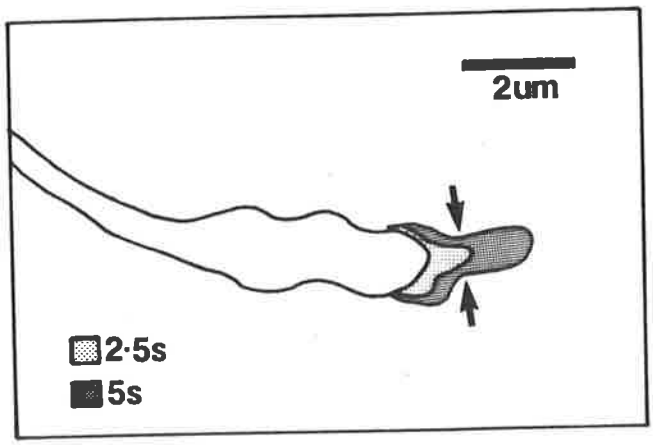

FIGURE 5.39 : Three superimposed images of a translocating sperm. The advance at the leading edge is shown after 2.5 sec. by the light shading and after 5 sec. by the dark shading. The arrows demonstrate the position of the constriction ring.

FIGURE 5.40 : Outlines of translocating sperm drawn from photographs taken at 2s intervals.
A-D, E-G show two cycles of the protrusion and swelling of the pseudopodium at the leading edge. The displacement of the new pseudopodium, to the left of the leading edge in E, causes a change in the direction of movement. Black arrows mark constriction rings, white arrows mark contraction wave.

FIGURE 5·40

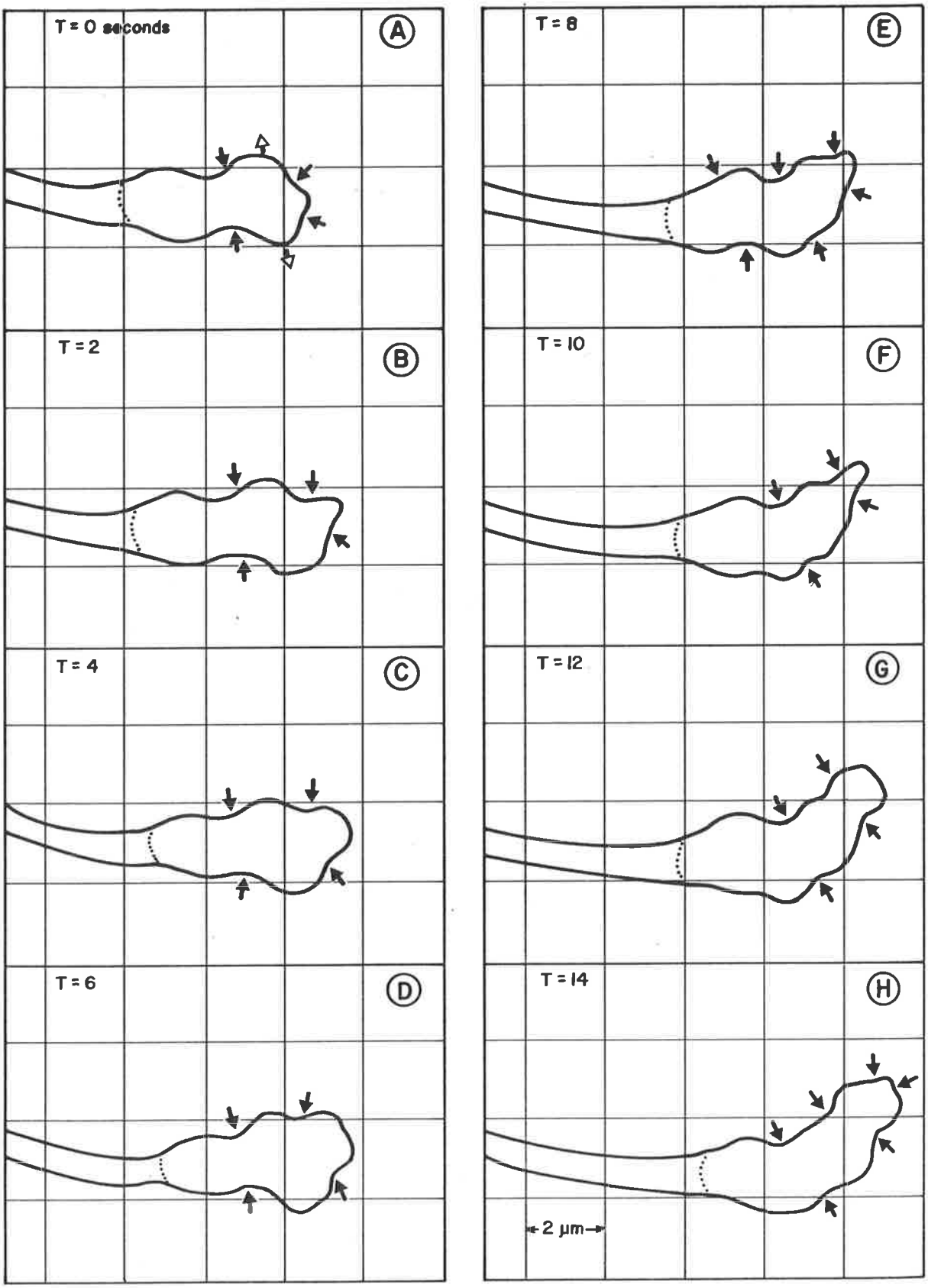

the sperm simultaneously (Figure 5.40E, H). The convexity (white arrows Figure 5.40), produced by the swollen pseudopodium with a constriction ring at its base, has been called a "contraction wave" (Senda, Tamura, Shibata, Yoshitake, Kondo and Tanaka, I975).

The sperm changes direction when a new pseudopodium forms on one side of the leading edge. Figure 5.40, frames E,F, and G, shows a sperm moving towards the left-hand side of the field. It demonstrates that the direction of movement is dictated by the point on the leading edge at which the new psuedopodium forms. As new pseudopodia are produced each 6-8 seconds, this change in direction can be accomplished rapidly. Sometimes, the sperm may move the cell body, i.e. the nuclear and cytoplasmic regions, from side to side, while continuing to advance in a straight line. This appears to be an active movement by the sperm, but its significance is not understood.

Figure 5.4I summarizes many important aspects of sperm locomotion. It shows 6 carefully alligned outlines of a translocating sperm at 2s intervals. The constriction rings have been joined by lines across the figure. The fact that these lines are straight and parallel emphasizes that the constriction rings remain stationary, relative to the substrate. Their equal spacing shows that this sperm was producing pseudopodia at a constant rate and would therefore have been travelling at a constant speed. As is generally the case, three constriction rings occur across the sperm at any one time. The junctions of the cytoplasmic and nuclear regions are joined by a dotted line. The constant slope of this line demonstrates that the cell body progresses at a constant rate, in comformity with the leading edge.

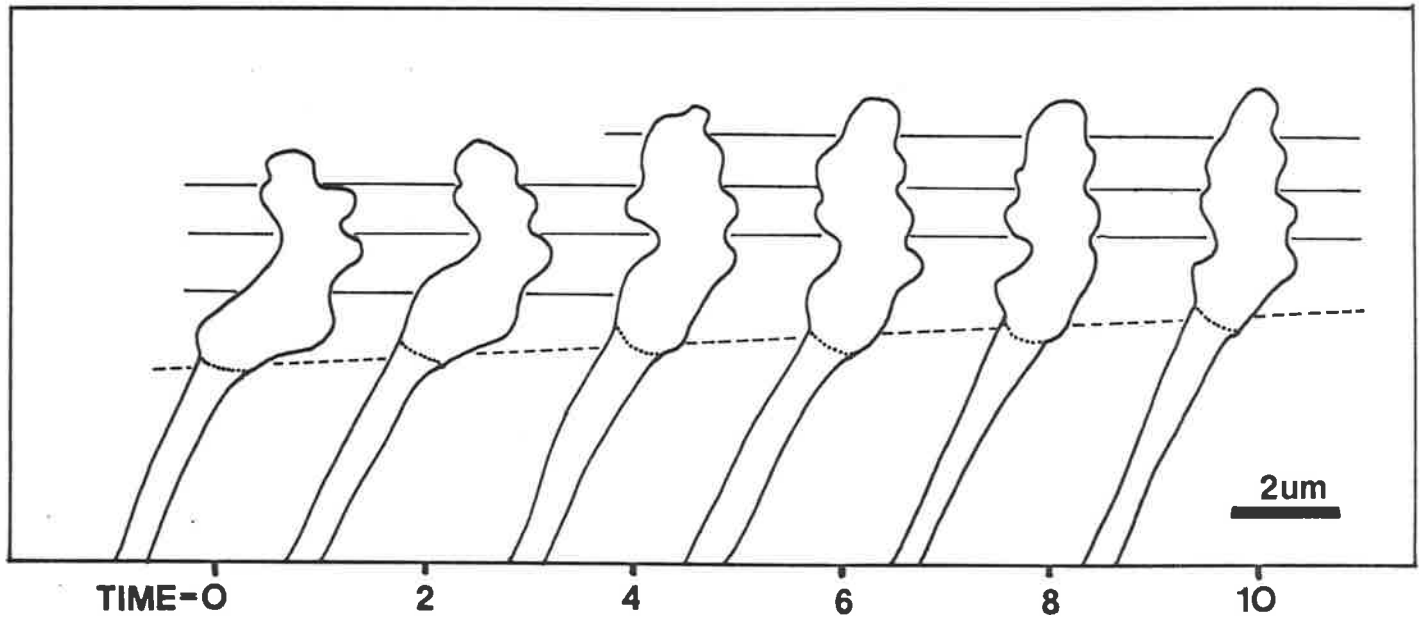

FIGURE 5.41 : Carefully aligned outlines of a translocating sperm at 2s intervals. Constriction rings, which remain stationary relative to the substrate, are joined by lines. The junctions of the nuclear and cytoplasmic regions are marked by dotted lines and joined by a dashed line.

When translocating sperm were perfused with cytochalasin B, I0-I00μM in I% DMSO, neither the form nor speed of their movement changed, This contrasted with the dramatic effect of this drug on white blood cells. After less than a minute's contact with I0μM cytochalasin, leukocytes abruptly stopped translocating. This effect was reversible, since they recommenced their migration a few minutes after perfusion with fresh medium. I% DMSO, alone, had no apparent effect on sperm or leukocytes.

Spermatozoa which were not attached to the substrate were common in most preparations. These sperm underwent the same pattern of pseudopod formation as translocating sperm. A small protruberance, with a constriction ring at its base, formed at the leading edge. The resultant contraction wave moved back along the sperm at the same speed as in translocating sperm.

Observations were also made on sperm *in utero*. This was possible only after dissecting the uterus out of the female, as other internal organs obscured the view in intact worms. Figure 5.42 shows sperm attached to the uterine epithelium, just posterior to the seminal receptacle. These sperm underwent the same cycle of pseudopod formation previously described for sperm *in vitro*.

Observations were generally made on sperm dissected into 0.85% sodium chloride, but on one occasion, sperm medium was used (see chapter 3.6). Although the form and speed of translocation was unchanged, the sperm survived for much longer periods in this medium. In one preparation, constantly maintained at 37^{o}C, some spermatozoa were still actively moving 11h after their dissection from the uterus.

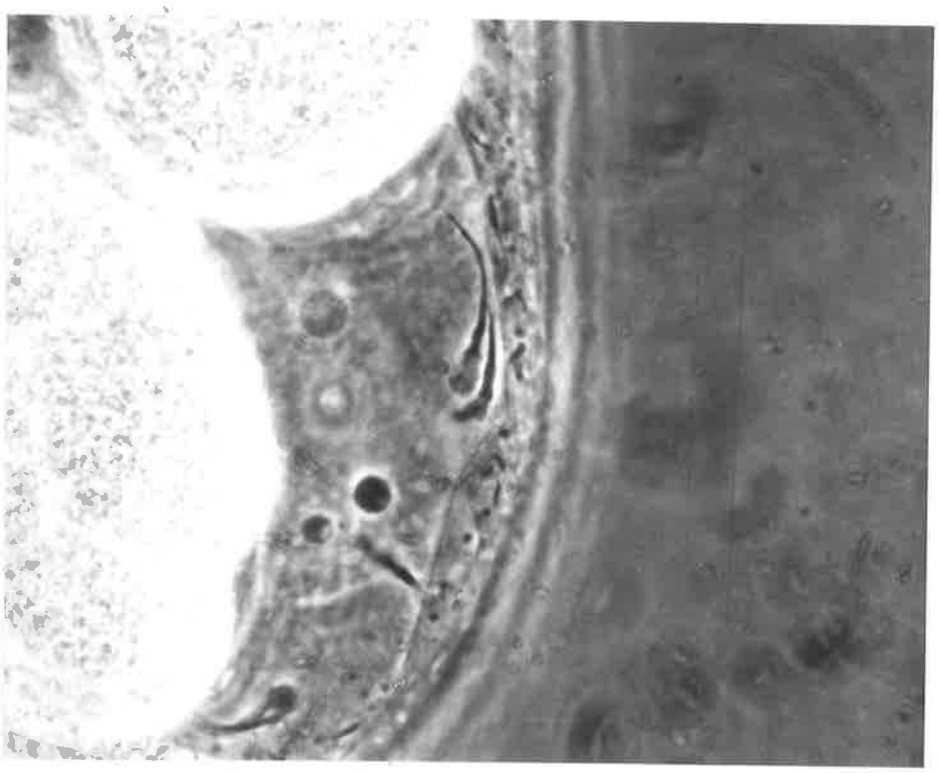

FIGURE 5.42 : Spermatozoa moving along the uterine epithelium, closeby are eggs.

5.4.2 Spermatozoa from males.

Thin sections of male worms (Figure 5.30B) show that some sperm in the seminal vesicle extend psuedopodia from their anterior ends. Indeed, when sperm were dissected from the seminal vesicle and observed at 37°C, a few produced pseudopodia (Figure 5.5). Often, these projections were short and, judging from their appearance in phase contrast, they protruded out into the medium. Moreover, they were formed in an irregular uncoordinated manner, sometimes from several points on the anterior margin. Occasionally, when they attached to the substrate, these sperm could translocate for short distances.

CHAPTER 6. SPERMATOGENESIS AND SPERMATOZOAN MATURATION IN *N. dubius*.

6.I Morphology of the testis.

The testis of *N. dubius* (Figure 6.I) resembles that of *N. brasiliensis* in both form and organization. It is a long, tubular organ which can be divided into four developmental zones. At the anterior, spermatogonia divide by mitosis while in the next region, spermatocytes undergo a long period of growth and development. Meiosis follows and finally, in the posterior testis and seminal vesicle, the spermatids differentiate into mature spermatozoa. The rachis originates as fine threads of cytoplasm joining the spermatogonia, but it soon enlarges into a central core which supports and connects the spermatocytes. It is an important structure throughout the testis, as the sperm cells separate from it only after they commence to differentiate into spermatozoa.

The most striking difference between the testes of the two species is their relative dimensions, the testis of *N. dubius* being twice the size of that of *N. brasiliensis* (3.7 - 3.8mm and I.8 - I.9mm respectively). In *N. dubius*, the developing sperm cells are approximately double the size of those in *N. brasiliensis*. For example, the cap cell is 20µm in diameter in *N. dubius*, compared with I0µm in *N. brasiliensis*. Similarly, the maximum size of the spermatocytes is 28-30µm in *N. dubius* and only I4µm in *N. brasiliensis*.

As a consequence of the larger size of the sperm cells, the dimensions of each of the four developmental regions of the testis is doubled in *N. dubius*. Within the first three regions, i.e. the zones of mitosis, growth and division, development proceeds in parallel with *N. brasiliensis*, however, in the zone of differentiation

FIGURE 6.1 : Phase contrast montage of the testes and seminal vesicle (Sv) of *N. dubius* showing spermatogonia (Sg) at the anterior and spermatocytes (Sc). After meiosis the spermatids differentiate into spermatozoa (Sz). There are many sperm in the testis, but rather few in the seminal vesicle, which is narrowed by large epithelial cells.

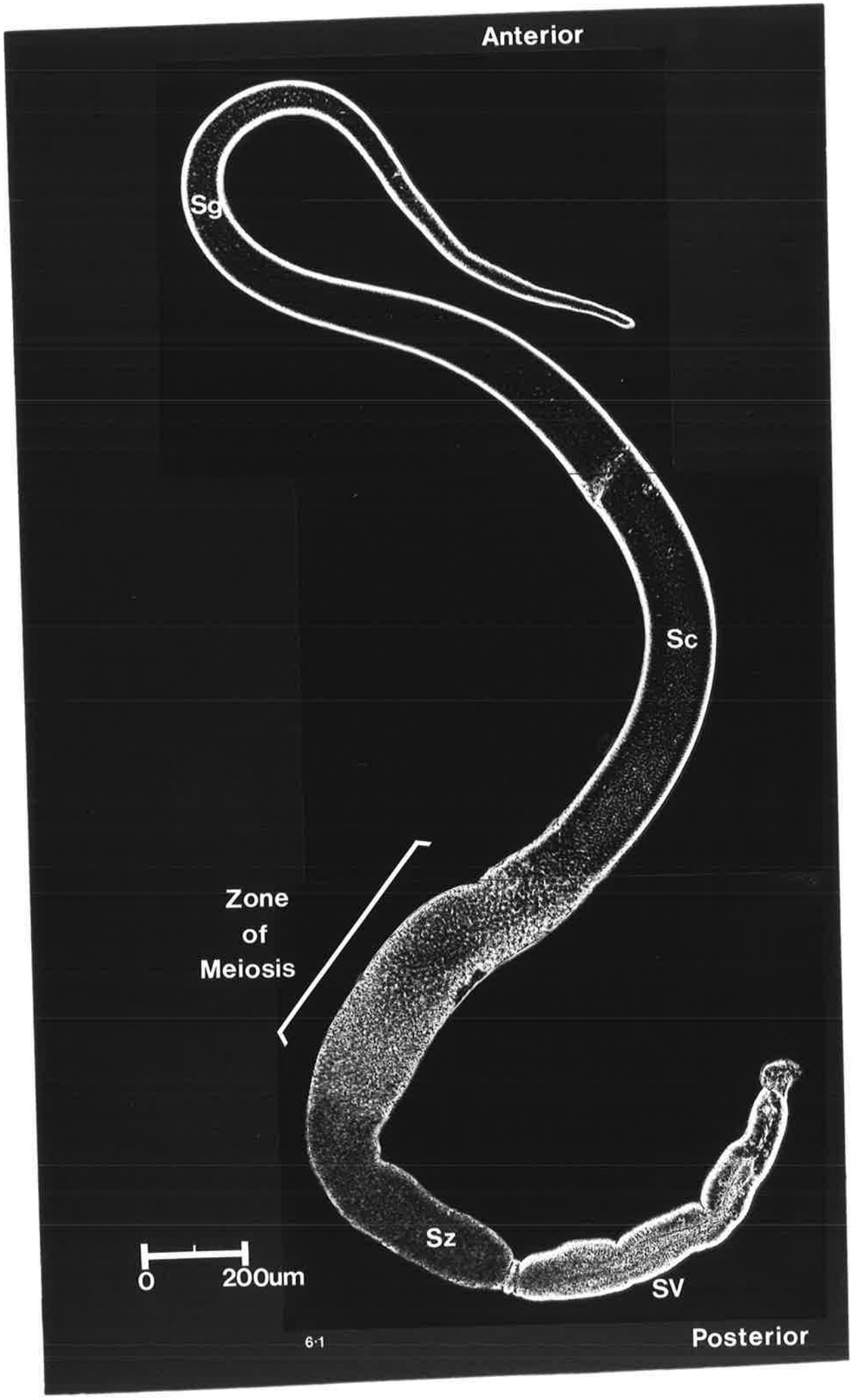

6-1

some differences are noted. Here the DNA of the spermatid condenses and is extruded into a tail within a disproportionately short region of the testis. Consequently, a greater length of the posterior testis of this species contains mature spermatozoa (300μm compared with 50μm in *N. brasiliensis*). Moreover, this region is marked off from the more anterior testis by a slight constriction of the epithelium, making it resemble the seminal vesicle of *N. brasiliensis*. The seminal vesicle proper, in *N. dubius*, also contains mature spermatozoa. These are rather few in number as the lumen is narrowed by large epithelial cells. Together, the posterior testis and seminal vesicle of *N. dubius* contain a greater number of mature sperm than the seminal vesicle of *N. brasiliensis*. This would be important given the greater egg-bearing capacity of the females of this species (see Chapter 4.2).

The mature spermatozoa of *N. dubius* (Figure 6.2), like those of *N. brasiliensis*, have an amoeboid anterior, a cytoplasmic region and a tail of DNA and, although the sperm of both species are I8μm long, the relative proportions of these three areas are different. Consequently the sperm can be readily distinguished (compare Figures 6.2 and 5.5). In *N.dubius*, the chromatin forms a short blunt projection, 3.5μm in length, which contrasts with the IIμm tail of *N. brasiliensis*. The cytoplasmic region of the sperm of both species is roughly cylindrical, but in *N. dubius* it measures I4μm, compared with 7μm in *N. brasiliensis*. The anterior amoeboid region which forms the pseudopodia used for translocation is similar in both species.

Comparisons made with the light microscope demonstrate that the early stages of spermatogenesis in *N. dubius* closely resemble those in *N. brasiliensis*, but during post-meiotic differentiation species-specific differences become obvious. It was important to

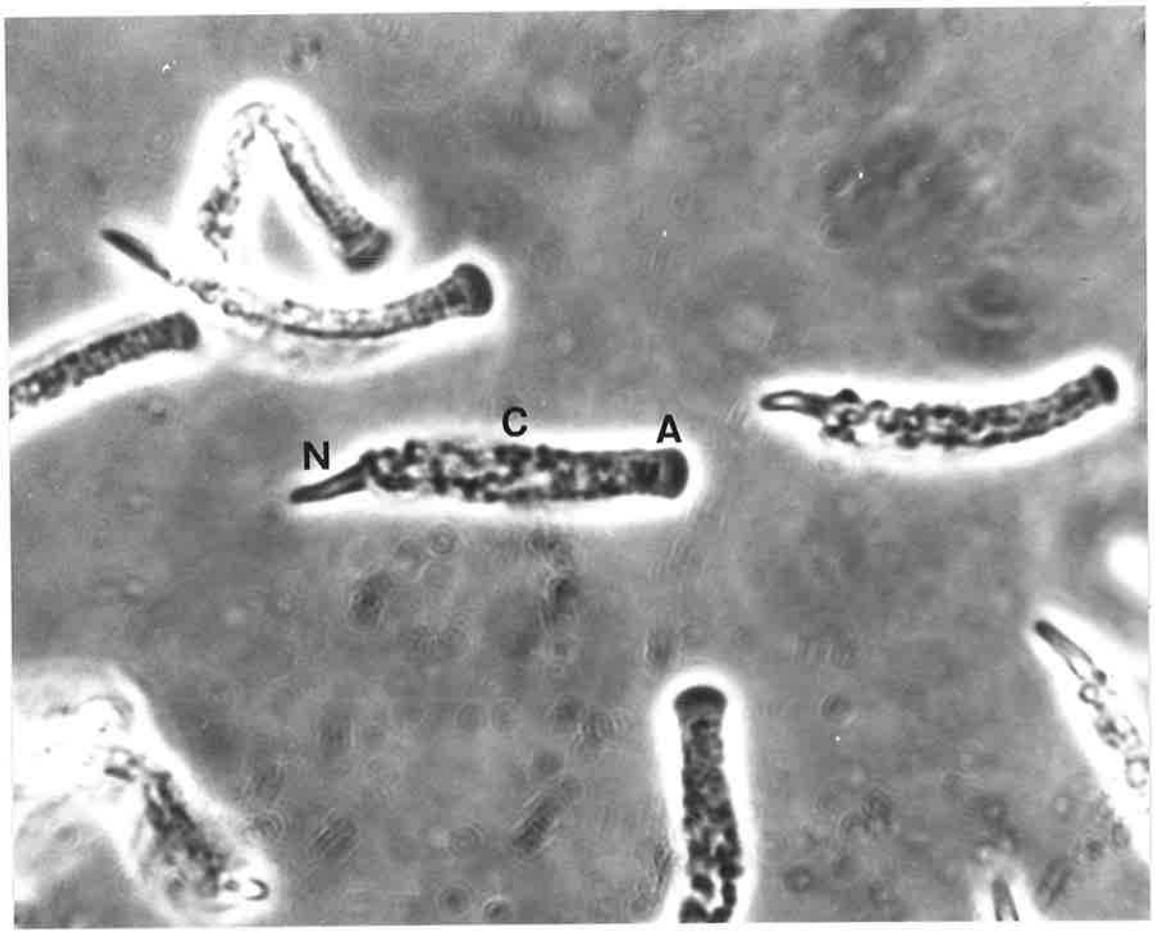

FIGURE 6.2 : Spermatozoa dissected from the seminal vesicle of a male of *N. dubius* showing nuclear tail (N), cytoplasmic region and amoeboid anterior (A).

confirm this with the electron microscope, as the higher resolving power of this instrument is capable of detecting differences between cells which would pass unnoticed in the light microscope.

6.2 Ultrastructure of the testis - spermatogenesis.

Spermatogonia and Early Spermatocytes.

A large nucleus, with a prominent nucleolus, occupies most of the spermatogonium (Figure 6.3). Numerous ribosomes, mitochondria, microtubules and some RER are seen in the cytoplasm. The mitochondria, with their pale matrices and plate-like cristae, are readily distinguished from the dense mitochondria of the testis epithelium (E). The early spermatocytes are characterized by synaptonemal complexes, around which the chromatin is condensed (Sy, Figure 6.4). Qualitatively, the cytoplasm is like that of spermatogonia, but it has increased in volume (Figures 6.4, 6.5). These early spermatogenic cells contain granular bodies (GB, Figures 6.4, 6.5) which resemble those seen in *N. brasiliensis*.

At the stage shown in Figure 6.5, the rachis has contracted into a central core of cytoplasm. It contains mitochondria, ribosomes and short fibrils (F) which give it a characteristic appearance. A narrow band of amorphous material lies immediately beneath its plasma membrane and is particularly noticeable where the spermatocytes and rachis join (arrowheads).

Late spermatocytes

As the spermatocytes move along the testis, they grow and differentiate. Their cytoplasm contains free ribosomes, mitochondria, and microtubules, as well as more RER and Golgi complexes than earlier stages (Figure 6.6). At about I300μm from the anterior tip of the testis, the spermatocytes begin to synthesize membranous organelles. They are formed from Golgi bodies, which are

FIGURE 6.3 : Late spermatogonium in the anterior testis of *N. dubius*. It contains a large nucleus, prominent nucleolus, numerous ribosomes, mitochondria, microtubules (arrows) and some RER. Mitochondria in the testis epithelium have a denser matrix than those in the sperm cells.

FIGURE 6.4 : Spermatocytes with large nuclei in which the chromatin is condensing around synaptonemal complexes. Microtubules (arrows) are numerous and in one cell a granular body lies near the nucleus.

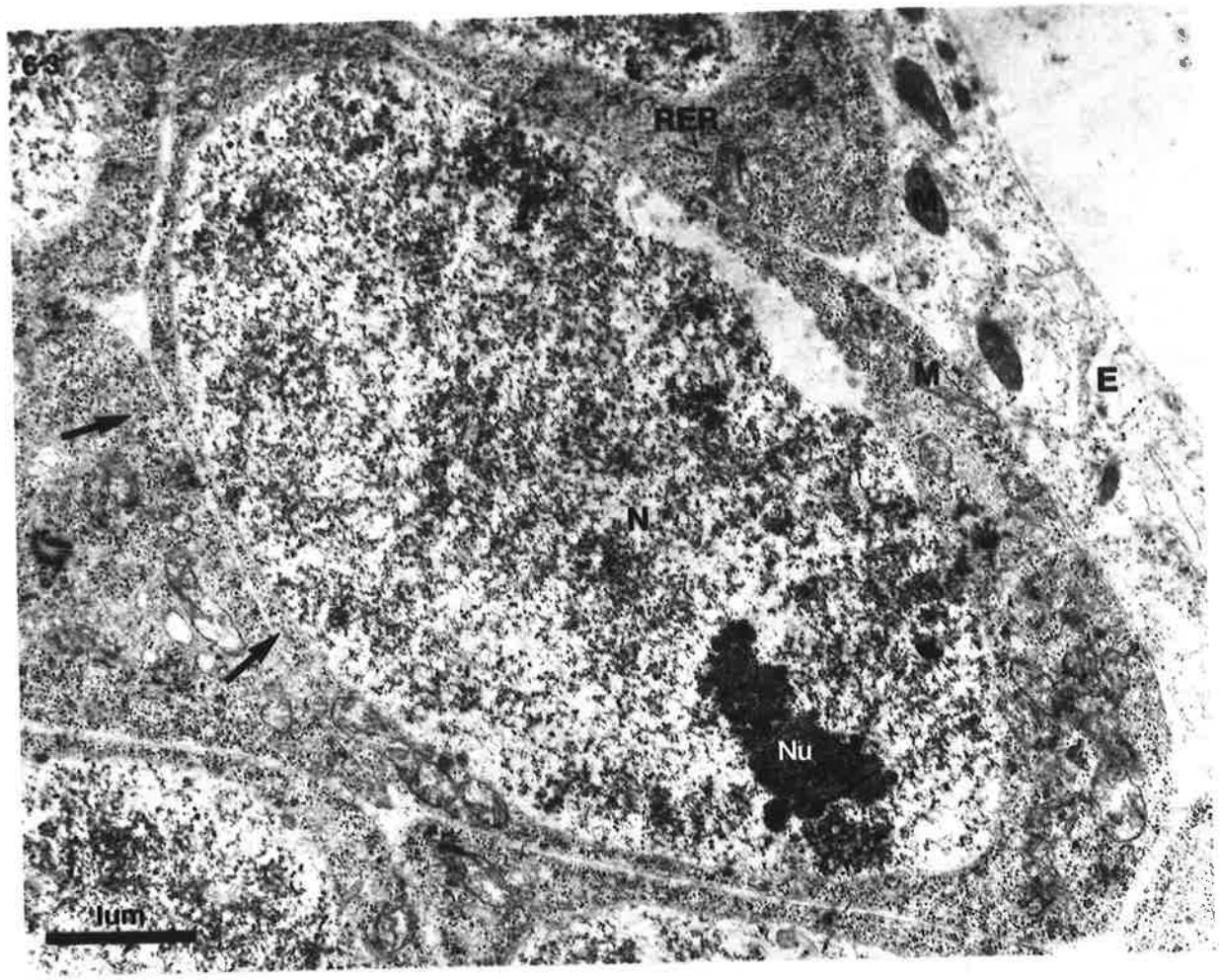
6-3
RER
M
E
N
Nu
1um

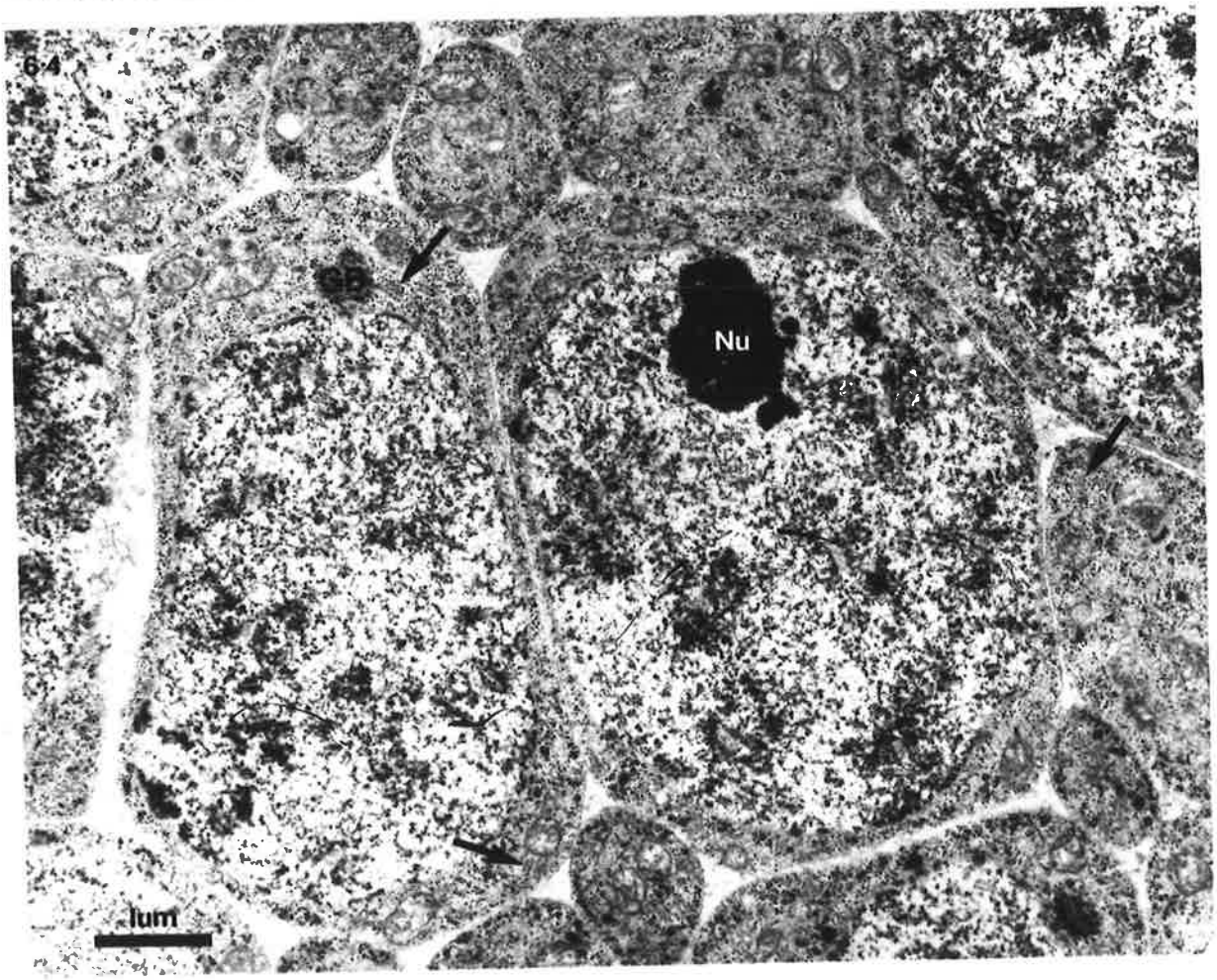
6-4
Nu
1um

FIGURE 6.5 : Longitudinal section showing early spermatocytes attached to the central axial rachis. The latter contains few ribosomes, but many short fibrils and its plasmalemma is lined by a dense material (arrow heads). Within the spermatocytes granular bodies are common; arrows point to microtubules beneath the plasma membrane and near the nucleus.

FIGURE 6.6 : Area at the junction of two spermatocytes and the rachis. At this stage, membranous organelles (long arrows) are beginning to be synthesized from the Golgi and RER. Short arrows show microtubules running between a spermatocyte and the rachis.

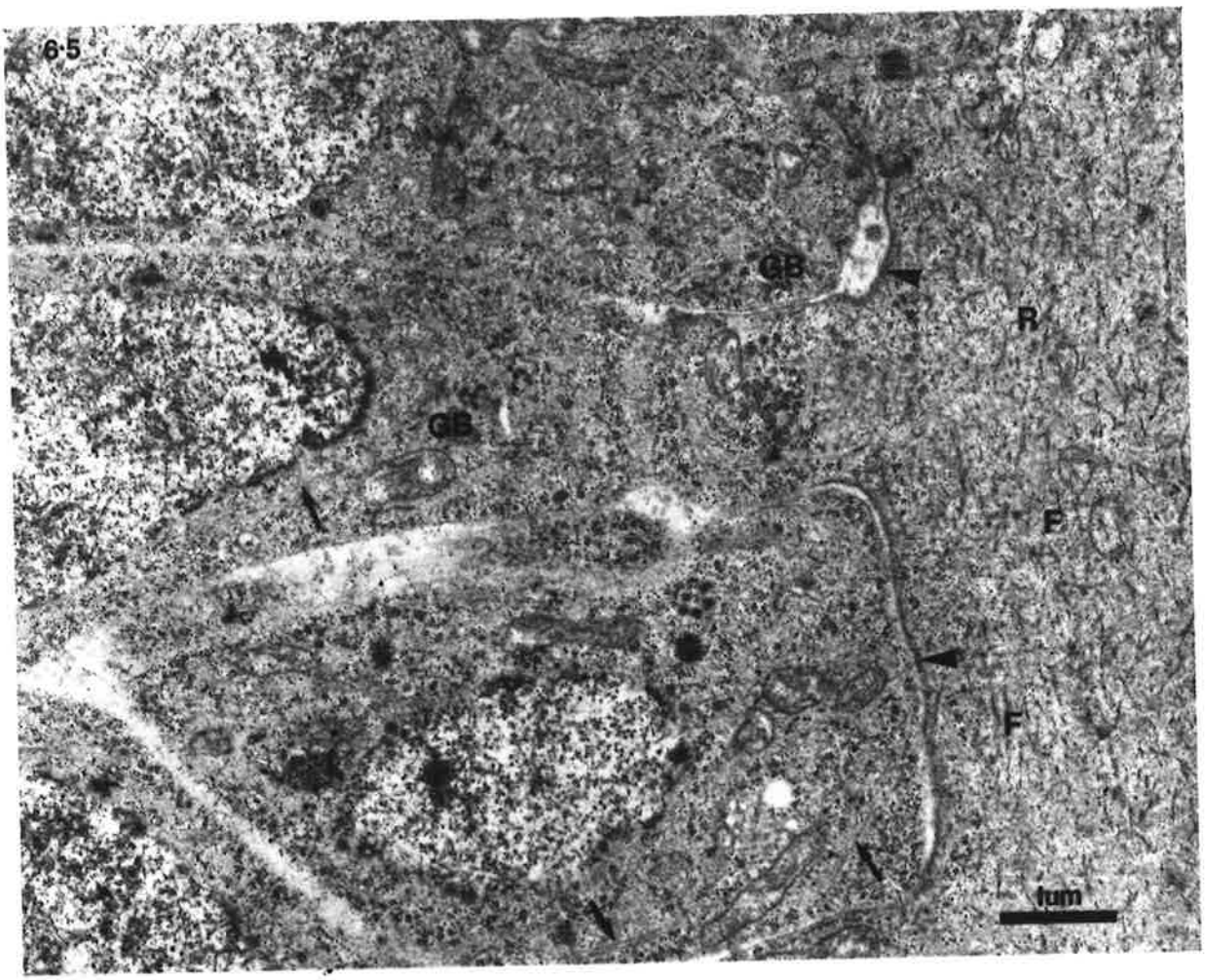
6·5
GB
GB
R
P
F
1um

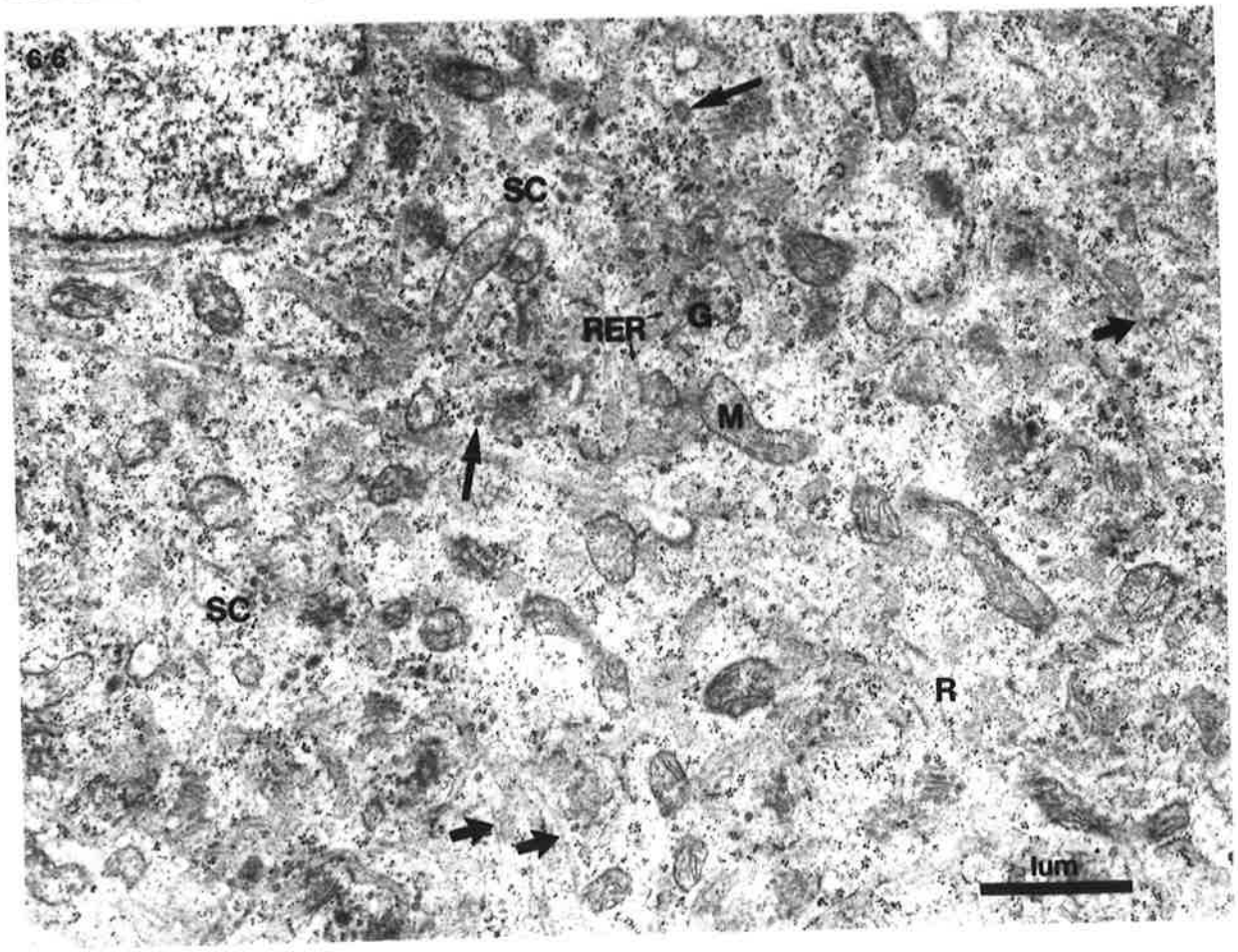
6·6
SC
RER
G
M
SC
R
1um

associated with tubular cisternae of RER (Figure 6.6). When they measure 0.3μm in diameter, an indentation forms on one side and is filled by a small deposit of material (arrow, Figure 6.7). Subsequently, this differentiates into a bundle of parallel fibres, labelled FB in Figure 6.8. Here the menbranous organelles have grown to a size of 0.7 - 0.8μm and the fibrous bodies occupy approximately one third of their volume. At this stage, some minor differences distinguish them from the membranous organelles in the spermatocytes of *N. brasiliensis*. In the latter, the vesicular part of the organelles forms a cup, which holds the fibrous body in a central cavity. In *N. dubius*, however, the vesicular part sits to one side and only a narrow arm encloses the fibrous body (compare Figures 6.8, 5.22). Whereas the membranous organelles of *N. brasiliensis* have pale inclusions, those of *N. dubius* contain one or more dense inclusions which are irregular in shape and variable in size (DI, Figures 6.8, 6.9).

The cytoplasm of spermatocytes at their latest stage of development is filled with membranous organelles, Golgi bodies, RER, ribosomes, microtubules and mitochondria (Figure 6.9). The nucleus is coarsly granular and often extends finger-like projections (Pr) into the cytoplasm. A thin layer of dense chromatin lines the inner leaflet of the nuclear envelope. The rachis contains extensive RER, as well as microtubules, mitochondria, and some membranous organelles (Figure 6.I0). Its plasma membrane still bears a thin layer of dense material (arrows).

Meiosis

As they approach meiosis, the wedge-shaped spermatocytes become spherical and measure I4-I5μm across (Figure 6.II). Although the rachis is branched and thread-like, the spermatocytes maintain their connection with it. The condensing chromosomes (Ch), surrounded by

FIGURE 6.7 : Tip of a spermatocyte near the testis epithelium; MOs have developed an indentation on one side (arrows) and in some, this is filled with a small deposit. RER and Golgi bodies are closely associated with the MOs.

FIGURE 6.8 : In late spermatocytes, up to 1/3 of the volume of each MO is occupied by a fibrous body. The vesicular part, which often contains one or more dense inclusions, lies to one side and only a narrow arm encloses the fibrous body.

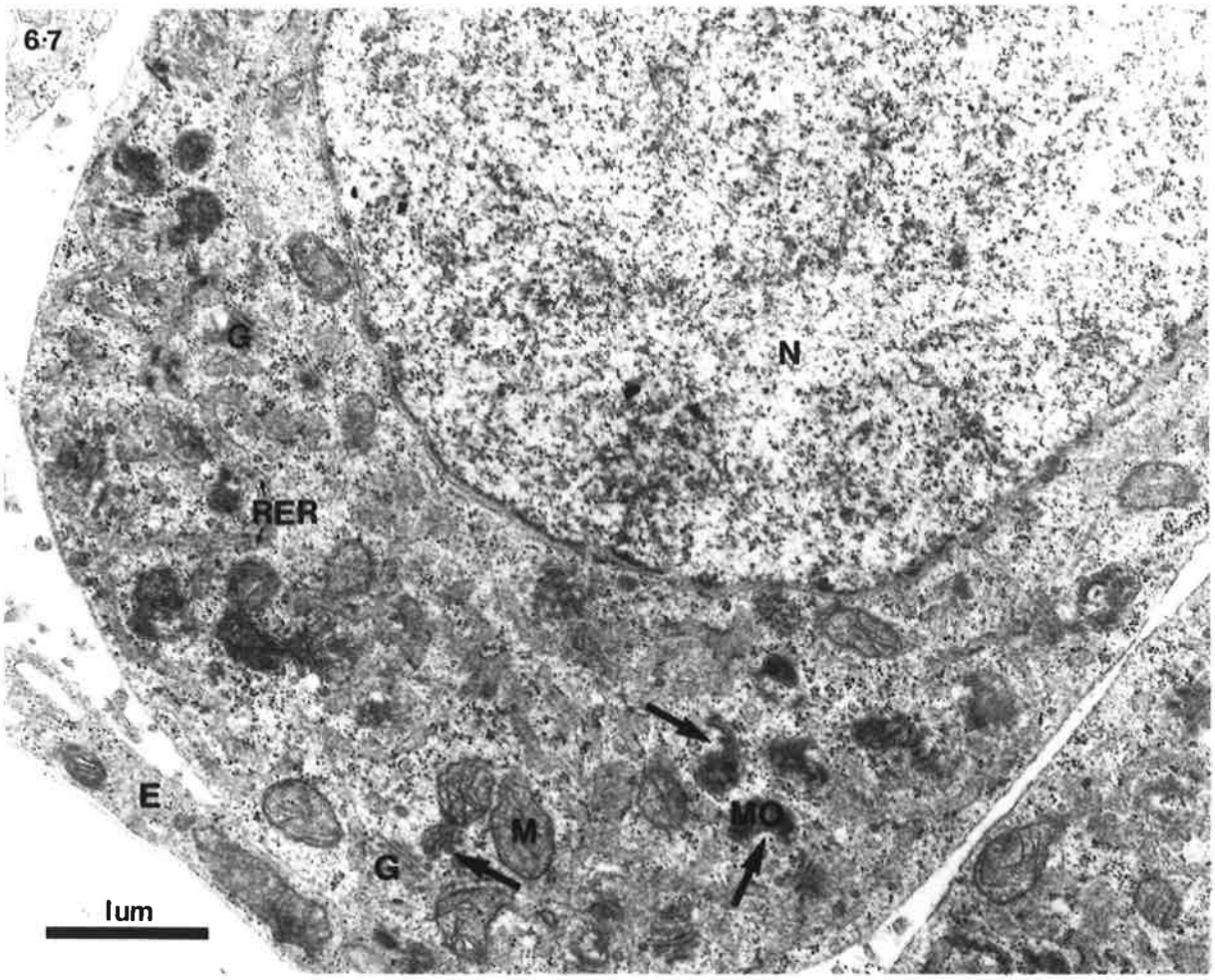
6·7
G
N
RER
E
M
G
MO
1um

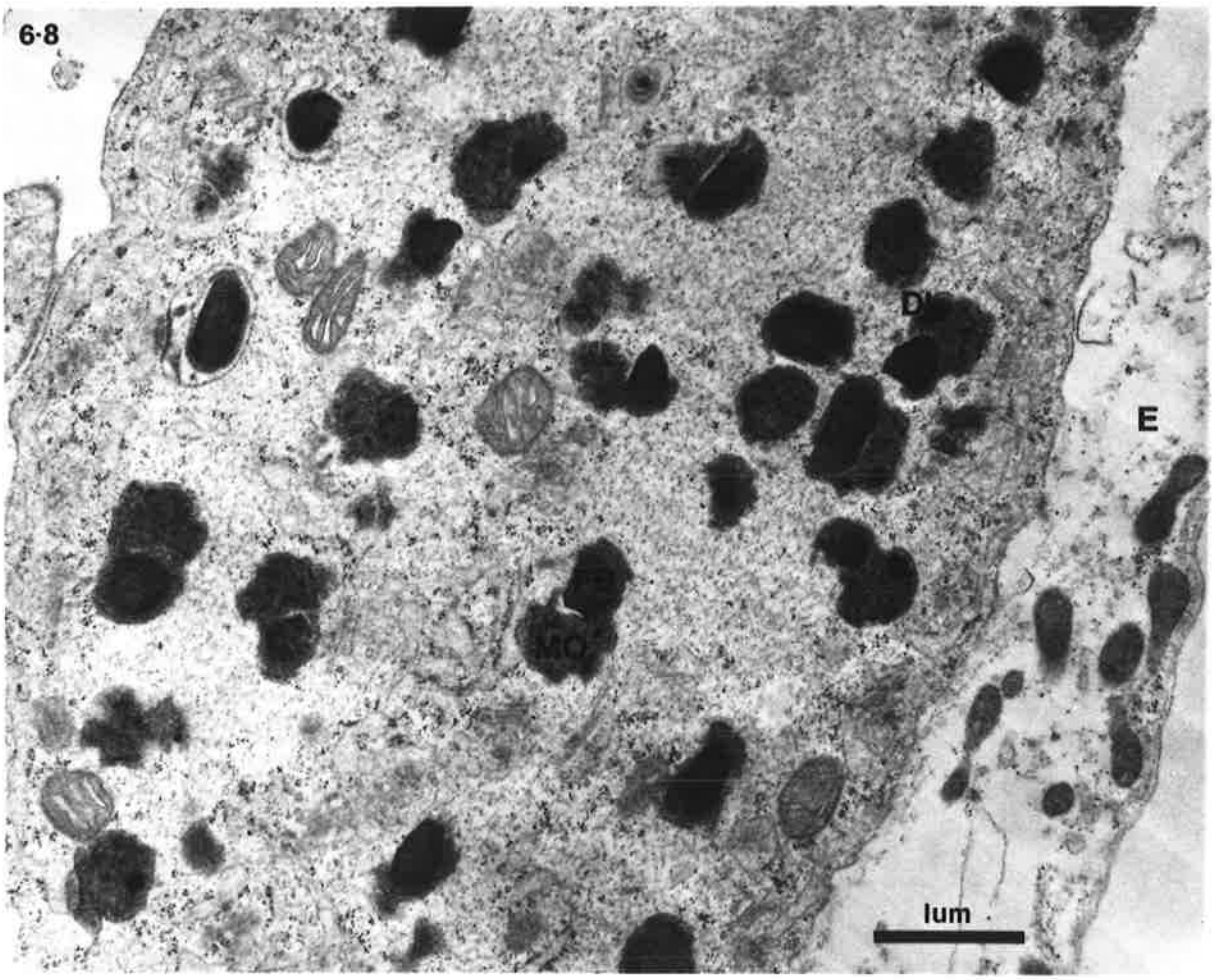
6·8
D
E
MO
1um

FIGURE 6.9 : Group of spermatocytes containing many MOs, associated RER and Golgi, mitochondria, microtubules (arrows) and ribosomes. The inner leaflet of the nuclear envelope is lined by a thin layer of dense chromatin which sometimes aggregates into dense patches. Thin finger-like protrusions of the nucleus extend out into the cytoplasm.

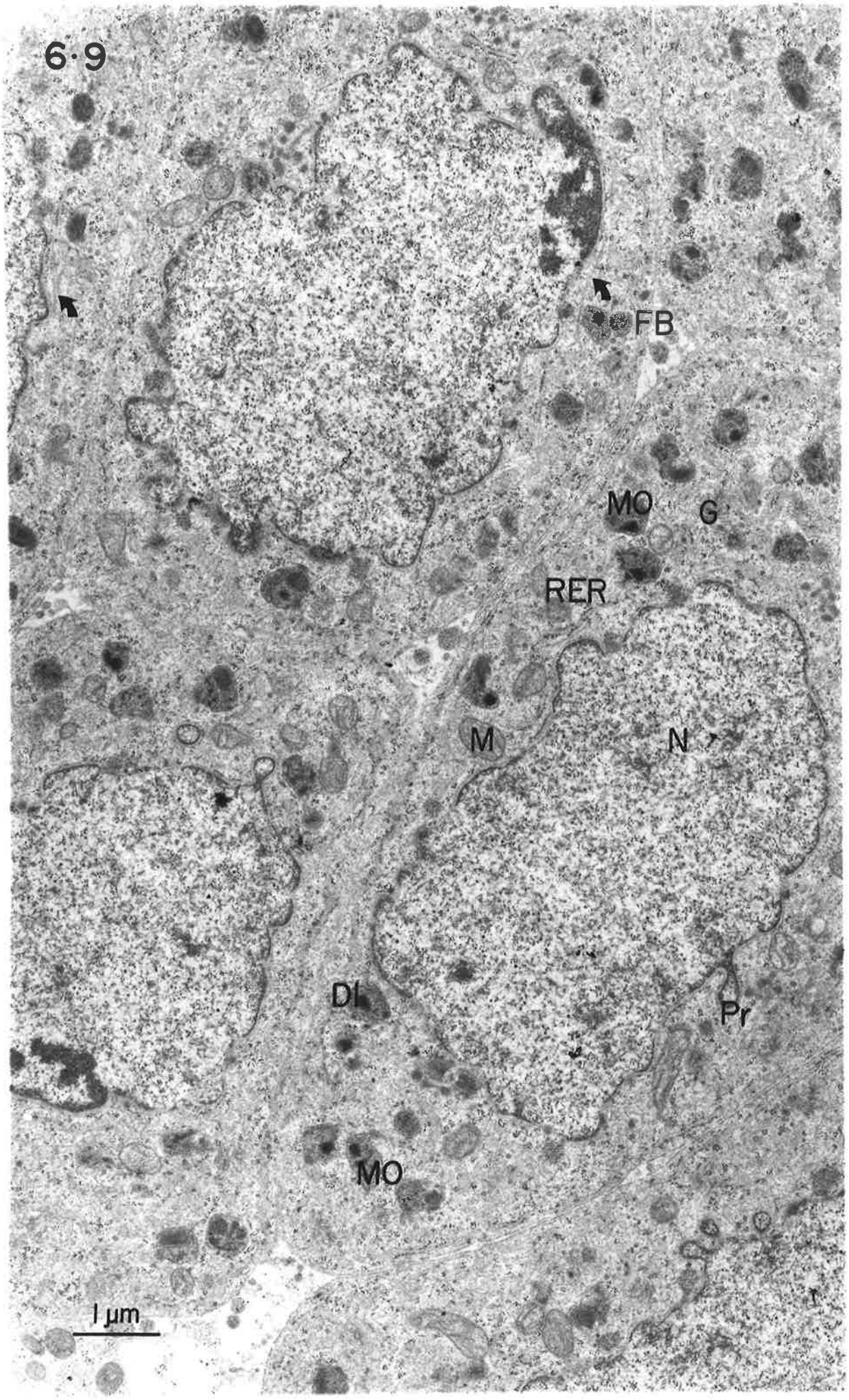
6·9
FB
MO
G
RER
M
N
Dl
Pr
MO
1 µm

FIGURE 6.10 : Two spermatocytes joined to the rachis. The cytoplasm of the latter is distinguished by anastomosing tubules of RER and short fibrils; it also contains mitochondria and MOs. Arrows point to material lining the plasmalemma of the rachis.

FIGURE 6.11 : A spermatocytes in which the chromosomes have condensed and the nuclear envelope has broken down in preparation for meiosis. Spindle fibres surround the chromosomes and the cytoplasmic organelles have moved to the periphery.

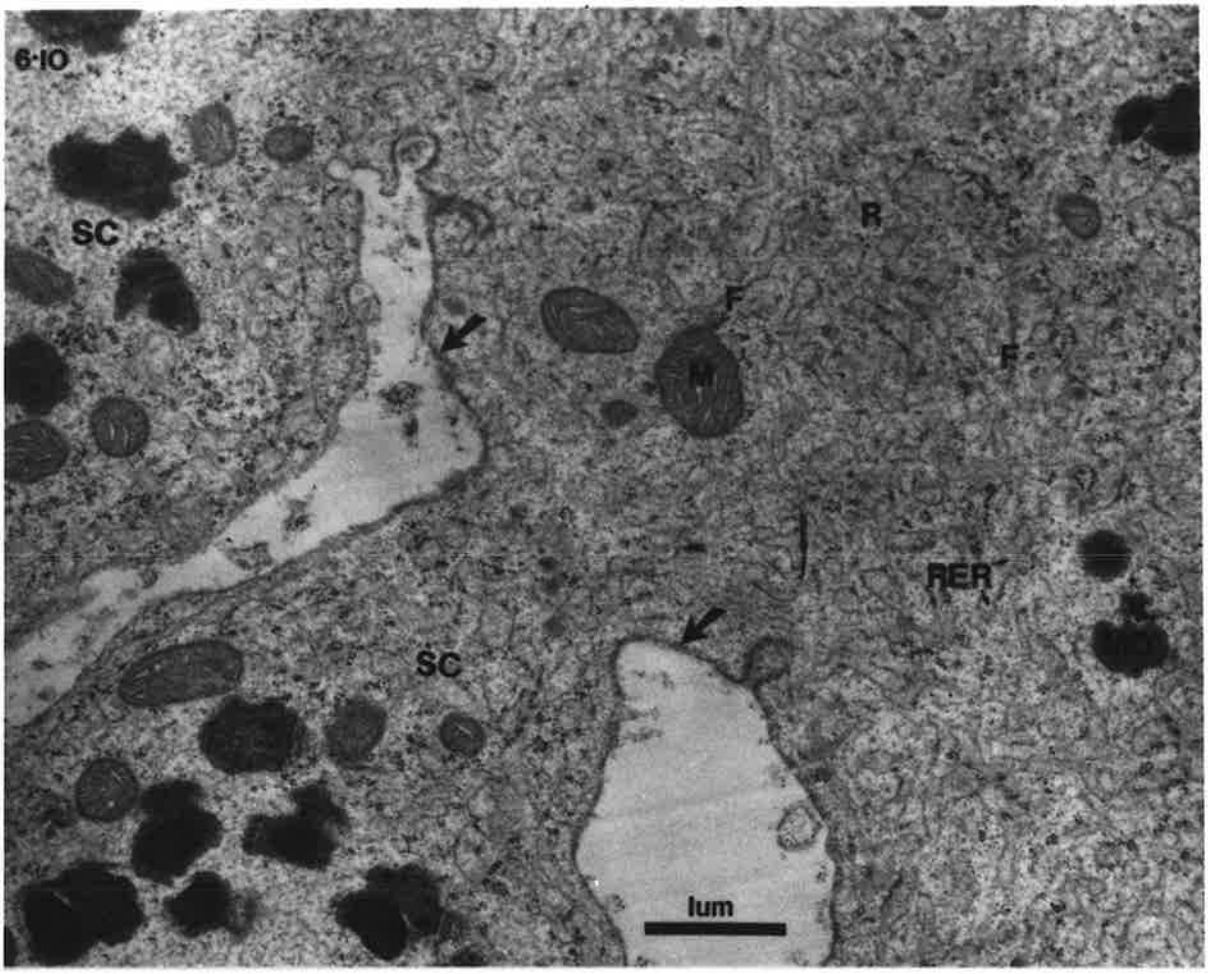
6·10
SC
R
F
M
F
RER
SC
lum

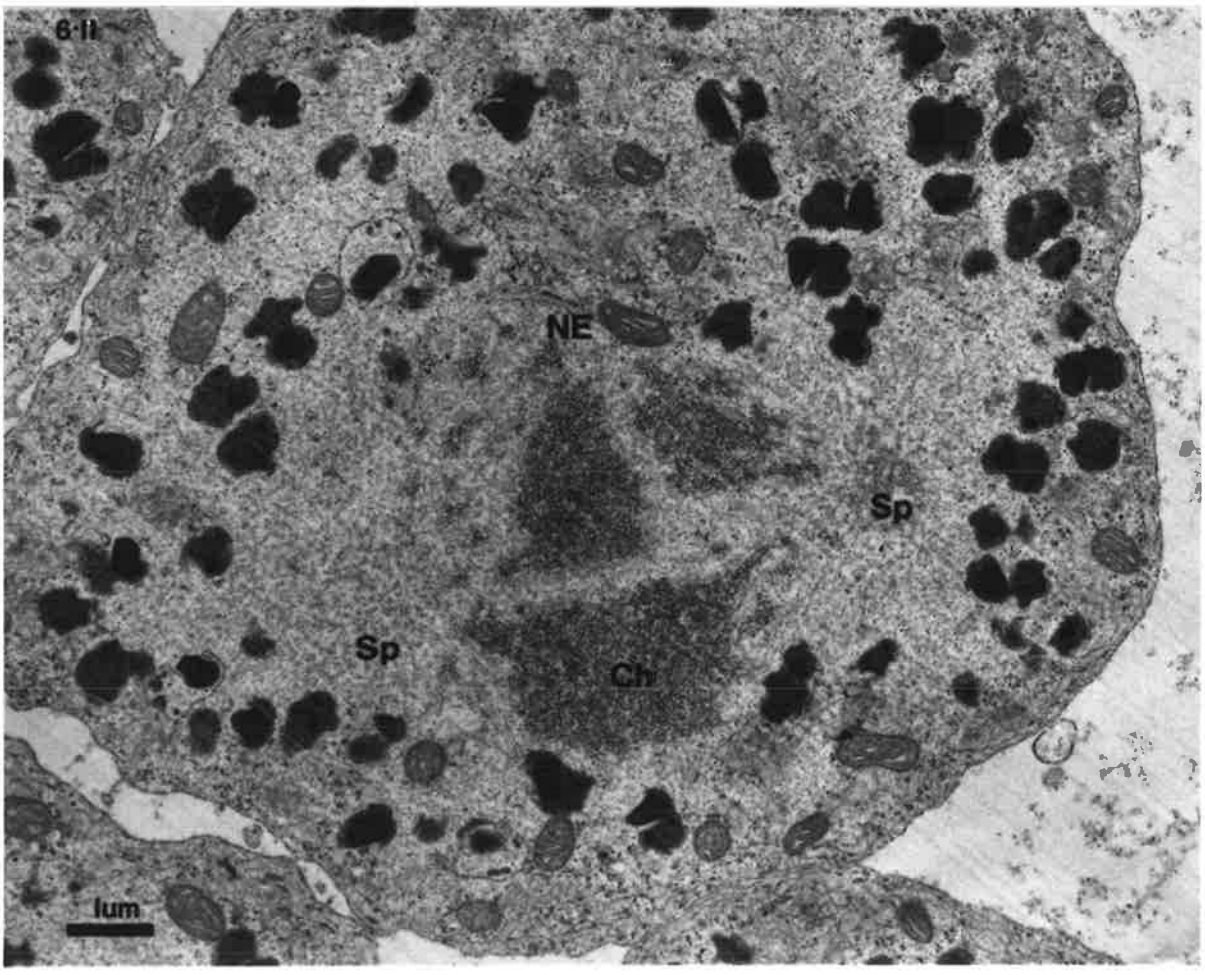
6·11
NE
Sp
Sp
Ch
lum

remnants of the nuclear envelope (NE), occupy the centre of the cell. On either side are the centrioles (C, Figure 6.I2) which act as organizing centres for the microtubules of the spindle (Sp, Figures 6.II, 6.I2). The membranous organelles, mitochondria, Golgi bodies, and RER have moved to the periphery and are distributed equally to the 4 spermatids during divison.

Spermatids

The spermatids are spherical, 8-9μm in diameter, and have a central mass of chromatin not bounded by a nuclear envelope (Cr, Figure 6.I3). Two centrioles (C), perpendicular to one another, lie on one side of the chromatin, while the other organelles remain at the outer perimeter of the cell. Narrow threads of rachis (R), identified by their characteristic cytoplasm, still connect the spermatids.

In the next stage of differentiation, the chromatin condenses into fine dense filaments (Cr, Figure 6.I4), leaving the centrioles sitting in a hollow to one side. Microtubules (arrows) are found around the centrioles as well as at the outer edge of the chromatin and in the surrounding cytoplasm. As the filaments of chromatin wind into a spiral, the nucleus elongates. Ultimately, it resembles an arrowhead, with the centrioles sitting in a hollow at its base (Figure 6.I5).

As the nucleus elongates, so does the spermatid. The RER, Golgi bodies and ribosomes move to the posterior of the cell, which is now occupied by the pointed tip of the nucleus. This is also the region in which the spermatids are connected to one another. The nuclear complex, including the centrioles, then moves backwards through the cytoplasm (Figure 6.I5). Microtubules may be involved in this movement as they extend forward from the centrioles to the anterior of the cell (arrows). As the chromatin evaginates to form

FIGURE 6.12 : Spermatocyte approaching meiosis; here the nuclear envelope is just beginning to break down. Many microtubules radiate out from the centriole on the left to form the aster.

FIGURE 6.13 : Spermatid just after division; the chromatin is a dense mass at the centre of the cell, unbounded by a nuclear envelope. Two centrioles, perpendicular to each other, lie on one side of the DNA. MOs and other organelles are at the edge of the cell. At the top right of the figure are remnants of the rachis.

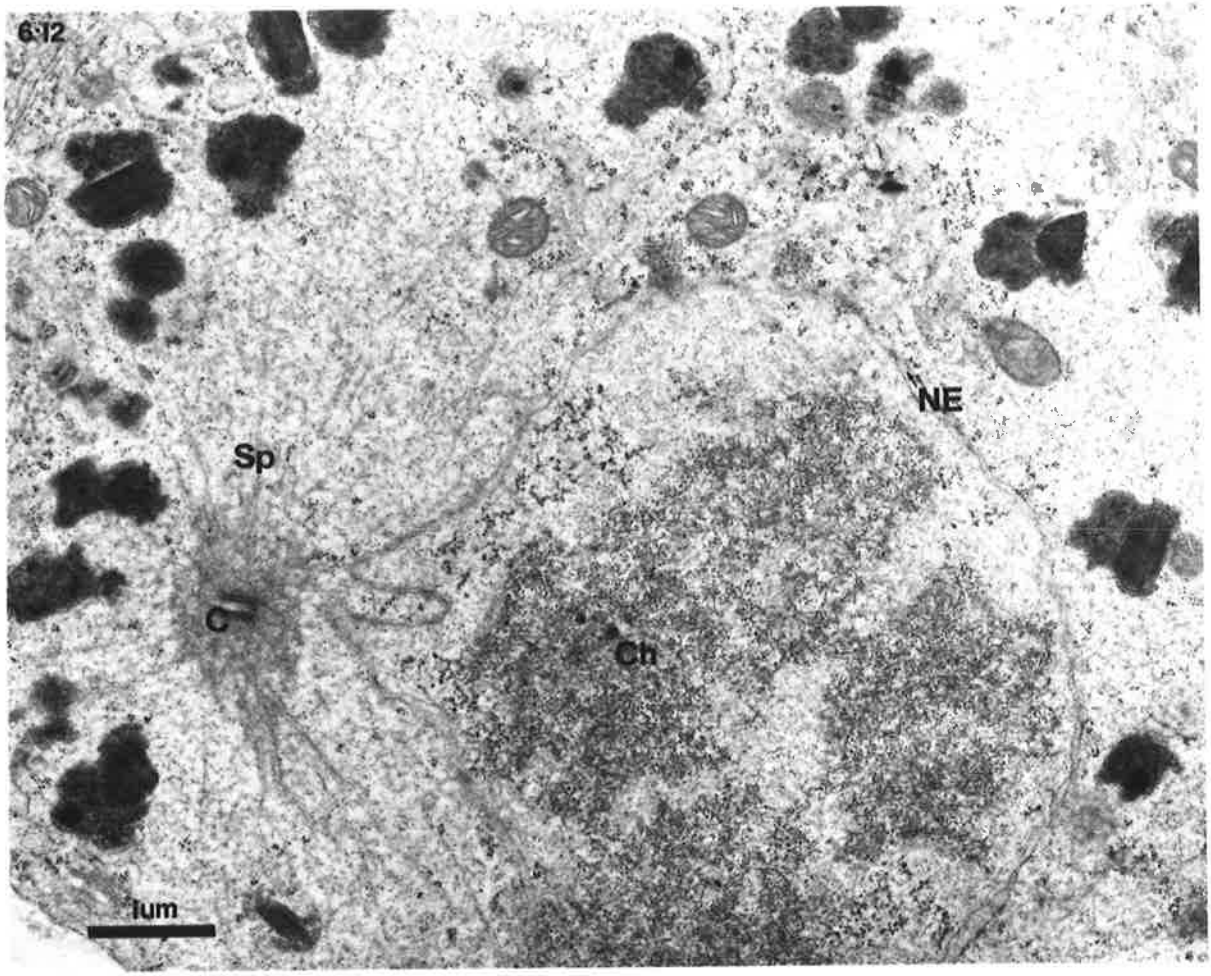
6·12
NE
Sp
C
Ch
lum

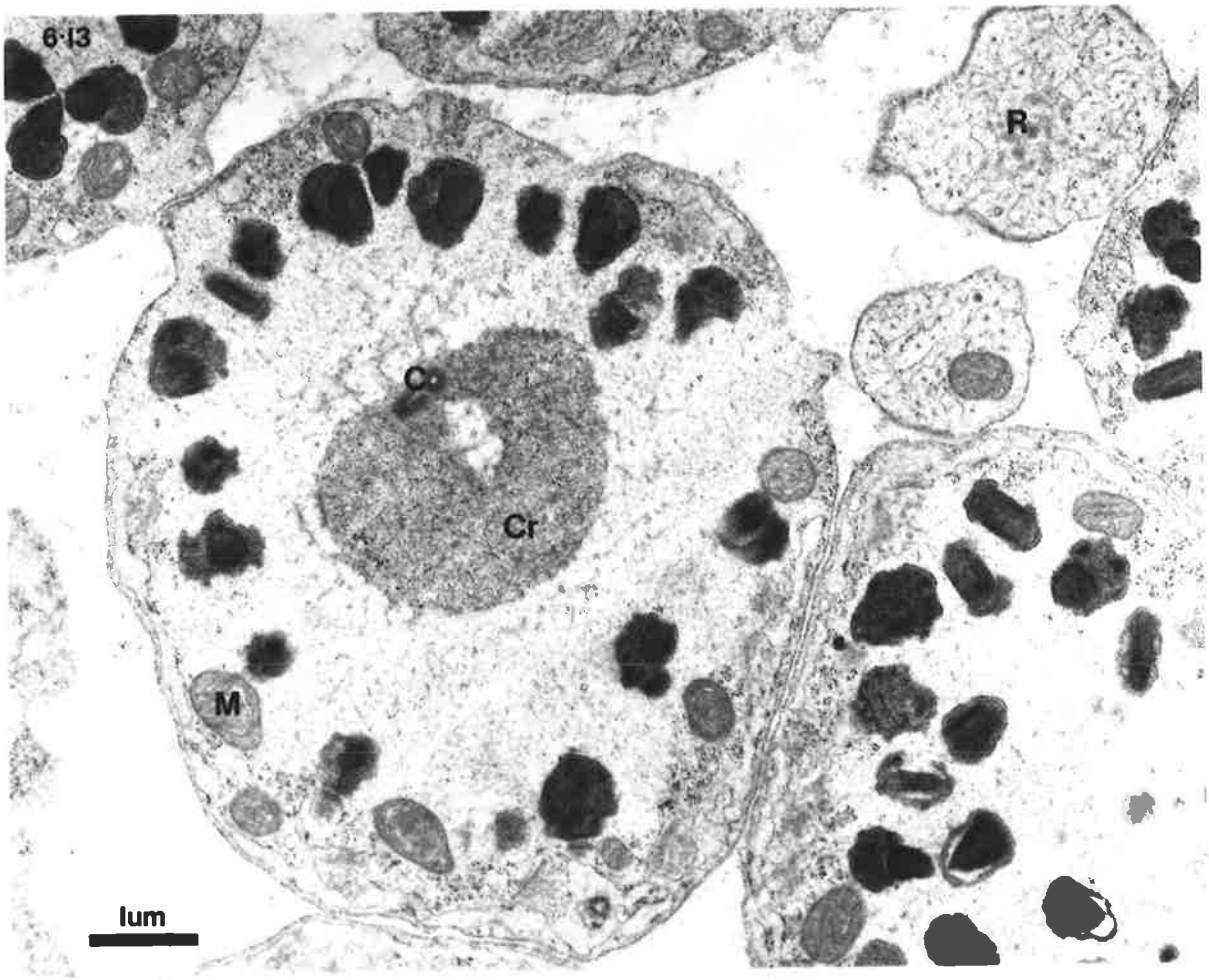
6·13
R
C
Cr
M
lum

FIGURE 6.14 : In these spermatids, the chromatin has condensed into filaments which are winding into a spiral. The centrioles sit in a hollow on one side and are surrounded by microtubules (arrows). The latter also encircle the chromatin and lie in the cytoplasm closeby. The MOs are now more cup-like, with the fibrous body in a central depression. Small invaginations (arrow heads) and sometimes a knob form on one side of them; dense inclusions are still present. Most of the other cytoplasmic organelles (except mitochondria) have moved to one end of the spermatids.

FIGURE 6.15 : The residual bodies from many sperm fuse to form large masses of cytoplasm like that shown here. Note how swollen the pools of RER have become. The chromatin of the sperm is now in the shape of an arrow head, with the centrioles at its base. Microtubules (arrows) run forwards from the DNA to the anterior. Knobs are visible on many MOs.

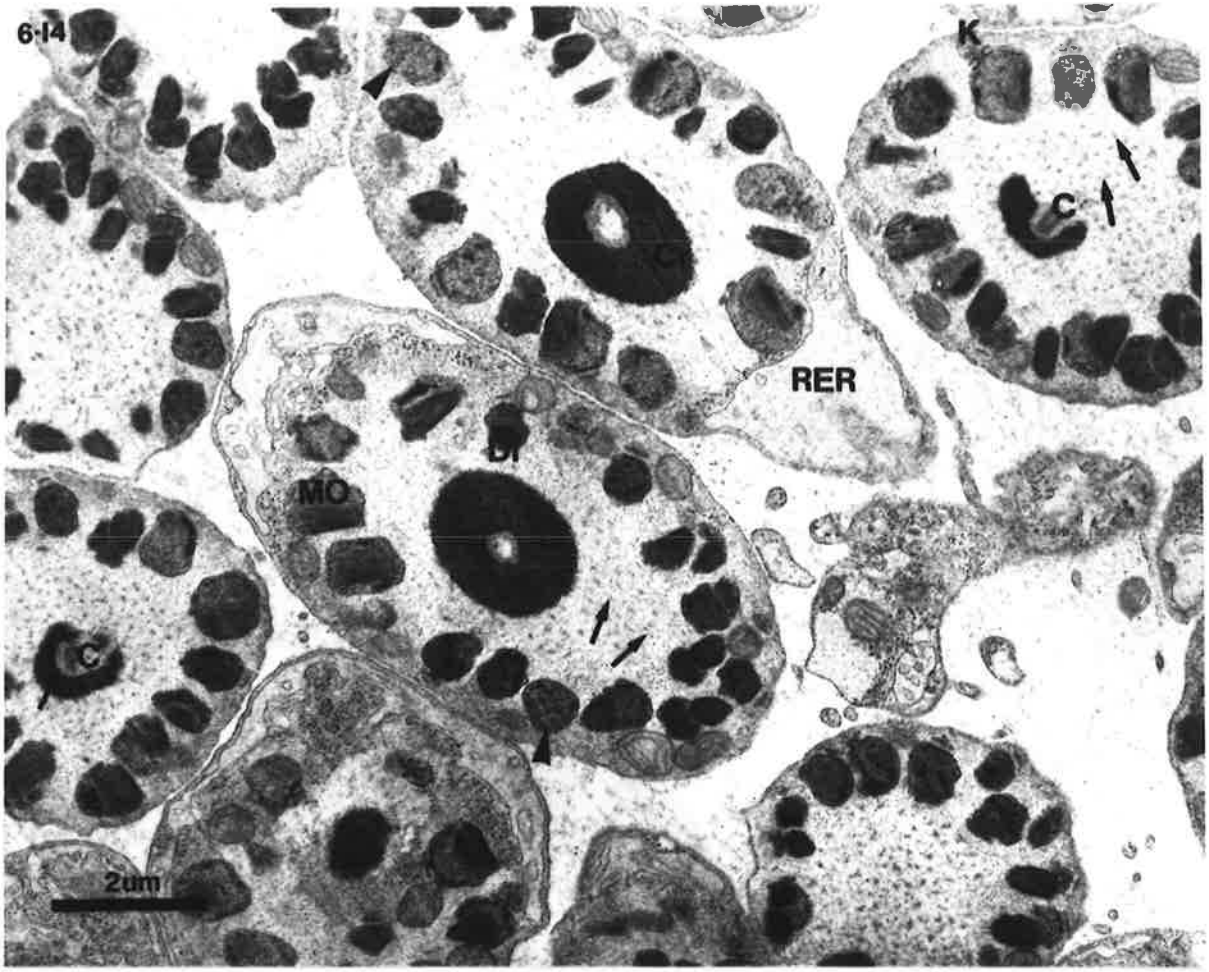
6·14
K
C
RER
MO
C
2um

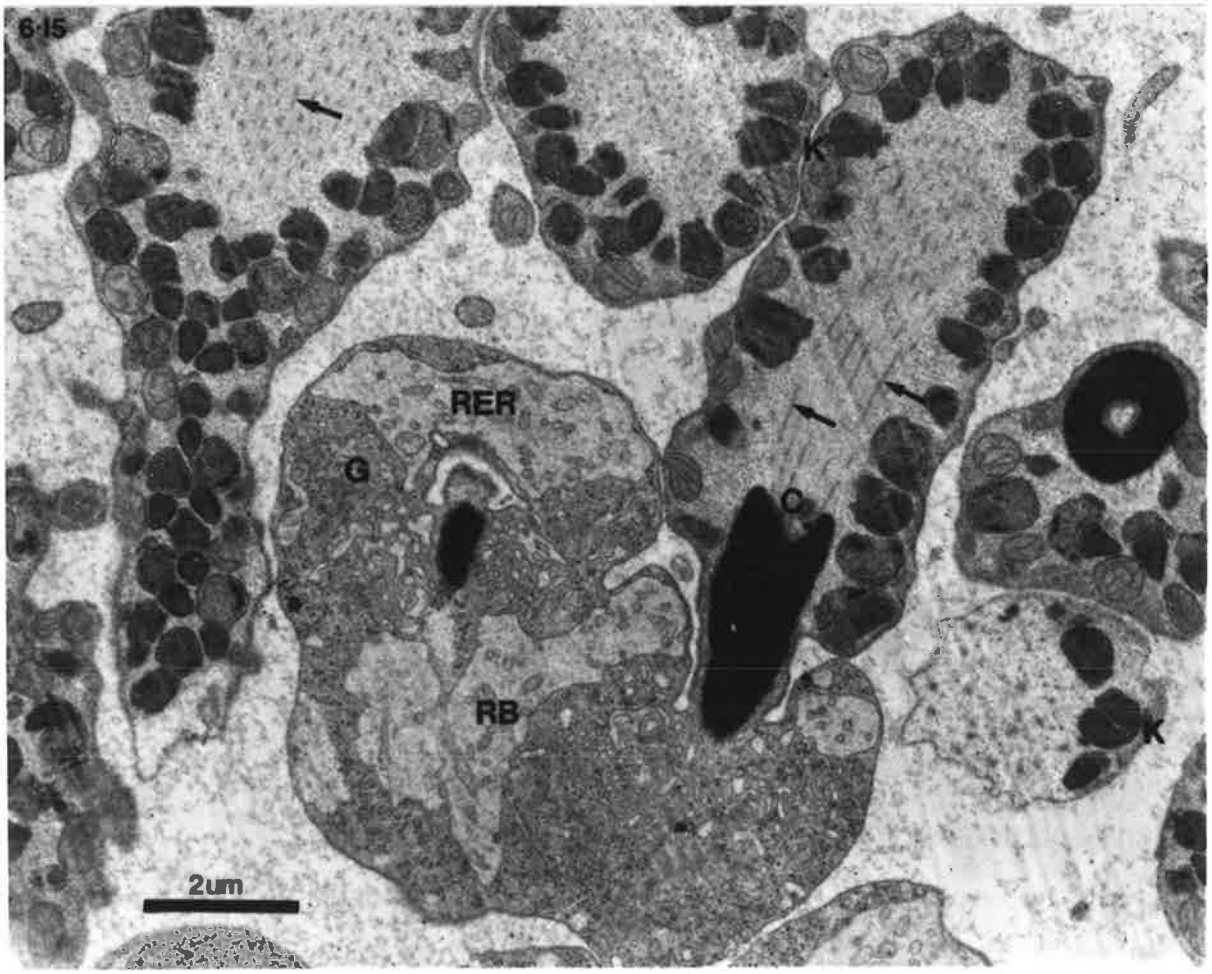
6·15
K
RER
G
C
RB
K
2um

the tail, the residual cytoplasm is extruded into a common pool (RB). At first, RER and Golgi bodies engage in considerable synthetic activity. They then begin to break down and finally the whole cytoplasmic mass is absorbed by the testis epithelium.

Some of the cytoplasmic organelles also undergo changes at this time. The membranous organelles, which now measure I.0 - I.Iμm, have become more like those of *N. brasiliensis* (Figure 6.I4). They are cup-shaped, with the central depression occupied by the fibrous body. Dense inclusions are still found within them. On the side opposite the fibrous body, a knob(K) and a number of tube-like invaginations (arrowheads) have formed.

Spermatozoa.

The final phase of development of the membranous organelles occurs during maturation of the spermatozoon. It can be traced in Figures 6.I6, 6.I7, and 6.I8. First, the fibrous body dissolves into the cytoplasm, allowing the remainder of the organelle to assume a spherical shape, 0.7μm across. The knob is large now and contains tiny vesicular elements (inset, Figure 6.I7); the invaginations around it have deepened. Subsequently, the majority of membranous organelles lose their dense inclusions and at the same time, a dense material precipitates in the cytoplasm nearby (arrows, Figures 6.I6, 6.I7, 6.I8). These small deposits soon fuse to form several large electron-dense clumps, which do not appear to be membrane-bound (inset, Figure 6.I6). Figure 6.I9 illustrates the development and differentiation of the membranous organelles in both *N. dubius* and *N. brasiliensis*. It summarizes many of the descriptions presented in Chapters 5 and 6 and depicts both similarities and differences between the membranous organelles of the two species. Freeze-fracture provides a three-dimensional view of the membranous organelles in the

FIGURE 6.16 : In these spermatozoa, the fibrous bodies have moved out from the vesicular parts of the MOs and are 'dissolving'. The MOs become more rounded and a dense material (arrows) is seen closeby. Inset shows this material at higher magnification. The chromatin of the sperm is now extremely dense.

FIGURE 6.17 : In these sperm the fibrous bodies have disappeared and an amoeboid region is evident at the anterior. Note that the plasmalemma is lined by flocculent material except in this region. The dense material which is presumed to come from the MOs has aggregated into small spheres. Inset shows the tiny vesicles in the knobs of the MOs.


6·16
K
K
MO
Cr
M
FB
0·4um

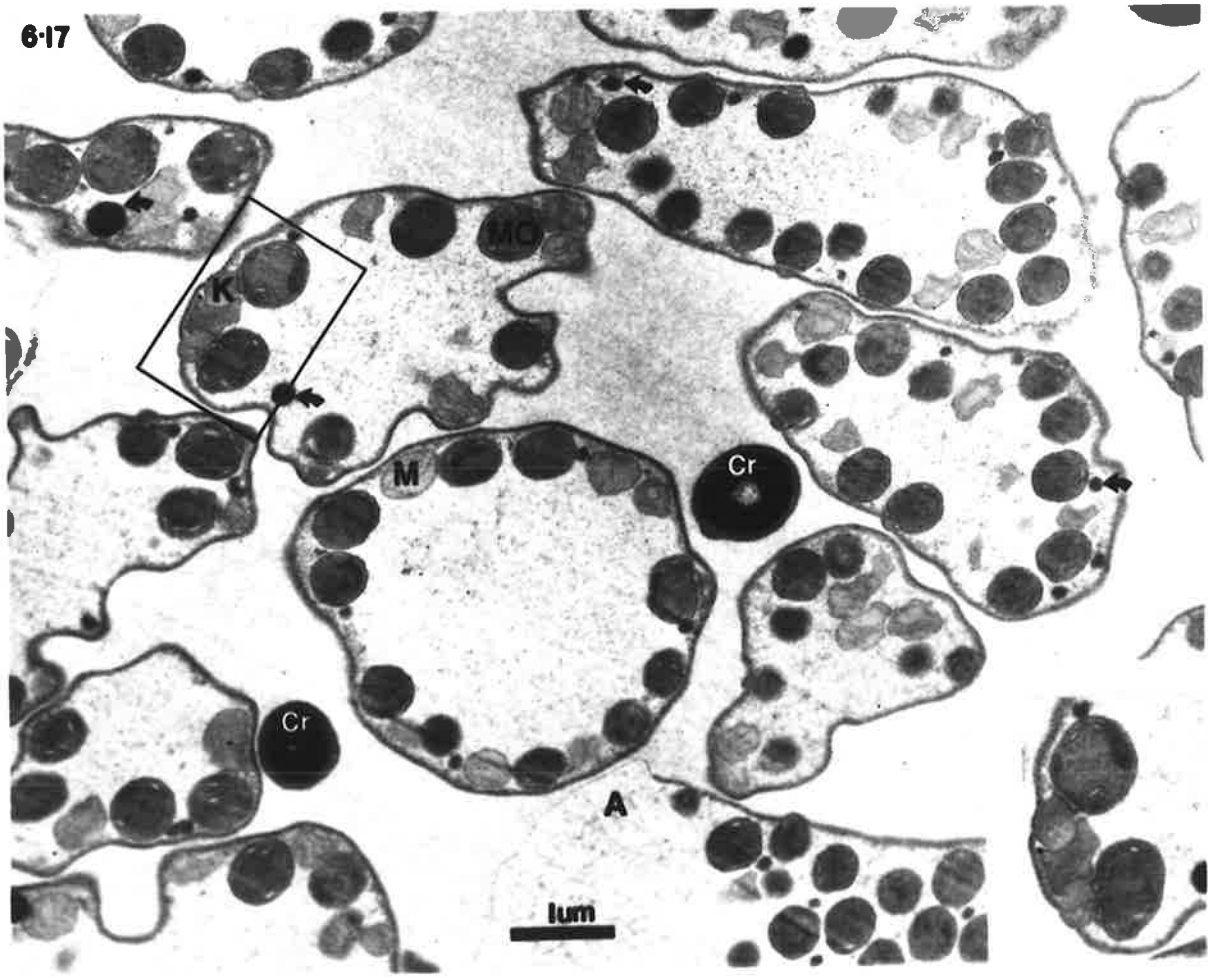
6·17
MO
K
M
Cr
Cr
A
1um

FIGURE 6.18 : Mature spermatozoa in the seminal vesicle. The amoeboid region of the sperm is large and contains a rather granular material and centrioles are still associated with the chromatin, which is very dense. The dense material which appeared to come from the MOs is still present in small spheres (arrows).

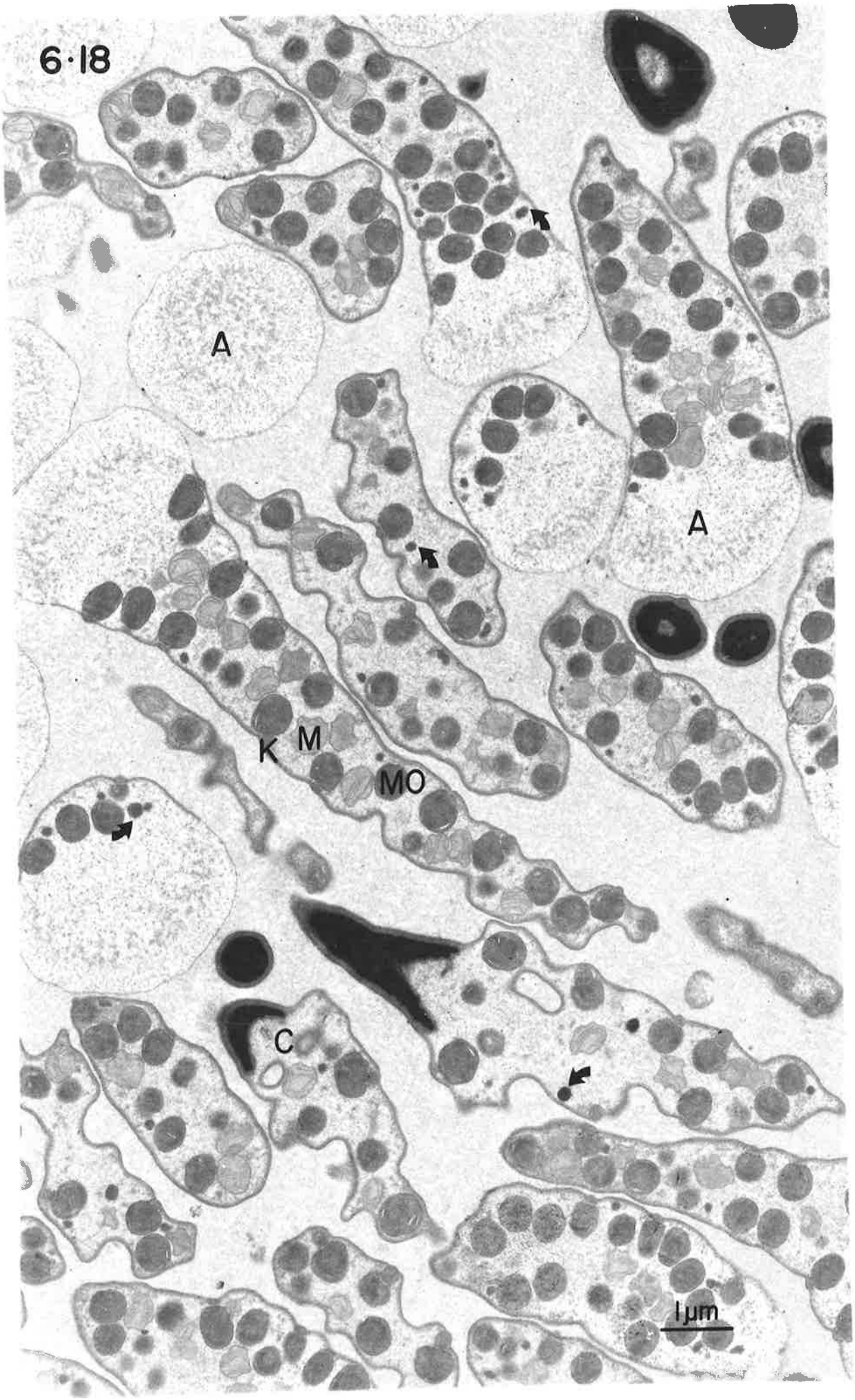
6·18
A
A
K
M
MO
C
1 µm

FIGURE 6.19 : Summary of the formation and differentiation of membranous organelles in *N. brasiliensis* and *N. dubius*. Their morphology is very similar initially, but as the fibrous body enlarges, interspecific differences become obvious. After activation in both species, the MOs fuse with the plasmalemma and release their electron-dense contents.

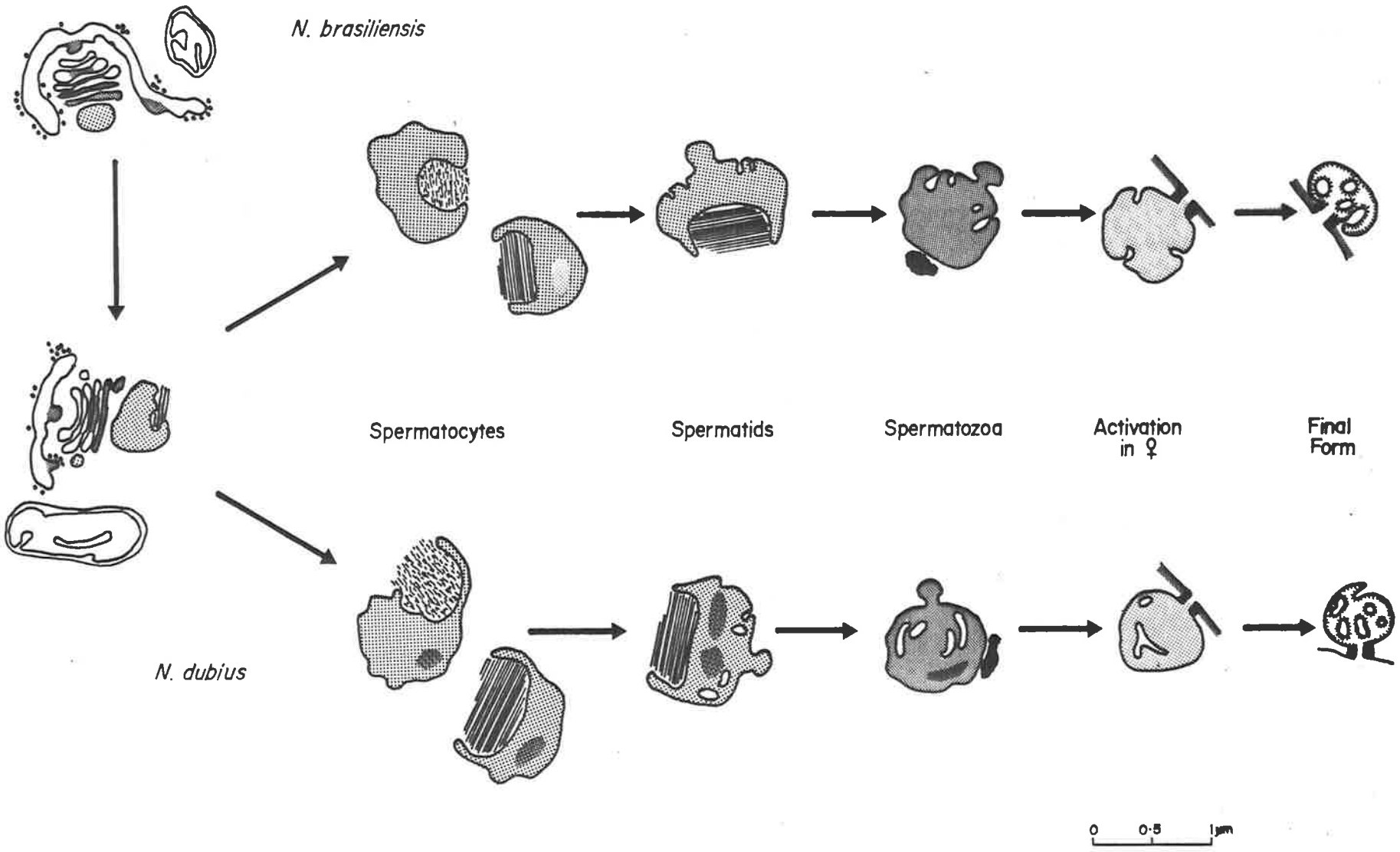
N. brasiliensis
Spermatocytes
Spermatids
Spermatozoa
Activation in ♀
Final Form
N. dubius
0 0·5 1μm

mature sperm (Figure 6.20 A,B). The knob (K) and its surrounding invaginations (arrows) are shown particularly clearly. On the PF-face, there are particle clusters, interspersed by bare patches of membranes, the EF-face, however, has very few particles.

After extruding the nucleus and residual body, the spermatozoa are oval and measure II-I2μm long. Organelles line their perimeter (Figure 6.I6), except in the amoeboid anterior (A, Figure 6.I7). The centre of the sperm is filled with an amorphous flocculent material and a dense layer, 6nm thick, lines the plasma membrane of the cytoplasmic, but not the amoeboid region. Sperm in the seminal vesicle have attained their final form (Figure 6.I8). They are longer and thinner now and the organelles have become more closely packed. Their DNA is so highly condensed that individual filaments are difficult to distinguish. Tests with I% SDS and 0.IM DTT, like those performed on the sperm of *N. brasiliensis* (Chapter 5.2), showed that ionic and not covalent bonding is responsible for holding the DNA in this condensed form. Although there is no nuclear envelope, an 85nm thick band of medium electron-density lies between the chromatin and the plasma membrane. A narrower band of similar material lines the indentation at the base of the chromatin. Figure 6.2I A, B and C shows the formation of this substance. Just after the nucleus is extruded, a coarse, granular material surrounds the chromatin. It soon loses this granularity and becomes more electron-dense. The two centrioles remain in the indentation at the cytoplasmic end of the nuclear tail (Figure 6.2I C).

6.3 Maturation of the sperm after insemination.

Light microscopy reveals that the spermatozoa of *N. dubius*, like those of *N. brasiliensis*, undergo substantial changes after insemination. Although the nucleus is unaltered, the cytoplasmic

FIGURE 6.20A,B : Cross-fracture of seminal vesicle showing mature sperm. The knob and invaginations (arrows) of the MOs are clearly visible; the EF-faces of their membranes have few particles but on the PF-faces, the IMPs are aggregated into clumps.

FIGURE 6.21A,B,C : Series of micrographs showing changes in the material surrounding the chromatin of maturing sperm. Initially (A) the material is granular (at this stage microtubules (arrows) may still be seen), it then loses its granularity (B) and becomes more electron dense (C). In C a centriole can be seen in the indentation at the cytoplasmic end.

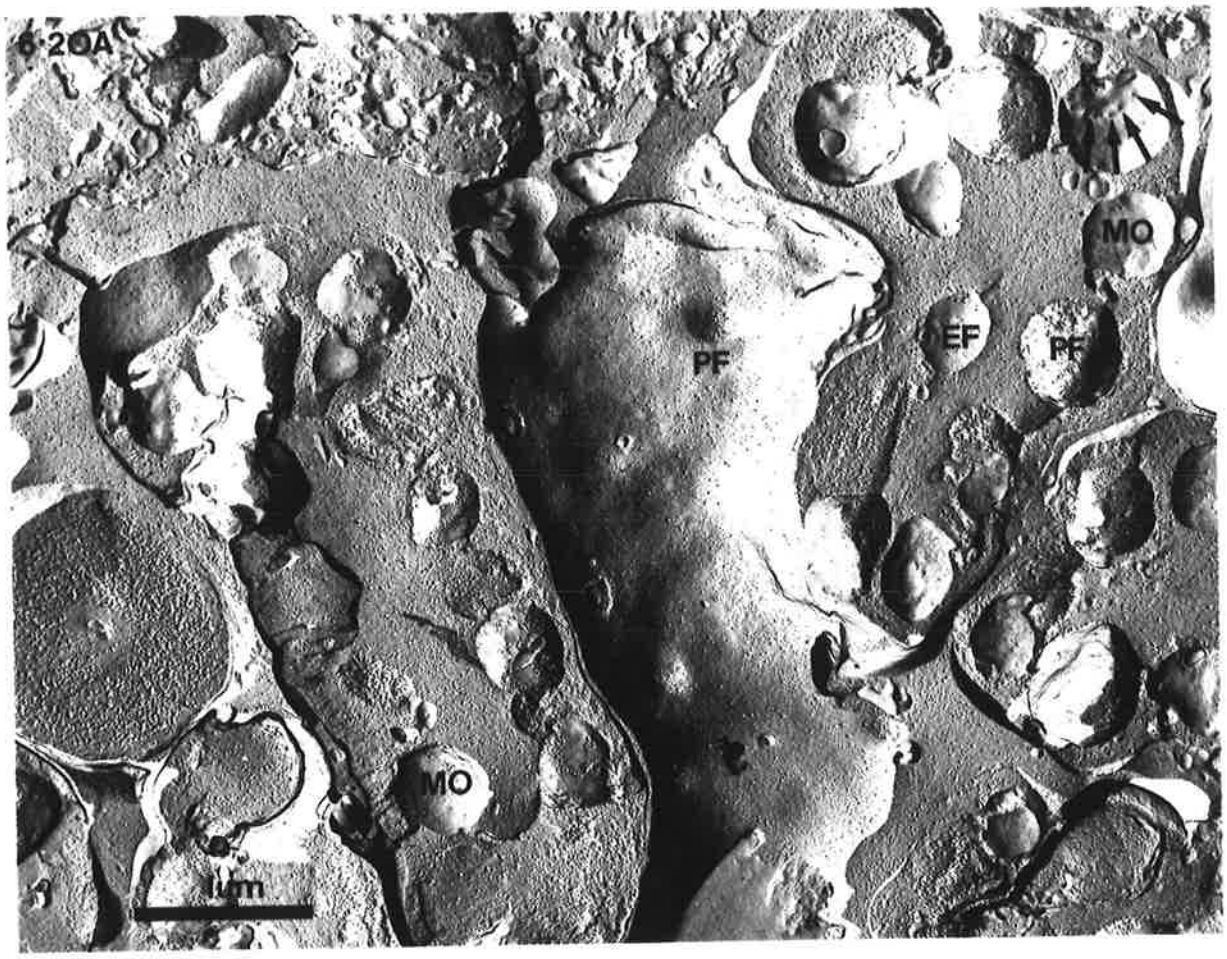
6·20A
PF
EF
PF
MO
MO
1um

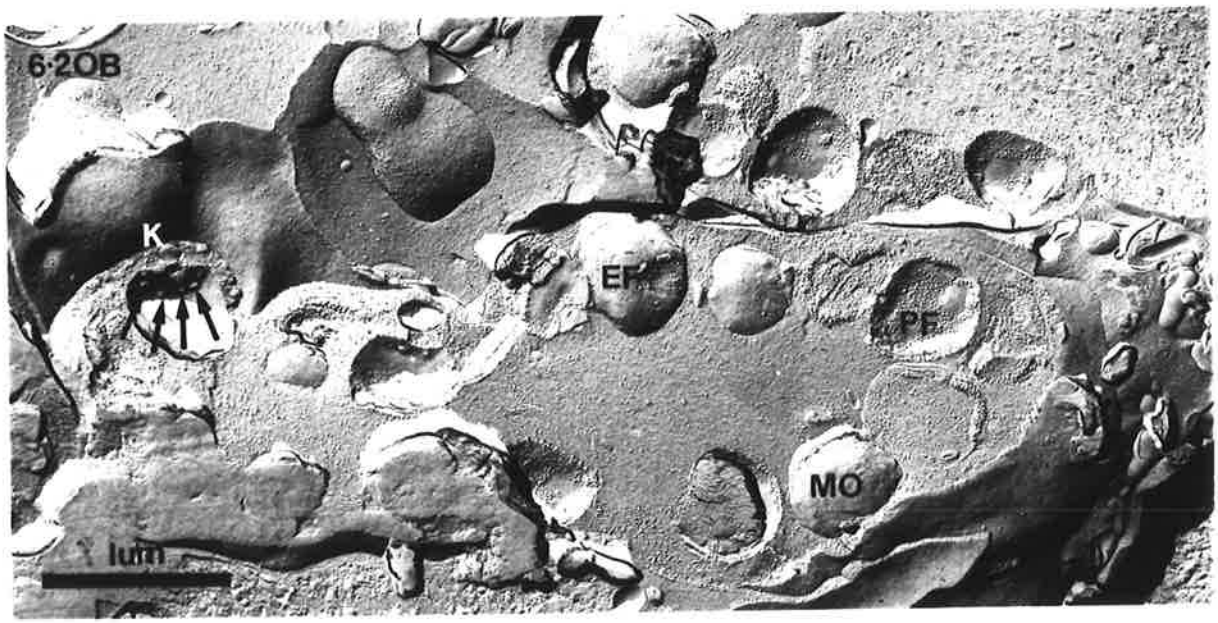
6·20B
K
EF
PF
MO
1um

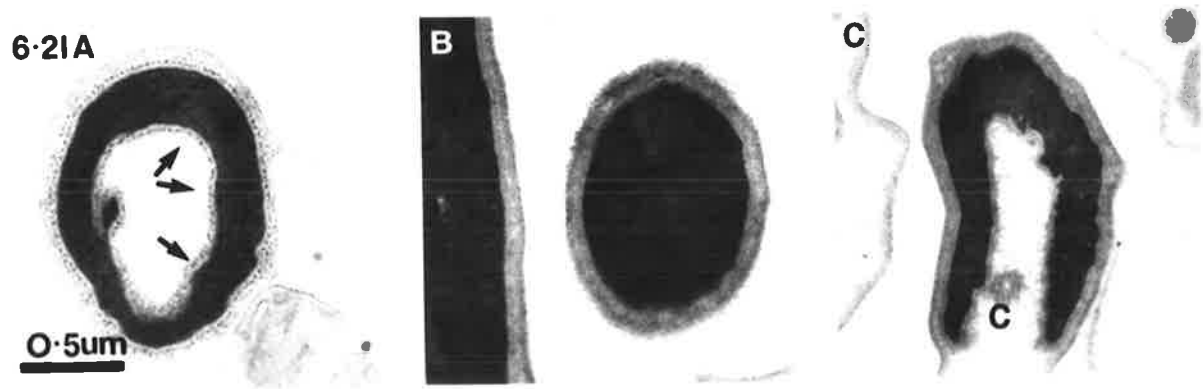
6·21A
0·5um
B
C
C

region shortens and the amoeboid anterior enlarges (Figure 6.22). Ultimately, the sperm become spherical, with virtually the entire anterior region capable of producing pseudopodia (Figure 6.23). Intermediate stages in this transformation are more easily found in this species, probably because the sperm are both larger and more numerous than in *N. brasiliensis*. Figure 6.24 shows " intermediate" sperm in the posterior uterus. A single membranous organelle (Stage I) is identical to those in sperm from males. At stage 2, the knob has fused with the plasma membrane and the dense contents have been released. The transformation to the final form (Stage 3) occurs when the invaginations of the membrane deepen and fill the interior of the organelle; this reduces their diameter to 0.35 - 0.45μm. At this stage, the amoeboid region (A) has begun to enlarge and has a dense granular appearance. Dense spheres are still seen in the cytoplasm and in one sperm they have fused to form a dense trilobed body (DS).

The sperm shown in Figure 6.25 are approaching maturity. The amoeboid anterior has increased in size and its contents are filamentous rather than granular. All the membranous organelles have fused with the plasma membrane and released their contents. The long tubular invaginations bear a fuzzy coat, 10nm thick, on their external side, while the cytoplasmic leaflet of the membrane is dense but without a coat. Freeze-fracture shows that shortly after fusion, the PF-face of the membranous organelles has a clumped distribution of particles (PF, Figure 6.26A) rather like that seen in unfused organelles. Later the particles become more evenly distributed (PF, Figure 6.26B). Particles are sparse on the EF-face (EF, Figure 6.26A).

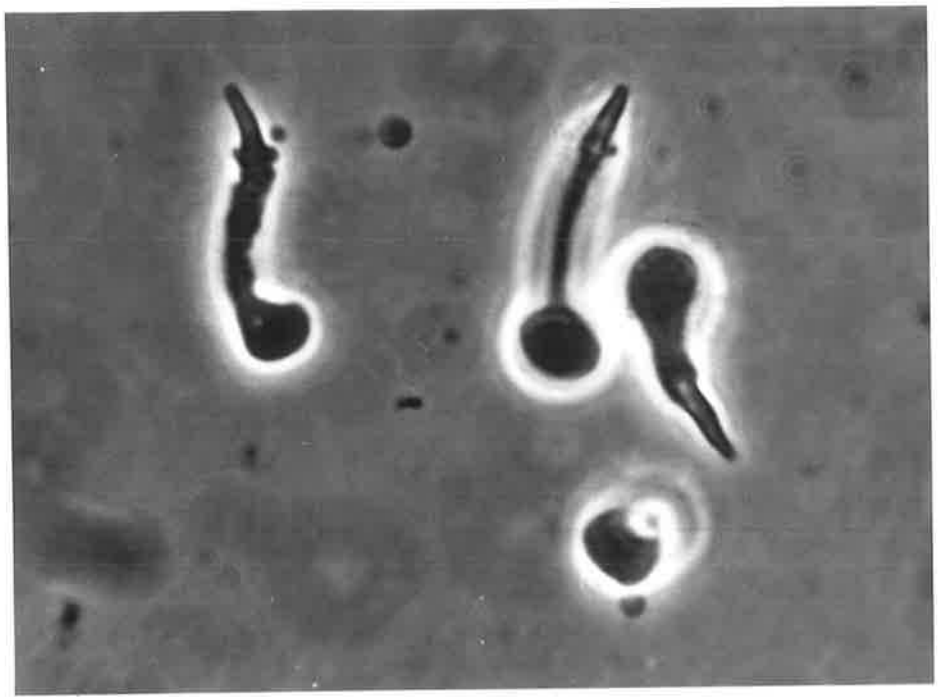

FIGURE 6.22 : A group of sperm in which activation has begun but is not yet complete. The amoeboid anterior has enlarged while the cytoplasmic region is shorter. The nuclear tail remains unchanged.

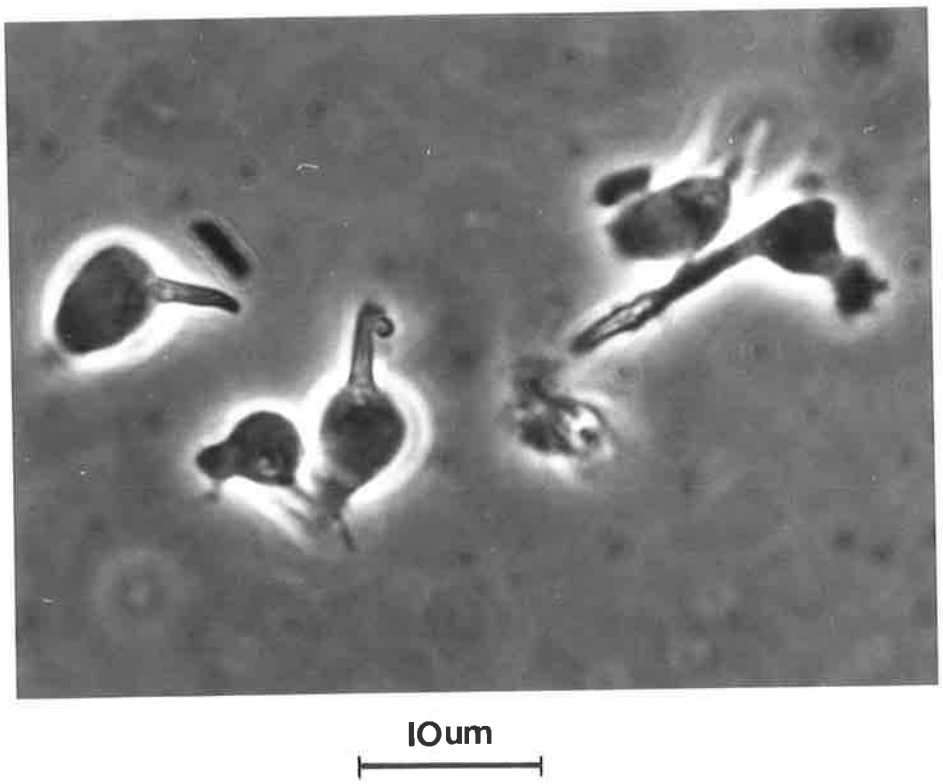

FIGURE 6.23 : Fully activated sperm from the seminal receptable of a female. The cytoplasmic region is almost spherical and from its anterior extend pseudopodia. The nucleus is still unchanged.

FIGURE 6.24 : Sperm undergoing activation in the posterior part of the female reproductive tract. One MO (1) is dense and resembles those of males; others (2) are large and electron lucent as they have released their contents; finally (3) invaginations form in their membranes. The small spheres of the dense material which was present in unactivated sperm are fusing into larger masses (DS). The amoeboid region of the sperm at the right of the figure appears to contain a granular material.

FIGURE 6.25 : Although all of the MOs have undergone fusion in this partially activated sperm, it is still in the elongate form. The substance of the amoeboid region is now filamentous. All the dense material, which was previously scattered in small clumps, has fused into a single dense sphere and the plasmalemma of the cytoplasmic region is lined by a flocculent material.

6·24

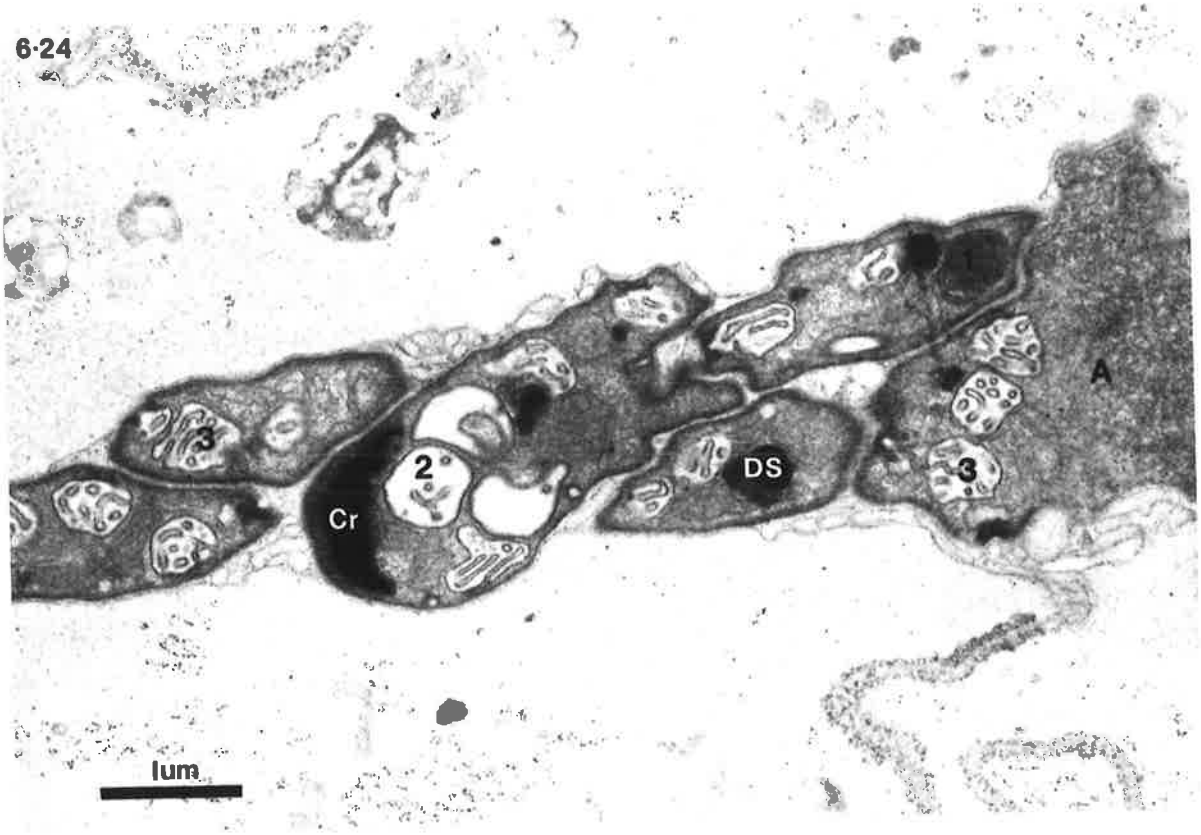

6·25

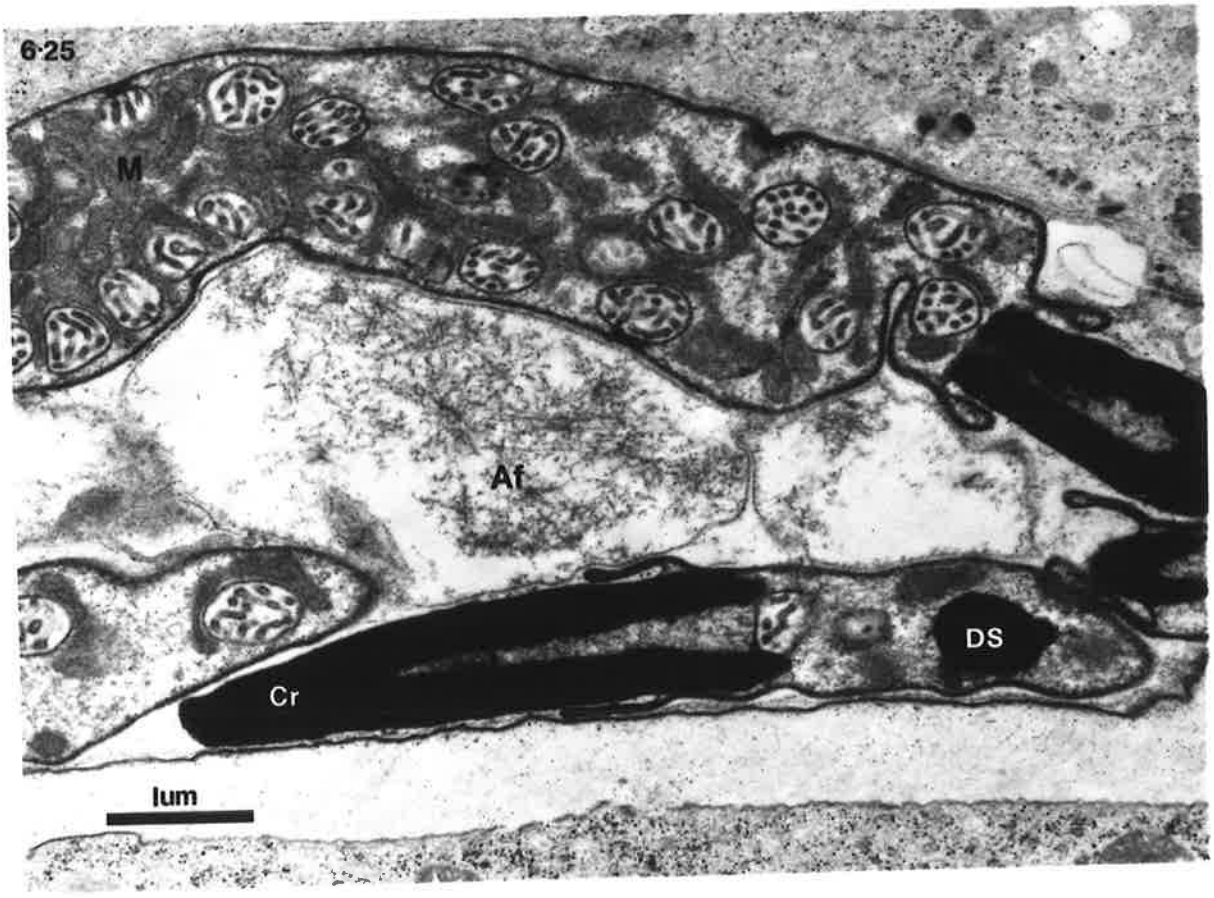

FIGURE 6.26A : A sperm cross-fractured soon after activation. The MO in the middle has released its contents through the pore (arrow) but the particles on the PF-face of the membrane are still clumped as they were in intact organelles.

FIGURE 6.26B : Some time after activation the particles on the PF-face of the MOs become randomly distributed. Invaginations are also evident.

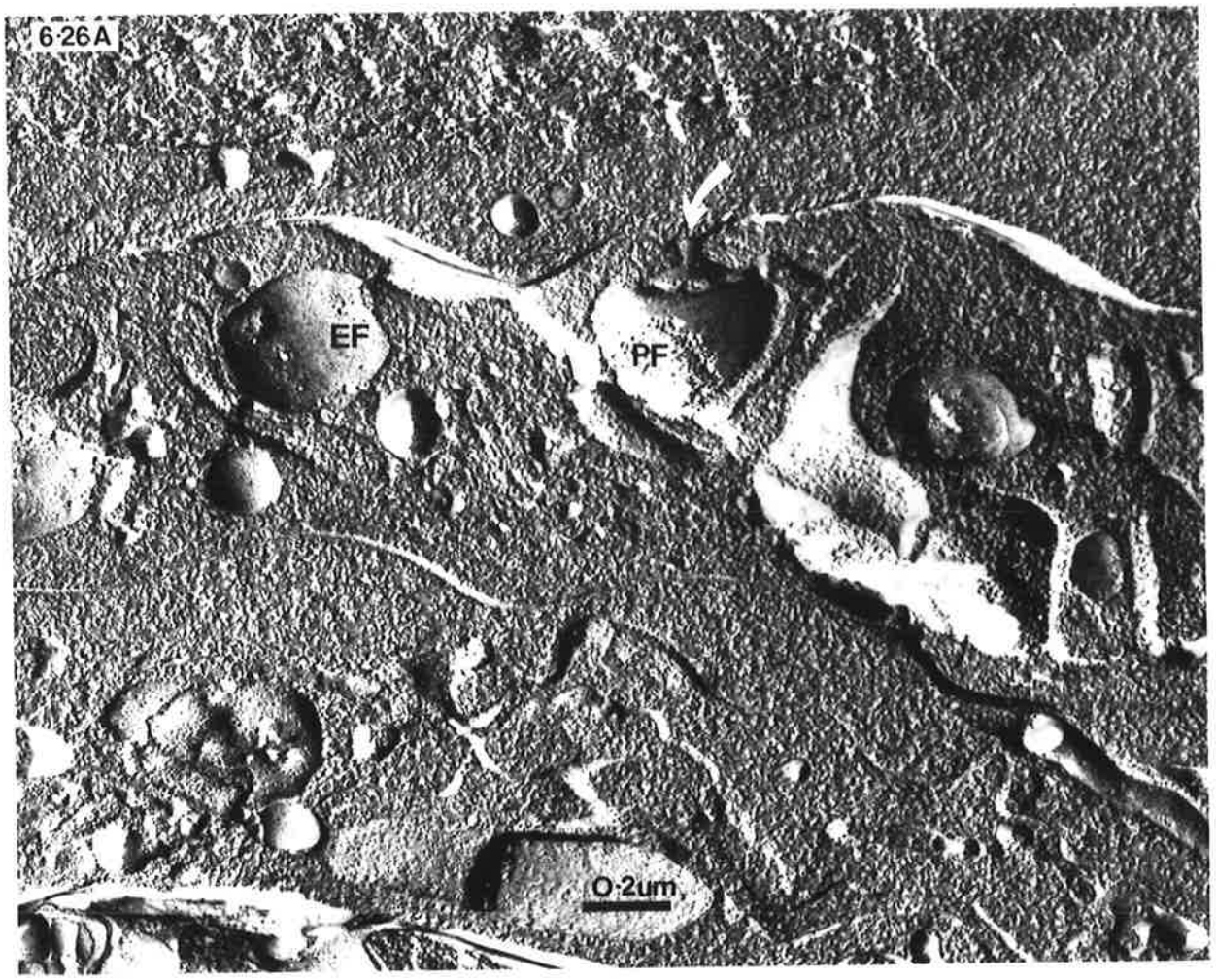
6·26A
EF
PF
0·2um

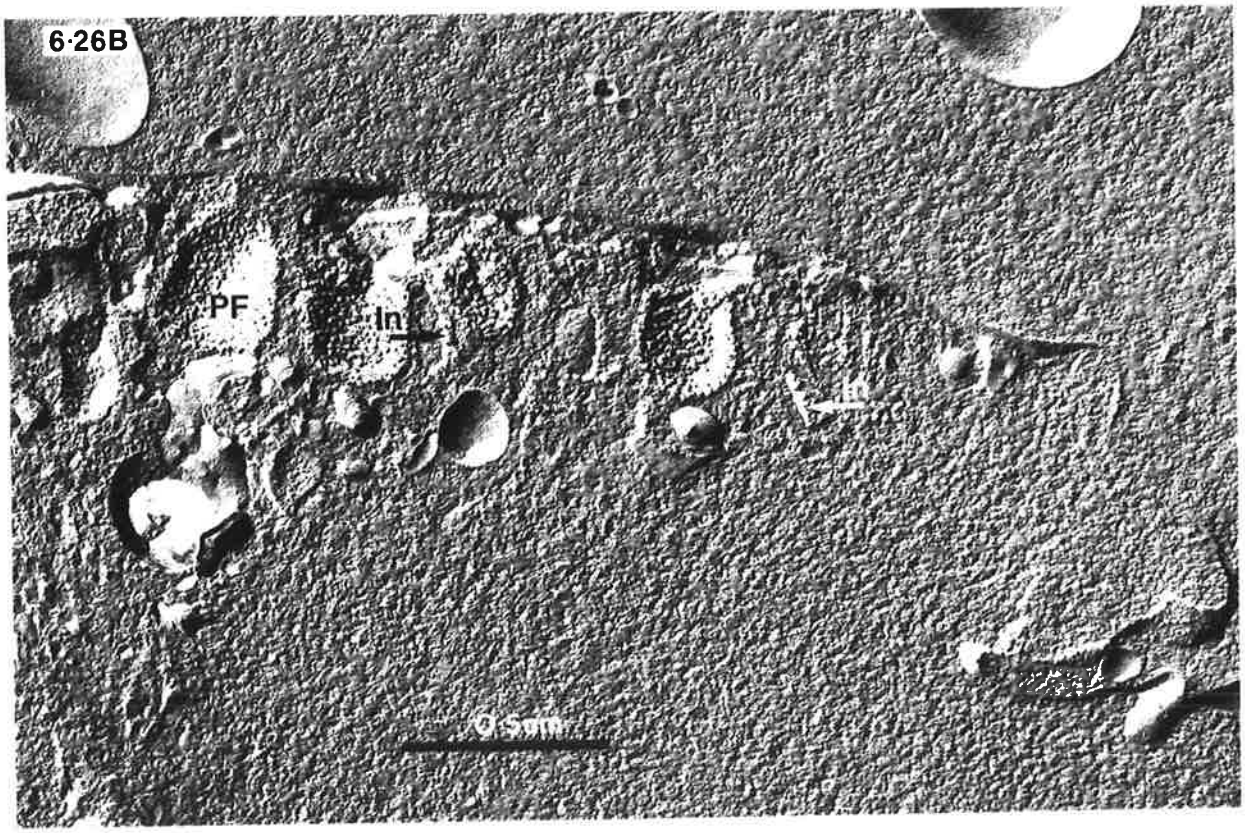
6·26B
PF
In
0·5um

Sperm in the seminal receptacle are generally fully activated (Figure 6.27). The dense layer which previously lined the plasma membrane (Figure 6.25) has disappeared. All that remains of it are dense rings of material, which form collars around the pores (P) joining the membranous organelles to the plasma membrane. The numerous dense spheres have migrated to the back of the sperm and fused into a trilobed body (DB, Figure 6.27). The pair of centrioles is also found in this region (inset, Figure 6.27).

The amoeboid region of activated sperm is extensive (A, figure 6.27). Filaments, usually aggregated in clumps, may fill the region, but more often they occupy only part of the area, while the rest appears empty. When tannic acid was added to the primary fixative, in an attempt to protect the filaments from osmium-induced denaturation, this distribution was unchanged (Figure 6.28). Both with and without tannic acid, many filaments appear to interact with the plasma membrane (arrows, Figures 6.27, 6.28).

FIGURE 6.27 : Fully activated sperm in the seminal receptacle. The dense layer which previously lined the plasma membrane has disappeared except for small rings around the pores joining the MO to the plasmalemma. The filaments in the amoeboid region often form chains which may interact with the plasma membrane (arrows). Mitochondria also occur near the membrane of this region. In the inset a centriole lies between the chromatin and a dense sphere.

FIGURE 6.28 : Sperm fixed with glutaraldehyde and tannic acid. The filaments are unchanged: they still occur in networks, interspersed by empty areas. Many filaments are attached to the plasma membrane (arrows).

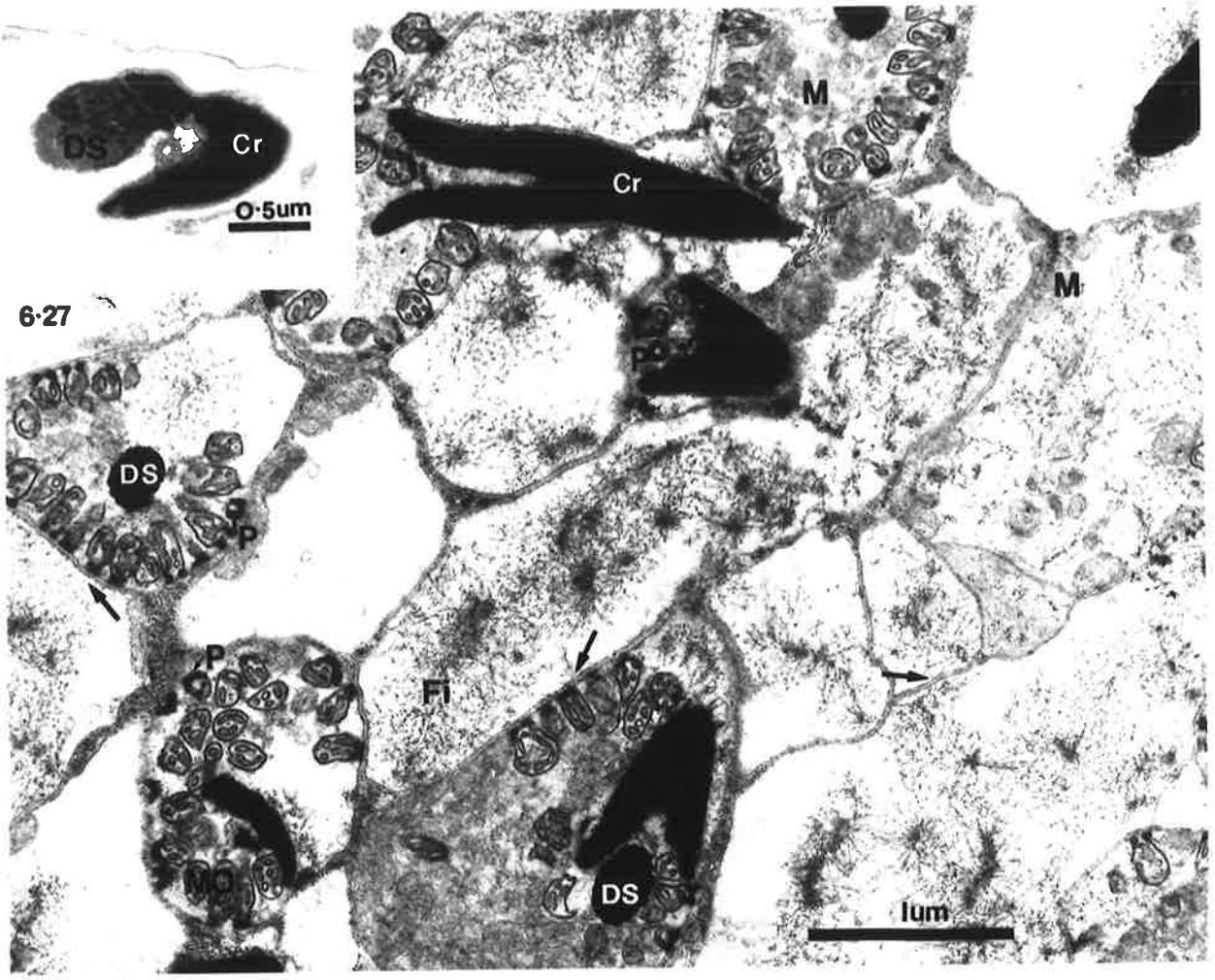

6·27

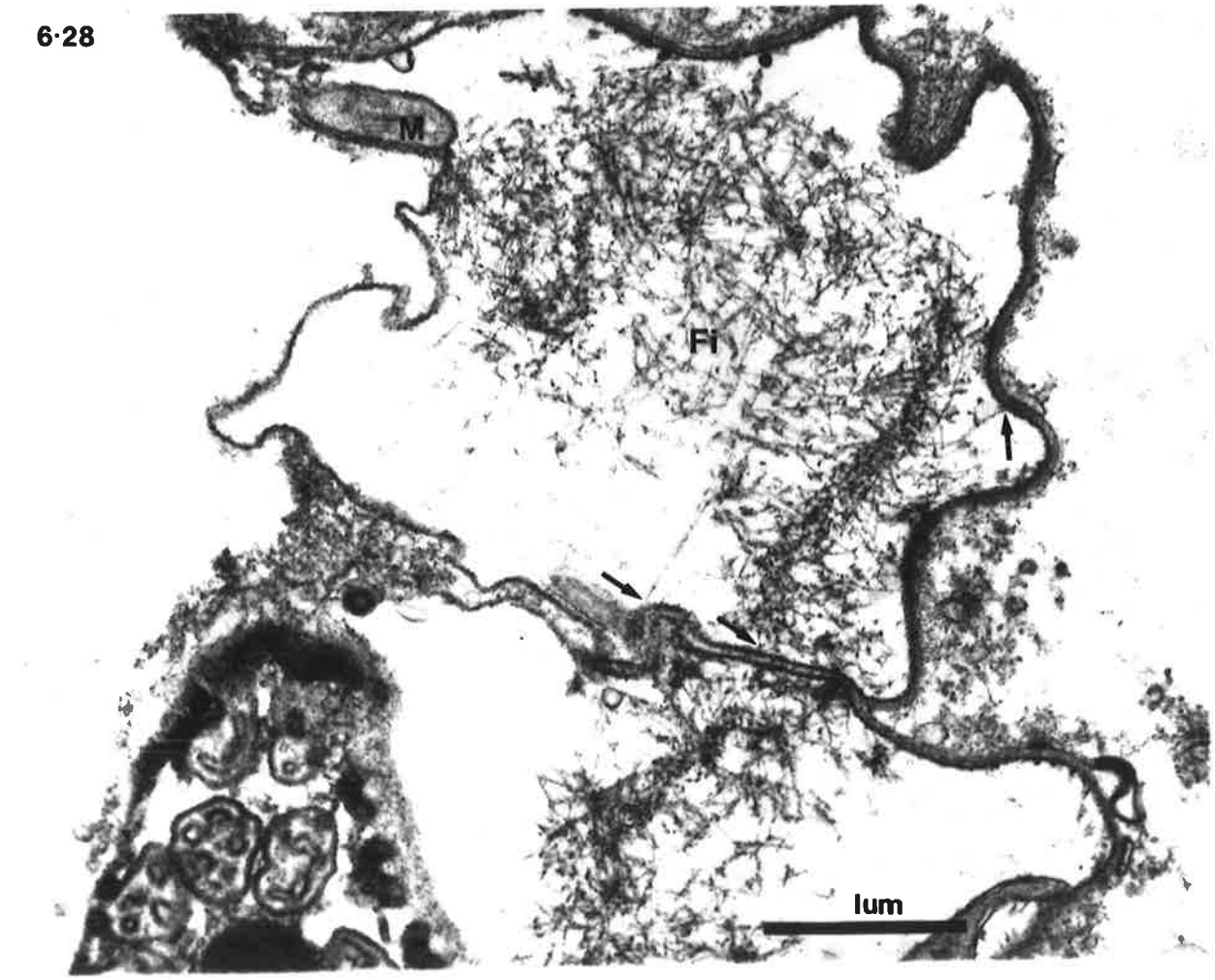

6·28

Chapter 7. DISCUSSION

7.1 Spermatogenesis and sperm maturation.

Cap cell and rachis

The large cap cell at the anterior end of the testis of *N. brasiliensis* and *N. dubius* is continuous with the testis epithelium. A similar relationship has been observed in the testis of *Aspiculuris tetraptera* (Anya, 1966) and *Dipetalonema viteae* Terry, Terry and Worms, 1961). McLaren (1973a) proposed that the cap cell is continuous with the rachis and provides a nucleus for this otherwise anucleate mass of cytoplasm. Observations with the light microscope have not revealed this proposed continuity and confirmation of McLaren's hypothesis awaits investigation with the electron microscope. It should be noted that a cap cell is also part of the germinal epithelium in the female reproductive tract of nematodes (Chitwood and Chitwood, 1950). It contains mitochondria, glycogen and a large nucleus (Wharton, 1979).

In an excellent experimental study, Kimble and White (1981) have shown that in *C. elegans* the cap cells in the testes of males or ovotestes of hermaphrodites are responsible for the control of germ cell development. Removal of the cap cells by laser microsurgery led to the arrest of mitosis and initiation of meiosis in the germ cells. Moreover, experimental manipulations of the position of the cap cells resulted in changes in the polarity of germ cell development, consistent with the hypothesis that the cap cells are the source of a diffusable meiotic inhibitory factor. The authors have proposed a simple model, whereby multiplication of the germ cells by mitosis allows the more proximal cells to escape the inhibitory influence of the cap cells and enter meiosis. This scheme could account for the sequence of maturation observed in all species of nematodes with telegonic gonads.

The rachis of *N. dubius* and *N. brasiliensis* is a large complex structure, extending throughout most of the testis and ultimately occupying one third of its width. The function of this organ in nematodes has been debated for many years. Although it has been contended that the absence of a rachis in many species demonstrates that it is of no great significance (Seurat, 1920; reported by Chitwood and Chitwood, 1950), the size and complexity of this structure in *N. dubius* and *N. brasiliensis* argues that it is of considerable importance. In other species, it has been implicated, although without direct evidence, in both the synchronous maturation (Lee, 1971; Lee and Lestan, 1973) and physical support (Foor, 1967; Lee 1971; McLaren, 1973a) of the germ cells. Furthermore, several authors suggest that it performs a nutritive function by contributing material to the developing germ cells (Prestage, 1960; McLaren, 1973a; Wolf, Hirsch and McIntosh, 1976).

When examining the function of the rachis of *N. dubius* and *N. brasiliensis*, both its size and contents in different regions of the testis should be considered. In the anterior germinal zone, it is little more than narrow bridges of cytoplasm between the spermatogonia. Like these germ cells it contains numerous ribosomes, as well as a few Golgi bodies, cisternae of RER and mitochondria. Soon the rachis can be distinguished from spermatogonial cytoplasm because a dense flocculent material forms fibrillar deposits within it and beneath its plasma membrane, especially at its junction with the sperm cells. By the time the spermatocytes begin their long period of growth and differentiation, the rachis has become a central core, containing more RER, but fewer Golgi bodies and mitochondria than the spermatocytes. In addition, microtubules and fuzzy fibrils are abundant between the cisternae of RER. Developing membranous organelles, with their associated Golgi bodies become common in the

rachis sometime after they first appear in the spermatocytes. The rachis continues to enlarge throughout the growth zone of the testis. It then shrinks rapidly as the spermatocytes approach meiosis. During this time, the membranous organelles disappear from the rachis, presumably moving back into the spermatocytes.

Since in *N. brasiliensis* and *N. dubius* the rachis contains vast quantities of ribosomes and RER, it appears to function as an extension of the spermatocyte cytoplasm, specialized for protein synthesis. The considerable quantities of raw materials needed to maintain such a high rate of synthesis probably come directly from the spermatocytes, via the bridges which connect them to the rachis. Microtubules noted in these bridges would facilitate this transport, as they are known to be involved in subcellular motility (Buckley, 1974). By regulating the movement of both these precursers and mRNA, the spermatocytes could maintain effective control over the activities in this extended cytoplasm. With the approach of meiosis, the spermatocytes reach the end of their period of growth and the rachis rapidly decreases in importance. Its component move back into the germ cells and it shrinks until once again it is represented by fine cytoplasmic bridges. This arrangement, in which a large pool of auxiliary cytoplasm outside the spermatocytes provides an increased volume of cytoplasm available for synthesis, avoids the increase in size of the spermatocytes which would otherwise be necessary. Moreover, the amount of additional plasma membrane required is reduced to a minimum.

Another function of the rachis could be to anchor the sperm cells in their correct positions and to regulate their progression along the testis. To this end, the plasma membrane at the junctions between rachis and spermatocytes is reinforced by a dense amorphous

material. A similar substance occurs in the rachis of the ovary of *A. lumbricoides* (Foor, 1967). In addition, the microtubules and fibrils noted throughout the rachis of *N. dubius* and *N. brasiliensis* appear to form a three-dimensional scaffolding which would be an important structural support for this large mass of cytoplasm.

By creating cytoplasmic continuity between all but the latest stages of germ cell development, the rachis provides a means of communication between these cells. In this way their synchronous development is ensured. This may have been the original function of the rachis and its enlargement into a complex synthetic organ in some species, may be a secondary development. Certainly, open communication between germ cells is a common feature of spermatogenesis throughout the animal kingdom (Cohen, 1977). In other animals, as in nematodes, these intercellular bridges arise from incomplete separation of the spermatogonia after mitosis and are believed to be responsible for the synchronous maturation of gametes (Fawcett, 1961; 1975a; Lunger, 1971; Jalton and Hardcastle, 1976).

Although spermatogonia in the hologonic testis of *C.hepatica* remain connected by spindle bridges after mitosis, these connections are only transient. The three functions performed by the rachis in the telegonic testis, viz. support, nutrition and regulation of development, have been assumed by sustentacular cells in the hologonic testis. These cells envelope the spermatogenic cells until the early spermatid stage (Neill and Wright, 1972). As such they are similar to Sertoli cells in the mammalian testis (Setchell, 1978) and nurse cells, nutrititive cells and support cells in invertebrates (Roosen-Runge, 1969; Lunger, 1971; Grant, Harkema and Muse 1976).

Spermatogonia

The spermatogonia of both *N. dubius* and *N. brasiliensis* are typical undifferentiated cells with large nuclei, prominent nucleoli and little cytoplasm. They are therefore like early germ cells from virtually all animals (Roosen-Runge, 1977), including other nematodes (Neill and Wright, 1972; McLaren, 1973a). The granular bodies with their associated dense spheres and tubular elaborations are curious structures. No similar complex has been reported in other nematodes, although micrographs of spermatogonia in *M. hapla* show many dense spheres in the cytoplasm, some of which are associated with granular masses (Figure 2A,B; Goldstein and Triantaphyllan, 1980). Unfortunately, the authors do not comment on these structures. In *R. pellio*, a granular mass labelled an "X body" is thought to be derived from the nucleus of spermatogonia. The authors were unable to comment on its nature and importance, but they did observe that the greater part of it is cast out with the residual cytoplasm (Beams and Sekhon, 1972). On the contrary, the granular bodies of *N. brasiliensis* and *N. dubius*, disappear from the cytoplasm of spermatocytes just before the membranous organelles are formed. They appear to be involved first in the proliferation of Golgi bodies in the spermatogonia, then they contribute material via these Golgi bodies to nearby secretion vesicles. The latter are easily identified by their electron-dense contents and unusual triangular shape. Although the Golgi bodies remain in the cytoplasm and ultimately become involved in the synthesis of the membranous organelles, the dense vesicles are short-lived and their fate is unknown.

Formation of the membranous organelles

The origin of the membranous organelles in the sperm of nematodes has long been a subject of controversy (see Chapter 1.2). It was therefore considered important to trace their formation and development in both *N. dubius* and *N.brasiliensis*. Jamuar (1966) was unable to determine their origin in his study of spermiogenesis in *N. brasiliensis*. Their association with fibrous bodies suggested to him that they were homologous with the "grains à batonnet" described as Golgi products in *P. equorum* (Favard, 1961). However, because of their superficial resemblance to mitochondria, he called them "mitochondrion-like inclusions".

The present study unequivocally demonstrates that in both *N. brasiliensis* and *N. dubius*, the membranous organelles originate in the early spermatocytes from dilated terminal saccules of Golgi bodies. As development proceeds, the characteristic electron-dense contents of these vesicles are augmented by dense secretions from the ER-associated Golgi complexes. When the membranous organelles measure about 0.3µm across a bundle of parallel fibres begins to form in an indentation on one side. Both parts of the complex continue to enlarge, until they reach their maximum size of 1µm diameter. At this time, the fibrous body occupies about 1/4 to 1/3 of the total volume. As the spermatids differentiate the fibrous body separates from the membranes and dissolves into the cytoplasm. Similar bodies have a transitory association with the membranous organelles in many other species. In several groups of plant-parasitic nematodes, however (Shepherd et al 1974; Shepherd and Clark, 1979; 1980), fibrous bodies form in the cytoplasm unassociated with other organelles. More specifically, membranous organelles are totally

absent from these species. It seems unlikely therefore, that the membranous organelles contribute to the growth of the fibrous bodies in *N. dubius* and *N. brasiliensis*. It is more probable that precursers are recruited directly from the cytoplasm, which is in direct contact with the fibrous body. This leaves the association of these two organelles unexplained. Wolf et al. (1976) have suggested that the fibrous material might be packaged into discrete bodies to prevent its loss when the residual cytoplasm is discarded. Observations of spermatogenesis in *G. rostochiensis* and *H. schachtii* support this proposal. In these species where the fibrous bodies are not associated with a membranous component, segregation of the residual cytoplasm occurs very early before the fibrous bodies are synthesized.

The nature and function of the fibrous material has puzzled researchers since it was first observed with the electron microscope. Several authors have agreed with the suggestion of Lee (1971) that it is a contractile protein which forms the substance of the amoeboid region of the sperm (Beams and Sekhon,1972; Shepherd and Clark, 1976). But its absence in the amoeboid sperm of *A tetraptera* (Lee and Anya, 1967) must also be considered. Perhaps in this species the fibrous material is free in the cytoplasm, while still protected, in some unknown way, from expulsion during partitioning of the residual cytoplasm.

The fibrous material in *C. elegans* constitutes 15% of the sperm protein and as such is the major sperm protein (MSP) (Klass and Hirsh, 1981). It has a MW of 15,000 and exists as a dimer *in vivo*. Evidence that this protein constitutes the fibrous bodies first came from pulse-labelling studies. These experiments demonstrated that MSP was synthesized in the primary spermatocytes at the same time that

fibrous bodies first appear (Klass and Hirsh, 1981). More recently its localization in the fibrous bodies of spermatocytes has been confirmed using affinity-purified antibody to MSP (Ward and Klass, in press). This technique has also allowed the fate of this material to be traced. When the fibrous bodies disassemble in the immature sperm, MSP becomes uniformly distributed throughout the cytoplasm. Subsequently, activation induces its migration into the amoeboid anterior of the sperm. Its role in sperm locomotion is discussed in Chapter 7.2. Since a similar protein, isolated from the sperm of *A. suum*, cross-reacts with affinity-purified antibody to MSP from *C. elegans*, the fibrous bodies may prove to have a similar nature and function in the sperm of other nematodes, including those of *N. brasiliensis* and *N. dubius*.

Spermiogenesis

The major events of meiosis are similar in *N. dubius* and *N. brasiliensis* and resemble those described for other species (Chapter 1.2; Neill and Wright, 1972; Favard, 1961). The spermatids of both *N. dubius* and *N. brasiliensis* remain connected by cytoplasmic bridges after completion of the second meiotic division. The ribosomes, RER and Golgi bodies, which are destined to form the residual body, then accumulate on one side of the spermatid and move into these bridges. Subsequently, the spermatids become detached and the cytoplasmic masses fuse with one another. The sperm of all species of nematodes undergo cytoplasmic reduction, but the specific movement of residual cytoplasm into the intercellular bridges joining the spermatids has been described only in *C. hepatica* (Neill and Wright, 1972), *C. elegans* (Ward, Argon and Nelson, 1981), *D. viteae* (McLaren, 1973a) and *A. blastophthorus* (Shepherd and Clark, 1976).

In the testes of *N. brasiliensis* and *N. dubius*, vast pools are formed by the fusion of many residual bodies. Here, the RER and

Golgi synthesize large numbers of secretory granules which appear to be lysosomal. Soon, the organelles within the residual cytoplasm begin to break down. Occasionally spermatids, presumed to be defective, are also seen undergoing degredation. Eventually, when most of the organelles are no longer recognizable, the whole area is phagocytosed by the testis epithelium. A similar fate has been reported in other species, e.g. *P. equorum* (Favard, 1961) *A. blastophthorus* (Shepherd and Clark, 1976) and *D. viteae* (McLaren, 1973a).

Several authors refer to the residual bodies of nematode spermatids as "cytophores" (Goldstein, 1977; McLaren, 1973a). This term is defined as "a central anuclear mass of cytoplasm by which clones of male germ cells may be united" (Roosen-Runge, 1977). Furthermore, the cytophores in platyhelminthes and other animals are described as arising from incomplete spermatogonial divisions. Its use in describing the residual cytoplasm cast out by the spermatids of nematodes is therefore not strictly correct and it would be more accurate to use the term"residual body". Moreover, this conforms with the terminology used to denote excess cytoplasm cast out from the spermatids of other animals (Roosen-Runge, 1977).

The accepted function of a residual body in all animals is to remove cytoplasmic organelles which are no longer required by the maturing spermatid. On the other hand, since RER and Golgi bodies are elaborated within the residual cytoplasm of *D. viteae*, McLaren (1973a) has suggested that these cytoplasmic masses are responsible for synthesizing enzymes to be used during spermiogenesis. In *N. dubius* and *N. brasiliensis* there is no evidence of proliferation of these organelles and the residual bodies seem only to be a means of removing excess cytoplasm or to occasionally dispose of defective sperm.

Nuclear morphogenesis after meiosis

The nuclear envelope does not reform after meiosis in *N. dubius* and *N. brasiliensis*. Jamuar (1966) described the spermatids of the latter as membrane-bound, but it appears from his micrographs that he was confusing the late spermatocytes with the spermatids. The absence of a nuclear envelope in post-meiotic spermatogenic cells is a common feature of nematodes, but its significance is not known. After fertilization it may be important for the DNA to be in direct contact with the oocyte cytoplasm, alternatively the DNA may need to be in direct communication with the sperm cytoplasm during spermiogenesis.

After meiosis in both *N. brasiliensis* and *N. dubius*, the central mass of DNA condenses into filaments which then wind into a spiral. As they do so, the chromatin elongates. In *N. dubius* this elongation stops when the DNA is a broad cone 3-4μm long, but it continues in *N. brasiliensis* until a narrow filament, 11μm long, is produced. In spite of their different dimensions, these two structures share many features including the disposition of their centrioles and microtubules, their movement back along the sperm with the aid of microtubules, as well as their conical, tail-like form.

Rapid dissolution of the nuclei of both *N. brasiliensis* and *N. dubius* with 1% sodium dodecyl sulphate, an ionic detergent, demonstrated that ionic and not covalent bonding is responsible for cross-linking the chromatin filaments. In this way these sperm differ from those of eutherian mammals but resemble the sperm of the majority of other animals (Bedford and Calvin, 1974). In eutherians, unique cysteine-protamines allow extensive -S-S- crosslinking (Balhorn, 1982). This has produced a structure of extraordinary rigidity, which is

believed to be advantageous in the penetration of the unusually thick zona pellucida around the eggs of these animals (Bedford, 1975). In other groups, the nuclear proteins of the sperm may be arginine - or tyrosine - protamines or they may be histone-like. Since a high degree of chromatin condensation can be correlated with a high content of basic proteins and a lesser proportion of somatic histones (Subirana, 1975), the proteins associated with the chromatin of *N. dubius* and *N. brasiliensis* are probably very basic.

Although nuclear condensation occurs in the sperm of virtually all animals and is believed to protect the DNA during transport and storage (Subirana, 1975), it is uncommon in nematode sperm. In general, the chromatin remains in the centre of the cell, either as distinct chromosomes, e.g. *P. silusiae, D. viteae,* or as a single dense mass e.g. *C. elegans, H. gallinarum.* Sperm with a nuclear tail have been described only in the trichostrongyle, *Nematodirus battus* (Martin and Lee, 1980a) and in the strongyle, *Ancylostoma caninum* (Foor, 1970). In both species, the chromatin is condensed into filaments and wound into a spiral, very much as it is in *N. brasiliensis* and *N. dubius*. In *N. battus,* it remains unchanged after insemination, whereas in *A. caninum* activation induces a mixing of nuclear and cytoplasmic regions (Foor, 1970).

While it is easy to understand the value of nuclear condensation in sperm, especially since they lack mechanisms for the repair of DNA (Subirana, 1975), it is more difficult to interpret the extrusion of the chromatin into a tail in the strongylids. The tail appears not to be important for locomotion in *N. brasiliensis* (Chapter 7.2) and *N. dubius* (Wright and Sommerville, 1977). Moreoever, the sperm of *C. elegans,* which have no tails, move at similar speeds and in a

similar way to tailed sperm (Nelson, Roberts and Ward, 1982). It might be expected that problems could arise when the long tail of *N. brasiliensis* is incorporated into the oocyte during fertilization. An ultrastructural study of sperm-egg interaction in this species may, however, show that the nuclear tail performs some hitherto unsuspected role in fertilization.

Centrioles

Although the two centrioles at the proximal end of the chromatin disappear after nuclear elongation in *N. brasiliensis*, they persist in *N. dubius* and can still be seen in the sperm after insemination. In both species the centrioles are similar. They consist of nine tubules, around a dense ring of material with an electron-lucent centre. They resemble centrioles in *A. lumbricoides* (Goldstein, 1977), *P. equorum* (Favard, 1961), *A. caninum* (Foor, 1970), *C. hepatica* (Neill and Wright, 1972) and *H. gallinarum* (Lee, 1971). Jamuar (1966) reported that centrioles in *N. brasiliensis* contained 18 microtubules, 9 of which were larger and more distinct. My observations suggest that the material between the nine singlets could be misinterpreted as extra tubules.

Activation

The spermatozoa of both *N. brasiliensis* and *N. dubius* change morphologically and ultrastructurally after insemination into the female reproductive tract. Modifications include enlargements of the amoeboid anterior, shrinking of the cytoplasmic region and fusion of the membranous organelles with the plasma membrane. In *N. dubius*, activation involves a dramatic transformation from an elongate to a globular shape, whereas in *N. brasiliensis* the changes are more minor. For this reason, intermediate stages are more easily recognised in

N. dubius. Although most sperm in the vagina and posterior uterus of both species are elongate or intermediate in shape, few have intact membranous organelles. This suggests that the first stage of activation involves fusion of the membranous organelles and that the morphological changes follow more slowly. The same sequence was noted during activation in *C. elegans* (Nelson and Ward, 1980). Experimental studies on other species have shown that activation occurs rapidly. *In utero*, the sperm of *B. pahangi* required less than an hour for transformation (Burghardt and Foor, 1975) and the sperm of *A. suum* and *C.elegans* can be activated *in vitro* in as little as 5 min (Burghardt and Foor, 1978; Nelson and Ward, 1980).

Since sperm were first observed to change shape after insemination, it was assumed that the female was the source of the stimulus for activation. Later, reports of activated or amoeboid sperm in males of some species, e.g. *D. viteae, P. silusiae,* suggested that the male reproductive tract might produce the stimulus. An attempt to confirm this in *N. dubius* was not successful (Wright, 1974). Males were ligatured just anterior of the cloaca whilst *in copula*. In this way, sperm were trapped in the posterior vas deferens where they were presumed to be in contact with secretory products of this region. The worms were then incubated in culture medium at 37^{o}C, and examined at intervals. Although sperm were clearly visible in the vas deferens, none underwent any morphological changes, even after 24 hours. This negative result does not necessarily mean that the vas deferens does not produce an activating substance, as other factors including the incubating conditions may have inhibited activation. A similar inhibition of activation has been observed in recently inseminated female worms incubated under the same conditions (Sommerville pers. comm.). More experiments, perhaps involving the transfer of worms back to their hosts, are

necessary to determine the source of the stimulus in this species.

The large size of *A. suum* allowed Foor and McMahon (1973) to test male secretions by injecting an extract of the vas deferens of males into the seminal vesicles of intact worms. In these animals, but not those injected with saline, sperm became activated. An elaborate sphincter, between the seminal vesicle and vas deferens, prevents secretory products of the later mixing with sperm prior to copulation (Foor, 1976). The observation that some sperm from mated, but not virgin,males of *C. elegans* are activated suggests a link between mating and sperm activation in this species, too (Ward, Hogan and Nelson, submitted for publication).

An investigation of the stimulus which induces activation in the sperm of *N. brasiliensis* and *N. dubius* was beyond the scope of this study. Nevertheless, a brief summary of the latest experimental work in this field is presented here, as it is relevant to the question of activation in nematodes generally.

Foor's group have approached the problem by studying the natural trigger produced by males of *A. suum*. Attempts to isolate a single activating substance from homogenates of the vas deferens have met with little success because the more heterologous fractions have a greater capacity to activate sperm (Abbas and Foor, 1978). The sperm activity substance (SAS) appears to have proteolytic activity as the serine protease inhibitor phenylmethylsulphonyl fluoride (PMSF) inhibits its activity (Fitzgerald and Foor, 1979) and proteases ($\propto$ chymotrypsin, trypsin and protease; 10µg/ml) cause sperm activation (Abbas and Cain, 1979). However, since high concentrations of soybean trypsin inhibitor failed to suppress SAS activity and no proteolytic activity against a number of substrates was detected in SAS extracts (Abbas and Cain, 1979), the mode of action

of SAS remains unclear.

Ward's group have approached the problem in a different way. They have tested numerous substances in an attempt to activate the sperm of *C. elegans in vitro* (Nelson and Ward, 1980). Among these were ionophores, cyclic nucleotides, ATP ase inhibitors and homogenates of *A. suum* vas deferens, *c. elegans* males and hermaphrodites. Only the ionophore monensin which transports Na^+ and K^+ was found to be active. Suspecting that cation transport was linked to H^+ efflux and an increase in intracellular pH, Ward and Hogan (1980) tested the effects of weak bases on sperm. Triethanolamine (TEA) and to a lesser extent ammonia induced activation and a rise of pH from 7.1 to 7.4. A similar pH increase occurs during monensin activation. Protease treatment can also activate sperm but without altering intracellular pH. Both TEA- and pronase-induced activation are blocked by mitochondrial inhibitors.(Ward, Hogan and Nelson submitted for publication). The authors have proposed a scheme to relate these different activators. They suggest that an increase in intracellular pH causes a release of a sperm protease on the surface of the cell. Proteolysis of some surface proteins could then cause a change in ionic permeability, which induces activation. As yet, they have been unable to detect a sperm protease of this kind. It would be interesting to test monensin and proteases on the sperm of *N. dubius* and *N. brasiliensis*. In this way, it may be possible to determine whether activation has a common basis in distantly related nematodes.

Once activation is triggered, a series of events follow which culminate in differentiated sperm fully equipped for locomotion, survival in the uterus and fertilization. Activation can therefore be thought of as a means of synchronizing the maturation of oocytes

and spermatozoa. This would be an obvious advantage in situations where mating was infrequent or unpredictable. Many natural populations of nematodes, either parasitic or free-living, are small enough to make this an important consideration. Similarly in the hermaphrodites, e.g. *C. elegans*, sperm are produced before oocytes in the ovotestis and their final development is synchronized by the sperm activating substance produced by the spermatheca (Ward and Carrell, 1979).

A strategy of this kind is not unique to nematodes but occurs in a wide variety of animals. In mammals, spermatozoa must undergo a period of maturation in the female reproductive tract before they become competant to fertilize an egg. This has been called "capacitation" (Austin, 1952) and is defined as "the conditioning transformations (membranous and otherwise) leading up to the overt acrosome reaction" (Koehler and Kinsey, 1977). Although sperm can be readily capacitated *in vitro* using simple media (Yanagimachi and Usui 1974; Kinsey and Koehler, 1978) the requirements for capacitation *in vivo* appear to be complex and sometimes highly specific. Recent evidence suggests that secretions of the male reproductive tract, which become adsorbed to the sperm head before insemination, are removed from the acrosomal membrane during capacitation (Cooper and Bedford 1980). Furthermore, integral membrane components such as glycoproteins, intramembranous particles and antigens are also cleared from areas of this membrane (Schwarz and Koehler, 1979; Kinsey and Koehler, 1978; Koehler, 1976). The possibility that similar changes occur on the surface during activation of the sperm of *N. brasiliensis* is explored in Chapters 8 and 9.

The membranous organelles after activation.

During activation, knobs on the outer side of the membranous organelles of *N. brasiliensis* and *N.dubius* fuse with the plasma membrane. In the sperm of several other species, e.g. *P. silusiae, R. pellis, C. elegans,* similar protrusions perform the same function. The sequence of exocytosis was followed in *N. brasiliensis* and *N. dubius* by examining sperm in the posterior reproductive tract of females. Following membrane fusion, as they release their contents, the membranous organelles lose their characteristic density and become large lucent spheres. Not all the membranous organelles fuse simultaneously, as empty and intact organelles may coexist in the same sperm. After the contents are discharged, the membranes fold into deep microvillous-like invaginations. The cytoplasmic leaflet of this membrane is more dense than the external layer but the latter bears a 10nm thick fuzzy coat. A permanent pore joins the membranous organelles of *N. brasiliensis* and *N. dubius* to the plasma membrane. Around the neck of this pore is an electron-dense collar. A similar structure occurs in the sperm of *B. pahangi, D. californicum, C. elegans* and *R. pellio* (Foor, 1974; Wright et al, 1972; Wolf et al, 1978; Beams and Sekhon, 1972).

The membranous organelles of nematodes can be compared with a number of structures found in the "aberrant" sperm of other invertebrates. These include the cellular processes of tick sperm (Reger, 1974), the spongy chambers of diplopod sperm (Bacetti, Dallai, Bernini and Mazzini, 1974) and "donut-shaped bodies" in the sperm of the rotifer *Asplancha brightwelli* (Aloia and Moretti, 1974). Some of these are PAS-positive and contain enzymes, while others fuse with the plasma membrane of the mature sperm. Although there is no evidence for their involvement in fertilization, all these structures have been called "acrosomal". The membranous organelles of nematode sperm, with their Golgi origins, PAS-positive contents and acid phosphatase activity

(Jamuar, 1966; Lee, 1971; Clark et al 1972) bear some resemblance to these structures, but their true relationships will not be understood until more is known about the evolution of sperm both within and between the major taxonomic groups.

Several authors have suggested that the membranous organelles have an acrosomal function (Favard, 1961; Jamuar, 1966; Lee, 1971; Clark et al, 1972). The acrosome of conventional sperm is considered a specialized lysosome which is PAS-positive and contains hyaluronidase, acid phosphatase, neuraminidase, phospholipase and the proteinase acrosin (Lung, 1974). During spermiogenesis it is synthesized by the Golgi and in the mature sperm it becomes flattened and wrapped around the anterior of the nucleus (Phillips, 1974; Setchell, 1978). Thus in their origin and contents, but not in their form and position in the sperm, the membranous organelles are like an acrosome. Further comparisons reveal more differences and fewer similarities between these organelles.

In both mammals and invertebrates, the acrosomal enzymes are released when the outer acrosomal membrane fuses with the overlying plasma membrane. In sea urchins this is triggered by a fucose sulphate component of the egg jelly (SeGall and Lennarz, 1979). Once released, the enzymes break down the egg coat, providing a pathway by which sperm may reach the oolemma. Fertilization is clearly different in nematodes. The electron-dense contents of the membranous organelles of *N. brasiliensis* and *N. dubius* are released in the posterior uterus, far from the oocytes. Similarly, in *A.suum* these organelles undergo no apparent change prior to contact between the sperm and oocyte (Foor, 1968). Moreover, my observations of fertilization in *N. brasiliensis* showed that the amoeboid anterior makes first contact with the oocyte. This has also been noted in

D. viteae (McLaren, 1973b), *A. suum* (Foor, 1968), *Physaloptera* (Foor, 1970) and *Dirofilaria immitis* (Harada et al, 1970). Under these circumstances, when the sperm first meets the oocyte, the membranous organelles would not be immediately adjacent to the oocyte surface (see McLaren, 1973b; Plate 1, C and D). Any enzyme released at this stage would need to diffuse some distance to the oocyte and would be unlikely to cause the localized removal of egg coat noted in the foregoing studies.

Clearly therefore, the membranous organelles have neither the form nor function of an acrosome. Foor (1968) suggests that nematode sperm have no need of such a structure since the thin egg coat is pushed aside by the pseudopods prior to membrane fusion. The nature of the egg investments in *N. brasiliensis* is explored in Chapter 8 and the question of acrosomal loss during evolution of the Nematoda is discussed in Chapter 10.

What then is the function of the contents of the membranous organelles? Anya (1976) suggested that the material might enable the cell body to stick to a substrate, but Ward, Roberts and Argon (1982) have shown that this region does not adhere during locomotion. They suggest that the material may be actually preventing adhesion. It is possible that in some way it changes the environment of the uterus, making it more suitable for sperm survival and motility. Alternatively, the material may adsorb to and thus alter the surface of the sperm, this facilitating sperm-egg interactions. One way of adressing this question would be to examine sperm which have no membranous organelles and compare their surface and locomotion with those sperm which do possess these structures.

In most kinds of secretory cells, the membrane of the secretory vesicles becomes part of the plasma membrane after exocytosis. On the contrary, the membranous organelles of nematode sperm persist after

releasing their contents. Their morphology may provide a clue to their continued importance. They effectively increase the surface area of the sperm in a compact manageable way. In fact, Burghardt (1976; reported by Burghardt and Foor, 1978) calculated that exocytosis of the membranous organelles results in a doubling of the surface area of the sperm of *A. suum*. This increased surface area may provide an absorptive surface for the uptake of nutrients from the uterine fluids, or may be important in ion exchange or the secretion of materials from the sperm. Freeze-fracture of the membranous organelles after fusion, showed a high density of intramembranous particles suggestive of a metabolically active membrane (see Chapter 9.3). It is interesting that in those groups of plant-parasitic nematodes in which membranous organelles do not occur, the surface area is increased by an enormous number of needle-like filopodia (Shepherd, Clark and Kempton, 1974; Shepherd and Clark, 1979, 1980). In *A. tetraptera*, the only other species without these organelles, cross sections of the testis (Lee and Anya, 1967) show cytoplasmic extensions which resemble the filopodia of the cyst nematodes. These observations support the proposal that an increased surface area is important to the sperm of nematodes. When this is not made available by membranous organelles, it appears to be provided by an elaboration of the plasma membrane in the form of filopodia.

Since fertilization was not examined at the ultrastructural level in *N. brasiliensis* and *N. dubius*, the ultimate fate of the membranous organelles in these species is not known. Observations on a number of other species, however, have shown that the membranous organelles enter the egg after fertilization and remain in the cytoplasm for some time (Favard, 1961; Harada et al, 1970; Lee and Lestan, 1971; McLaren, 1973b).

The significance of this persistance is not known. These organelles may play some role in the early development of the egg, but alternatively they may be absorbed into the egg only to be broken down later.

Dense Spheres

As the spermatids of *N. dubius* near the end of their differentiation into mature sperm, a dense amorphous material accumulates in small deposits near the membranous organelles. This material fuses into larger, dense spheres, 0.25 - 0.35μm across, which are not membrane bound. A similar material forms in *N. brasiliensis* but as it is not as dense, it is less obvious. After insemination, this substance coalesces into an extremely dense, lobed structure in *N. dubius*, which comes to lie at the base of the conical nucleus. In *N. brasiliensis* it forms one or more dense spheres just posterior to the pseudopodial region. I believe that this structure may be analagous to the refringent body of ascarid sperm. After fertilization, this body contributes material towards the formation of the enormous numbers of ribosomes which suddenly appear in the ooplasm at this time (Foor, 1968; Kaulenas and Fairbairn, 1968). The newly-fertilized oocytes of *Physaloptera* (Foor, 1970), *D. viteae* (McLaren, 1973b) and *H. gallinarum* (Lee and Lestan, 1971) are also filled with ribosomes, but there is a refringent cone in the sperm of these species. Published micrographs show small accumulations of dense material in the sperm cytoplasm of these and other species, e.g. *D. californicum* (Wright et al, 1973), *N. battus* (Martin and Lee, 1980), *Gnathostoma* (Foor, 1970). This material may be analagous to the dense spheres in the sperm of *N. dubius* and *N. brasiliensis* and may provide ribosomal precursers to the newly-fertilized oocyte. A thorough study of the nature and origin of this material would be required to confirm this hypothesis.

RNA in the mature spermatozoa

The dense halo which exists around the chromatin of a number of species has been shown to contain RNA (Clark et al 1972; Wolf et al 1978; Goldstein and Triantaphyllou, 1980). A similar material occurs around the chromatin of *N. dubius* and *N. brasiliensis* and it would be interesting to know if this too contains RNA. The source of this material is not known. A sequence of micrographs of the maturing sperm of *N. dubius* shows that it condenses from a granular substance around the elongating chromatin, suggesting it may have originated from the nucleus after meiosis. Again further work is required to understand the function of this material.

7.2 Movement of the sperm of *N. brasiliensis*.

During translocation *in vivo* and *in vitro*, a cycle of events occurs at the leading edge of the sperm of *N. brasiliensis*. First, a small protrusion with a basal constriction ring, forms at the anterior. As the protrusion spills outwards and enlarges, the constriction ring remains stationary relative to the substrate. In effect, therefore, the constriction ring moves back along the sperm. Before it is halfway back, a new protrusion forms at the anterior. If this new protrusion is extended from one side of the leading edge, the sperm changes direction. Thus, the position at which the protrusion forms dictates the direction of locomotion.

The cycle of events which occurs in the sperm of *N. brasiliensis* is also seen during translocation of the sperm of *N. dubius* (Wright and Sommerville, 1977). These changes in shape are also typical of moving leukocytes, both *in vitro* (Ramsey, 1974; Senda, Tamura, Shibata, Yoshitake, Kondo and Tanaka, 1975; Englander, 1980) and *in vivo* (Shure, 1980). Locomotion has been reported in the sperm of only two other species of nematodes, *A. suum* (Nelson and Ward, 1981) and

C. elegans (Nelson et al, 1982). A cycle of events at the leading edge has not been recorded in either species, but descriptions of protrusions from the anterior and changes in contour along the sides of the sperm match those presented here for *N. brasiliensis*. In all cases, turns are preceeded by lateral extensions of the pseudopodium. The surface of the sperm of *N. brasiliensis* appears smooth, but in *C. elegans* and *A. suum* the sperm are covered by projections. In the latter, these are small and spiky, whereas in *C. elegans* they are short and stubby. They move back along the sperm slightly faster than its forward progress.

Membrane flow has been followed during locomotion of the sperm of *C. elegans* using a number of markers, such as fluorescent lectins and latex beads (Roberts and Ward, 1982a). These revealed continuous, directed movement of macromolecules from the tip of the pseudopod to its base. Moreover, fluorescent phospholipids were cleared from the pseudopod at the same rate as lectins. The results are therefore consistent with membrane flow over the pseudopod. New membrane components are added at the leading edge and old membrane is disassembled at the junction of the pseudopod and cell body. Ward, Roberts, Nelson and Argon (1982) suggest that the permanent pores which connect the membranous organelles to the plasma membrane are responsible for stabilizing the membrane over the cell body. Evidence in favour of this comes from the fer -1 mutant. Here, the membranous organelles fail to fuse with the plasma membrane, topographical assymetry is never established and the sperm are immotile (Roberts and Ward, 1982a).

The examination of membrane flow across the sperm of *N. brasiliensis* during locomotion was planned to follow preliminary lectin-labelling studies of fixed sperm (Chapter 8). Unfortunately the lectins did not bind avidly enough to enable their movement to be traced during sperm translocation. Lectin-labelling of moving leukocytes reveals the

same kind of centripetal transport of macromolecules back over the surface of the cells (Ryan, Borysenko and Karnorsky, 1974). This suggests that bulk membrane flow accompanies locomotion in these cells as it does in nematode sperm.

If it is assumed that leukocytes and the sperm of all nematodes move in a similar way, the data on locomotion in these different cells can be pooled and the following hypothetical model of movement in the sperm of *N. brasiliensis* can be proposed. At regular intervals, in both attached and unattached sperm, constriction rings are produced by a localized region of circular contraction across the leading edge. Addition of membrane at the anterior tip, then causes the resultant protrusion to enlarge. In adherent cells, areas of attachment to the substrate occur beneath the pseudopodium anterior to the constriction ring. As membrane is added at the anterior, the constriction ring moves backwards along the sperm. In attached sperm, however, it remains stationary relative to the substrate, resulting in the forward displacement of the sperm. Some kind of longitudinal contraction must cause the forward movement of cytoplasm. This jet-like flow, which carries the membrane subunits, is directed towards the point of growth of the anterior membrane by the constriction ring. Thus, the constriction ring is always perpendicular to the direction of movement (Fig 5.58). A change in direction could be accomplished by the formation of a new constriction ring on one side of the anterior margin. This would redirect the flow of cytoplasm and cause a new pseudodium to form laterally. Alternatively, turns could be initiated when a new point on the leading edge becomes the site of membrane growth. In this case a constriction ring would form at the base of the resultant protrusion. The mechanism by which cells change direction is an

important question, especially in relation to chemotaxis. Leukocytes are well known for their ability to direct their movement along a chemical gradient (Ramsey, 1974; Keller, Wissler, Hess and Cottier, 1978). It can be shown that a stationary leukocyte is able to sense a gradient across its surface, but exactly how it can do this is not known (Zigmond, 1978). Although chemotaxis has not been demonstrated in nematode sperm, the sperm of *N. brasiliensis* can be observed moving towards and congregating in the seminal receptacle of females. These sperm may be exhibiting chemotaxis but it is also possible that they are guided by changes in the surface across which they move i.e. they show "contact guidance".

One prediction from this hypothetical model is that both sperm and leukocytes should contain contractile elements capable of producing both circular and longitudinal forces. In amoeboid leukocytes, a three-dimensional actin network has been identified in the cell cortex and associated with the plasma membrane (Boyles and Bainton, 1979; Pryzwansky, Schilwa and Porter, 1981). Force is generated by the superprecipitation of actin and myosin filaments, while directionality is thought to derive from changes in the cross-linking of actin filaments (Stossel, Hartwig, Yin and Stendall, 1980).

On the basis of these observations one would expect to find actin filaments in the amoeboid anterior of nematode sperm. Micrographs of the sperm of both *N. dubius* and *N. brasiliensis* reveal a network of filaments approximately 7nm in diameter. These occur in clumps, separated by empty areas of cytoplasm. It is unlikely that this discontinuous pattern is an artifact of fixation, caused by osmium breaking and rearranging filaments of a continuous network (Pollard, Fujiwara, Niederman and Maupin-Szamier, 1976), since addition of tannic acid to the primary fixative, a procedure known to preserve cytoplasmic

filaments (Pollard and Maupin, 1978; Seagull and Heath, 1979) produced identical images. The identity of these filaments was investigated with cytochalasin, a compound shown to prevent the polymerization of actin filaments (Lin, Tobin, Grumet and Lin, 1980; McLean-Fletcher and Pollard, 1980). Since it had no effect on the translocating sperm of *N. brasiliensis*, the polymerization of actin seems not to be important in locomotion, however, this does not exclude the possibility that stable actin filaments play a role in cytoplasmic contraction in these sperm.

Although filaments occur in the pseudopod of the sperm of *A. suum* (Nelson and Ward, 1981; Abbas and Cain, 1979), none were observed in *C. elegans* despite extensive searching and various regimes of fixation (Nelson et al, 1982). In both species, fluorescent anti-actin antibody is localized in the pseudopodial region of activated sperm, but cytochalasin had no effect on sperm locomotion. Moreover, since actin represents less than 1% of the total sperm protein it is unlikely to play a major part in motility (Nelson and Ward, 1981; Nelson et al, 1982). In *C. elegans* the major sperm protein (MSP) constitutes 15% of the total protein in the sperm. Since MSP becomes localized in the pseudopods during activation and has the ability to form filaments, it has been implicated in amoeboid locomotion (Ward and Klass, in press). Analysis of defects in mutants unable to synthesise MSP should enable its function in *C. elegans* to be established. It would be interesting to examine the material of the fibrous bodies of *N. brasiliensis* and *N. dubius* more closely and to determine its fate and function in these species. Antibodies, raised against the fibrous bodies in *C. elegans* or *A. suum*, could also be used to determine if the material in these sperm bears any relationship to that in *N. brasiliensis* or *N. dubius*.

Although some sperm dissected from the seminal vesicles of males of *N. brasiliensis* can translocate for short distances, in general these sperm do not possess a fully developed capacity for locomotion. Instead, they form pseudopodia in an irregular and uncoordinated manner. Sections through the seminal vesicle,show that a granular amorphous material fills the small amoeboid region of these sperm. Occasionally, one finds a sperm with filaments in this region and it is tempting to speculate that only these sperm would be able to translocate. Support for this idea comes from the observation that during sperm activation in the female reproductive tract (Figs 5.52; 6.18), the contents of the amoeboid anterior change from a granular to a filamentous form.

The mean speed of 12.3 µm/min for the sperm of *N. brasiliensis* migrating across albumin, is slightly faster than measured for *N. dubius* (7.3 µm/min, Wright and Sommerville, 1977), but is very close to the published speeds for *C. elegans* and *A. suum* on acid washed glass (respectively 11 µm/min, Nelson and Ward 1981; 9.4 µm/min, Nelson et al, 1982) and for leukocytes (10±1.0 µm/min, Ramsey, 1974). The sperm of *C. elegans* moved faster (21µm/min) over a glass surface coated with *Ascaris* uterine extract (Nelson et al, 1982). This is not surprising as it would presumably resemble the substrate encountered *in vivo*.

The medium into which sperm were dissected did not affect the speed of movement, but it did influence sperm longevity. While sperm survived for a maximum of three hours in a simple salt solution, in the sperm medium recommended by Ward et al (1979) some were still active after 11 hours at 37^{o}C. It seems that low ionic strength, neutral pH and the presence of protein or other macromolecules are of key importance in sustaining sperm motility. (Nelson et al, 1982).

7.3 Conclusions

The results presented in Chapters 5 and 6 and discussed here, demonstrate that the original concept of a two-species model for the study of nematode sperm is a viable one. The mature sperm, as well as their developmental stages, are very similar in the two species. Important organelles, such as the fibrous bodies and membranous organelles, are virtually indistinguishable and have identical origins. Furthermore, the nature of the changes undergone during activation are the same in principle, even though the details of the morphological transformation differ slightly. Finally, spermatozoon motility is essentially the same in the two species and, judging from the ultrastructure of the amoeboid regions, it shares a common structural basis.

Comparison of the mature sperm of *N. brasiliensis* and *N. dubius* shows that the latter is more suitable for studies in which the light microscope is used. This is because, although the length of the sperm is similar in the two species, the cytoplasmic and amoeboid regions occupy a much greater proportion of the total length in *N. dubius*. Moreover, the morphological changes which accompany activation are more dramatic in this species. Since pairs of *N. dubius*, but not *N. brasiliensis*, remain *in copula* for some time after their removal from the host, the former would be suitable for studies of reproductive behaviour, insemination and sperm activity post-insemination. Preliminary studies of this kind have been performed by Sommerville and Weinstein (1964).

N. brasiliensis has been extensively used as a model for the study of the action of the immune mechanisms of the host against its nematode parasites. Although it is known that immune hosts can reduce parasite fecundity (Ogilvie and Hockley, 1968), few attempts have been made to determine the more specific effects of the host's immune system on the reproduction of its parasites. Lee's work has

shown that the spermatogenic cells of worms under immune attack undergo extensive changes associated with the presence of lysosome-like bodies, within the germ cells themselves (Martin and Lee, 1980b) or in the walls of the vas deferens (Lee, 1969). The full and detailed account of spermatogenesis in *N. brasiliensis* presented in Chapter 5 would provide a base from which the specific effects of host immunity on reproduction in males can be determined.

Although nematodes have often been used as gerontological models, little is known about the effects of aging on their reproduction (reviewed by Zuckerman and Himmelhock, 1980). Because *N. brasiliensis* is expelled from the rat within two weeks after infection, it is unsuitable for studies of this nature. *N. dubius*, however, may prove to be more useful, since worms are known to survive in mice for many months. Preliminary observations of worms from very old infections, suggest that their fecundity is reduced (Sommerville pers. comm). A comparison of the spermatogenic cycle in aged worms with the account presented in Chapter 6 could determine in what way aging affects the reproductive potential of male worms.

SECTION III

ASPECTS OF THE CELL BIOLOGY OF THE SPERM OF *N. BRASILIENSIS*

CHAPTER 8. THE SURFACE OF THE GAMETES

8.I Introduction

Virtually all cells are covered by a surface coat, which in the electron microscope appears as a fuzzy mat of filaments, 10 - 20nm thick, originating from the outer leaflet of the plasma membrane. It is made up of the carbohydrate side chains of integral glycoproteins and glycolipids, as well as extrinsic or peripheral oligosaccharides and glycoproteins, bound to the surface of the membrane electrostatically. This coat is important to the cell in many ways. Luft (1976) likens it to the fur of an animal pelt in providing both protection and strength and limiting the permeability of substances to the cell membrane proper.

Of more interest here, is that the cell surface can be said to determine the 'sensory world' of the cell (Denburg, 1978). It bears markers which identify the cell and receptors which enable it to recognize and interact with other individuals. In this way, cells can exchange information about one another. Cell adhesion is often a result of cell-cell interactions of this kind. The simplest model of this process predicts initial binding between the two cell surfaces, followed by the formation of stable attachments (Glaser, 1980). In some situations (Dazzo, 1980; Stoolman and Rosen, 1981) but not others (Barondes, 1980; Chin, Rubin and Den, 1981) binding can be shown to involve a carbohydrate-protein interaction. Since these proteins interact with specific sugar groups they are classed as lectins. Compelling evidence that sperm-egg binding is mediated by this kind of interaction has come from the study of fertilization in sea urchins. The egg-binding receptor, a protein called bindin, is the major component of the acrosomal vesicle of the sperm (Glabe and Vacquier, 1977). With the triggering of the acrosome reaction,

bindin becomes exposed on the elongating acrosomal process and shortly afterwards can be localized on the vitelline surface (Moy and Vacquier, 1979). A glycoprotein with a high affinity for bindin has now been isolated from the egg surface and has been partially characterized (Vacquier, 1980; Glabe, Grabel, Vacquier and Rosen, 1982).

While it can often be demonstrated that the particular part of the egg to which sperm bind, e.g. the chorion of the ascidian egg (Rosati, de Santis and Monroy, 1978) or the zona pellucida of mouse eggs (Bleil and Wassarman, 1980) contains lectin binding sites (Nicolson, Yanagimachi and Yanagimachi, 1975), it is more difficult to show that these molecules are specific sperm-receptors. Inhibition of *in vitro* fertilization with lectins (Schmell, Earles, Breaux and Lennarz, 1977; Oikawa, Yanagimachi and Nicolson, 1973) does not necessarily confirm this, as lectins bound to the egg surface can stearically hinder sperm binding. Enzymatic treatment of the gamete surfaces may be needed to demonstrate the nature of their receptor molecules. For example, in the prawn, *Sicyonia ingentis*, the receptor on the egg appears to be a trypsin-sensitive protein which binds to a complementary periodate-sensitive polysaccharide, located at the anterior tip of the sperm (Clark, Yundin and Kleve, 1981). Similar enzyme treatments have revealed that gamete recognition in the brown alga, *Fucus serratus*, relies on lectin-ligand interactions (Bolwell, Callow, Callow and Evans, 1979).

While endogenous lectins may be implicated in cell-cell interactions such as sperm-egg binding, exogenous lectins, usually derived from plant seeds, may be used as specific molecular-probes to explore the architecture and dynamics of the cell surface. One technique involves estimating the degree of cell agglutination induced by addition of lectins to cell suspensions. This technique relies on the ability of polyvalent lectins to cross-link and aggregate the surface molecules

to which they bind. Successful experiments, using sperm suspensions, have provided information on the density, mobility and position of carbohydrates on the sperm surface (Nicolson and Yanagimachi, 1972). Negative results are more difficult to interpret, as lack of agglutination may be caused by factors other than a lack of receptors (Yanagimachi and Nicolson, 1976). The tagging of lectins with I^{125}, has enabled the quantification of lectin binding to cells. Edelman and Millette (1971) found a similar number of ConA receptors on sperm, lymphocytes, thymus cells and erythrocytes of mice. Similarly, the number of lectin receptors does not vary substantially between sperm of different species (rabbit, 1.0×10^7; hamster, 1.9×10^7; mouse, 4.9×10^7) especially when relative areas are considered (Millette, 1977; Nicolson, Lacorbiere and Yanagimachi, 1972). Lectin-binding sites can be localized on the cell surface by tagging the lectins with fluorescein isothiocyanate (FITC) for visualization in the light microscope, or ferritin or colloidal gold (Horisberger and Rosset, 1977) for detection in the TEM. Horseradish peroxidase can also be used to mark ConA binding sites, as a dense black precipitate forms when the lectin-horseradish peroxidase complex reacts with diaminobenzidine (Bernhard and Aurameas, 1971). As would be expected, the lectin-labelling pattern is consistent no matter which marker is used to visualize the sites of lectin binding (Millette, 1977).

Lectin labelling demonstrates a dramatic regionalization of the mammalian sperm surface. In the sperm of mice, while lentil and yellow pea agglutinin label the entire surface, ConA binds mainly to the acrosome and green pea lectin only to the post-acrosomal region and tail. Red lentil labels all but the post-acrosomal area (Gall, Millette and Edelman, 1974). Lectins label the sperm of different species in a similar way. Thus, ConA and WGA bind more intensely to the acrosome in sperm of the hamster (Koehler and Kinsey, 1977),

guinea-pig (Schwarz and Koehler, 1979), rabbit (Nicolson, Usui, Yanagimachi, Yanagimachi and Smith, 1977), ram (Courtens and Fournier-Delpech, 1979), human, rat and bull (Baccetti, Bigliardi and Burrine, 1978). An exception is in the mouse, where WGA binds more avidly to the tail than the head (Edelman and Millette, 1971).

The majority of lectin-labelling experiments have been performed on sperm from laboratory animals or common domestic species. Of the other mammals studied, the hydrax, armadillo and possum also have patchy distributions of lectin binding sites (Bedford and Millar, 1978; Temple-Smith and Bedford, 1976), but sperm of the shrew label uniformly with ConA (Cooper and Bedford, 1976). There have been few studies of invertebrate sperm using the lectin-labelling technique. In sea urchins one of the two species examined bound ConA on the sperm head (Aketa, 1975), while 23 out of the 50 lectins obtained from various seed extracts caused head-head agglutination of clam sperm (Badel and Brilliantine, 1969). These studies then suggest that the heads of invertebrate sperm, like those of mammals, bear the majority of lectin receptors. This trend was not noted in the sperm of two species of frogs, since here, agglutination with various lectins occurred at random positions on the sperm (del Pino, Cabado and Fonio, 1981).

Lectin-induced redistribution of surface receptors has been used successfully to explore membrane dynamics in sperm. As might be expected from the distinct regionalization seen with lectin labelling, there is little lateral mobility of membrane components in sperm. When live guinea-pig sperm were labelled at $10^{\circ}C$, reincubated at $37^{\circ}C$ and compared with sperm which had been prefixed, no difference in the binding patterns of FITC-ConA, -SBA or -WGA was detected (Schwarz and Koehler, 1979). Although Koehler (1978) noted some clumping of ConA receptors on the hamster sperm tail when unfixed labelled sperm were incubated at $37^{\circ}C$, no such aggregation was seen on the sperm head where

receptors are more dense.

Lectins have also been used to probe the consequences of maturational changes on the sperm surface. Mammalian sperm undergo substantial modifications during epididymal transit. These include changes to the phospholipid and enzymic composition of the membrane (Scott, Voglmayr and Setchell, 1967; Chulavatnatol and Yindepit, 1976; Terner, MacLaughlin and Smith, 1975) and modifications of the surface proteins and glycoproteins (Voglmayr, Fairbanks, Jackowitz and Colella, 1980; Young and Goodman, 1980). Maturation is also reflected in alterations to lectin binding patterns. During epididymal transit, ConA binding was reduced on the flagella of bull, human, ram, hydrax and armadillo sperm (Baccetti *et al.*, 1978; Courtens and Fournier-Delpech, 1979; Bedford and Millar, 1978) and over the head of rat sperm (Baccetti *et al.*, 1978; Olson and Danzo, 1981, Dooher, 1981). WGA, and to a lesser extent RCA, also have a decreased affinity for sperm after epididymal maturation (Nicolson *et al.*, 1977). An exception to this general pattern is seen in rabbits, where lectin labelling is similar on sperm from all regions of the epididymis (Nicolson *et al.*, 1977). Although in some cases, receptor loss might occur through shedding, there is good evidence that substances from epididymal and seminal fluid become adsorbed to the sperm surface and mask lectin binding sites (Young and Goodman, 1980; Voglmayret *et al.*, 1980). Thus, a report that rabbit sperm from the cauda epididymis strongly bound ConA (Gordon, Dandekar and Bartoszewicz, 1975) may have little relevance to the situation *in vivo*, as sperm were washed prior to labelling. This procedure would probably remove surface coating and expose otherwise cryptic lectin-binding sites (Koehler, 1981). Capacitation is another maturational change which has been examined with lectins. Studies using a number of lectins on sperm from different animals show the same general trend: capacitation involves the formation of patches,

entirely free of bound lectin, over the acrosomal region (Kinsey and Koehler, 1978; Gordon *et al.*, 1975; Schwarz and Koehler, 1979; Lewin, Weissenburg, Sobel, Marcus and Nebel, 1979; Koehler and Sato, 1978).

It is clear from these studies of sperm, that as well as determining the chemical nature of surface molecules, lectins can provide information about their distribution and mobility at different stages of cell maturation. For this reason, lectin-labelling was used to examine the molecular organization of the surface of the sperm of *N. brasiliensis*. It was anticipated that the segregation of the cytoplasmic organelles into different parts of the sperm during spermiogenesis might be reflected in regionalization of the sperm surface. Furthermore, it was predicted that the morphological changes which follow insemination would be accompanied by changes to the surface molecules. The surface architecture of unfertilized oocytes was also examined, since only a study of both sperm and eggs can provide an insight into the nature of gamete interactions.

In conjunction with lectin labelling, ruthenium red was used to examine the charge distribution and ultrastructural features of the surface coats of both eggs and sperm. Many techniques are available for enhancement of the cell coat, including staining with tannic acid (Simionescu and Simionescu, 1976), modification of the PAS method to show neutral mucopolysaccharides (Hughes, 1975) and the detection of charged groups using colloidal iron hydroxide (Gasic, 1968), alcian blue (Behnke and Zelander, 1970), ionized ferritin (Danon, Goldstein, Marikovsky and Skutelsky, 1972) and ruthenium red (Luft, 1971b). The inorganic dye ruthenium red (RR) was chosen here because, in conjunction with osmication, it provides a high resolution, high contrast technique which stains extraneous coats on a wide range of cell types, e.g. muscle, heart, lung, intestine, cartilage, erythrocytes (Luft, 1971b) and amoebae (Szubinska and Luft, 1971).

8.2 Results

8.2.1 Ruthenium Red Labelling

Preliminary Comments

Although RR can penetrate blocks of tissue to a depth of 100µm (Luft, 1971b), both sperm and oocytes were unstained after intact testes and uteri were immersed in the dye during fixation. Penetration was poor even in small (500µm) segments of reproductive tract. Subsequently, it was found that sperm dissected from worms stuck to the bases of polypropylene petri dishes and could be stained with RR, then fixed and processed *in situ*. These preliminary tests were performed on immature stages of the sperm of *N. dubius* which were available at the time. In these specimens, the cell coat appeared as fine black filaments extending out from the cell surface (Figure 8.1). Satisfied that the technique was working well, I proceeded with staining of the gametes of *N. brasiliensis*.

Ruthenium red labelling of eggs

Unfertilized eggs are surrounded by a cell coat, 40-45nm thick (Figure 8.2), which with routine staining is moderately electron-dense. The outer edge of the coat is delimited by a narrow electron-dense border (Figure 8.3). The coat stains with ruthenium red (Figure 8.4A). This stain highlights gaps which occur in the coat at intervals (Figure 8.4B). The plasma membrane is continuous across these gaps, but the extraneous coat appears to be absent for a distance of 150-250 nm. Often, the cytoplasm bulges out through this gap to form a bump or even a stumpy microvillous (Figure 8.4C). Neuraminidase changes the surface substantially (Figure 8.5A-C). The unstained preparation (Figure 8.5A) suggests that there is less RR binding to the surface now. This is confirmed in stained sections (Figures 8.5B,C). Moreover, the coat appears to have been partially digested by neuraminidase.

FIGURE 8.1 : RR staining of the surface of spermatids of *N. dubius* reveals a fine filamentous cell coat. Section unstained.

FIGURE 8.2 : Section through the posterior ovary of *N. brasiliensis* showing the cell coat on unfertilized eggs. Section stained with lead and uranium.

FIGURE 8.3 : Higher power micrograph of the egg coat. Section stained.

8·1

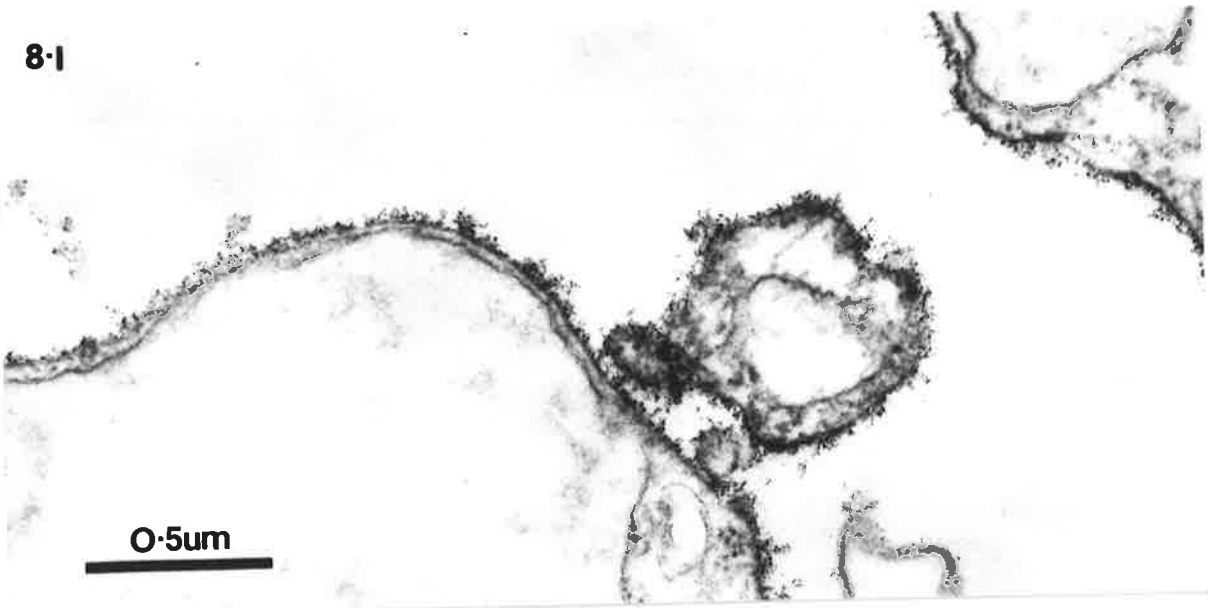

8·2

8·3

FIGURE 8.4A : RR staining of the egg coat. Unstained section.

FIGURE 8.4B : RR staining highlights gaps in the egg coat of *N. brasiliensis*. Section stained with lead and uranium.

FIGURE 8.4C : The cytoplasm sometimes bulges out through the gaps in the cell coat and forms a stumpy microvillous. RR stained, section counterstained.

8·4A

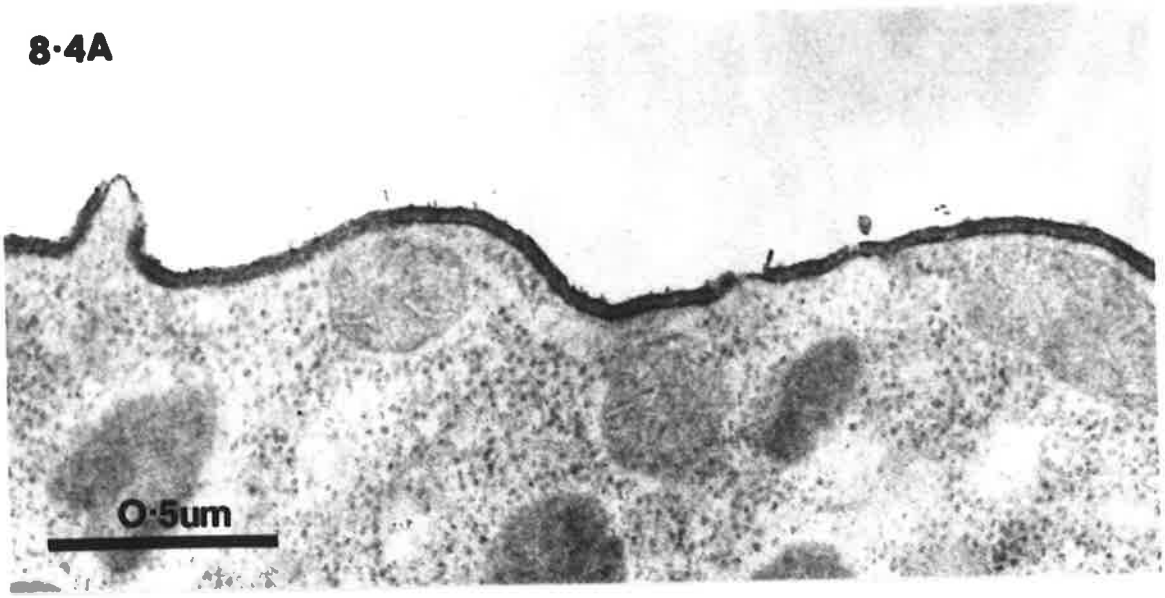

B

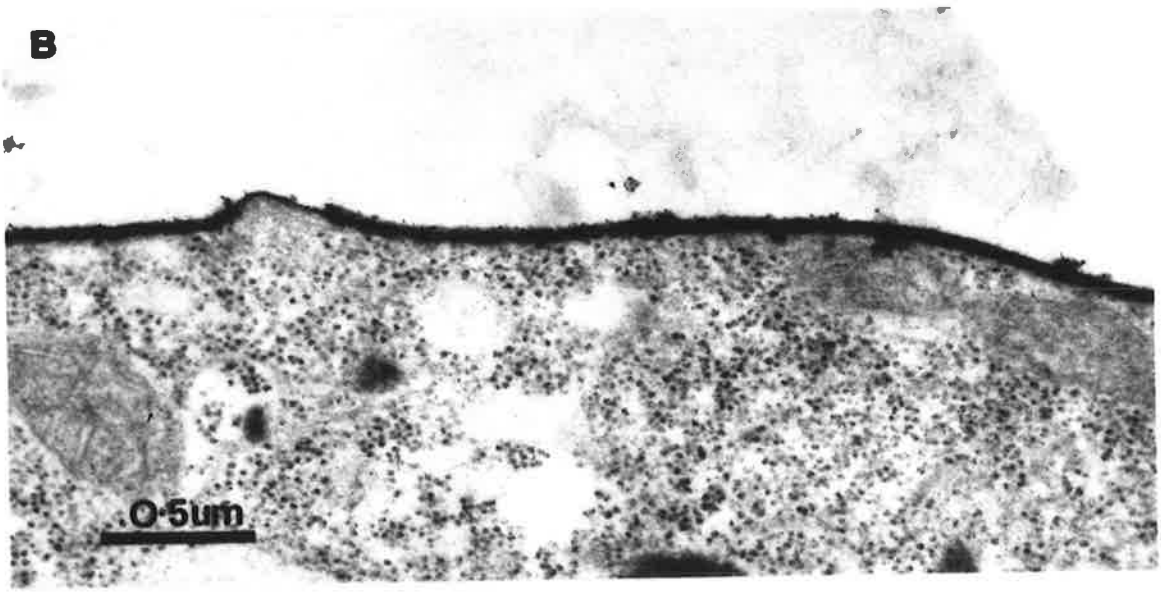

C

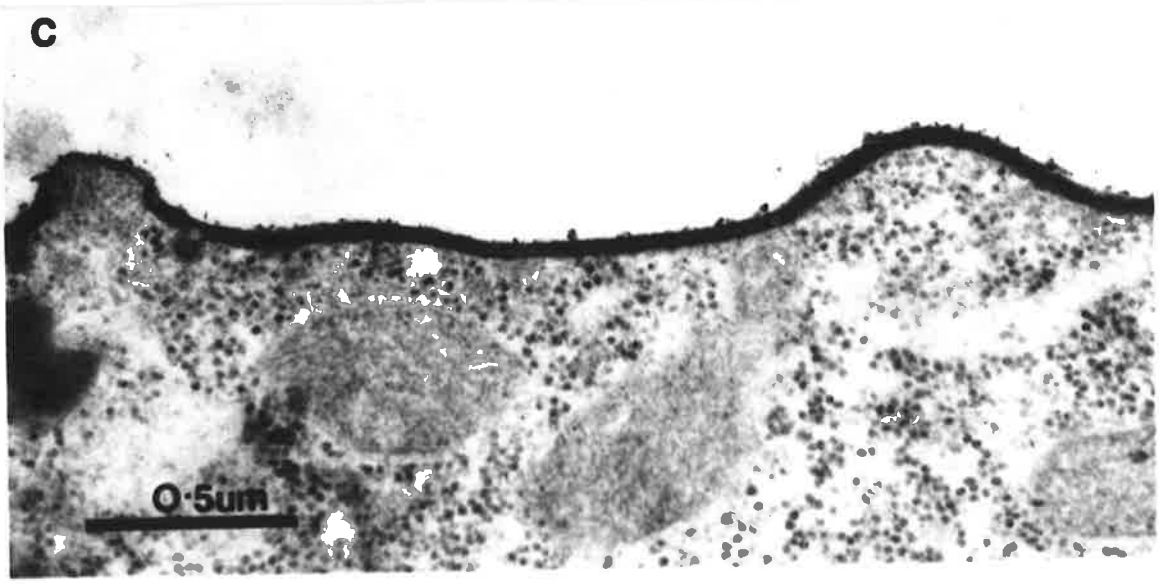

FIGURE 8.5A : Neuraminidase virtually abolishes RR staining of the egg coat. Moreover, it partially digests the coat. Unstained section.

FIGURE 8.5B : The outer surface of the egg coat is covered by a tangled mat of filaments after incubation with neuraminidase. Black RR staining is no longer visible. Section stained with lead and uranium.

FIGURE 8.5C : The external part of the cell coat, which previously formed a dense border, takes on a pentilaminar appearance after neuraminidase treatment. Section stained with lead and uranium.

8·5A

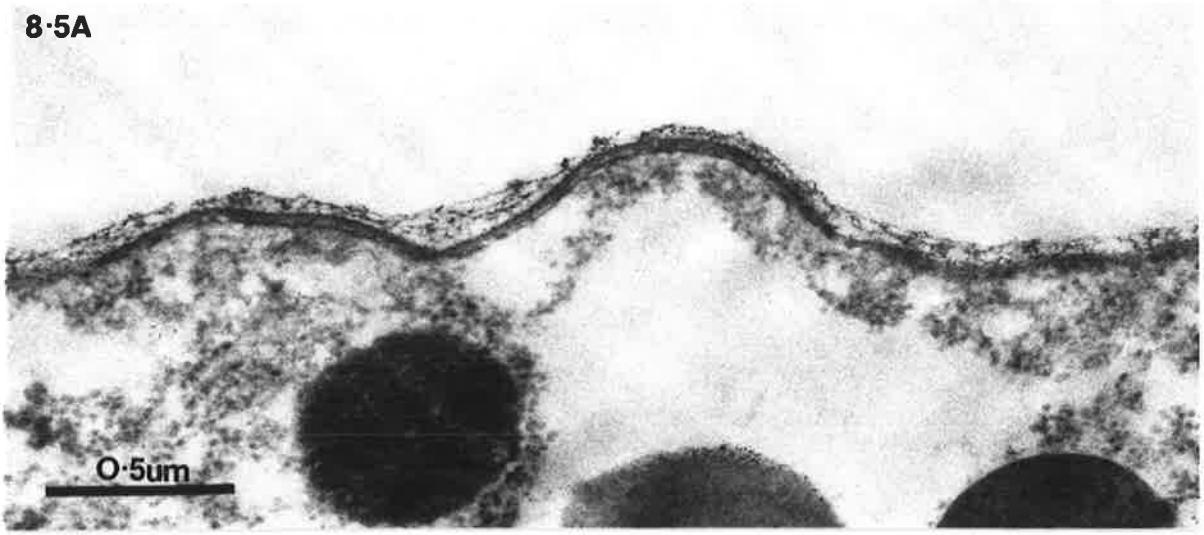

B

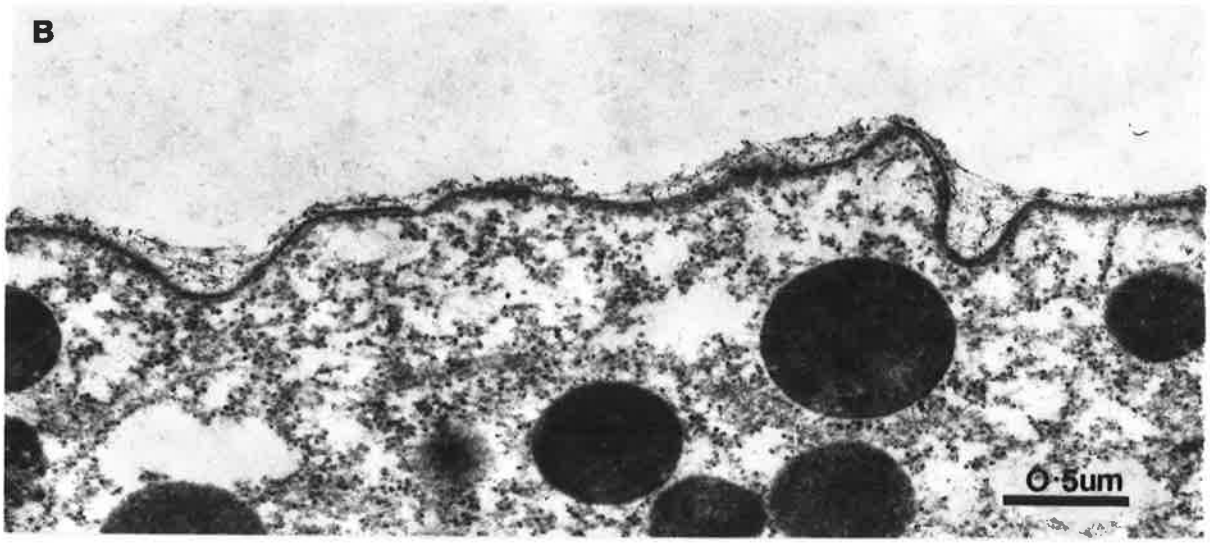

C

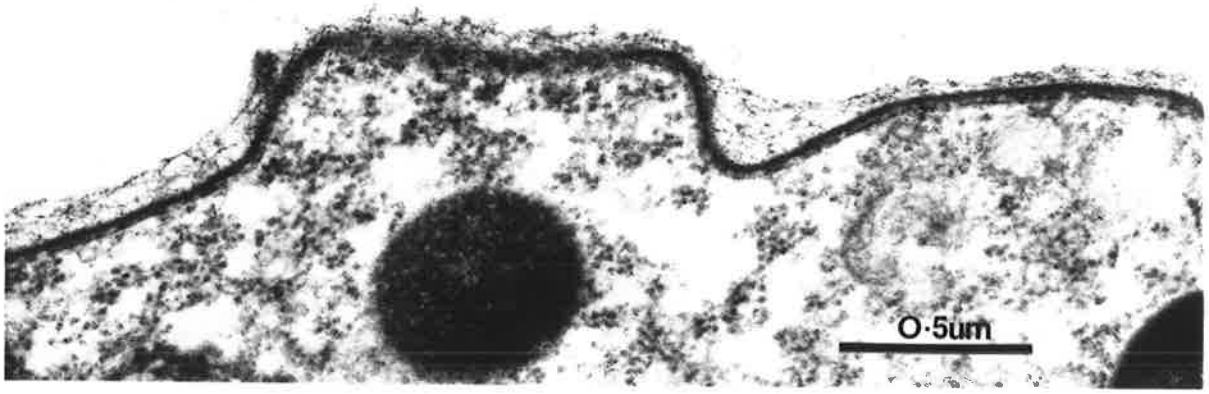

Although the characteristic band of extracellular material is still present, it is less dense and a mass of tangled filaments, resembling cobwebs, clings to it. Enlargements of the cell surface after neuraminidase treatment show a multilaminate structure at the outer edge (Figure 8.5C).

Ruthenium Red labelling of sperm from males

With conventional staining (lead and uranium) spermatozoa from the seminal vesicles of males appear to have virtually no cell coat (see Figure 5.30). Occasionally, fine filaments may be seen extending from the outer side of the plasmalemma, especially if tannic acid is used in conjunction with glutaraldehyde (Figure 8.6A). When RR is added to the fixative, a fine black stain lines the plasma membrane. There is some variation in staining intensity between sperm (Figure 8.7, compare F,G,H), but in general there is slightly more stain over the amoeboid region than elsewhere (Figure 8.7F). Staining the sections lightly with lead and uranium enhances the black precipitate of RR slightly (Figure 8.7B unstained section, F,G stained lead, uranium). When sperm are incubated with neuraminidase prior to labelling with RR (Figure 8.7E), there is some reduction in staining (compare with Figure 8.7D) but it is not abolished entirely (Figure 8.7I,J).

RR labelling of sperm from females

When sperm from females are stained with RR and examined in sections which have not been counterstained, the most striking feature is the density of cytoplasmic staining (Figure 8.8A,B). This is especially obvious when these images are compared with those obtained when RR is omitted from the fixatives (Figure 8.8, compare A and D, B and C). All sperm examined, including specimens from separate experiments performed on different days with fresh solutions, showed this

FIGURE 8.6A : Sperm dissected from males of *N. brasiliensis* show a sparse cell coat when tannic acid is added to the glutaraldehyde during fixation. Tannic acid also enhances cytoplasmic staining.

B : Cytoplasmic staining is also enhanced when sperm from females are stained with tannic acid. The fuzzy coat on the internal membranes of the membranous organelles is also stained with tannic acid. A very sparse cell coat exists on the sperm surface.

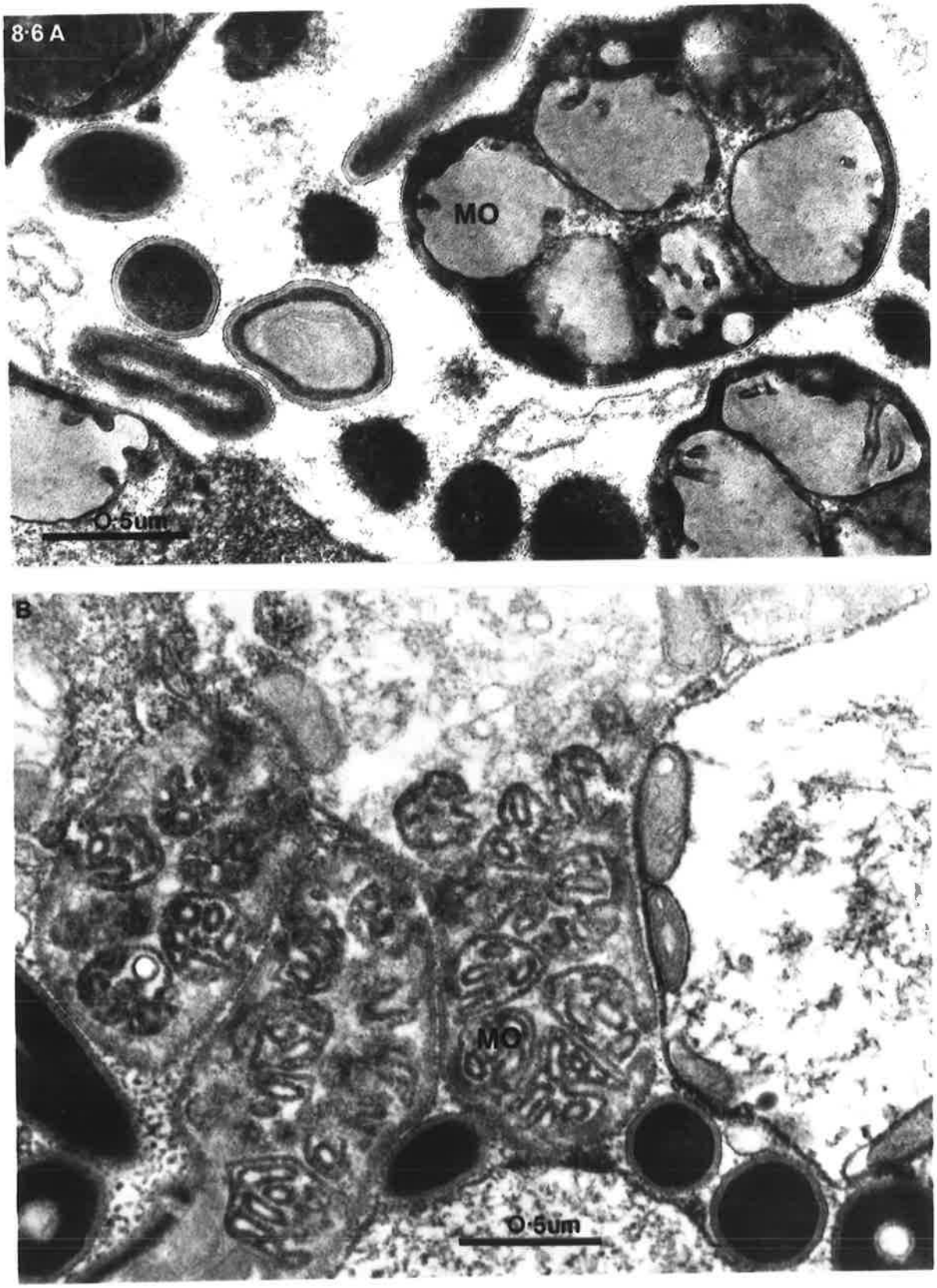
8·6 A
MO
0·5um
B
MO
0·5um

FIGURE 8.7 : RR staining of sperm from the seminal vesicles of males.

A,C, Control specimens (RR omitted from fixative) showing amoeboid region and cytoplasmic region. Sections unstained.

B,D,F,G,H, RR-stained material exhibits a fine black deposit on the surface of the cytoplasmic (c), nuclear (n) and amoeboid regions (a). In F, the stain is slightly thicker over the amoeboid anterior. B,D,H unstained sections. F,G stained with lead and uranium.

E,I,J, specimens fixed in glutaraldehyde then incubated in neuraminidase before labelling with RR. The surface is changed by the enzyme and there is a little less RR staining. E unstained section. I,J stained with lead and uranium.

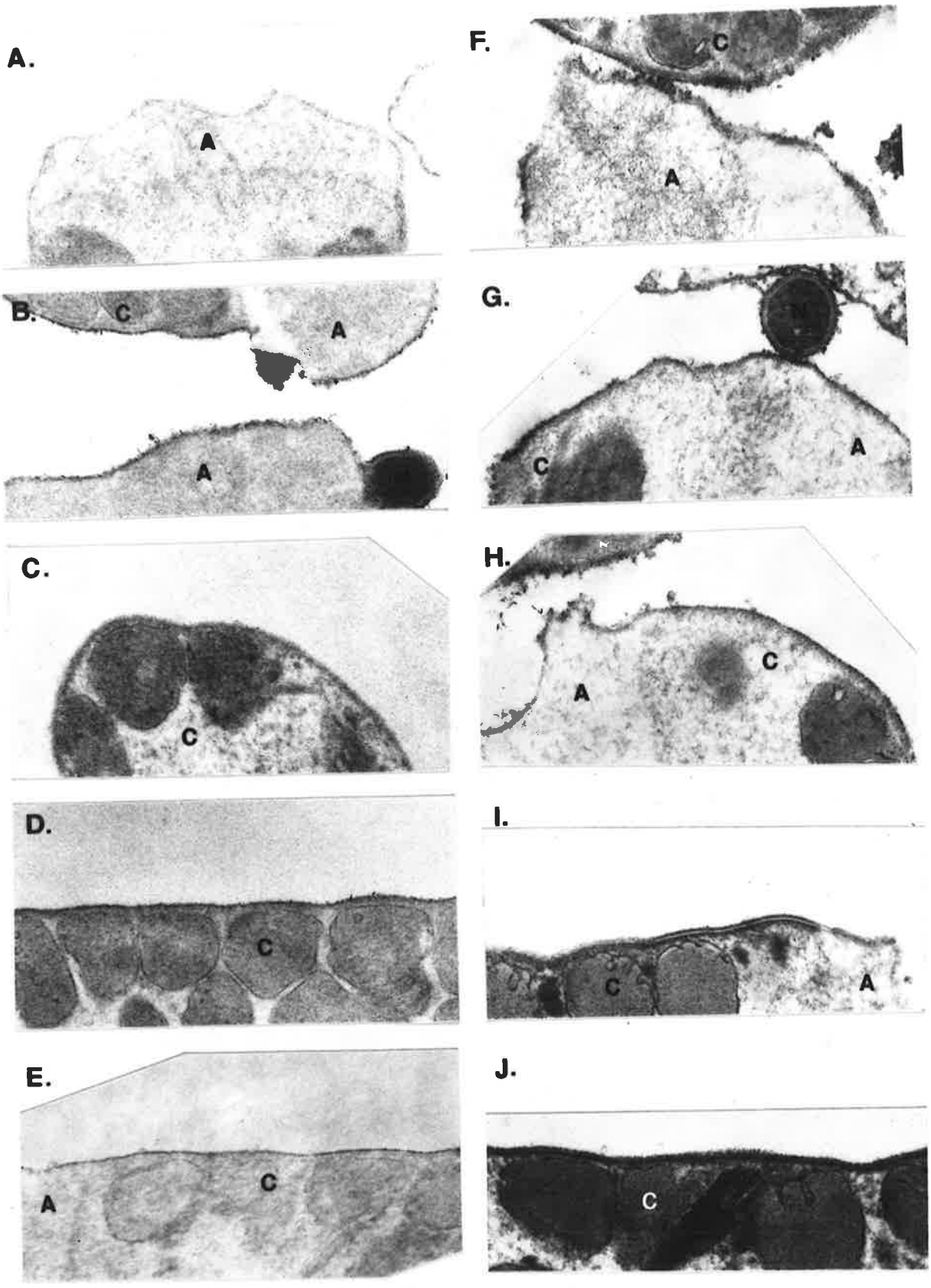

8·7

1um

FIGURE 8.8 : RR staining of sperm from the uterus of females.

C,D, Control preparations, RR omitted from fixitives, showing amoeboid, cytoplasmic and nuclear regions. Unstained sections.

A,B,F,H,I, RR stained specimens. Note the dense cytoplasmic staining even in sections without counterstain (A,B,I). The internal membranes of the membranous organelles are clearly labelled (A,F) and there is some surface material in the amoeboid region (B). F,H, stained with lead and uranium.

E,G,J, fixed specimens were incubated in neuraminidase for 3 hrs at 37^0C before staining with RR. There is some reduction in staining of the membranes of the membranous organelles (J) but otherwise the staining pattern is little changed. E,J stained with lead and uranium; G unstained section.

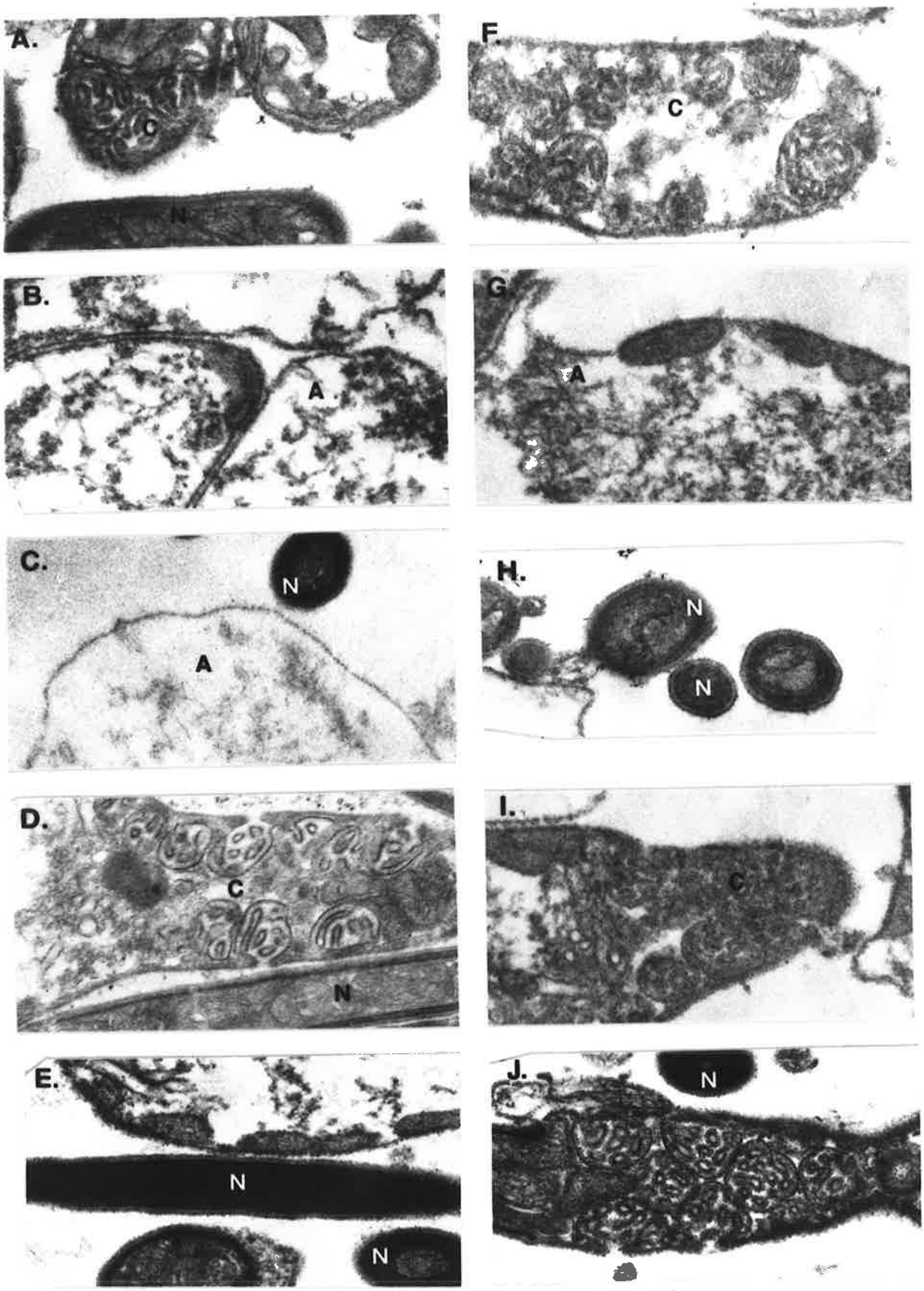

8·8

1um

internal staining, suggesting that it is not a consequence of occasional cell damage.

The surface staining with RR in the nuclear and cytoplasmic regions of the sperm is very sparse (Figure 8.8A,H,F) and is not reduced significantly by neuraminidase (Figure 8.8E,I,J). The internal membranes of the membranous organelles have bound large quantities of the dye, giving them a bold appearance even in sections which have no counterstain (Figure 8.8, compare A with D). Enzymic digestion with neuraminidase has reduced this a little (Figure 8.8J). The amoeboid region bears some surface coat material (Figure 8.8G) which is especially evident when two membranes lie adjacent (Figure 8.8B). There is some reduction in the density of this material after treatment of the sperm with neuraminidase (Figure 8.8E). Figure 8.6B shows that if tannic acid is applied to sperm in the same way as RR, i.e. added to the fixative, the staining pattern is very similar. As well as enhancing cytoplasmic contrast, the tannic acid has stained the internal membranes of the membranous organelles and some extracellular material.

8.2.2 Lectin Labelling

Lectin labelling experiments, preliminary comments

As it was important to ensure that my techniques of labelling and fluorescence microscopy were satisfactory, a preliminary labelling experiment was performed using guinea pig and mouse sperm. These species were chosen because they are readily available and the lectin labelling pattern of their sperm is well documented (Schwarz and Koehler, 1979; Koehler, 1981). Figure 8.9A,B shows the results which I obtained using ConA - FITC on these sperm. Since these micrographs are virtually identical to those in the literature (Figure 7C, Koehler, 1981; Figure 2, Schwarz and Koehler, 1979), I was assured that my techniques were adequate. In subsequent experiments in which

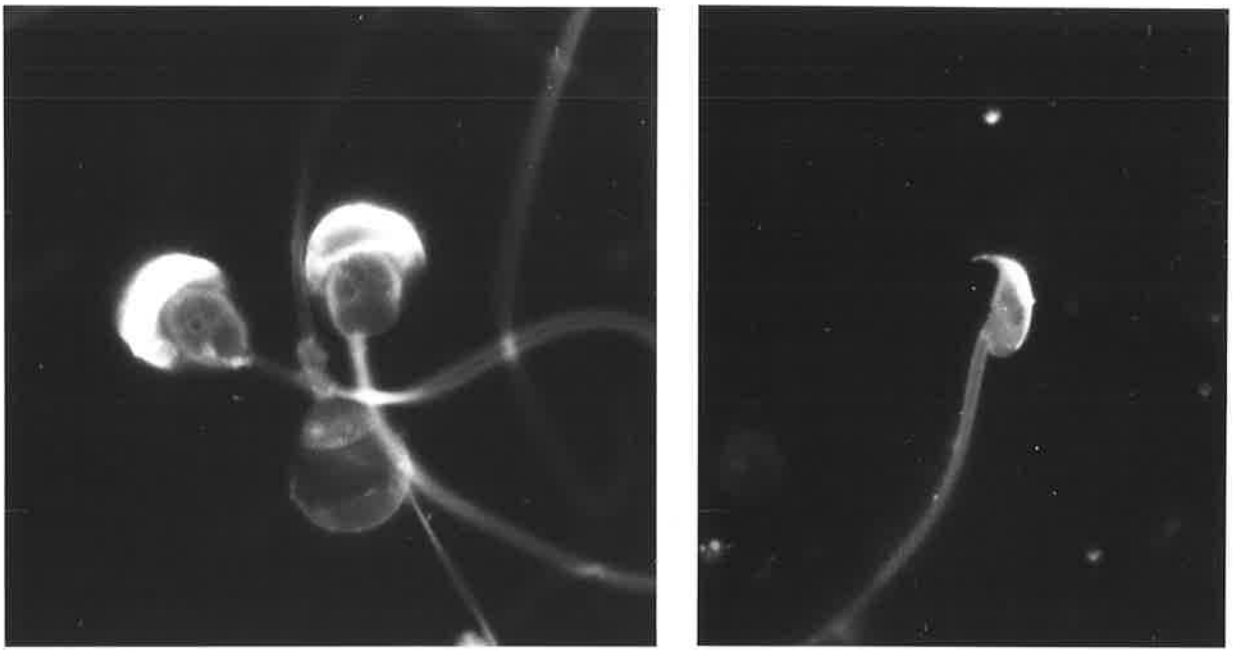

FIGURE 8.9A : ConA-FITC labelling of epididymal guinea-pig sperm showing intense fluorescence over the acrosome.

FIGURE 8.9B : The acrosomal region of the mouse sperm is intensely stained with ConA-FITC. The rest of the surface bears some stain.

Both micrographs magnified 1,600 times.

nematode sperm were labelled, the sperm of one of these mammalian species was included to act as a positive control.

ConA

Unfertilized oocytes approaching the oviduct autofluoresce intensely when illuminated with UV light (Figure 8.10A). Oocytes labelled with ConA - FITC showed an additional halo of fluorescence around their edges (Figure 8.10B). This surface labelling was punctuated by tiny gaps (arrows Figure 8.10C). Control specimens incubated with ConA - FITC and its sugar inhibitor, α-methyl-mannoside, autofluoresced but had no surface labelling (Figure 8.10D). When mature sperm from the seminal vesicles of male worms are labelled with ConA - FITC, the cell body and the nuclear tail fluoresce (Figure 8.11A). Sperm which have been inseminated into females also bind ConA - FITC over these regions, but labelling is slightly more intense over the cytoplasmic area (Figure 8.11B). Fluorescence over the amoeboid anterior is weak. Control sperm, labelled with ConA - FITC in the presence of α-methyl mannoside were indistinguishable from unlabelled sperm.

WGA

A comparison of WGA - FITC labelling in the presence or absence of the inhibitor ovomucoid (Figure 8.14A,B) demonstrates that this lectin does not bind to the surface of unfertilized oocytes. Sperm from males show weak fluorescence over their cytoplasmic and nuclear regions (Figure 8.12A). After insemination the labelling of these areas is unchanged (Figure 8.12B).

RCA_{11}

RCA_{11} - FITC does not label the surface of unfertilized oocytes, but the cytoplasmic region, and to a lesser extent the nucleus, of sperm from males fluoresces when labelled with this lectin (Figure

FIGURE 8.10A : Unlabelled, fixed oocyte autofluorescing under UV light.

FIGURE 8.10B : Unfertilized oocyte labelled with ConA-FITC shows intense surface labelling.

FIGURE 8.10C : Oocytes labelled with ConA-FITC showing surface labelling which is punctuated by tiny gaps (arrows).

FIGURE 8.10D : Oocytes incubated with ConA-FITC and sugar inhibitor, α methyl mannoside, show autofluorescence but no surface label.

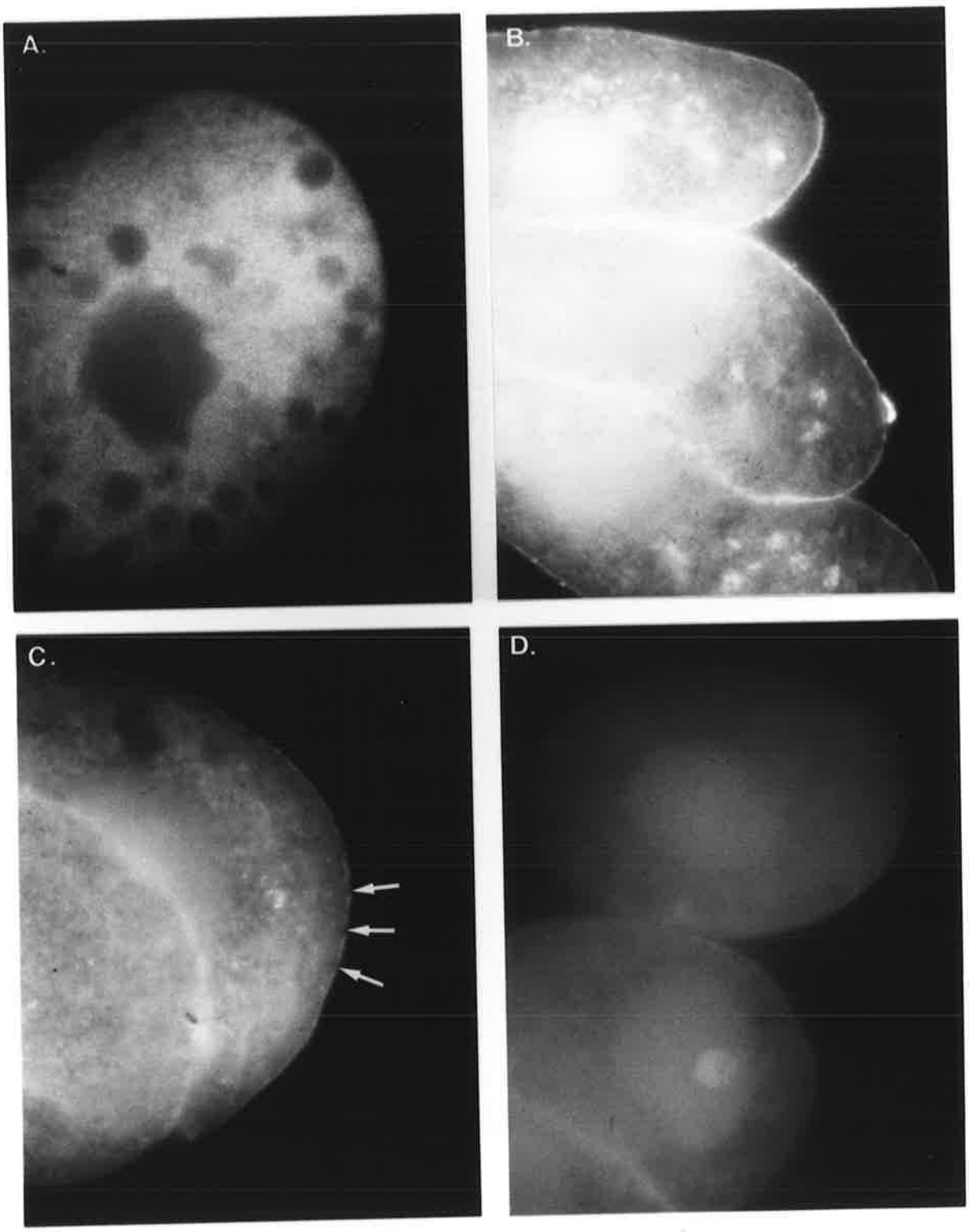

8·10

20um

FIGURE 8.11A : Sperm from the seminal vesicle of males stained with ConA -FITC. Fluorescence is over cell body and nuclear tail. Note how little label has bound compared with mammalian sperm (FIGURE 8.9).

FIGURE 8.11B : Sperm from the uterus of females stained with ConA-FITC. The labelling over the cytoplasmic region is slightly more intense than previously.

FIGURE 8.12A : Sperm from males fluoresce only weakly with WGA-FITC

FIGURE 8.12B : Labelling on sperm from females is also weak with WGA-FITC.

FIGURE 8.13A : RCA-FITC labels the cytoplasmic region of sperm from males slightly more than the nuclear region. Labelling is less intense than with ConA-FITC.

FIGURE 8.13B : RCA-FITC labelling on sperm from females is more intense over the cytoplasmic region.

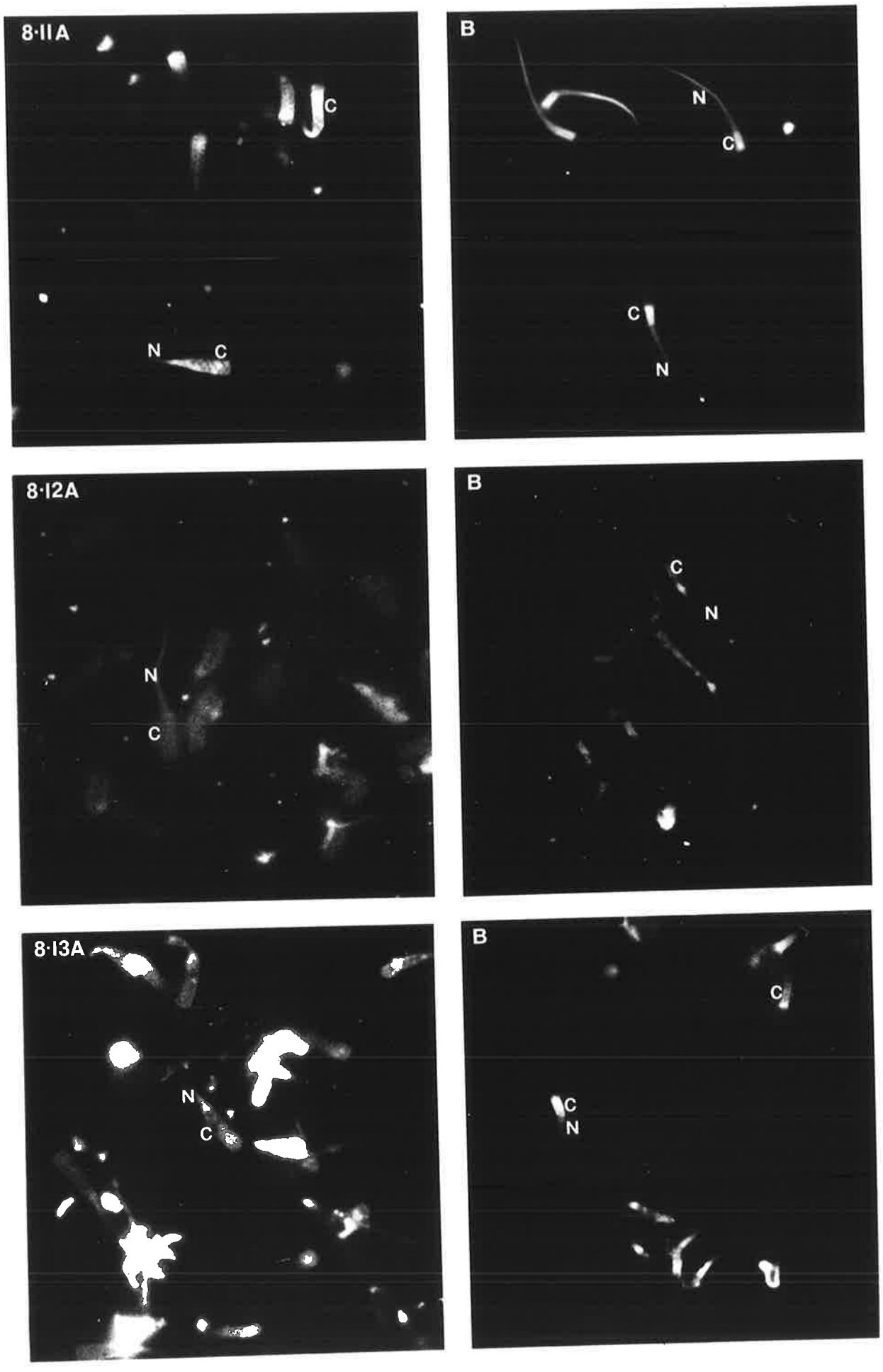
8·11A
C
N
C
B
N
C
C
N
8·12A
N
C
B
C
N
8·13A
N
C
B
C
C
N
20um

FIGURE 8.14A : WGA-FITC labelled oocyte. No surface fluorescence can be detected.

FIGURE 8.14B : Oocyte labelled with WGA-FITC in the presence of the inhibitor ovomucoid. There is no surface fluorescence.

FIGURE 8.14C : Unfertilized oocytes unlabelled, but autofluorescing under UV illumination.

FIGURE 8.14D : SBA-FITC labelled oocyte. No surface fluorescence can be detected.

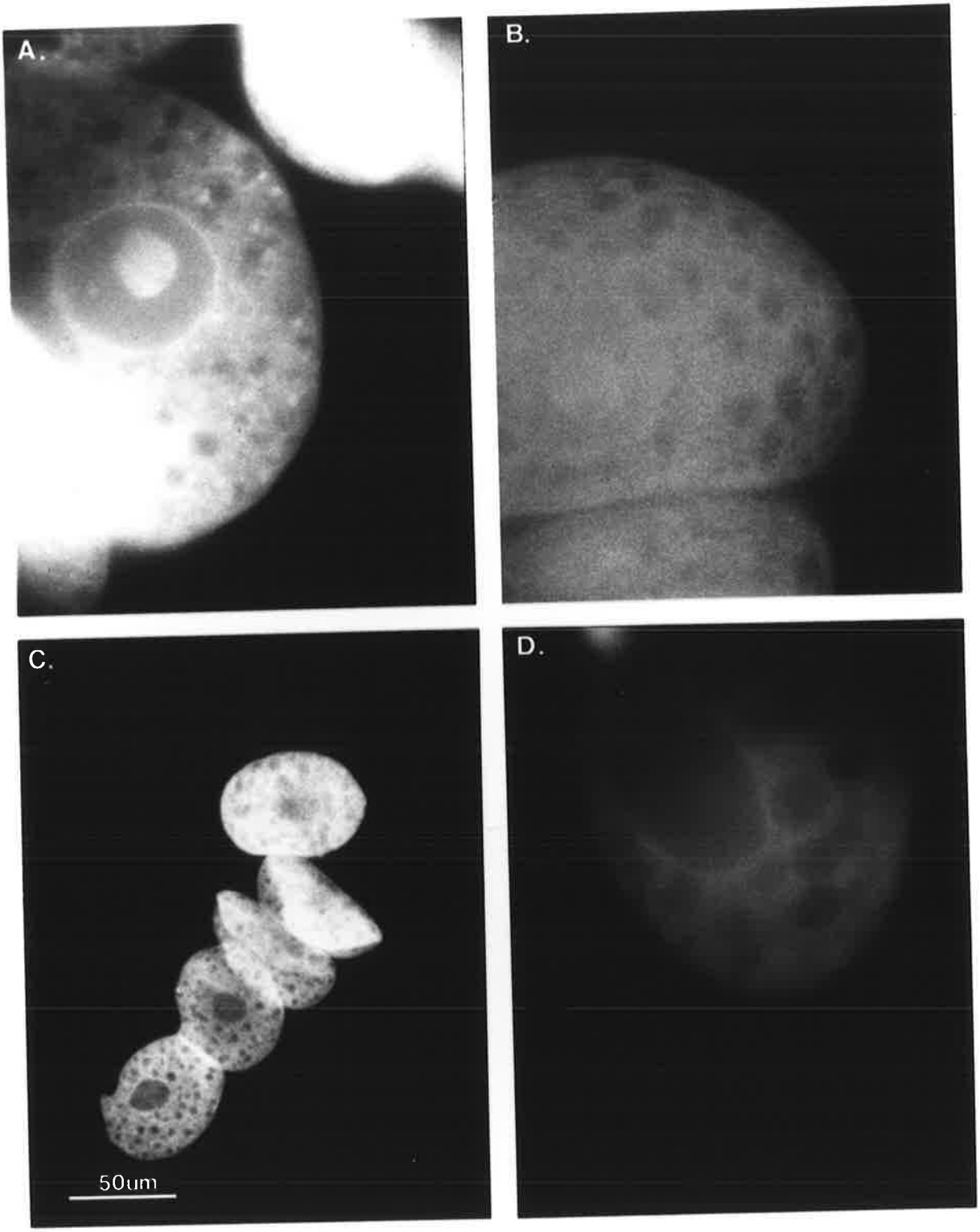

8·14

20um

8.13A). After insemination, the greater intensity of labelling over the cytoplasmic region is accentuated a little (Figure 8.13B). Controls were unlabelled.

SBA

This lectin did not label unfertilized oocytes of *N. brasiliensis* (Figure 8.15), nor sperm from either the male or female reproductive tracts.

8.3 Discussion

8.3.1 Ruthenium Red Labelling

Specificity of RR staining

In precipitation experiments, Luft (1971a) showed that ruthenium red reacted with acidic proteins, mucins, pectins, hyaluronic acid, chondroitin sulphate and some phospholipids and fatty acids. In addition, he concluded from titrations that there was an approximate stoichiometric interaction of RR with the ionizable carboxylic acid residues on several pectins. It was recognised, however, that in tissue the situation was more complex; although some specimens stained red in the light microscope, the characteristic brown-black deposit could not be obtained unless the tissue was also exposed to osmium tetroxide. Luft suggested three mechanisms to explain the observed staining pattern. All of them relied on the initial interaction of RR with an acidic polysaccharide, followed by an interaction with osmium. This left several aspects of the staining with RR unexplained, including its reaction with lipids. In 1976, Blanquet undertook a thorough study of the stain, in which, by the use of neuraminidase, poly-l-lysine, phospholipase, esterification and lipid extraction, he showed that osmium - RR stains carboxyl, phosphate and sulphate groups

in membranes. He proposed a model in which osmium reacts with unsaturated lipids in the plasma membrane to form stable cyclic osmic acid diesters. These molecules associate with RR to produce an electron-dense positive marker which 'stains the most available acidic groups of the outer hydrophilic leaflet, viz., carboxyl groups of sialoglycoconjugate compounds (sialoglycolipids and sialoglycoproteins) and amino acid residues, sulphate groups of glycolipids and glycosaminoglycans and phosphate groups of phospholipid polar heads exposed to the outer surface of the lipid bilayer', (Blanquet, 1976). This is the best explanation of the staining reaction of RR to date and will be used to interpret the staining pattern observed on the oocytes and sperm of *N. brasiliensis*.

RR staining of the egg coat

The 40-45nm - thick coat outside the plasma membrane of unfertilized oocytes of *N. brasiliensis* stains black with ruthenium red. This suggests that it contains many negatively charged groups. Since the density of staining is reduced by neuraminidase, which cleaves N-acetylneuraminic acid (commonly known as sialic acid) from glycoproteins and glycolipids (Gottschalk and Drzeniek, 1972), a sizeable proportion of the negative charge probably derives from sialic acid. Furthermore, neuraminidase substantially alters the structure of the egg coat, suggesting that the presence of sialic acid is important in maintaining its integrity.

The investments of unfertilized eggs have been studied in only a few species of nematodes. In each case some kind of cell coat covers the oolemma. It is a fuzzy, filamentous layer, only 35nm wide in *Dipetalonema viteae* (McLaren, 1973b) but 100nm thick in *Heterakis gallinarum* (Lee and Lestan, 1971). The egg coat of *Ascaris suum* and *Physaloptera* resembles that of *N. brasiliensis* in having a more dense outer boundary (Foor, 1968; Foor, 1970). This is an unusual feature,

as cell coats are generally described as having a 'gradually decreasing density toward their free surface' (Luft, 1976). This latter appearance is probably caused by a continual shedding and renewal (Luft, 1976) which may not be occurring in these mature oocytes. The significance of the laminar appearance of the outer boundary after neuraminidase digestion is not understood.

RR staining of sperm from males

The outer leaflet of the plasmalemma of sperm from males is stained by RR. As this staining is unaffected by neuraminidase, it probably represents negatively charged phospholipids in the outer lipid layer of the membrane. In addition, a sparse extracellular coat, a little thicker on the amoeboid region, is stained with RR. In some sperm this is removed by neuraminidase. In some micrographs (Figure 11I,J), however, it is difficult to assess the effect of this enzyme. Here, the electron-lucent midportion of the membrane appears wider, suggesting that the membrane has been altered. A fuzzy layer still coats the plasma membrane, although the observation that it no longer stains black suggests that at least some of its components have been removed. The variability noted with neuraminidase may be a consequence of its use on fixed tissue. Although in some cases (Lumsden, Oaks and Alworth, 1970; Blanquet, 1976) it has been used successfully on cells after fixation, in other studies (Ackerman, 1972; Ackerman and Clark, 1972) it has been found that prior fixation may prevent the removal of sialic acid by this enzyme. Moreover, some sialic acid residues bound to glycoproteins (Gress and Lumsden, 1976) and glycolipids (Labat and Schmid, 1969) are not susceptible to neuraminidase digestion. Thus the validity of drawing conclusions about the presence or absence of sialic acid, based solely on digestion by neuraminidase, is open to question.

RR staining of sperm from the female reproductive tract

The interpretation of the staining of sperm taken from the uterus of inseminated females is complicated because of cytoplasmic staining by ruthenium red. Penetration of this dye through membranes is unusual and is generally attributed to mechanical damage during fixation (Luft, 1971b). There are, however, several tissues in which RR stains the cytoplasm of the cells. In these cases, Luft postulates that the plasmalemma has a low finite permeability to the dye, allowing organelles with a high affinity for RR to stain. Since all spermatozoa examined had dense cytoplasmic staining, it is unlikely that staining was caused by damage to the plasma membrane. Instead, it suggests that the organelles in the sperm have a high affinity for RR and that the membrane has become more permeable to the dye.

The sparse surface staining by RR, which is not significantly reduced by neuraminidase, probably represents negatively charged phospholipids of the membrane. There is a rather amorphous cell coat over the amoeboid region which, judging from only slight reduction with neuraminidase, contains few sialic acid groups. The fuzzy coat which is associated with the internal membranes of the membranous organelles must bear a negative charge as it stains with RR. Since the staining was reduced by neuraminidase this charge could be at least partially due to sialic acid.

Evaluation of the RR staining technique

Several aspects of these results have been difficult to interpret. Although spermatids of *N. dubius* have a typical cell coat, the surface staining on the sperm of *N. brasiliensis* does not resemble that seen on other cells studied with this technique (Luft, 1971b). The staining was sparse and the typical fine filamentous deposit seen on almost all other cells was absent. The marked contrast between the surfaces of mature sperm of *N. brasiliensis* and immature cells of

N. dubius is curious; it may be an expression of fundamental developmental changes during spermatogenesis or simply an example of interspecific variation. In this regard, it would be interesting to examine both early stages of *N. brasiliensis* and mature sperm of *N. dubius*.

Another difficulty with the technique is that the appearance of the stain reaction differed in sperm from males, compared with those from females. The unstained sections of sperm before insemination showed a distinct, albeit narrow, black deposit along the membrane. In contrast, the staining in sperm after insemination was greyish rather than black. Since samples of sperm taken from males and females were processed simultaneously and with the same solutions, these factors cannot account for the observed differences. Perhaps the cytoplasmic staining, noted only in sperm dissected from females, is interferring with the formation of the usual black surface precipitate. This cytoplasmic staining, itself, presented another difficulty, as it tended to obscure the contrast needed to evaluate surface staining. It did, however, reveal a change in membrane permeability after insemination, but the significance of this observation is not known.

A number of refinements could improve the technique. Incubation of specimens with poly-l-lysine provides an additional control, as this positively-charged polymer should abolish all staining with RR. Other enzymatic digestions would help to identify the RR binding sites on the cell surface. For example, hyaluronidase, phospholipase C and proteases can identify the contribution of hyaluronic acid, phospholipids and polypeptides to the observed staining pattern (Huet and Herzberg, 1973; Himmelhoch and Zuckerman, 1978). Ferritin is a commonly used ultrastructural label, which when cationized becomes a useful marker of negative charge. In general, it does not penetrate cells and has the advantage over RR and colloidal iron hydroxide in

being suitable for use on fixed or unfixed tissue, at physiological pH (Danon *et al.*, 1972; Himmelhoch, Kisiel and Zuckerman, 1977; Jakoi, Marchase and Reedy, 1981). Moreover, as the density of particles can be counted, binding can be quantitated. Although the use of this technique was considered in this study, it was not pursued, largely because of the lack of negative charge on the sperm, as demonstrated by RR.

Surface charge of spermatozoa

To my knowledge no previous attempt has been made to investigate the surface charge of nematode sperm. Wright and Sommerville (1977) suggested that the surface of *N. dubius* sperm might be positively charged as sperm stuck to albumin but not to poly-l-lysine, they did not, however, attempt to measure the surface charge. Since Roberts and Ward (1982) were able to stick latex spheres carrying a positive charge to the sperm of *C. elegans*, we can infer that these sperm carry at least some negatively charged groups on their surface. A number of techniques have been used to investigate the surface charge of both vertebrate and invertebrate sperm. Early electrophoretic studies showed that sperm carried a net negative charge, the flagellum having a higher charge density than the head (Nevo, Michaeli and Schindler, 1961; Bedford, 1963). Cytochemistry with ruthenium red (Anderson, 1968) and colloidal iron hydroxide (CIH) (Cooper and Bedford, 1976; Fléchon, 1979) confirmed this. Epididymal maturation of sperm causes an increase in CIH binding (Yanagimachi, Noda, Fujimoto and Nicolson, 1972; Holt, 1980) while *in utero* incubation either decreases it (Courtens and Fournier-Delpech, 1979), or leaves it unchanged (Yanagimachi, Nicolson, Noda and Fujimoto, 1973). It is not clear whether this binding can be attributed to sialic acid as neuraminidase does not reduce CIH binding (Yanagimachi *et al.*, 1972). Moreover, Nicolson and Yanagimachi (1972) demonstrated that while

sialic acid on the heads of rabbit and hamster sperm was labelled with influenza virus (specific for sialic acid), this area was largely unlabelled by CIH. Bedford and Cooper (1978) proposed that labelling could be detecting negative charge due to groups other than sialic acid (e.g. sulphate). Evidence against this comes from an unpublished observation by Cooper (cited by Bedford and Cooper, 1978) that removal of sialic acid by acid hydrolysis abolished CIH binding. Furthermore, SDS - PAGE, together with the galactose-oxidase-H^3 sodium borate labelling technique, has shown the presence of a surface sialoglycoprotein on cauda epididymal sperm which was not detected in caput sperm (Olson and Hamilton, 1978). Thus, CIH binding may be due to neuraminidase-insensitive derivatives of sialic acid (Yanagimachi *et al.*, 1972). As appears the case with most cytochemical techniques, 'the interpretation of CIH labelling studies is far from straightforward' (Koehler, 1978).

8.3.2 Lectin labelling

The chemistry of lectins

Before discussing the results of the lectin-binding experiments, it is appropriate to summarize briefly our current knowledge of the chemistry of lectins and the way in which they interact with other macromolecules. Lectins are carbohydrate-binding proteins or glycoproteins which are abundant in legume seeds and occur in lesser amounts in a variety of plants and animals. Our knowledge of the nature of lectin-binding molecules on the surface of cells is based mainly on inhibition studies. Thus as N-acetyl-glucosamine prevents WGA from binding to cells, it has been assumed that this lectin binds to N-acetyl-glucosamine-like residues on the cell surface. The situation is known to be more complicated than this, because binding may also be influenced by other residues in the oligosaccharide chain,

as well as the polypeptide backbone to which they are linked (Sharon and Lis, 1975). For example, the trisaccharide of N-acetyl-glucosamine is 3,000 times more potent an inhibitor of WGA than the monosaccharide (Allen, Neuberger and Sharon, 1973). Since neuraminidase reduces WGA binding to the surface of cells (Adair, Kornfield, 1974; Bhavanandan and Katlic, 1979) this lectin also appears to bind to N-acetyl-neuraminic acid. Although some reviewers of the chemistry of lectins acknowledge this affinity (Nicolson, 1974; Kabat, 1978), others consider this binding to be a non-specific electrostatic interaction between the basic lectin and sialic acid (Lis and Sharon, 1977; Roth, 1978). This is because although Greenaway and Levine (1973) demonstrated that WGA bound N-acetyl-neuraminic acid, they were unable to saturate the lectin with this ligand. Several later studies have shown that WGA does specifically interact with sialic acid (Bhavanandan and Katlic, 1979; Adair and Kornfield, 1974). One of these used proton magnetic resonance to show that a 1:1 association complex fitted the data for the binding of WGA to both N-acetyl-neuraminic acid and N-acetyl-glucosamine. Although N-acetyl-galactosamine also interacted with the lectin, it did so in a different way (Jordan, Bassett and Redwood, 1977).

Concanavalin A, purified from the jackbean, *Canavlia ensiformis*, is the most commonly used lectin and consequently has been extensively studied. At neutral pH it exists as a tetramer, but below pH 5.6 it dissociates to a dimer. There is one binding site per subunit and this can combine with a variety of oligosaccharides bearing α-D-mannose and α-D-glucose at core or terminal sites (Nicolson, 1974; Lis and Sharon, 1977). The castor bean, *Ricinus communis* contains at least two lectins. The one designated RCA_1 is a tetramer of MW 120,000 which has haemagglutinating activity and binds to terminal β-D-galactose residues. RCA_{11} or RCA_{60} exists as a dimer, having one

subunit in common with RCA_1 and one unique subunit. In addition to binding to β-D-galactose, RCA_{11} is specific for N-acetyl-galactosamine, but has no haemagglutinating activity. Although RCA_{11} shares many properties with the *Ricinis* toxin, ricin D, (Lis and Sharon, 1977; Kabat, 1978) it is not clear whether the two are identical molecules (Nicolson, 1974). The lectin from the soybean, *Glycine max*, is similar to RCA_1 in that it is a tetramer of MW 120,000. Moreover, both lectins are glycoproteins containing mannose and N-acetyl-glucosamine residues. Periodate oxidation shows that the integrity of the carbohydrate moity is not required for activity (Lis and Sharon, 1977). SBA will bind to terminal ∝- or β-linked N-acetyl-galactosamine and to a lesser extent to terminal ∝- or β-galactose residues (Kabat, 1978). Subterminal sugars are bound only weakly (Lis and Sharon, 1977).

Lectin binding to oocytes

Of the four lectins used in this study only ConA bound in detectable quantities to the surface of unfertilized oocytes, although low levels of binding by other lectins may have been masked by the autofluorescence of oocytes. The lack of substantial binding by RCA and SBA, which commonly label the surface of cells (Nicolson, 1974), is surprising especially considering the thickness of the egg coat. It is possible that we are only measuring lectin binding to the dense outer layer of the coat as this region may prevent penetration of the lectins into the inner region. If this were true, incubation with neuraminidase, which substantially changed the structure of the coat, may render these residues accessible. This approach has succeeded in exposing cryptic ricin receptors on red blood cells (Adair and Kornfield, 1974) and RCA_1 binding sites on 3T3 and Sendai virus-transformed 3T3 cells (Nicolson, 1973).

The discontinuities in the surface labelling of oocytes incubated with ConA - FITC probably represent the gaps in the cell coat noted

with RR staining. To confirm this association, the labelling pattern obtained using ConA tagged to an ultrastructural marker such as ferritin would need to be examined with the TEM. There was no correlation between RR and WGA labelling of the egg surface. The neuraminidase-sensitive RR staining of unfertilized eggs was interpreted as evidence of sialic acid in the egg coat yet this ligand should be labelled by WGA. It is possible that some kind of stearic hindrance is preventing WGA binding to the egg surface. Similar discrepancies can be found in the literature. For example, WGA labelling of the heads and tails of rabbit sperm decreases dramatically during epididymal transit (Nicolson *et al.*, 1977) yet negative surface charge, presumed to be due to sialic acid, increases during the same time (Yanagimachi *et al.*, 1972). Although the authors suggest that sialic acid may be masking the N-acetyl-glucosamine residues (Nicolson *et al.*, 1977), this seems contradictory since WGA also binds to sialic acid (Nicolson, 1974). Unfortunately, comparisons cannot be made between surface labelling on the oocytes of *N. brasiliensis* and other species of nematodes because molecular probes like lectins have not yet been used to examine the surface of unfertilized nematode eggs.

Lectin labelling of spermatozoa

As well as partially characterizing the surface of the sperm of *N. brasiliensis*, this lectin labelling study has disclosed regionalization of the sperm surface and minor maturational changes associated with insemination. Of the four lectins tested, ConA had the highest affinity for sperm, SBA showed no detectable binding, fluorescence with WGA - FITC was weak, while RCA_{II} labelled the cytoplasmic region more strongly than the nuclear tail. Sperm which had been inseminated into females were labelled in a similar way to those from males, except that with ConA, fluorescence was more intense over the cytoplasmic region. The enlarged amoeboid anterior of sperm dissected

from uteri had a low affinity for all the lectins.

The low intensity of fluorescence shown by the sperm of *N. brasiliensis* when labelled with fluorescein-conjugated lectins, suggests a low density of lectin-binding sites on the sperm surface. Binding by ConA demonstrates the presence of glucose or mannose residues and the low affinity for WGA suggests a lack of sialic acid and N-acetyl-glucosamine. Although SBA and RCA_{11} have similar carbohydrate specificities, they have different affinities for the sperm surface. This suggests that factors other than the presence or absence of simple sugars may be influencing lectin-binding patterns.

Given the distinct regionalization of the cytoplasmic organelles in the sperm of *N. brasiliensis*, the different lectin-binding properties of the different areas of the sperm are not surprising. There are several ways in which a cell can maintain membrane or surface specializations (Nicolson, Poste and Ji, 1977). Surface molecules may be constrained by cytoskeletal elements, or peripheral membrane components inside or outside the cell. Alternatively, associations of the membrane molecules themselves, e.g. lipid domains or protein-protein aggregations may prevent free diffusion of cell surface molecules. The dense amorphous material which lines the cytoplasmic region of the sperm of *N. brasiliensis* may constrain surface molecules in this area. In the nuclear region, the close association between the chromatin and the overlying plasma membrane may play a part in restricting the movement of surface molecules.

In a recent study of cell surface domains of guinea pig sperm, monoclonal antibodies were used to show two ways in which antigen domains can become established. One antibody (AH-1) binds to the entire head of testicular sperm and becomes restricted to the anterior head only after epididymal maturation. This localization is maintained by immobilization, as the antigens cannot be aggregated by

antibody. In contrast, the PH-1 antigen cannot be detected on testicular sperm, but first appears on epididymal sperm already confined to the posterior head. Since the PTA-1 antigen forms antibody-induced patches which do not leave the posterior tail region, localization of this antigen can be explained by a membrane modification acting as a barrier to migration between the posterior and anterior tail regions (Myles, Primokoff and Bellué, 1980).

The mobility of surface molecules can also be explored by observing lectin-induced receptor redistribution on unfixed cells (Schwarz and Koehler, 1979). Unfortunately, the low labelling intensity of the sperm of *N. brasiliensis* precluded the use of this technique in the present study. It has, however, been used in an elegant series of experiments which trace membrane flow during activation and locomotion in the sperm of *C. elegans* (Roberts and Ward, 1982a,b). Unactivated sperm label uniformly with SBA, WGA, RCA and LCA (*Lens culinaris* agglutinin) (Argon, 1979). 30 - 60s after activation, the pseudopodia are cleared of fluorescent lectins, with fluorescence being removed first from the tips of the pseudopodia. The same centripetal movement of lectin binding sites continues during locomotion. Furthermore, by initially incubating sperm with non-fluorescent lectin, then pulse labelling with FITC - WGA the authors were able to demonstrate that new receptors are added at the tips of the pseudopods. As yet they are unable to define the source of these new lectin binding molecules, but suggest that they may be incorporated from a cytoplasmic pool. This study is one of the best examples of the way in which lectins may be used to probe membrane dynamics. It is ironical that these experiments were performed using nematodes whose sperm, until now, have been poorly studied using modern techniques.

Lectin labelling of the activated sperm of *C. elegans* also revealed small dots of fluorescence on the cell body (Argon, 1979). This

is believed to represent labelling of the inside of the membranous organelles. Further analysis of lectin-labelling of the sperm of *C. elegans*, using I^{125} and SDS - PAGE, demonstrated seven WGA-binding glycoproteins with molecular weights from 5 - 200k (Argon, 1979). This diversity of lectin-binding molecules on the surface of this relatively small cell emphasizes a point made by Roth (1978). He states that the term 'lectin receptor' is misleading as it implies a single molecule with the specific function of coupling to a lectin. In fact, there are usually several molecules on the surface of a cell which, by chance, have carbohydrate sequences capable of combining with particular lectins.

The only other investigation of the surface of nematode gametes has been made on *Ascaris suum*. Here, immunocytochemistry has shown that new surface antigens appear on both eggs and sperm during their final maturational changes just prior to fertilization (Wu and Foor, 1980; Bradley and Burghardt, 1976). A further investigation of the sperm, using I^{125} labelling in conjunction with SDS - PAGE, has shown some similarities and some differences between the surface molecules of activated and unactivated sperm (Abbas and Cain, 1980). The two forms of the sperm share four major glycoproteins, two of which stain with ConA. The activated sperm have two unique high molecular weight components which the authors believe may be derived from glandular secretions of the male.

Evaluation of the labelling technique

The technique by which sperm are fixed, stained and processed while attached to a substrate provides a means by which small numbers of sperm can be processed for cytochemistry. Its use here with RR and fluorescein-labelled lectins was taken as a test of its usefulness for both light and electron microscopy. It has proved satisfactory for light microscopy and SEM (Wright and Sommerville, 1977) but it was

found impracticable for TEM. This is largely because the sperm, being roughly 2 x 18μm, are difficult to locate and to section. These disadvantages could be tolerated with the numbers of sperm which can be obtained from 5 or 6 males, but it is impossible to dissect large numbers of sperm from the reproductive tracts of females. Those groups working with *C. elegans* and *A. suum* have an advantage in this regard as the sperm of these species can be activated *in vitro*, thus avoiding the need to dissect females. Moreover, Klass and Hirsh (1981) have overcome the disadvantage of working with a small nematode by designing a procedure by which sperm are literally squeezed from males in a Carver Laboratory Press. Until either a better way to isolate sperm from females or a method for *in vitro* activation is found, progress on the cytochemistry and biochemistry of activated sperm of *N. brasiliensis* and other species of nematodes will be slow. A similar situation existed a few years ago in the field of mammalian reproduction. It was not until the development of techniques for *in vitro* capacitation that significant progress was made towards understanding the molecular and biochemical features of this phenomenon.

8.3.3 Surface properties of the gametes of *N. brasiliensis* - Conclusions

Unfertilized oocytes of *N. brasiliensis* are covered by a 40 - 45nm thick coat which is punctuated by small gaps, about 200nm across. Its staining characteristics with RR and neuraminidase suggest that it bears a negative charge which is largely due to sialic acid and its high affinity for ConA reveals that it contains mannose and glucose residues.

Different regions of both activated and unactivated sperm have different surface characteristics. RCA_{II} binding sites are more abundant over the cytoplasmic region than the nuclear tail and this

difference is accentuated after activation. Similarly, mannose and glucose residues which are labelled by ConA are more numerous over the cytoplasmic region of activated sperm. The amoeboid region has a low affinity for ConA, SBA, WGA and RCA but negative charge appears more dense here. Only some of this charge can be attributed to sialic acid, the rest is presumably derived from phospholipids. Following insemination, the sperm membrane becomes more permeable to RR, resulting in dense cytoplasmic staining. After the membranous organelles have discharged their contents, their internal membranes become covered by a fuzzy coat containing sialic acid.

This characterization of the surface of the gametes of *N. brasiliensis* allows some speculation about the nature of sperm-egg interactions in this species. Lectin-carbohydrate binding forms the basis for all such interactions studied to date. In this species, the amoeboid region of the sperm makes first contact with the egg and therefore presumably bears egg-receptors. Since this region has a low affinity for exogenous lectin, it may bear molecules which are themselves lectin-like and which bind to sugars on the egg surface. Perhaps some of the ConA-binding sites, shown here to be common in the egg coat, are part of a sperm-binding molecule. This prediction could be tested by attempting to inhibit fertilization with ConA. Unfortunately, although some stages of the spermatogenic cycle can be completed *in vitro* (Ward *et al.*, 1981; Grevengood, Lande and Foor, 1981) fertilization has not yet been accomplished outside the animal. Thus, experiments of this kind await further advances in the development of *in vitro* techniques suitable for nematode tissue.

CHAPTER 9. THE MEMBRANE OF THE SPERM

9.1 Introduction

Cell membranes form the interface between cells and their environment and, by controlling ion fluxes, the uptake of nutrients and electrostatic potential, the membrane is in many ways responsible for the homeostasis of cells. In addition, a variety of receptors in the plasmalemma enables cells to respond to exogenous stimuli such as hormones, neurotransmitters and antigens. Freeze-fracture has proved a useful technique in the study of membranes as it allows large areas of the surface of cells to be visualized in the TEM. The technique involves fracturing frozen tissue under a vacuum, then casting a replica of it by evaporating carbon and platinum onto the exposed face. As the platinum is evaporated at an angle of 45°, there is a 'shadow-cast effect' which shows the surface in three-dimensional relief. When replicas are examined in the TEM the membranes are seen as flat faces containing globular particles, 5-20nm in diameter. It is now commonly agreed (Branton, 1966; Zingsheim and Plattner, 1976; Bullivant, 1977) that the hydrophobic interior of the membrane is revealed by freeze-fracture. The particles are therefore called intramembranous particles (IMPs) and are thought to represent integral membrane proteins (McNutt, 1977). The fracture face formed from the extra-cellular leaflet of the lipid bilayer is designated the 'E' fracture face or EF-face, while the other, which derives from the protoplasmic leaflet, is called the 'P' fracture face or PF-face (Branton, Bullivant, Gilula, Karnovsky, Moor, Mühlethaler, Northcote, Packer, Satir, Satir, Speth, Staehelin, Steere and Weinstein, 1975). Deep etching sublimes away surrounding ice to reveal the true surface of the membrane, designated ES when belonging to the exterior half and PS when derived from the protoplasmic leaflet.

A number of studies of sperm membranes have been made using freeze-fracture. Earlier work described landmarks not easily seen in thin sections, e.g. the posterior striated ring between neck and head and the oblique rods or serrations in the equatorial segment (Koehler, 1966, 1970, 1973. Pedersen, 1972a,b; Flechon, 1974). More detailed descriptions of particle arrays in different regions of the plasma and acrosomal membranes of the sperm of man, mouse, rat and guinea pig followed (Koehler, 1972; Stackpole and Devorkin, 1974; Friend and Fawcett, 1974). More recently, one marsupial (Olson, Lifsics, Fawcett and Hamilton, 1979) and several invertebrate sperm (Reger and Fitzgerald, 1979; Reger, Itaya and Fitzgerald, 1979; Tilney, Clain and Tilney, 1979) have been studied by freeze-fracture. As might be expected from their unusual morphology, the invertebrate sperm have unique particle arrays on their membranes.

The high degree of regional specialization noted in the membrane of the guinea pig sperm is typical of mammalian sperm in general (Friend and Fawcett, 1974; Fawcett, 1975b). Both faces of the plasma membrane over the acrosomal region are composed of domains, separated by smooth regions containing scattered particles. Within the domains, the fracture face is indented in a honeycomb pattern, often referred to as 'quilted'. The PF-face of the outer acrosomal membrane may have a similarly patterned appearance (Friend and Fawcett, 1974), while the EF-face has a uniform population of globular particles (Friend, Perrelet and Yanagimachi, 1977). The rear margin of the equatorial segment is marked by a palisade of oblique rods which point towards the anterior of the head. Fusion between the acrosomal and plasma membranes usually occurs in front of these elevations. At the junction of the head and tail is a circumferential groove, with fine vertical striations called the posterior or striated ring. A particle-free zone often occurs in front of it, on both PF- and EF-faces (Friend, 1977).

An important specialization occurs on the PF-face of the midpiece of the sperm tail. Concentric strands of 6-8nm particles wind around the sperm at the same pitch as the gyres of the mitochondrial helix beneath. This pattern stops abruptly at the annulus which separates the midpiece from the principle piece. On the membrane of the latter are randomly scattered particles and, occasionally, domains of linear or hexagonal particle arrays (Koehler and Gaddum-Rose, 1975). On the principle piece, a staggered row of 8-9nm intramembranous particles occurs on the PF-face, opposite the primary dense fibre. This is believed to be related to a longitudinal surface ridge, composed of a double row of particles running almost the full length of the principle piece. This 'zipper' as it has been called (Koehler and Gaddum-Rose, 1975) has binding sites for ConA, WGA and RCA_1 (Enders, Werb and Friend, 1981).

Recently, in an attempt to do more than just describe patterns of particles on membrane faces, some workers have tried to correlate the freeze-fracture images of sperm with their physiological state. *In vitro* conditions which stimulate capacitation cause the disruption of some of the regular patterns seen in epididymal sperm. For example, the characteristic honeycomb pattern in the acrosomal and plasma membranes of the guinea pig sperm disappear after acrosomal disruption (Friend and Rudolf, 1974). In hamster sperm, the particles on the equatorial segment, which were previously randomly distributed, become clustered after acrosomal loss (Kinsey and Koehler, 1978). Similarly, Friend *et al.* (1977) reported the clearance of globular and fibrillar particles from the PF- and EF-faces of acrosomal and plasma membranes, prior to their fusion in the acrosome reaction. Behind the resultant line of fusion, in the postacrosomal region, further particle clearing occurred, possibly in preparation for sperm-egg fusion.

Particle changes in the midpiece, resulting from incubation in

capacitating media, can be correlated with a change in cell motility. Epididymal guinea pig sperm, with linear strands of small particles overlying the mitochondrial helix, move with a stiff windshield-wiper action. In activated sperm, the tail appears more flexible and beats with a lashing motion, while the strings of particles dissociate to form a random array (Koehler and Gaddum-Rose, 1975). These linear strands on the midpiece seem particularly susceptible to other physiological changes in the sperm. The metabolic inhibitor cyanide both halts flagellar motion and causes the particles to disperse, sometimes into small clumps (Friend, 1977). As sperm degenerate in the lower reproductive tract of males after vasectomy, large bare patches appear between the strands of particles on the membrane of the midpiece (Friend, Galle and Silber, 1976).

The freeze-fracture technique has provided a useful means of extending and supplementing current morphological descriptions of sperm. Moreover, it has been demonstrated that physiological changes in mammalian sperm can be reflected in their freeze-fracture morphology. This technique was therefore considered a potentially useful tool for the study of nematode sperm; first to examine regional specialization of the membrane and second, to explore the effect of activation on the plasmalemma of the sperm. The initial work, consisting of a comparison of fixed and glycerinated uteri of *N. dubius* with unfixed tissue, examined the effect of fixation and cryoprotection on particle density and distribution. Next, sperm in the reproductive tracts of males of *N. brasiliensis* and *N. dubius* were compared with those in females and both regional specializations and particle densities were noted. Changes resulting from activation were further analysed by extensive measurements of particle sizes on the different membrane faces of the sperm of *N. brasiliensis*.

9.2 Results

9.2.1 Particle density

Favourable fractures of the reproductive tract from males produce replicas of mature spermatozoa in the lumen of the seminal vesicle. Sperm viewed in this way superficially resemble those seen with the SEM (Wright and Sommerville, 1977). The nuclear and cytoplasmic regions can be distinguished on morphological grounds (Figure 9.1). In the cytoplasmic region, the membrane seems to cling to the membranous organelles and outlines them quite clearly (Figure 9.2). On the PF-face, the knobs of the membranous organelles can be distinguished as protrusions (Figure 9.1K), while on EF-faces, they appear as small depressions (Figure 9.2K). The particle distributions on both faces of the membrane are random. On the PF-face, the particle density is similar in the region over the nucleus (1,153 particles/μm^2) and over the cytoplasm (909 particles/μm^2). Very few EF-faces of the membrane of the nuclear region were obtained, but on the EF-face over the cytoplasm particle density was very low (203 particles/μm^2).

If the anterior uterus of females is freeze-fractured, replicas of spermatozoa after activation can be obtained. Figure 9.3 shows such a group of sperm. Sperm are so tightly packed here that initially it was difficult to identify the fracture faces. However, outlines drawn on transparent overlays, together with three-dimensional images produced from stereo pairs, helped to determine the relative positions of the faces and the general topography of the replica. Identification of the different regions of the sperm was easier. Both the PF- and EF-faces of the cytoplasmic region are characterized by pores which join the membranous organelles to the plasma membrane (Figures 9.3 and 9.4). Anterior to this, the membrane of the amoeboid area swells out (Figures 9.4 and 9.5) and is often closely applied to the membrane of an adjacent sperm (Figure 9.3). Cross fractures of this area sometimes

FIGURE 9.1 : Freeze-fracture replica of sperm in the seminal vesicle of a male of *N. brasiliensis*, showing PF-face of nuclear (Nuc) and cytoplasmic (Cyt) regions. Note bumps (K) formed by knobs of the MOs.

FIGURE 9.2 : PF- and EF-faces of sperm of *N. brasiliensis* in the seminal vesicle of a male. The outlines of membranous organelles (MO) and their knobs (K) are obvious.

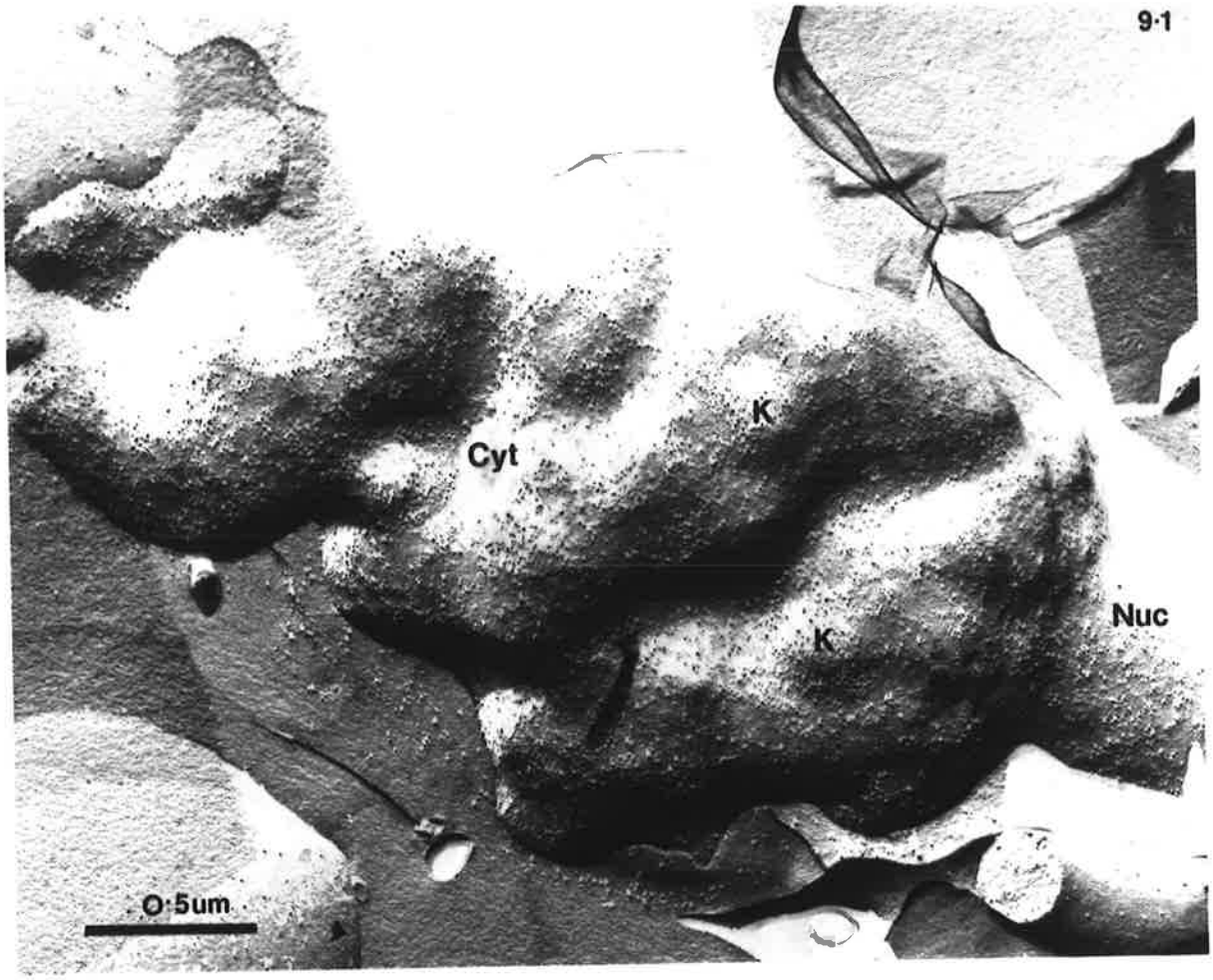
9·1
Cyt
K
K
Nuc
O·5um


9·2
MO
PF
K
EF
K
O·5um

FIGURE 9.3 : Cross fracture of upper uterus of a female of *N. brasiliensis*, showing PF- and EF-faces of sperm membranes in the nuclear (Nuc), cytoplasmic (Cyt) and amoeboid (Am) regions. Note particle-free vesicles (V) in the amoeboid region. Long arrows denote particle aggregations on PF-face of amoeboid region, short arrows show pores joining MOs to plasmalemma. X denotes cross-fracture.

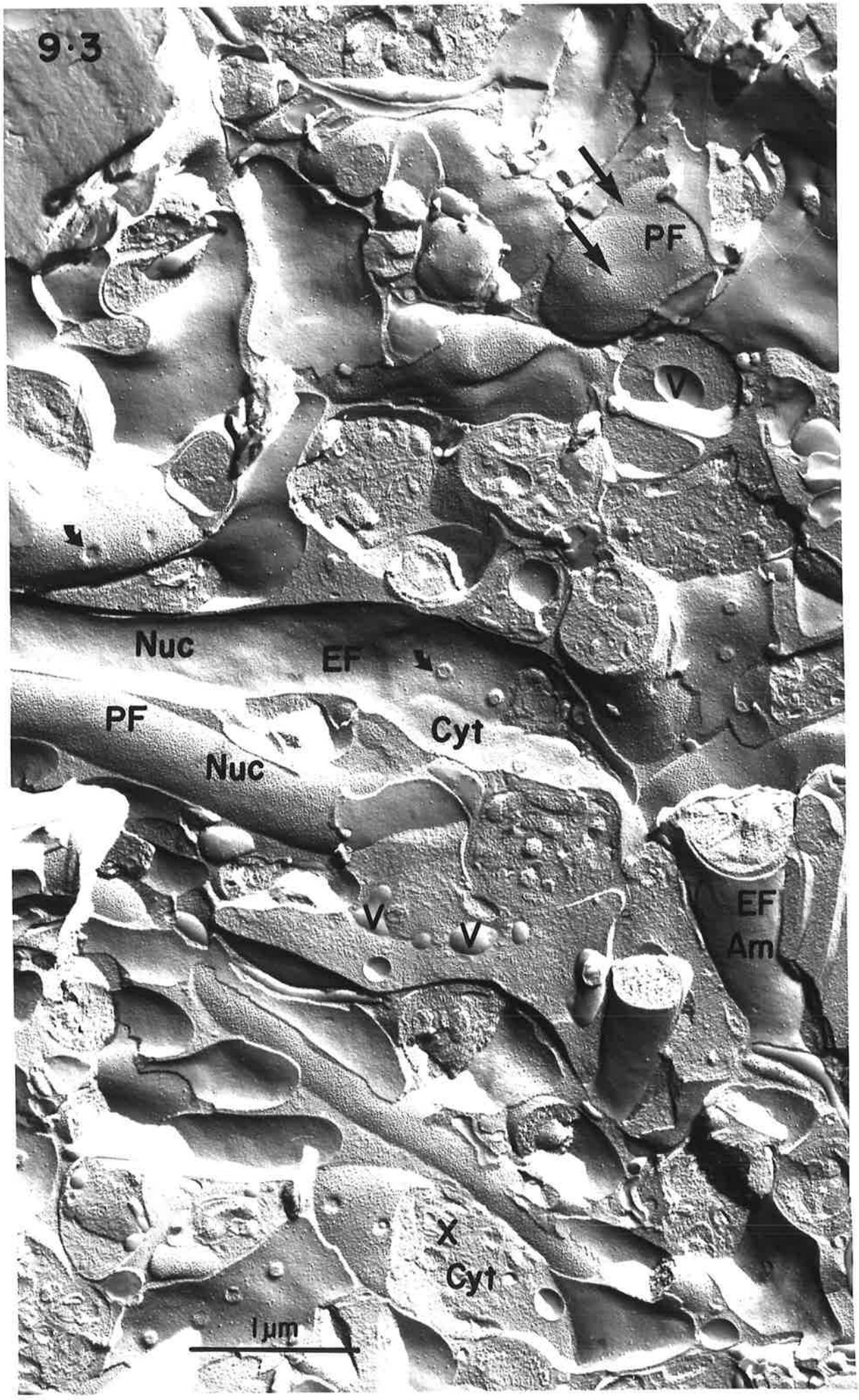
9·3
PF
V
Nuc
EF
PF
Cyt
Nuc
V
V
EF
Am
X
Cyt
1 µm

FIGURE 9.4 : PF-face of sperm in uterus of female of *N. brasiliensis* showing cytoplasmic (Cyt) and amoeboid (Am) regions. Large arrows outline particle aggregations over amoeboid region, while short arrows denote pores joining MOs to plasmalemma. Around these pores are rings of large particles (small arrows). Ex denotes extracellular fluid and X Am shows cross-fracture of amoeboid region; note the similar appearance of these two areas.

FIGURE 9.5 : EF-faces of two sperm in the uterus of a female, showing pores on the cytoplasmic region (Cyt) which join MOs to the plasma membrane. The amoeboid region (Am) bears few particles. *N. brasiliensis*.

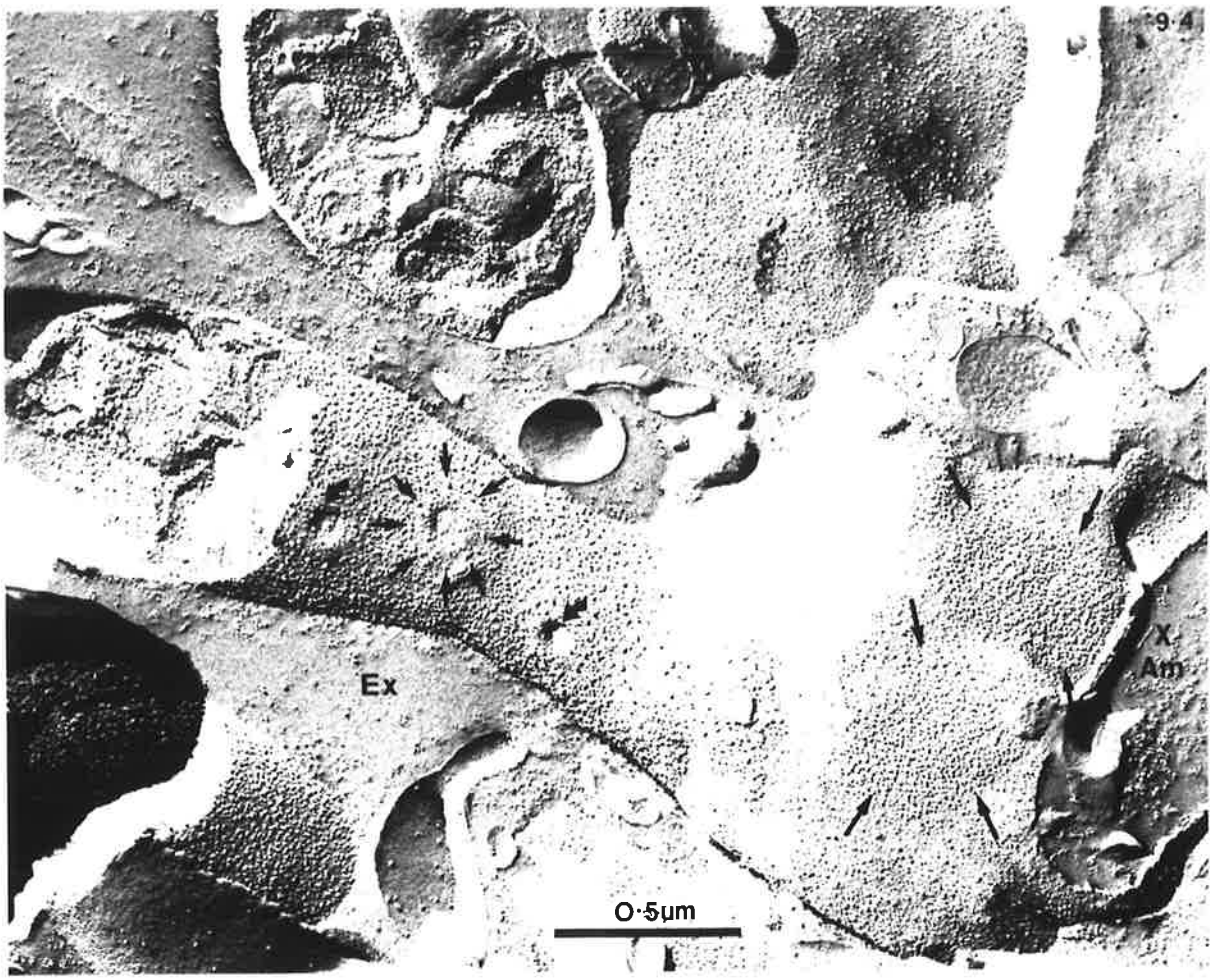
9·4
Ex
X
Am
0·5μm

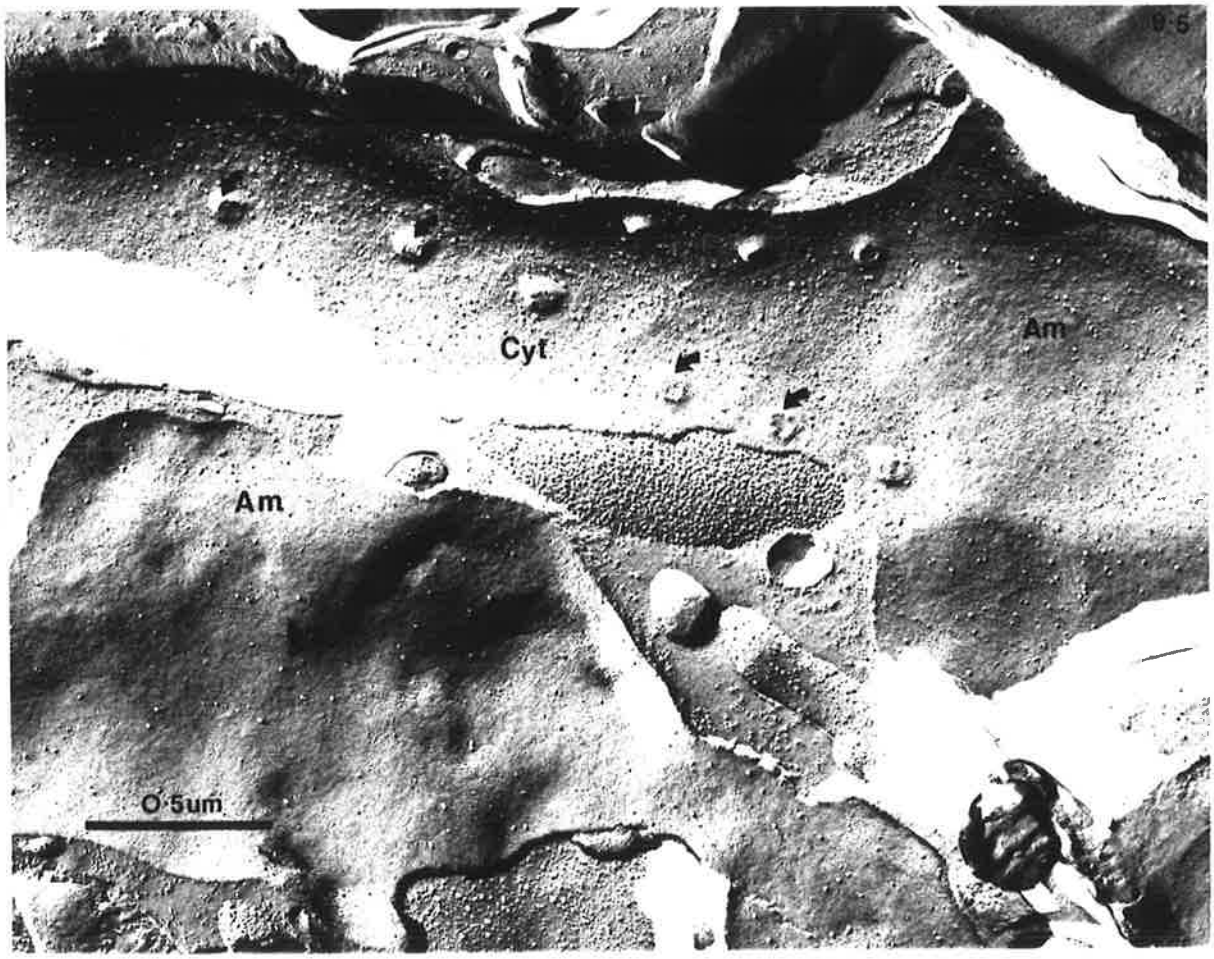
9·5
Cyt
Am
Am
0·5um

show a featureless homogeneous groundplasm (Figure 9.6, X, Am), but in other replicas, aggregates of both globular and irregular material are scattered across a very smooth surface (Figure 9.4, X, Am). A closer examination of each of these replicas, shows that the material in these cross-fractures, resembles the extracellular matrix (Ex). This suggests that this region contains a large amount of soluble material and its appearance may be governed by the conditions under which fracturing was performed. Vesicles of various sizes are also seen in cross fractures of the amoeboid region (Figures 9.3, 9.7). Both PF- and EF-faces of these vesicles are virtually particle-free. They probably represent the empty vesicles seen in thin sections of this part of the sperm (Chapter 5.2). The nuclear region of the sperm resembles a long narrow tube, running back from the cytoplasmic region (Figure 9.3). There is a hint of the spiral arrangement of the underlying chromatin in some images (Figure 9.8).

Table 9.1 lists the mean particle densities for different regions of sperm in the uterus of females. On the PF-face, the greatest density occurs over the nuclear region ($\bar{x}$ = 3,423 particles/μm^2). The mean density is 2,234 particles/μm^2 in the cytoplasmic area and 1,572 particles/μm^2 on the amoeboid region. On the EF-face, the density is very low over the nucleus (102 particles/μm^2) and is greatest in the cytoplasmic area (347 particles/μm^2). The value of 186 particles/μm^2 for the amoeboid region is intermediate between these two

The distribution of particles across the membrane faces is random, except in the amoeboid area where particle aggregations, measuring up to 0.8μm in diameter may occur (arrows, Figure 9.4). Fortuitous fractures, showing part of the membrane face as well as cytoplasm, reveal cytoplasmic organelles adjacent to these particle aggregations (Figures 9.6, 9.7). Thin sections identify these organelles as mitochondria (see Chapter 5.2), suggesting that particle aggregations on

FIGURE 9.6 : Cross-fracture of a uterus of *N. brasiliensis* showing several sperm. Material of the amoeboid region (X Am) and extracellular fluid (Ex) have a similar appearance. Arrow at top right points to a particle cluster on the PF-face of the membrane over the amoeboid region. Immediately beneath this (crossed arrow) is a cross-fractured mitochondrion.

FIGURE 9.7 : Beneath a particle cluster on the PF-face (arrow) lies a mitochondrion (crossed arrow), also in the cytoplasm of the amoeboid region are particle-free vesicles (v). *N. brasiliensis*.

FIGURE 9.8 : A group of nuclear tails of sperm in the uterus of a female of *N. brasiliensis*. Note high density of particles on PF-face of the membrane. Cross-fractures show mitochondria (M) within the tube of chromatin (Ch).

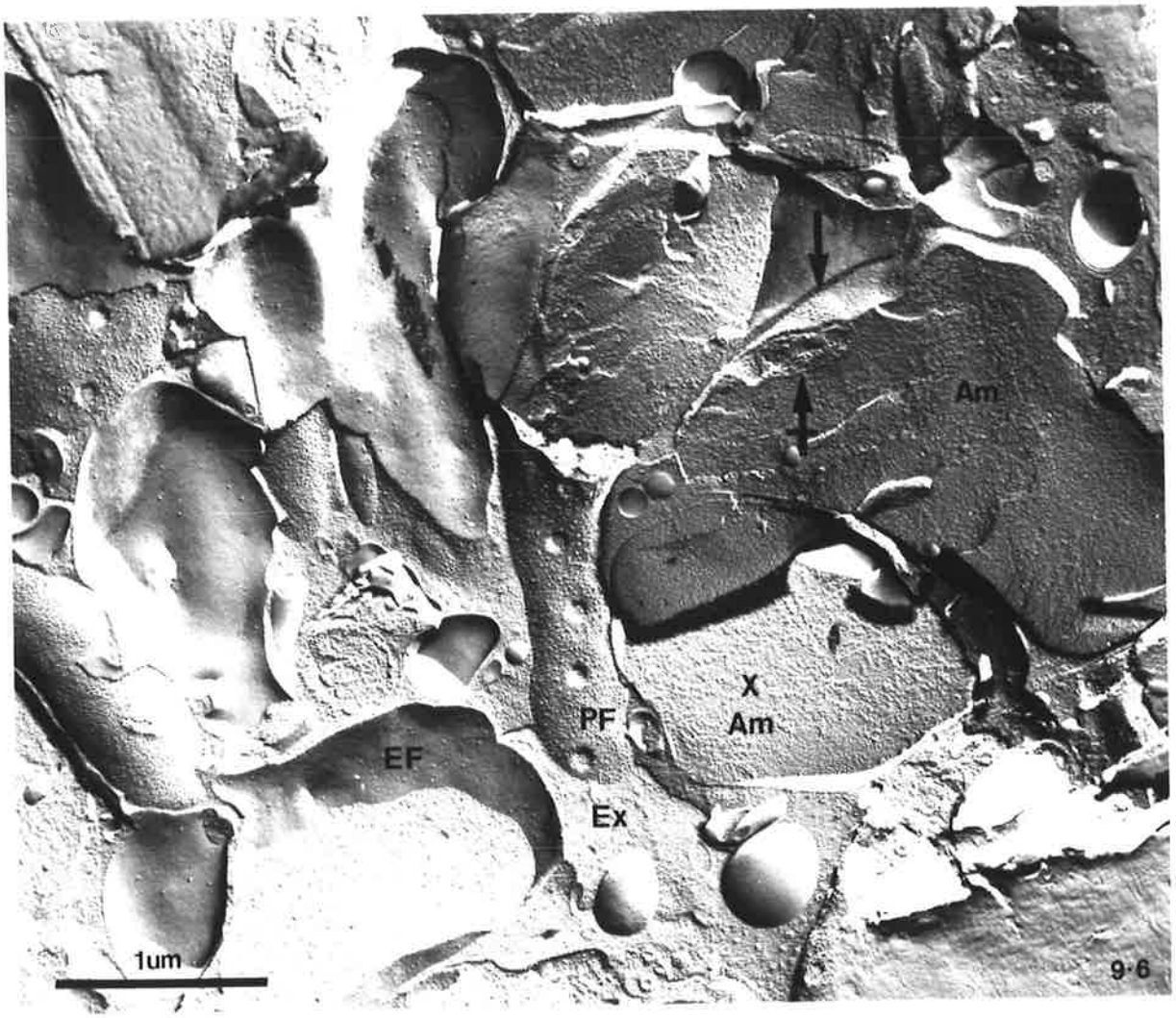
Am
X
Am
PF
EF
Ex
1um
9·6

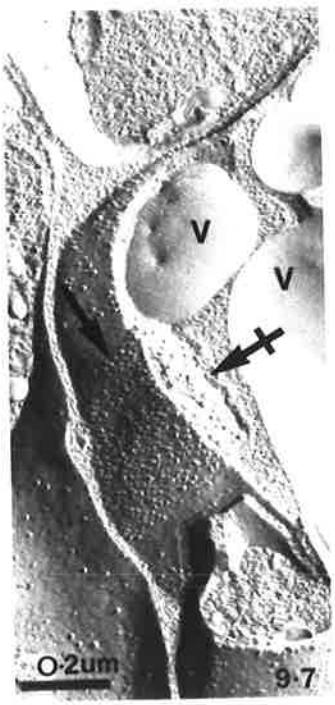
V
V
0·2um
9·7

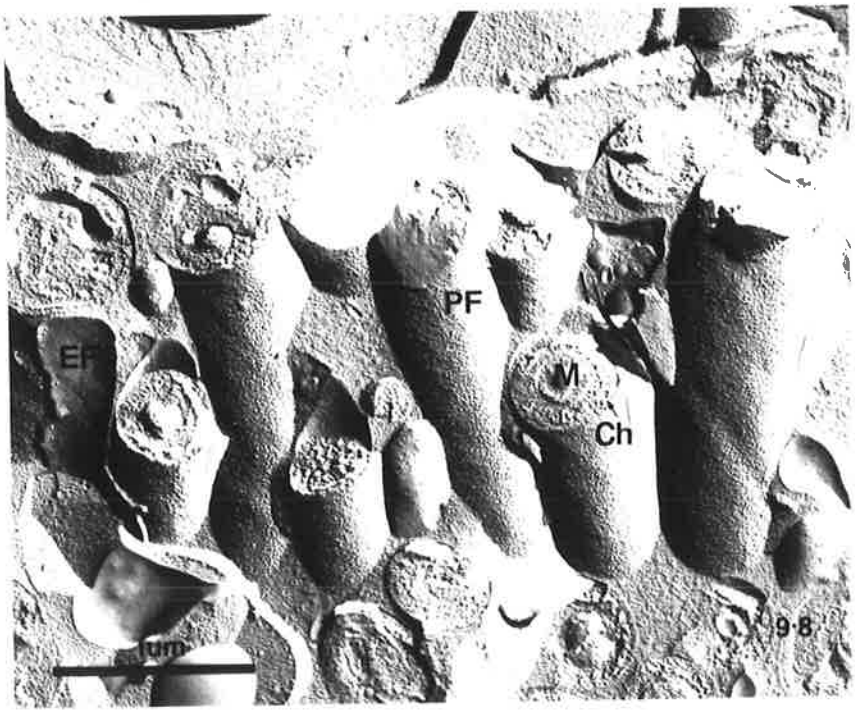
PF
EF
M
Ch
1um
9·8

the amoeboid region are associated with mitochondria in the underlying cytoplasm.

The membrane faces and the regions to which they belong are easily recognized in the sperm of *N. dubius* as they closely resemble homologous areas in the sperm of *N. brasiliensis*. In sperm from males (Figures 9.9, 9.10), the PF-face of the cytoplasmic region has characteristic bumps (K) caused by protrusion of the knobs of the underlying membranous organelles. Particles are clustered over these protrusions, but elsewhere they have a random distribution. The EF-face of this region (Figure 9.10) has a low density of particles. The nuclear region is characterized by longitudinal ribs (arrows, Figure 9.11) which presumably relate to the form of the underlying chromatin. The particle density on both the PF- and EF-faces here is similar to that of the cytoplasmic region.

The particle density on the EF-face of both the cytoplasmic and amoeboid regions of sperm in females is low (Figures 9.12, 9.13). Cross-fractures of the amoeboid region show that the cytoplasm here resembles the uterine fluid around the sperm (compare Ex and X, Am, Figure 9.12). Figures 9.13 and 9.14 demonstrate that on the PF-face of the membrane, particle density increases substantially after insemination. An interesting specialization occurs on this face in the cytoplasmic region; a 0.2μm diameter ring of large, prominent particles surrounds the pores which join the membranous organelles to the plasma membrane. Sometimes, complementary pits can be seen on the EF-face (Figure 9.12). More critical examination of replicas of the sperm of *N. brasiliensis* revealed similar rings of particles in this species (arrows, Figures 9.4, 9.6). Although they can be distinguished because they are large and often occur in pairs, they were not obvious initially because of the high density of other large particles elsewhere on this fracture face.

FIGURE 9.9 : PF-face (cytoplasmic) of sperm of *N. dubius* in seminal vesicle of male. Clusters of particles occur over the knobs (K) of the MOs.

FIGURE 9.10 : PF- and EF-faces of sperm in seminal vesicle of male of *N. dubius*. Knobs (K) of the MOs are obvious.

FIGURE 9.11 : Cross fracture of seminal vesicle of *N. dubius* showing PF- and EF-faces of the nuclear region (Nuc) and PF-face of the cytoplasmic (Cyt) region. Particles are sparse on EF-face of the MOs but are dense and clumped on PF-faces.

9·9

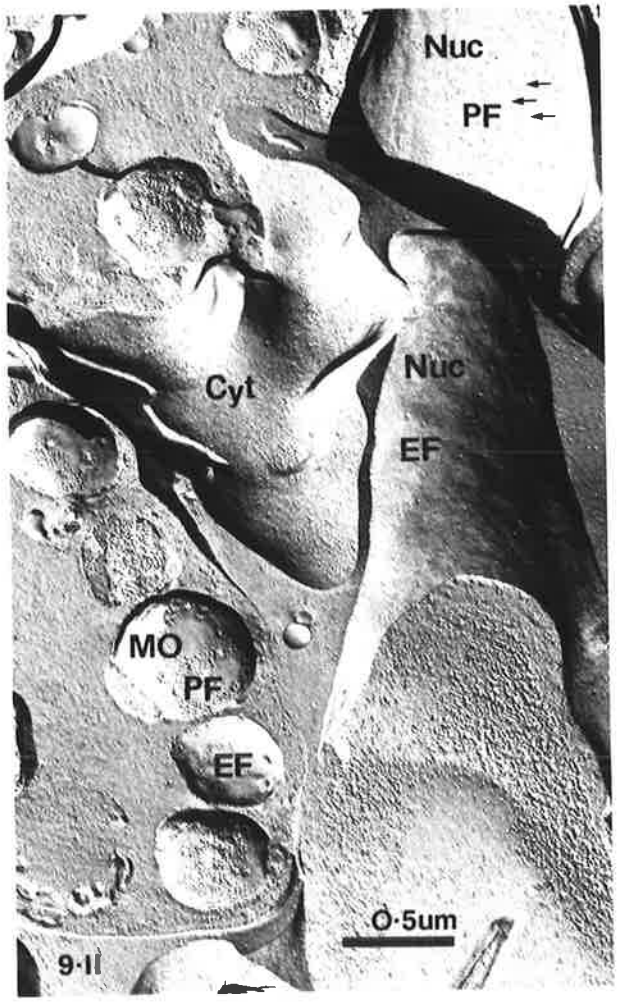

9·11

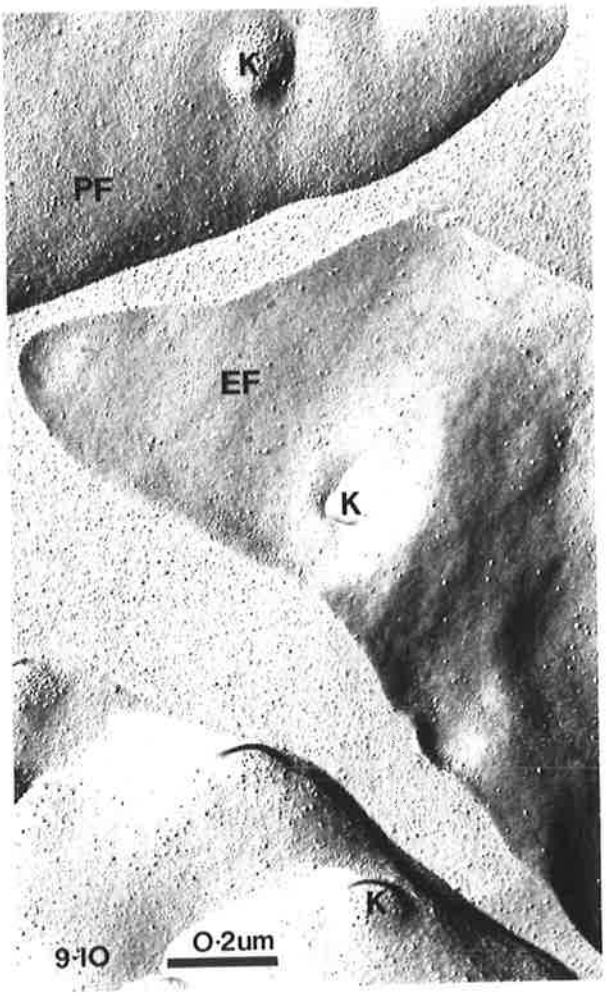

9·10

FIGURE 9.12 : EF-face of the cytoplasmic (Cyt) and amoeboid (Am) region of sperm in the uterus of a female *N. dubius*. Pores joining MOs to plasma membrane are obvious. Pits around them (arrows) are presumably left by complementary particles on PF-face (see Figure 9.13). Specimen fixed and cryoprotected.

FIGURE 9.13 : Several sperm in the uterus of a female of *N. dubius*. On the PF-face, note rings of particles around pores joining MOs to plasma membrane. EF-face of the amoeboid region has few particles. Cross-fractured chromatin (X Ch) has a characteristic appearance. Specimen fixed and cryoprotected.

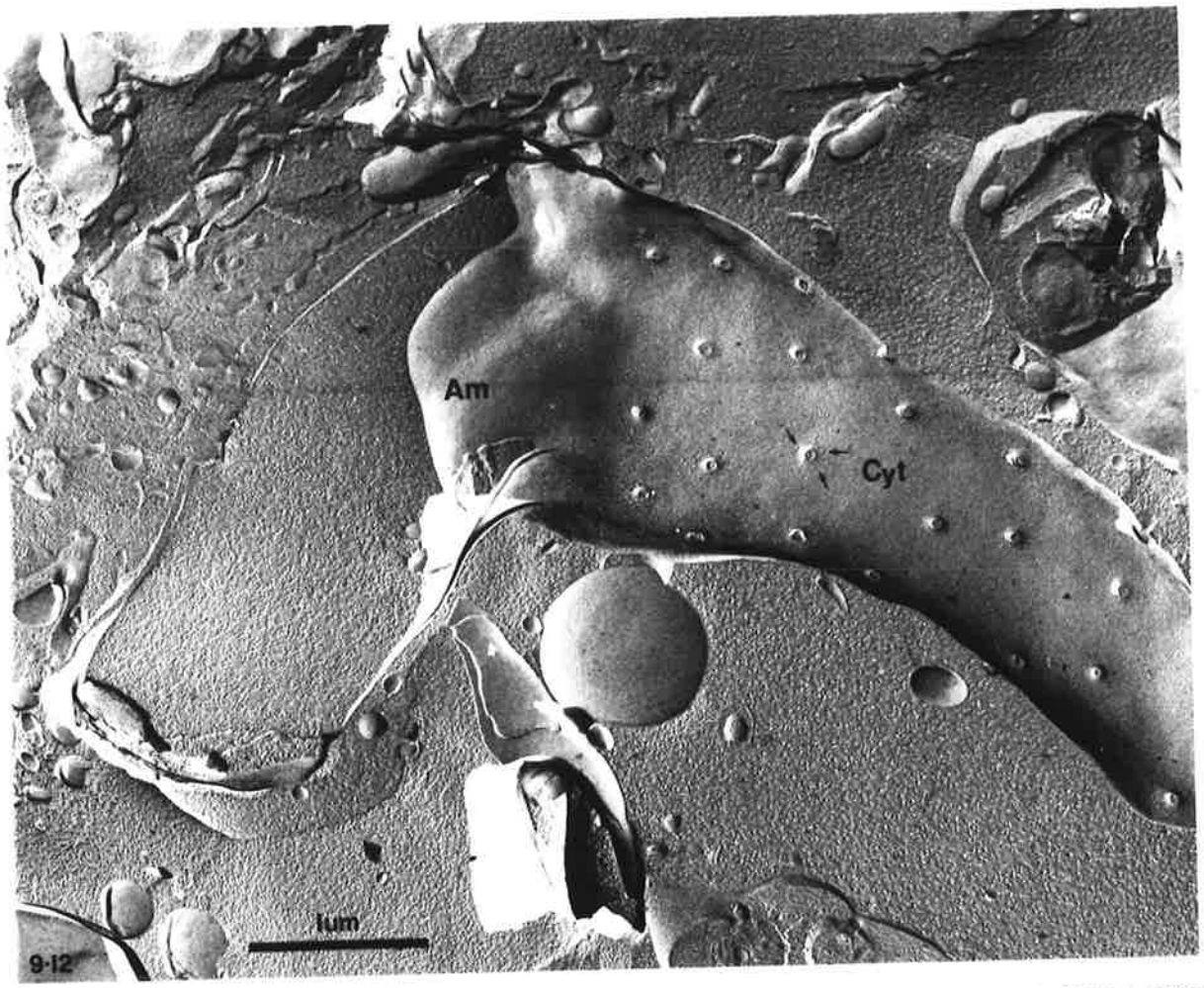
Am
Cyt
1um
9·12

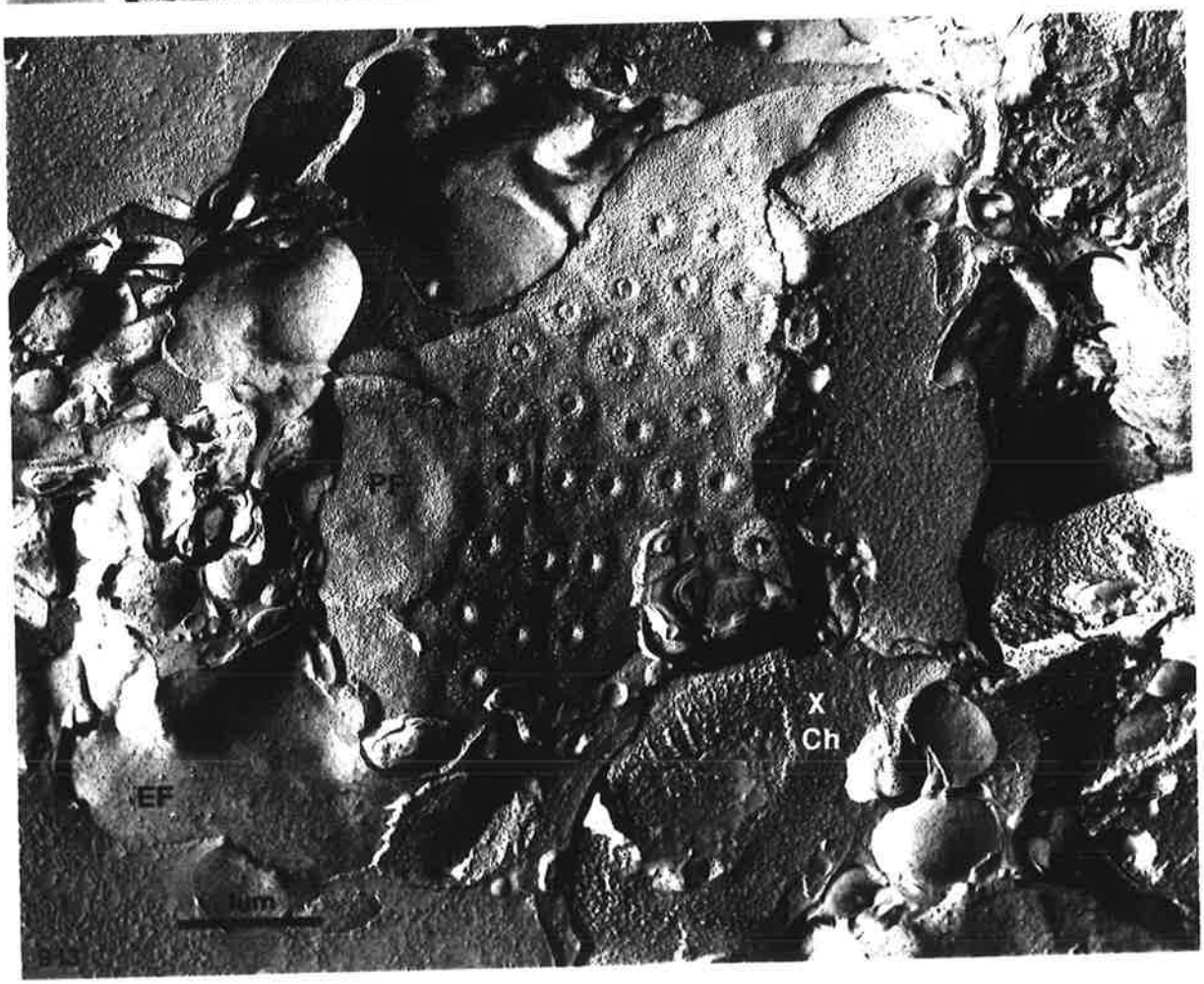
PF
X
Ch
EF
1um

Particle density and distribution is the same in uteri which have been fixed and cryoprotected with glycerol prior to fracture and those which were used 'fresh' (Figures 9.15, 9.16). In Figure 9.16, the numerous pits and indentations are caused by sublimation of ice during deep-etching. The membrane faces themselves are intact and, in the cytoplasmic region, bear characteristic pores with their associated ring of PF-face particles (arrows). In one area of the PF-face the outline of unfused membranous organelles can be discerned, yet on the surrounding membrane, the density of particles is high. This suggests that the increase in particle density which occurs after insemination precedes exocytosis of the membranous organelles.

In summary, the major change to the membranes of the spermatozoa of *N. brasiliensis* after insemination is an increase in particle density in all but one region of the sperm (Table 9.1). The greatest increase occurs on the PF-face of the nuclear region (197%), but the change of 146% seen on the PF-face of the cytoplasmic area is also substantial. The membrane of the amoeboid region of sperm inseminated into females presumably derives from the membrane of the cytoplasmic part of sperm from the testis. In this transition there is a 73% increase in particle density on the PF-face, but no change on the EF-face. On the EF-face of the cytoplasmic region however, there is an increase of 71% in the particle density after activation. A similar increase in particle density follows insemination in *N. dubius*.

9.2.2 Particle size

In an attempt to characterize this dramatic increase in particle density, particle sizes were measured. The resultant histograms (Figure 9.17) show that similar size classes of particles occur on all membrane faces, but their relative proportions differ in the different regions.

The graph of the PF-face of the cytoplasmic region of sperm from

FIGURE 9.14 : PF-face of the nuclear region of sperm in the uterus of a female (*N. dubius*). The density of particles is very high here. Specimen fixed and cryoprotected.

FIGURE 9.15 : Also a PF-face of nuclear region but the specimen was unfixed and not cryoprotected. The membrane with its high density of particles resembles that seen in FIGURE 9.14.

FIGURE 9.16 : Unfixed, non-glycerinated uterus of *N. dubius* cross-fractured to reveal both PF- and EF-faces of the cytoplasmic region. The particle densities resemble those of fixed specimens. Pores joining membranous organelles to plasma membrane are clearly shown. Arrow points to an outline of an MO before fusion, note high density of particles in this region; see also the ring of particles around an open pore (white arrow).

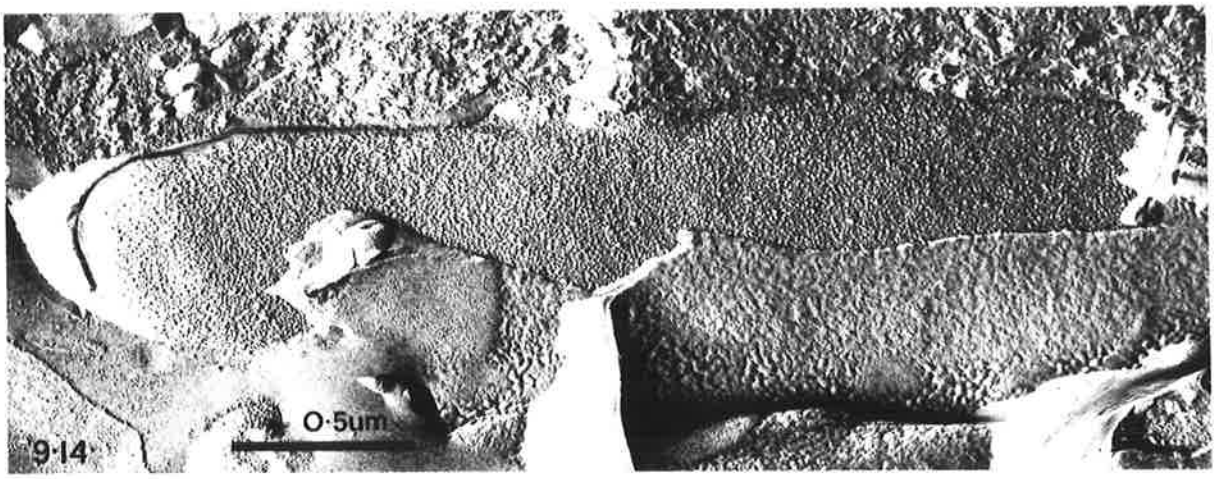
0·5um
9·14

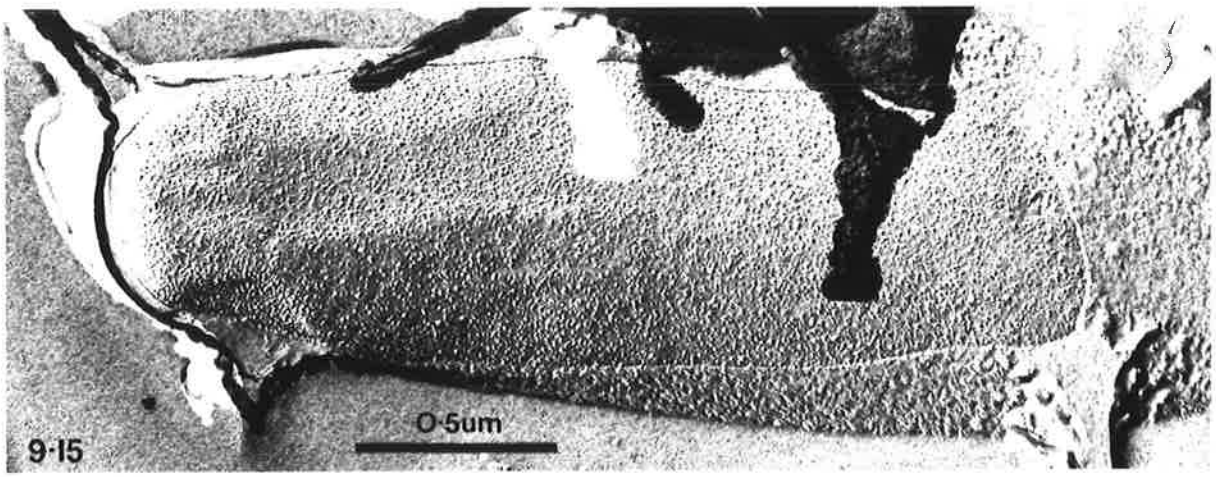
0·5um
9·15

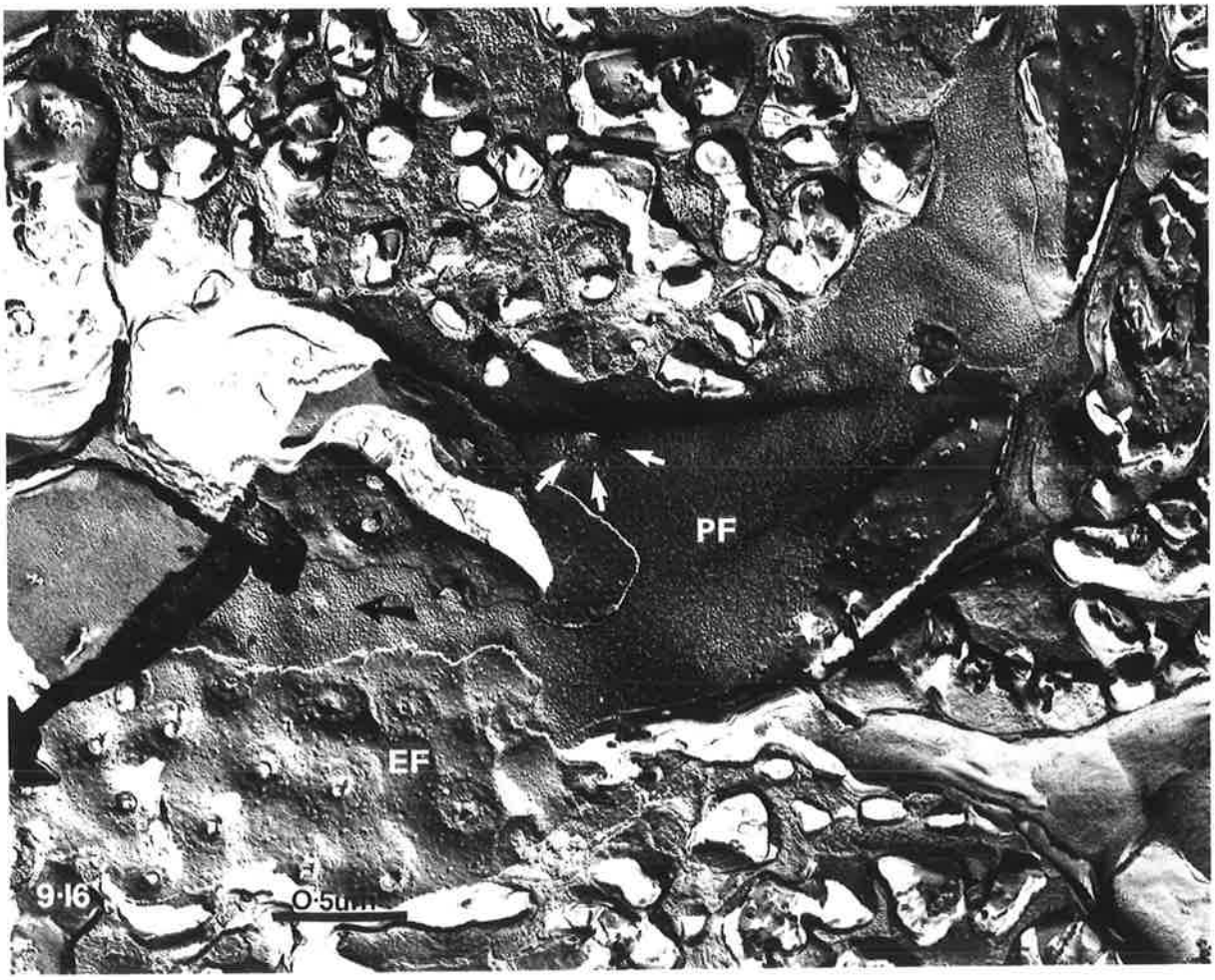
PF
EF
0·5um
9·16

TABLE 9.1

Region	PF ♂	PF ♀	% Change	EF ♂	EF ♀	% Change
Nucleus	1153 ± 150	3423 ± 401	197*		102 ± 31	
Cytoplasm	909 ± 227	2234 ± 345	146*	203 ± 66	347 ± 45	71*
Amoeboid	-	1572 ± 393	73* c.f.cyt ♂		186 ± 67	-8 c.f.cyt ♂

Mean particle density (particles/μm^2) ± S.D. on EF- and PF- faces in different regions of sperm from males and females. % change in particle density after insemination is also shown. * denotes which of these changes are significant at the 5% level using a two-tailed Mann-Whitney U Test. N.brasiliensis

FIGURE 9.17 : A-E, G-I. Histograms showing the frequency of particles in different size classes. Particle density ± S.D. for each face is also shown. The percentages illustrate the proportion of particles ≤10nm and >10nm. The major peak occurs at 9.7nm with minor peaks at 11.3 - 11.6, 13nm and sometimes 14.2nm.

F. Here, the higher density of particles on sperm in females has been taken into account by graphing the density of particles in each size class; the density of small, but not large particles is similar in males and females.

N.brasiliensis

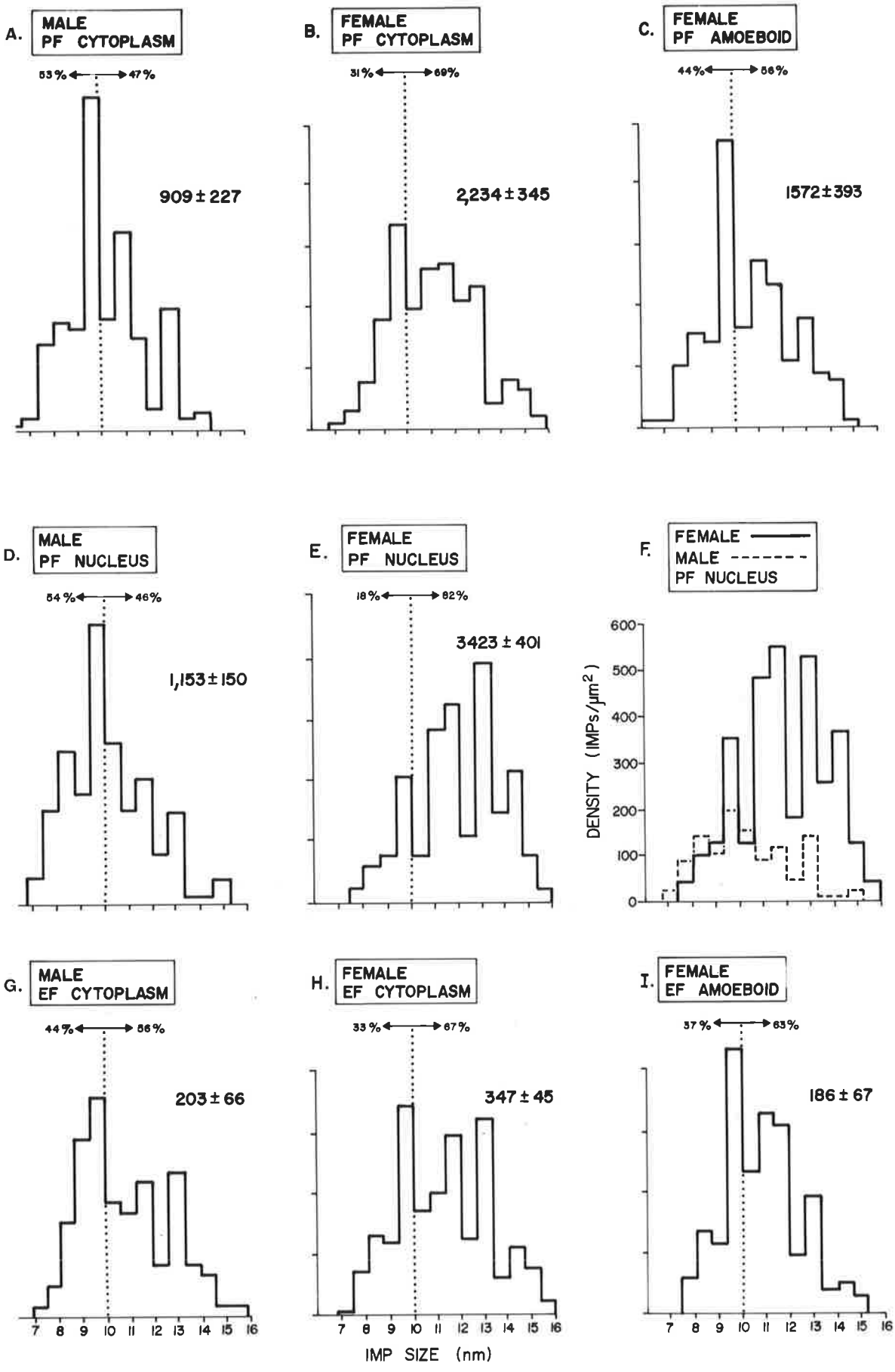
A.
MALE
PF CYTOPLASM
53%
47%
909 ± 227
B.
FEMALE
PF CYTOPLASM
31%
69%
2,234 ± 345
C.
FEMALE
PF AMOEBOID
44%
56%
1572 ± 393
D.
MALE
PF NUCLEUS
54%
46%
1,153 ± 150
E.
FEMALE
PF NUCLEUS
18%
82%
3423 ± 401
F.
FEMALE
MALE
PF NUCLEUS
DENSITY (IMPs/μm²)
600
500
400
300
200
100
0
G.
MALE
EF CYTOPLASM
44%
56%
203 ± 66
H.
FEMALE
EF CYTOPLASM
33%
67%
347 ± 45
I.
FEMALE
EF AMOEBOID
37%
63%
186 ± 67
7 8 9 10 11 12 13 14 15 16
IMP SIZE (nm)

males (Figure 9.17A) is a representative histogram. There is a major modal class at 9.7nm and smaller peaks at 11nm and 13nm. Since for some analyses, it is useful to calculate the proportion of particles in different size categories (Staehelin, 1976). I chose to divide the particles into two groups, those of 10nm and less and those greater than 10nm. This division was selected as the 9.7nm size class was, with only one exception, the major modal class and the magnitudes of the two other peaks rose and fell in unison and so could be considered together. Dividing the histogram of the PF-face of the cytoplasmic region in sperm from males in this way, shows that 53% of the particles are less than or equal to 10nm in diameter. Turning to the same face in sperm from females (Figure 9.17B) it is clear that the majority of particles are greater than 10nm (69%). The major modal class is still at 9.7nm but it is reduced in magnitude from 27.2% to 16.7%. The minor peaks have increased accordingly. Although the larger of these two is still at 13nm, the smaller is spread over two size classes and the 'class mark' is now at 11.3nm. While discussing the cytoplasmic region we should also consider the amoeboid region as it is presumably derived from the former when sperm are activated in the female reproductive tract. Once again, the histogram for the PF-face has a major modal class at 9.7nm and minor peaks at 11.6nm and 13nm, while 56% of the particles are greater than 10nm (Figure 9.17C).

If the particles sizes are considered in conjunction with particle density, some interesting trends appear. In Table 9.2, the density of small ($\leq$10nm) and large (>10nm) particles has been calculated from the total particle density and the percentage of particles in the two size groups. After activation the density of small particles on the PF-face of the cytoplasmic region increases from 482 to 693 particles/μm^2. The density of larger particles increases even more substantially after

TABLE 9.2

Region	Density (IMPs/μm^2)	% ≤10nm	Density ≤10nm	% >10nm	Density >10nm
♂ Cytoplasm	909	53%	482	47%	418
♀ Cytoplasm	2234	31%	693	69%	1541
♀ Amoeboid	1572	44%	692	56%	880

Mean number of IMPs/μm^2 ≤10nm and >10nm on the PF-face of different regions of sperm from the male and female reproductive tracts. Values calculated from the mean density on each face and the % of particles which occur in each size category.

activation (418 to 1,541 particles/μm^2). Similar trends occur in the amoeboid region.

Turning now to the plasma membrane overlying the chromatin, the histogram of particle size for sperm from males has four modal classes. The major one is at 9.7nm, with others at 8.4nm, 11.6nm and 13nm (Figure 9.17D). As in the cytoplasmic region, the majority of particles (54%) measure ≤10nm. The corresponding graph for sperm from females shows a major departure from the general shape of all the other histograms (Figure 9.17E). The main modal class is at 13nm, with minor modes at 11.3nm, 14.2nm and 9.7nm. The latter has the smallest peak of the four as only 18% of the particles are 10nm or less. The huge increase in the density of particles which occurred on this face after activation (from 909 to 3,423 particles/μm^2) can be taken into account by calculating and graphing the density rather than the percentage of particles in each size class (Figure 9.17F). Now it is clear that the density of particles ≤10nm is virtually unchanged after activation, but that there is a huge increase in the density of 11.3nm and 13nm particles as well as the addition of a new particle (14.2m) to the membrane. These densities reflect real changes in the numbers of particles as the area of membrane overlying the nucleus does not change after insemination.

The density of particles on the EF-face of the membrane is substantially and consistently lower than on the PF-face (Table 9.1). Few fractures of this face in the nuclear region were located, therefore only the cytoplasmic and amoeboid regions will be considered. The histograms of particle size on the EF-face resemble those for the PF-face. In the cytoplasmic region of sperm from both males and females the same three peaks occur at 9.7nm, 13nm and 11.6nm (Figure 9.17G,H). After activation, particle density increases by 71% and the proportion of large particles also rises (♂ 56%, ♀67%). This suggests that the increase in density of the larger size classes (11.6nm, 13nm)

is more substantial than for the smaller particles (≤10nm). In the amoeboid region the slight decrease in particle density was not significant, but the histogram of particle sizes has changed (Figure 9.17I). The proportion of particles >10nm has increased from 56% to 63% by the addition of particles to the 11.3nm size class, while the numbers of particles in the other size classes have been reduced accordingly.

9.2.3 Summary of results

Although the nuclear and cytoplasmic regions of sperm from males of *N. brasiliensis* can be distinguished on morphological grounds, the particle size and density is similar in both regions. After insemination, when the sperm develop a large amoeboid region, there is a significant increase in particle density on all but one of the membrane faces. The histograms of particle size demonstrate that while some of the new particles are ≤10nm, the greater proportion belong to the 11 - 11.6nm and 13nm size classes.

There are two specialized particle arrays on the membranes of sperm from females. Particle clusters, 0.5μm across, occur on the PF-face of the amoeboid region. Favourable fractures show mitochondria underlying these particle aggregations. On the PF-face of the cytoplasmic region, a ring of large particles surrounds the pore joining the membranous organelles to the plasma membrane. A similar specialization is seen in the sperm of *N. dubius*. Further observations of the sperm of the latter revealed increased particle densities on the PF-faces of the membrane after insemination. Moreover, a comparison of fixed and unfixed specimens revealed no difference in particle density or distribution.

9.3 Discussion

9.3.1 The nature of IMPs

Many studies have been undertaken to determine the nature of the particles visualized with freeze-fracture. Evidence that they are protein comes from reconstitution experiments, where particles appear on fracture faces only after the addition of a protein, be it erythrocyte Band 3 protein (Yu and Branton, 1976), rhodopsin (Hong and Hubbell, 1972), glycophorin (Segrest, Gulik-Krzywicki and Sardet, 1974), or cytochrome oxidase (Montal, 1974). Furthermore, protein digestion can remove particles from erythrocyte ghost membranes (Engstrom, 1970; reported by Branton, 1971) and inhibition of protein synthesis during development causes a decrease in particle density in *Acholeplasma laidlawii* cells (Tourtellotte and Zupnik, 1973). Although more recent work suggests that pure lipid bilayers may be particulate (Robertson and Vergara, 1980), it is generally accepted that intramembranous particles are proteins surrounded by a boundary layer of lipid (Bullivant, 1977; Zingshein and Plattner, 1976).

There is now good evidence that many of the particles in the membrane of the erythrocyte represent the two major transmembrane proteins, glycophorin and Band 3 protein (Bretscher and Raff, 1975; McNutt, 1977). As glycophorin is a sialoglycoprotein bearing receptors for WGA, PHA, ABO antigens and influenza virus (Marchesi, Tillack, Jackson, Segrest and Scott, 1972; Zingsheim and Plattner, 1976) and Band 3 bears a ConA receptor (Findlay, 1974), both proteins are easily labelled. A comigration of these tagged transmembrane proteins follows experimental aggregation of particles (Pinto da Silva and Nicolson, 1974; Bretscher and Raff, 1975). Spectrin, a peripheral protein on the inner side of the membrane, is closely associated with the particles, as it too comigrates during particle aggregation (Shotten, Thompson, Wofsy and Branton, 1978).

In more complex nucleated cells there is no consistent correlation between cell surface receptors and IMPs. For example, when particles in the membrane of *Entamoeba histolytica* were aggregated with glycerol, ConA receptors remained randomly distributed (Pinto da Silva and Martinez-Palomo, 1974). Similarly, cross-linking and redistribution of virtually all lymphocyte cell surface proteins produced no particle movement on the PF-face and only minor redistribution on the EF-face (Kuby and Wofsy, 1981). These surface proteins must penetrate through the membrane as there is good evidence that they are associated with the cytoplasmic actin network (Flanagan and Koch, 1978). Thus, the results led the authors to speculate that IMPs might not adequately represent lymphocyte transmembrane protein organization.

The recently developed technique of combining freeze-fracture and cytochemistry (Pinto da Silva, Kachar, Torrisi, Brown and Parkinson, 1981) may provide a better understanding of the relationship between cell surface receptors and IMPs. Results from one study support previous findings for complex nucleated cells, since cell surface receptors, unlike IMPs, were found to be localized mainly on the EF-face of the plasmalemma (Pinto da Silva, Torrisi and Kachar, 1981). Bretscher and Raff (1975) have presented an explanation for this kind of observation. They postulate the existence of two types of transmembrane proteins in nucleated cells. One group has both polypeptide and oligosaccharide exposed at the cell surface, but little mass within the membrane. These would not be visualized in freeze-fracture but would bind ligands. The other group has a considerable mass within the membrane and are therefore seen as particles. They do not extend far out from the membrane and so are not readily labelled. This group would include proteins involved in the formation of cell junctions and those which transport ions and sugars.

Many exceptions demonstrate that these groups are not distinct and

mutually exclusive. The particles of the ciliary necklace in the quail oviduct cilia bind ConA and WGA. They also bear a negative charge which is partly due to sialic acid as it can be abolished with neuraminidase. The particles appear to be anchoring sites for the fibrillar material which links the microtubules to the plasma membrane (Sandoz, Boisvieux-Ulrich and Chailley, 1979). Although not a plasmalemma, the outer part of the tegument of *Schistosoma* has membrane-like properties. When live worms are labelled with ConA or WGA, receptors which were formerly distributed randomly move to the tips of the tegumental spines. Freeze-fracture shows that at the same time EF-face particles become paired and they too accumulate on the spines. It was therefore concluded that in this membrane, ConA and WGA binding sites are associated with intramembranous particles (Torpier and Capron, 1980).

The nature of intramembranous particles is best understood in highly specialized cells where one membrane protein is more abundant than the rest. Correlated thin sectioning, negative staining and freeze-fracture has identified particles in kidney membranes as Na^+/K^+ ATPase (Deguchi, Jørgensen and Maunsbach, 1977). Similarly, in photosensitive membranes, particles represent molecules of the visual pigment rhodopsin (Besharse and Pfenninger, 1980). In these cells and in the purple membrane of *Halobacterium halobium* (Fisher and Stoeckenius, 1977) the ratio of protein molecules to particles is not 1:1, suggesting that each intramembranous particle is an aggregate of several molecules (Willmer, Skaer and Treherne, 1979). In chloroplast membranes, these aggregates are thought to form functional complexes. For example, the large EF-face particles are believed to be the structural equivalent of photosystem II and the PF-face particles correspond to photosystem I complexes (Staehelin, 1976).

9.3.2 Freeze-fracture of the sperm of *N. brasiliensis* and *N. dubius*

In general terms, an increase in particle density on a membrane can be brought about by either the addition of particles or the removal of membrane. Either or both of these mechanisms could account for the increase in particle density which occurs in the sperm membranes after insemination. Membrane could be removed by the formation of small particle-free vesicles, like those seen in the amoeboid region of the sperm, or there may be a movement of membrane into the membranous organelles. Nevertheless, a decrease in surface area, if indeed it occurs, cannot explain the differential increase in density of the large particles (>10nm) on the membrane.

Different methods of processing tissue can significantly alter the membrane and its particles. Particle movements including aggregation and disruption of regular arrangements may follow glycerination (Pinto da Silva and Martinez-Palomo, 1974), fixation (Hasty and Hay, 1978; Green, 1981) and processing at low temperatures (Kachar, Serrano and Pinto da Silva, 1980; Feltkamp and van der Waerden, 1982), while fixation can change both particle size (Gros, Potreau and Mocquard, 1980) and density (Willmer *et al.*, 1979). The changes in particle size and density noted in this study are unlikely to be due to such factors as identical conditions were used for all specimens. Moreover, comparison of replicas of uteri of *N. dubius* processed in different ways showed that particle density and distribution is unaffected by fixation and glycerination.

Assuming the particles are proteins, they must be preformed as the protein synthesizing machinery of the sperm is cast out with the residual cytoplasm after meiosis. These proteins may be present in the membrane as single molecules which only aggregate to form visible complexes after activation, or they may be present in the cytoplasm and inserted into the membrane after insemination. Although, in

general, the majority of proteins are assembled into membranes while being synthesized by membrane-bound ribosomes, there is also evidence that preformed proteins can move from the cytoplasm into the membrane (Wickner, 1980; Sabatini, Kreibich, Morimoto and Adesnik, 1982). It seems unlikely that particles are contributed by the membranous organelles as they do not become depleted of IMPs during activation. Furthermore, the PF-face of the cytoplasmic region of 'intermediate' sperm from *N. dubius* were observed to have a high density of IMPs before all of the membranous organelles had undergone exocytosis.

Although in general, IMPs have not been shown to bear surface receptors, in studies of sperm membranes many particle arrays have been correlated with the cell coat. In the plasma membrane of the head of the guinea pig spermatozoon, the 'quilted honeycomb pattern' seen with freeze-fracture can be correlated with a glycocalyx resembling contiguous circles when sectioned tangentially (Friend and Fawcett, 1974). Dispersal of crystalline arrays of particles in the plasma membrane of the head of rat sperm coincides precisely with the removal of a dense glycocalyx from the same region during epididymal transit (Suzuki and Nagano, 1980). In the midpiece of the tail of the guinea pig, grazing sections reveal linear densities in the cell coat in the region where strands of particles are seen in freeze-fracture (Friend, 1977). The changes in these particle arrays which accompany capacitation are believed to be related to surface modifications detected by the lectin SBA (Schwarz and Koehler, 1979).

Studies of the surface of the sperm of *N. brasiliensis* revealed little external coat and only a slight increase in lectin binding to the cytoplasmic region following insemination (Chapter 8). Thus changes noted here with freeze-fracture cannot be readily correlated with alterations to the sperm surface. Thin sections of activated

sperm, do however show a dense layer of material beneath the plasma membrane of the cytoplasmic region. This material may have a structural relationship with the dense particles seen on the PF-face of this membrane. Certainly in other sperm, filamentous material beneath the membrane has been correlated with IMPs. An example of this is in the midpiece of the sperm of the oppossum. Here, regular rows of particles overlie strips of an amorphous material attached to the cytoplasmic side of the plasmalemma. It has been inferred that the filamentous material anchors the particles into rows and together they serve to maintain the unusual scalloped topography of the membrane (Olson *et al.*, 1977). Similar associations between intramembranous particles and cytoplasmic filaments have been proposed in the sperm of the isopod *Armadillium vulgare* (Reger *et al.*, 1979) and the squid, *Loligo pealeii* (Olson and Linck, 1980).

The particles in the membrane of the sperm of *N. brasiliensis* may function as structural supports between the filamentous material and the membrane. This association would help to maintain the cell's shape and the position of the membrane over this region during amoeboid locomotion. Conversely, the filamentous material could serve to anchor the IMPs while they perform a quite different function. In some cells, particles have been identified as ion channels which regulate the passage of ions through the membrane. In such systems, environmental changes (e.g. low salinity) may stimulate changes in the numbers of these molecules (Willmer *et al.*, 1980). It has been suggested that a change in ionic permeability of the membrane accompanies activation of the sperm of *C. elegans* (Ward, Hogan and Nelson, submitted for publication). If a similar change occurred in the sperm of *N. brasiliensis*, it could account for the enormous increase in particle density which follows insemination in this species.

One specialization noted on the PF-face of the cytoplasmic region

of sperm in females was a ring of large particles around each pore connecting the membranous organelles to the plasma membrane. Grazing sections show that the filamentous material lying beneath the plasma membrane of this region is perceptably thicker around these pores (see Figure 5.37). The diameter of the rings of particles corresponds to the width of these thickened regions. This relationship also exists in the sperm of the related species *N. dubius*, where the dense collar and the rings of particles are even more prominent. It seems then that the permanent connection between the membranous organelles and the plasma membrane is reinforced by a thickening of the subplasmalemmal material and that this collar is anchored to the plasma membrane by a ring of large intramembranous particles. In *A. suum*, intermediate steps in the fusion of the membranous organelles are marked by the formation of a rosette of particles on the PF-face of the plasma membrane. After fusion, however, this array loses its highly ordered appearance and thin sections reveal no collar of material around the neck of the pore (Burghardt and Foor, 1978).

Specialized arrays of particles may also act as sites of membrane to membrane attachment. For example, parallel rows of IMPs on the membranes of the cilia of *Glaucoma ferox* are associated with regularly spaced intercilliary bridges of a flocculent material (Montesano, Didier and Orci, 1981). In the intracellular membranes of *Paramecium*, four regions of membrane to membrane attachment appear as rings of particles on the PF-faces (Plattner, Miller and Bachmann, 1973). Thus particle aggregates in the amoeboid region of sperm from females of *N. brasiliensis* may represent sites of close contact between the plasma and underlying mitochondrial membranes. Thin sections (see Figure 5.38) show that the membranes are closely apposed and a dense material fills the narrow gap between them.

In the amoeboid region, cytoplasmic filaments insert into the

membrane (Chapter 5.3). It is difficult to see whether or not intramembranous particles are involved in this attachment as filaments are poorly preserved during freeze-fracture. In the literature, there is evidence both for and against the notion that particles act as anchors for the attachment of microfilaments (Bluemink and Tertoolen, 1978; Tilney and Mooseker, 1976).

The function of the high density of particles on the PF-face of the nuclear region is unknown. The DNA of spermatids is 'switched-off' during spermiogenesis (Temple-Smith and Bedford, 1976), becoming a highly condensed, inert mass in the spermatozoon. The chromatin of all nematode sperm lacks a nuclear envelope and perhaps the high density of particles is somehow related to this.

CHAPTER 10. CONCLUSIONS

10.1 The form and function of spermatozoa

In 1956, Franzén recognized a correlation between sperm type and mode of fertilization. He observed that 'primitive' sperm, with their simple head, midpiece and tail in radial symmetry, occur in animals with external fertilization. Sperm which undertake internal fertilization are 'modified', usually by elongation of the midpiece and remodelling of the nucleus and acrosome. More unorthodox solutions to the problems of internal fertilization have produced 'aberrant' sperm in some groups, including the nematodes. Recently, Afzelius (1979) summarized these relationships when he stated that sperm morphology is determined by both phylogeny and the functional demands of fertilization.

The environment of fertilization may act directly on sperm, or it may influence the structure of the egg and thus indirectly affect the sperm. For example, since the acrosome is particularly sensitive to hypotonicity, it has been sacrificed in some groups with external fertilization in freshwater. The lack of an acrosome in the sperm of marine teleosts can thus be readily explained, as this group are believed to be descended from freshwater teleosts (Baccetti and Afzelius, 1976). The eggs of terrestrial invertebrates, such as insects, are surrounded by thick impermeable egg coats, designed to reduce water loss. Since sperm enter these eggs via micropyles, the acrosome is superfluous and has been reduced or lost (Baccetti, 1979).

In nematodes the egg coat is thin, i.e. 40 - 50nm thick, and in *N. brasiliensis* it is punctuated by gaps 0.2µm across. It seems not to be a formidable barrier to sperm penetration, as micrographs of fertilization in *A. suum* show that it is pushed aside by the pseudopodia (Foor, 1968). It follows that an acrosome containing lytic enzymes is

not required for fertilization in nematodes. Here then is another example of the functional demands of fertilization determining sperm morphology.

Several factors may have reduced the importance of egg investments in nematodes. Since eggs travel only a short distance from the ovary to the site of fertilization, they do not require the same protection as eggs moving long distances through the female reproductive tract or in the external environment. Furthermore, the impermeable egg shell, which is added after fertilization, protects the zygote and embryo from desiccation. In mammals, the zona pellucida is also the major barrier to penetration by heterologous sperm (Adams, 1974) and is involved in the block to polyspermy (Austin, 1976). It is likely that in nematodes these functions have been assumed by other structures such as the oolemma and vitelline (fertilization) membrane.

A further modification to the sperm of a number of groups of invertebrates, including nematodes, is loss of the functional flagellum. In some cases, the sperm have developed new forms of locomotion which may be based on an amoeboid flow of cytoplasm, as in nematode sperm, or may involve new organizations of microtubules. If the sperm remain immotile, they must rely on other mechanisms, such as contractions of the female reproductive tract, to bring them into the vicinity of the egg. Similarly, since flagellar beating is important during penetration of the egg investments, mechanisms like the 'explosive' acrosome reaction of decapods have evolved to propel the otherwise immotile sperm through the chorion (Talbot and Chanmanon, 1980).

Dallai *et al.* (1975) had difficulty in seeing any advantage in the loss of the flagellum. However, Cohen (1975) argues that the manufacture of a complex flagellum may present so many difficulties, that it has been abandoned in favour of either, other forms of motility or, other mechanisms to bring the eggs and sperm together. The demands of

fertilization would determine how easily this transformation could be accomplished. The change from flagellar to amoeboid locomotion may have presented few problems to the sperm of ancestral nematodes. They are believed to have been small animals, thus, sperm would have been required to travel only short distances along the female reproductive tract. If Cohen (1975) is correct that the formation of a flagellum is a difficult process, it can be envisaged that the advantages of removing a difficult and probably lengthy step in sperm development would more than outweigh the disadvantage of the reduced mobility of the sperm. There is an alternative and equally tenable hypothesis which explains amoeboid locomotion in nematode sperm. It comes from two observations: first, while aflagellate sperm occur only sporadically in other groups, the sperm of all species of nematodes are aflagellate and second, functional cilia and flagella are missing from the somatic cells of all larval and adult nematodes. Thus, both nematodes and their sperm may be devoid of these organelles because the instructions for their synthesis are incomplete, or as argued by Crofton (1966) cilia (and flagella) are incompatable with the high turgor-pressure system of nematodes.

Dallai *et al.* (1975) believe that amoeboid locomotion could easily be acquired by aflagellate spermatozoa because this form of movement is 'ancestral' and 'universal in almost all cells'. This appears to be an oversimplification at least in terms of nematodes. Studies of sperm movement in *C. elegans* (Roberts and Ward, 1982a) and *N. brasiliensis* (Chapter 5.4) suggest that locomotion does not rely on actin, the ubiquitous contractile protein implicated in all non-muscle cell movement. Thus, it remains to be seen if nematode sperm have evolved a novel means of amoeboid movement, representing a divergence from more conventional mechanisms of non-muscle cell motility.

10.2 Conclusions

The first part of this study examined the reproductive biology of *N. dubius* and *N. brasiliensis*, two species of nematodes which have been extensively used as experimental models. Spermatogenesis and sperm maturation in these two species were compared and found to be very similar. Indeed, the differences were so minor that for many purposes the two species can be considered interchangeable. Since each is suitable in certain fields of study, together they provide a model system which has many advantages over the use of a single species.

An evaluation of the particular kinds of investigations which would be suitable for study with these species is made after consideration of the second part of the present study. In this section, a conventional approach was taken in which a number of specific techniques were used to examine aspects of the cell biology of *N. brasiliensis*. These investigations revealed a number of interesting features of the sperm surface, including regional specialization and modifications to the membrane and surface coat after insemination. Problems arose, however, whenever the procedures included the use of free sperm, since they were difficult to obtain in large numbers, especially from females. Since many of the major techniques of cell biology such as electrophoresis, immunocytochemistry and cytochemistry require cellular suspensions or cell homogenates, they are likely to prove unsuitable for use with the sperm of *N. brasiliensis* or *N. dubius*. This may severely limit the usefulness of these sperm as models in studies of a broader significance, such as cell-cell interactions, cell fusion and cell motility.

An alternative approach is to view sperm from a more ecological perspective, where they are examined in relation to their environment within the reproductive tract of the whole animal. A number of features of *N. brasiliensis* and *N. dubius* make them suitable for in-

vestigations of this kind, as well as for more general studies of the reproductive biology of nematodes. They are dioecious and can either be returned to their hosts after examination and manipulation or maintained *in vitro*. Copulation can be controlled to some extent by isolating the sexes before maturity, then introducing pairs into hosts at specific times. Moreover, in *N. dubius* copulation may continue for some time after the removal of worms from their hosts.

Sperm redundancy is one area which has attracted a great deal of interest. Investigations in this field have addressed such questions as why so many sperm are required to ensure that a single egg is fertilized, or why a particular sperm fertilizes an egg when many others fail (Jones, 1975). It is now believed that a high proportion of the crossings-over which occur during meiosis result in the production of defective sperm and that sperm redundancy is a means of making enough 'acceptable' sperm to accomplish fertilization (Cohen, 1977). It is therefore surprising that in hermaphrodites of *C. elegans*, every sperm produces a zygote (Ward and Carrel, 1979). If this is also shown to be true of the dioecious species, nematode sperm, already considered atypical, will be set even further apart from the sperm of other organisms.

REFERENCES

Abbas, M. & Cain, G.D. (1979) : *In vitro* activation and behaviour of the amoeboid sperm of *Ascaris suum* (Nematoda). *Cell. Tissue Res.* 200, 273-284.

\- (1980) : Iodination of surface components of the spheroidal and amoeboid spermatozoa of *Ascaris suum* (Nematoda). *Biol. Reprod.* 22, 1007-1014.

Abbas, M. & Foor, W.E. (1978) : *Ascaris suum*: free amino acids and proteins in the pseudocoelom, seminal vesicle and glandular vas deferens. *Exp. Parasitol.* 45, 263-273.

Ackerman, G.A. (1972) : Localization of pyroantimonate - preciptable cation and surface coat anionic binding sites in developing erythrocytic cells and macrophages in normal human bone marrow. *Z. Zellforsch.* 134, 153-166.

Ackerman, G.A. & Clark, M.A. (1972) : A cytochemical evaluation of pyroantimonate binding to the plasmalemma of blood and bone marrow cells and its relationship to cellular maturation. *J. Histochem. Cytochem.* 20, 880-895.

Adair, W.L. & Kornfield, S. (1974) : Isolation of receptors for wheat germ agglutinin and the *Ricinus communis* lectins from human erythrocytes using affinity chromatography. *J. Biol. Chem.* 249, 4696-4704.

Adams, C.E. (1974) : Species specificity in fertilization. In 'Physiology and Genetics of Reproduction'. Part B. pp.69-79. Eds. E.M. Coutinho and F. Fuchs. (Plenum Press: New York, London.)

Afzelius, B.A. (1979) : Sperm structure in relation to phylogeny in lower metazoa. In 'The Spermatozoon'. pp.243-252. Eds. D.W. Fawcett and J.M. Bedford. (Urban-Schwarzenberg Inc.: Baltimore-Munich.)

Aketa, K. (1975) : Physiological studies on the sperm surface component responsible for sperm-egg bonding in sea urchin fertilization. II Effect of concanavlin A on the fertilizing capacity of sperm. *Exp. Cell Res.* 90, 56-62.

Allen, A.K., Neuberger, A. & Sharon, N. (1973) : The purification, composition and specificity of wheat germ agglutinin. *Biochem. J.* 131, 155-162.

Aloia, R.C. & Moretti, R.L. (1974) : Spermiogenesis and cytochemistry of the functional spermatozoon of the Rotifer *Asplanchna brightwelli*. *Biol. Reprod.* 11, 301-318.

Anderson, W.A. (1968) : Cytochemistry of sea urchin gametes. II Ruthenium red staining of gamete membranes of sea urchins. *J. Ultrastruct. Res.* 24, 322-333.

Anya, A.O. (1966) : Studies on the structure and histochemistry of the male reproductive tract of *Aspiculuris tetraptera* (Nematoda : Oxyuridae). *Parasitol.* 56, 347-358.

- (1976) : Physiological aspects of reproduction in nematodes. *Adv. Parasitol.* 14, 267-351.

Argon, Y. (1979) : Sperm lectin receptors. *Carnegie Inst. Wash. Yearbook* 78, 49-52.

Austin, C.R. (1952) : The 'capacitation' of mammalian sperm. *Nature* 170, 326.

- (1976) : Specialization of gametes. In 'The Evolution of Reproduction'. Book 6. pp.149-182. Eds. C.R. Austin and R.V. Short. (Cambridge University Press: Cambridge.)

Baccetti, B. (1979) : Evolution of the acrosomal complex. In 'The Spermatozoon'. pp.305-329. Eds. D.W. Fawcett and J.M. Bedford. (Urban-Schwarzenberg: Baltimore-Munich.)

Baccetti, B. & Afzelius, B.A. (1976) : The Biology of the Sperm Cell. *Monographs in Dev. Biol.* 10. (Karger: Basel, Switzerland.)

Baccetti, B., Bigliardi, E. & Burrini, A.G. (1978) : The cell surface during mammalian spermiogenesis. *Dev. Biol.* 63, 187-196.

Baccetti, B., Dallai, R., Bernini, F. & Mazzini, M. (1974) : The spermatozoon of Arthropoda. XXIV Sperm metamorphosis in the Diplopod *Polyxenus*. *J. Morph.* 143, 187-246.

Badel, P. & Brilliantine, L. (1969) : Agglutination of spermatozoa of clams and human A, B and O blood groups by phytagglutinins. *Proc. Soc. Exp. Biol. Med.* 130, 621-627.

Baker, N.F. (1954) : Trichostrongylidosis - the mouse as an experimental animal. *Proc. 91st Ann. Meeting, Amer. Vet. Med. Assn.* Seattle, U.S.A. p.185-192.

Balhorn, R. (1982) : A model for the structure of chromatin in mammalian sperm. *J. Cell Biol.* 93, 298-305.

Barondes, S.H. (1980) : Endogenous cell surface lectins: Evidence that they are cell adhesion molecules. In 'The Cell Surface: Mediator of Developmental Processes'. pp.349-363. Eds. S. Subtelny and N.K. Wessells. (Academic Press: New York.)

Bartlett, A. & Ball, P.A.J. (1972) : *Nematospiroides dubius* in the mouse as a possible model of endemic human hookworm infection. *Ann. Trop. Med. Parasitol.* 66, 129-134.

Baylis, H.A. (1926) : On a trichostrongylid nematode from the wood-mouse (*Apodemus sylvaticus*). *Ann. a Mag. Nat. Hist. ser 9*, 18, 455-464.

Beams, H.W. & Sekhon, S.S. (1972) : Cytodifferentiation during spermiogenesis in *Rhabditis pellio*. *J. Ultrastruct. Res.* 38, 511-527.

Bedford, J.M. (1963) : Changes in the electrophoretic properties of rabbit spermatozoa during passage through the epididymis. *Nature* 200, 1178-1180.

\- (1975) : On the functional significance of -S-S- crosslinks in the sperm heads with particular reference to eutherian mammals. In 'The Functional Anatomy of the Spermatozoon'. pp.343-347. Ed. B.A. Afzelius. (Pergamon Press: Oxford.)

Bedford, J.M. & Calvin, H.I. (1974) : The occurrence and possible functional significance of -S-S- crosslinks in sperm heads, with particular reference to eutherian mammals. *J. Exp. Zool.* 188, 137-156.

Bedford, J.M. & Millar, R.P. (1978) : The character of sperm maturation in the epididymis of the ascrotal hydrax, *Procavia capensis* and armadillo, *Dasypus novemcinctus*. *Biol. Reprod.* 19, 396-406.

Begg, D.A. & Rebhun, L.I. (1978) : Visualization of actin filament polarity in thin sections. *Biophys. J.* 21, 23a.

Behnke, O. & Zelander, T. (1970) : Preservation of intercellular substances by the cationic dye alcian blue in preparative procedures for electron microscopy. *J. Ultrastruct. Res.* 31, 424-438.

Bernhard, W. & Avrameas, S. (1971) : Ultrastructural visualization of cellular carbohydrate components by means of concanavlin A. *Exp. Cell Res.* 64, 232-236.

Besharse, J.C. & Pfenninger, K.H. (1980) : Membrane assembly in retinal photoreceptors. I. Freeze-fracture analysis of cytoplasmic vesicles in relationship to disc assembly. *J. Cell Biol.* 87, 451-463.

Bhavanandan, V.P. & Katlic, A.W. (1979) : The interaction of wheat germ agglutinin with sialoglycoproteins. The role of sialic acid. *J. Biol. Chem.* 254, 4000-4008.

Bird, A.F. (1971) : 'The Structure of Nematodes.' (Academic Press: New York, London.)

Blanquet, P.R. (1976) : Ultrahistochemical study on the ruthenium red surface staining. II. Nature and affinity of the electron dense marker. *Histochem.* 47, 175-189.

Bleil, J.D. & Wassarman, P.M. (1980) : Mammalian sperm-egg interaction: identification of a glycoprotein in mouse egg zonae pellucidae possessing receptor activity for sperm. *Cell* 20, 873-882.

Bluemink, J.G. & Tertoolen, L.G.J. (1976) : Freeze-fracture electron microscopy of the plasma membrane of *Xenopus* egg: evidence for particle associated filaments. *Cytobiologie* 16, 358-366.

Bolla, R.I., Bonner, T.P. & Weinstein, P.P. (1972) : Genic control of the postembryonic development of *Nippostrongylus brasiliensis*. *Comp. Biochem. Physiol.* 41B, 801-811.

Bolla, R.I. & Weinstein, P.P. (1980) : Acid protease activity during development and ageing in *Nippostrongylus brasiliensis*. *Comp. Biochem. & Physiol.* 66B, 475-481.

Bolwell, G.P., Callow, J.A., Callow, M.E. & Evans, L.V. (1979) : Fertilization in brown algae. II. Evidence for lectin-sensitive complementary receptors involved in gamete recognition in *Fucus serratus*. *J. Cell Sci.* 36, 19-30.

Bone, L.W., Gaston, L.K. & Reed, S.K. (1980) : Production and activity of the Kav 0.64 pheromone fraction of *Nippostrongylus brasiliensis*. *J. Parasitol.* 66, 268-273.

Boyles, J. & Bainton, D.F. (1979) : Changing patterns of plasma membrane-associated filaments during the initial phases of polymorphonuclear leucocyte adherance. *J. Cell Biol.* 82, 347-368.

Brambell, M.R. (1965) : The distribution of a primary infestation of *Nippostrongylus brasiliensis* in the small intestine of laboratory rats. *Parasitol.* 55, 313-324.

Branton, D. (1966) : Fracture faces of frozen membranes. *Proc. Natl. Acad. Sci.* 55, 1048-1056.

- (1971) : Freeze-etching studies of membrane structure. *Phil. Trans. Roy. Soc. Lond.* B. 261, 133-138.

Branton, D., Bullivant, S., Gilula, N.B., Karnovsky, M.J., Moor, H., Mühlethaler, K., Northcote, D.H., Packer, L., Satir, B., Satir, P., Speth, V., Staehelin, L.A., Steere, R.L. & Weinstein, R.S. (1975) : Freeze-etching nomenclature. *Science* 190, 54-56.

Breed, W.G. & Sarafis, V. (1979) : On the phylogenetic significance of spermatozoal morphology and male reproductive tract anatomy in Australian rodents. *Trans. Roy. Soc. S.A.* 103, 127-135.

Bretscher, M.S. & Raff, M.C. (1975) : Mammalian plasma membranes. *Nature* 258, 43-49.

Brown, J.C. & Hunt, R.C. (1978) : Lectins. *Int. Rev. Cytol.* 52, 277-349.

Bryant, V. (1973) : The life cycle of *Nematospiroides dubius*, Baylis, 1926 (Nematoda : Heligmosomidae). *J. Helminthol.* 47, 263-268.

Buckley, I.K. (1974) : Subcellular motility: correlated light and electron microscopic study using cultured cells. *Tissue and Cell* 6, 1-20.

Bullivant, S. (1977) : Evaluation of membrane structure facts and artefacts produced during freeze-fracturing. *J. Micros.* 111, 101-116.

Burghardt, R.C. & Foor, W.E. (1975) : Rapid morphological transformations of spermatozoa in the uterus of *Brugia pahangi* (Nematoda : Filarioideae). *J. Parasitol.* 61, 343-350.

- (1978) : Membrane fusion during spermiogenesis in *Ascaris*. *J. Ultrastruct. Res.* 62, 190-202.

Burton, P.R., Hinkley, R.E. & Pierson, G.B. (1975) : Tannic acid-stained microtubules with 12, 13 and 15 protofilaments. *J. Cell Biol.* 65, 227-233.

Chabaud, A.G. (1965) : Ordre des Strongylida. In 'Traité de Zoologie Anatomie, Systématique, Biologie'. Volume IV. Part 3. pp.869-931. Ed. P.P. Grassé. (Masson et Cie: Paris.)

- (1974) : Keys to the Subclasses, orders and superfamilies. In 'C.I.H. Keys of the Nematode Parasites of Vertebrates'. No.1. Eds. R.C. Anderson, A.G. Chabaud & S. Willmott. (Commonwealth Agricultural Bureaux: London.)

Chaicumpa, V., Prowse, S.J. Ey, P.L. & Jenkin, C.R. (1977) : Induction of immunity in mice to the nematode parasite, *Nematospiroides dubius*. *Ajebak* 55, 393-400.

Chin, J.H., Rubin, L.L. & Den, H. (1981) : Endogenous β-galactoside specific lectins from chick embryo are not involved in myoblast fusion or synaptogenesis *in vitro*. *J. Cell Biol.* 91, 102a.

Chitwood, B.G. & Chitwood, M.B. (1950) : 'Introduction to Nematology'. (University Park Press: Baltimore).

Chulavatnatol, M. & Yindepit, S. (1976) : Changes in surface ATP-ase of rat spermatozoa in transit from the caput to the cauda epididymidis. *J. Reprod. Fert.* 48, 91-97.

Clark, W.H.Jr., Moretti, R.L. & Thomson, W.W. (1967) : Electron microscope evidence for the presence of an acrosome reaction in *Ascaris lumbricoides* var. *suum*. *Exp. Cell Res.* 47, 643-647.

- (1972) : Histochemical and ultracytochemical studies of the spermatids and sperm of *Ascaris lumbricoides* var. *suum*. *Biol. Reprod.* 7, 145-159.

Clark, W.H.Jr., Yudin, A.I. & Kleve, M.G. (1981) : Primary binding in the gametes of the marine shrimp *Sicyonia ingentis*. *J. Cell Biol.* 91, 174a.

Cohen, J. (1975) : Gametic diversity within an ejaculate. In 'The Functional Anatomy of the Spermatozoon'. pp.329-339. Ed. B.A. Afzelius. (Pergamon Press: Oxford.)

- (1977) : 'Reproduction'. (Butterworths: London.)

Cooper, G.W. & Bedford, J.M. (1976) : Assymmetry of spermiation and sperm surface charge patterns over the giant acrosome in the musk shrew *Suncus murinus*. *J. Cell Biol.* 69, 415-428.

Courtens, J.L. & Fournier-Delpech, S. (1979) : Modifications in the plasma membranes of epididymal ram spermatozoa during maturation and incubation *in utero*. *J. Ultrastruct. Res.* 68, 136-148.

Crofton, H.D. (1966) : 'Nematodes'. (Hutchinson University Library: London.)

Croll, N.A. (1976) : The location of parasites within their hosts: the influence of host feeding and diet on the dispersion of adults of *Nippostrongylus brasiliensis* in the intestine of the rat. *Int. J. Parasitol.* 6, 441-448.

Croll, N.A. & Ma, K. (1978) : The location of parasites within their hosts: the passage of *Nippostrongylus brasiliensis* through the lungs of the laboratory rat. *Int. J. Parasitol.* 8, 289-296.

Croll, N.A. & Wright, K.A. (1976) : Observations on the movements and structure of the bursa of *Nippostrongylus brasiliensis* and *Nematospiroides dubius*. *Can. J. Zool.* 54, 1466-1480.

Cross, J.H.Jr. (1960) : The natural resistance of the white rat to *Nematospiroides dubius* and the effect of cortisone on this resistance. *Exp. Parasitol.* 46, 175-185.

Dallai, R., Baccetti, B., Bernini, F., Bigliardi, E., Burrini, A.G., Giusti, F., Mazzini, M., Pallini, V., Renieri, T., Rosati, F., Selmi, G. & Vegni, M. (1975) : New models of aflagellate arthropod spermatozoa. In 'The Functional Anatomy of the Spermatozoon'. pp.279-287. Ed. B.A. Afzelius. (Pergamon Press: Oxford.)

Danon, D., Goldstein, L., Marikovsky, Y. & Skutelsky, E. (1972) : Use of cationized ferretin as a label of negative charges on cell surfaces. *J. Ultrastruct. Res.* 38, 500-510.

Dazzo, F.B. (1980) : Lectins and their saccharide receptors as determinants of specificity in the *Rhizobium* - legume symbiosis. In 'The Cell Surface: Mediator of Developmental Processes'. pp.277-304. Eds. S. Subtelny and N.K. Wessells. (Academic Press: New York.)

Deguchi, N., Jørgensen, P.L. & Maunsbach, A.B. (1977) : Ultrastructure of the sodium pump. Comparison of thin sectioning negative staining and freeze-fracture of purified membrane-bound (Na^+/K^+)-ATPase. *J. Cell Biol.* 75, 619-634.

del Pino, E.J., Cabado, M.O. & Fonio, M.C. (1981) : Lectin-mediated sperm agglutination of *Bufo arenarum* and *Leptodactylus chaquensis* spermatozoa. *Gamete Res.* 4, 97-104.

Denburg, J.L. (1978) : The biochemistry of intercellular recognition. *Adv. Comp. Physiol. & Biochem.* 7, 105-226.

Dick, T.A. & Wright, K.A. (1974) : The ultrastructure of the cuticle of the nematode *Syphacia obvelata* (Rudolphi, 1802). III. Cuticle associated with the male reproductive structures. *Can. J. Zool.* 52, 179-182.

Dobson, C. (1982) : Passive transfer of immunity with serum in mice infected with *Nematospiroides dubius*: influence of quality and quantity of immune serum. *Int. J. Parasitol.* 12, 207-213.

Dobson, C. & Owen, M.E. (1978) : Effect of host sex on passive immunity in mice infected with *Nematospiroides dubius*. *Int. J. Parasitol.* 8, 359-364.

Dooher, G.B. (1981) : Differences in the rate of redistribution of receptors for concanavalin A *in vivo* and *in vitro* on spermatozoa from normal mice and from sterile mice carrying different T/t locus haplotypes. *Gamete Res.* 4, 105-111.

Downey, N.E. & Connolly, J.F. (1963) : A method for the enumeration of Trichostrongylid third stage larvae. *J. Helminthol.* 37, 255-260.

Durette-Desset, M.C. (1968) : Identification des Strongles des mulots de campagnols décrits par Dujardin. *Ann. de Parasitol. (Paris)* 43, 387-404.

Edelman, G.M. & Millette, C.F. (1971) : Molecular probes of spermatozoon structures. *Proc. Nat. Acad. Sci.* 68, 2436-2440.

Ehrenford, F.A. (1954) : The life cycle of *Nematospiroides dubius* Baylis (Nematoda : Heligmosomidae). *J. Parasitol.* 40, 480-481.

Enders, G., Werb, Z. & Friend, D.S. (1981) : Lectin binding to sperm zipper particles. *J. Cell Biol.* 91, 116a.

Englander, L.L. (1980) : Human leukocyte locomotion: cytoplasmic flow and contacts with the substratum. *J. Cell Biol.* 87, 89a.

Fahmy, M.A.M. (1956) : An investigation on the life cycle of *Nematospiroides dubius* (Nematoda : Heligmosomidae) with special reference to the free-living stages. *Z.f. Parasitenkunde.* 17, 394-399.

Favard, P. (1961) : Evolution des ultrastructures cellulaires au cours de la spermatogenese de l'*Ascaris*. *Ann. Sc. Nat. Zool.* 3, 53-152.

Fawcett, D.W. (1961) : Intercellular-bridges. *Exp. Cell Res.* Supp.8, 174-187.

- (1975a) : Gametogenesis in the male: prospects for its control. In 'Developmental Biology of Reproduction'. pp.25-53. Eds. C.L. Markert and J. Papaconstantinou. (Academic Press: New York.)

- (1975b) : The mammalian spermatozoon. *Dev. Biol.* 44, 394-436.

Feltkamp, C.A. & van der Waerden, A.W.M. (1982) : Low temperature-induced displacement of cholesterol and intramembrane particles in nuclear membranes of mouse leukemia cells. *Cell Biol. Intern. Reports* 6, 137-145.

Findlay, J.B.C. (1974) : The receptor proteins for ConA and *Lens culinaris* phytohemagglutinin in the membrane of the human erythrocyte. *J. Biol. Chem.* 249, 4398-4403.

Fisher, K.A. & Stoeckenius, W. (1977) : Freeze-fractured purple membrane particles: protein content. *Science* 197, 72-74.

Fitzgerald, L.A. & Foor, W.E. (1979) : *Ascaris suum*: electrophoretic characterization of reproductive tract and perienteric fluid polypeptides and effects of seminal and uterine fluids on spermiogenesis. *Exp. Parasitol.* 47, 313-326.

Flanagan, J. & Koch, G.L.E. (1978) : Cross-linked surface Ig attaches to actin. *Nature* 273, 278-281.

Fléchon, J-E. (1974) : Freeze-fracturing of rabbit spermatozoa. *J. Microscopie* 19, 59-64.

- (1979) : Sperm glycoproteins of the boar, bull, rabbit and ram: II Surface glycoproteins and free acidic groups. *Gamete Res.* 2, 53-64.

Foor, W.E. (1967) : Ultrastructural aspects of oocyte development and shell formation in *Ascaris lumbricoides*. *J. Parasitol.* 53, 1245-1261.

- (1968) : Zygote formation in *Ascaris lumbricoides* (Nematoda). *J. Cell Biol.* 39, 119-134.

- (1970) : Spermatozoan morphology and zygote formation in Nematodes. *Biol. Reprod.* Suppl.2, 177-202.

- (1973) : Action of the glandular vas deferens in the nematode *Ascaris lumbricoides*. *31st. Ann. Proc. Elect. Micr. Soc. Amer.* p.177.

- (1974) : Morphological changes of spermatozoa in the uterus and glandular vas deferens of *Brugia pahangi*. *J. Parasitol.* 60, 125-133.

- (1976) : Structure and function of the glandular vas deferens in *Ascaris suum* (Nematoda). *J. Parasitol.* 62, 849-864.

Foor, W.E., Johnson, M.H. & Beaver, P.C. (1971) : Morphological changes of spermatozoa of *Dipetalonema viteae in utero*. *J. Parasitol.* 57, 1163-1169.

Foor, W.E. & McMahon, J.T. (1973) : Role of the glandular vas deferens in the development of *Ascaris* spermatozoa. *J. Parasitol.* 59, 753-758.

Forrester, D.J. (1971) : *Heligmosomoides polygyrus* (= *Nematospiroides dubius*) from wild rodents of northern California: natural infections, host specificity and strain characteristics. *J. Parasitol.* 57, 498-503.

Franzén, A. (1956) : On spermiogenesis, morphology of the spermatozoon, and biology of fertilization among invertebrates. *Zool. Bidr, Uppsala* 31, 355-482.

Friend, D.S. (1977) : The organization of the spermatozoal membrane. In 'Immunobiology of Gametes'. pp.5-30. Eds. M. Edidin and M.H. Johnson. (Cambridge University Press: Cambridge.)

Friend, D.S. & Fawcett, D.W. (1974) : Membrane differentiations in freeze-fractured mammalian sperm. *J. Cell Biol.* 63, 641-664.

Friend, D.S., Galle, J. & Silber, S. (1976) : Fine structure of human sperm, vas deferens epithelium, and testicular biopsy specimens at the time of vasectomy reversal. *Anat. Rec.* 184, 584.

Friend, D.S., Orci, L., Perrelet, A. & Yanagimachi, R. (1977) : Membrane particle changes attending the acrosome reaction in guinea pig spermatozoa. *J. Cell Biol.* 74, 561-577.

Friend, D.S. & Rudolf, I. (1974) : Acrosomal disruption in sperm. Freeze fracture of altered membranes. *J. Cell Biol.* 63, 466-479.

Gall, W.E., Millette, C.F. & Edelman, G.M. (1974) : Chemical and structural analysis of mammalian spermatozoa. In 'Physiology and Genetics of Reproduction'. Part A pp.241-257. Eds. E.M. Coutinho, F. Fuchs. (Plenum Press: New York.)

Gasic, G.J., Berwick, L. & Sorrentino, M. (1968) : Positive and negative colloidal iron as cell surface electron stains. *Lab. Invest.* 18, 63-71.

Glabe, C.G., Grabel, L.B., Vacquier, V.D. & Rosen, S.D. (1982) : Carbohydrate specificity of sea urchin sperm bindin: a cell surface lectin mediating sperm-egg adhesion. *J. Cell Biol.* 94, 123-128.

Glabe, C.G. & Vacquier, V.D. (1977) : Species specific agglutination of eggs by bindin isolated from sea urchin sperm. *Nature* 267, 836-838.

Glaser, L. (1980) : From cell adhesion to growth control. In 'The Cell Surface: Mediator of Developmental Processes'. pp.79-97. Eds. S. Subtelny and N.K. Wessells. (Academic Press: New York.)

Glassburg, G.H., Zalisko, E. & Bone, L.W. (1981) : *In vivo* pheromone activity in *Nippostrongylus brasiliensis* (Nematoda). *J. Parasitol.* 67, 898-905.

Glauert, A.M. (1974) : Fixation, dehydration and embedding of biological specimens. In 'Practical Methods in Electron Microscopy'. Volume 3. pp.1-207. Ed. A.M. Glauert. (Nth-Holland Publ. Co.: Amsterdam.)

Goldstein, P. (1977) : Spermatogenesis and spermiogenesis in *Ascaris lumbricoides* var. *suum*. *J. Morph.* 154, 317-338.

Goldstein, P., & Triantaphyllou, A.C. (1980) : The ultrastructure of sperm development in the plant-parasitic nematode *Meloidogyne hapla*. *J. Ultrastruct. Res.* 71, 143-153.

Gordon, M., Dandekar, P.V. & Bartoszewicz, W. (1975) : The surface coat of epididymal, ejaculated and capacitated sperm. *J. Ultrastruct. Res.* 50, 199-207.

Gottschalk, A. & Drzeniek, R. (1972) : Neuraminidase as a tool in structural analysis. In 'Glycoproteins. Their Composition, Structure and Function'. Part A. p.381-402. Ed. A. Gottschalk. (Elsevier: Amsterdam.)

Grant, W.C., Harkem, A.R. & Muse, K.E. (1976) : Ultrastructure of *Pharyngostomoides procyonis* Harkem 1942 (Diplostomatidae). I Observations on the male reproductive system. *J. Parasitol.* 62, 39-49.

Green, C.R. (1981) : Fixation-induced intramembrane particle movement demonstrated in freeze-fracture replicas of a new type of septate junction in Echinoderm epithelia. *J. Ultrastruct. Res.* 75, 11-22.

Greenaway, P.J. & Levine, D. (1973) : Binding of N-acetyl neuraminic acid by wheatgerm agglutinin. *Nature New Biol.* 241, 191-192.

Gress, F.M. & Lumsden, R.D. (1976) : Ultrastructural cytochemistry of the tegumental surface membrane of *Paragonimus kellicotti*. *Rice Univ. Studies: Studies in Parasitology* 62, 111-143.

Grevengood, C., Lande, M.A. & Foor, W.E. (1981) : *In vitro* culture of *Ascaris suum* tissues. *Proc. 56th Ann. Meeting, Amer. Soc. Parasitol.* p.52.

Gros, D., Potreau, D. & Mocquard, J-P. (1980) : The myocardial plasma membrane during development: influence of glutaraldehyde fixation on the density and size of intramembranous particles. *J. Cell Sci.* 43, 301-317.

Haley, A.J. (1961) : Biology of the rat nematode *Nippostrongylus brasiliensis* (Travassos 1914). I Systematics, hosts and geographic distribution. *J. Parasitol.* 47, 727-732.

- (1962) : Biology of the rat nematode *Nippostrongylus brasiliensis* (Travassos 1914). II Preparasitic stages and development in the laboratory rat. *J. Parasitol.* 48, 13-23.

Haley, A.J. & Parker, J.C. (1961) : Size of adult *Nippostrongylus brasiliensis* from light and heavy infections in laboratory rats. *J. Parasitol.* 47, 461.

Halton, D.W. & Hardcastle, A. (1976) : Spermatogenesis in a monogenean, *Diclidophora merlangi*. *Int. J. Parasitol.* 6, 43-53.

Harada, R., Maeda, T., Nakashima, A., Sadakata, Y., Ando, M., Yonamine, K., Otsuji, Y. & Sato, H. (1970) : Electronmicroscopical studies on the mechanism of oogenesis and fertilization in *Dirofilaria immitis*. In 'Recent Advances in Researches on Filariasis and Schistosomiasis in Japan'. pp.99-121. Ed. M. Sasa. (Univ. of Tokyo Press & Univ. Park Press.)

Harding, H.R., Carrick, F.N. & Shorey, C.D. (1981) : Marsupial phylogeny: new indications from sperm ultrastructure and development in *Tarsipes spenserae*? *Search* 12, 45-47.

Hasty, D.L. & Hay, E.D. (1978) : Freeze-fracture studies of the developing cell surface. II Particle-free membrane blisters on glutaraldehyde-fixed corneal fibroblasts are artefacts. *J. Cell Biol.* 78, 756-768.

Hertwig, O. (1890) : Vergleich der Ei und Samenbilslung bei Nematoden. *Archiv. Mikros. Anat.* 36, 1-38.

Himmelhoch, S., Kisiel, M.J. & Zuckerman, B.M. (1977) : *Caenorhabditis briggsiae*: electron microscope analysis of changes in negative surface charge density of the outer cuticular membrane. *Exp. Parasitol.* 41, 118-123.

Himmelhoch, S. & Zuckerman, B.M. (1978) : *Caenorhabditis briggsiae*: aging and the structural turnover of the outer cuticle surface and the intestine. *Exp. Parasitol.* 45, 208-214.

Holt, W.V. (1980) : Surface bound sialic acid on ram and bull spermatozoa: deposition during epididymal transit and stability during washing. *Biol. Reprod.* 23, 847-857.

Hong, K. & Hubbell, W.L. (1972) : Preparation and properties of phospholipid bilayers containing rhodopsin. *Proc. Natl. Acad. Sci.* 69, 2617-2621.

Hope, W.D. (1974) : Nematoda. In 'Reproduction in Marine Invertebrates'. Volume I. pp.391-469. Ed. A.C. Giese. (Academic Press: New York.)

Horisberger, M. & Rosset, J. (1977) : Colloidal gold, a useful marker for transmission and scanning electron microscopy. *J. Histochem. Cytochem.* 25, 295-305.

Huet, C.H. & Herzberg, M. (1973) : Effect of enzymes and EDTA on ruthenium red and concanavalin A labelling of the cell surface. *J. Ultrastruct. Res.* 42, 186-199.

Hughes, R.C. (1975) : The complex carbohydrates of mammalian cell surfaces and their biological roles. In 'Essays in Biochemistry'. Volume II. pp.1-36. Eds. P.N. Campbell and W.N. Aldridge. (Academic Press: London.)

Hughes, R.L. (1965) : Comparative morphology of spermatozoa from five marsupial families. *Aust. J. Zool.* 13, 533-543.

Jakoi, E.R., Marchase, R.B. & Reedy, M.C. (1981) : Distribution of anionic sites on surfaces of retinal cells: a study using cationized ferretin. *J. Ultrastruct. Res.* 76, 96-106.

Jamuar, M.P. (1966) : Studies of the spermiogenesis in a nematode, *Nippostrongylus brasiliensis*. *J. Cell Biol.* 31, 381-396.

Jones, R.C. (1975) : Fertility and infertility in mammals in relation to sperm structure. In 'Biology of the Male Gamete'. pp.343-365. Eds. J.G. Duckett and P.A. Racey. (Academic Press: London.)

Jordan, F., Bassett, E. & Redwood, W.R. (1977) : Proton magnetic resonance studies on wheat germ agglutinin - amino sugar interaction. Evidence for involvement of a tryptophan residue in the binding process. *Biochem. Biophys. Res. Commun.* 75, 1015-1021.

Kabat, E.A. (1978) : Dimensions and specificities of recognition sites on lectins and antibodies. *J. Supramolec. Struct.* 8, 79-88.

Kachar, B., Serrano, J.A. & Pinto da Silva, P. (1980) : Particle displacement in epithelial cell membranes of rat prostate and pancreas induced by routine low temperature fixation. *Cell Biol. Int. Reports* 4, 347-356.

Kaulenas, M.S. & Fairbairn, D. (1968) : RNA metabolism of fertilized *Ascaris lumbricoides* eggs during uterine development. *Exp. Cell Res.* 52, 233-251.

Keller, H.U., Wissler, J.H., Hess, M.W. & Cottier, H. (1978) : Distinct chemokinetic and chemotactic responses in neutrophil granulocytes. *Eur. J. Immunol.* 8, 1-7.

Kimble, J.E. & White, J.G. (1981) : On the control of germ cell development in *Caenorhabditis elegans*. *Dev. Biol.* 81, 208-219.

Kinsey, W.H. & Koehler, J.K. (1976) : Fine structural localization of Concanavalin A binding sites on hamster spermatozoa. *J. Supramol. Struct.* 5, 185-198.

- (1978) : Cell surface changes associated with *in vitro* capacitation of hamster sperm. *J. Ultrastruct. Res.* 64, 1-13.

Klass, M.R. & Hirsh, D. (1981) : Sperm isolation and biochemical analysis of the major sperm protein from *Caenorhabditis elegans*. *Dev. Biol.* 84, 299-312.

Koehler, J.K. (1966) : Fine structure observations in frozen-etched bovine spermatozoa. *J. Ultrastruct. Res.* 16, 359-375.

- (1970) : A freeze-etching study of rabbit spermatozoa with particular reference to head structures. *J. Ultrastruct. Res.* 33, 598-614.

- (1972) : Human sperm ultrastructure: a freeze-etching study. *J. Ultrastruct. Res.* 39, 520-539.

- (1973) : Studies on the structure of the postnuclear sheath of water buffalo spermatozoa. *J. Ultrastruct. Res.* 44, 355-368.

- (1976) : Changes in antigenic site distribution on rabbit spermatozoa after incubation in 'capacitating' media. *Biol. Reprod.* 15, 444-456.

- (1978) : The mammalian sperm surface: studies with specific labelling techniques. *Int. Rev. Cytol.* 54, 73-108.

- (1981) : Lectins as probes of the spermatozoon surface. *Arch. Androl.* 6, 197-217.

Koehler, J.K. & Gaddum-Rosse, P. (1975) : Media induced alterations of the membrane associated particles of the guinea-pig sperm tail. *J. Ultrastruct. Res.* 51, 106-118.

Koehler, J.K. & Kinsey, W.H. (1977) : Changes in sperm membrane structure during capacitation: a brief review. *Scanning Electron Microscopy* 2, 325-332.

Koehler, J.K. & Sato, K. (1978) : Changes in lectin labelling pattern of mouse spermatozoa accompanying capacitation and the acrosome reaction. *J. Cell Biol.* 79, 165a.

Kuby, J.M. & Wofsy, L. (1981) : Intramembrane particles and the organization of lymphocyte membrane proteins. *J. Cell Biol.* 88, 591-598.

Labat, J. & Schmid, K. (1969) : Neuraminidase resistant sialyl residues of α_1 - acid glycoprotein. *Experientia* 25, 701.

Lane, C. (1923) : Some strongylata. *Parasitol.* 15, 348-364.

Lee, D.L. (1969a) : Changes in adult *Nippostrongylus brasiliensis* during the development of immunity to this nematode in rats. *Parasitol.* 59, 29-39.

- (1969b) : *Nippostrongylus brasiliensis*: some aspects of the fine structure and biology of the infective larva and the adult. *Symp. British Soc. for Parasitol.* 7, 3-16.

- (1971) : The structure and development of the spermatozoon of *Heterakis gallinarum* (Nematoda). *J. Zool. Lond.* 164, 181-187.

- (1973) : Evidence for a sensory function for the copulatory spicules of nematodes. *J. Zool. Lond.* 169, 281-285.

Lee, D.L. & Anya, A.O. (1967) : The structure and development of the spermatozoan of *Aspiculuris tetraptera* (Nematoda). *J. Cell Sci.* 2, 537-544.

Lee, D.L. & Lestan, P. (1971) : Oogenesis and egg shell formation in *Heterakis gallinarum* (Nematoda). *J. Zool. Lond.* 164, 189-196.

Lewin, L.M., Weissenburg, R., Sobel, J.S., Marcus, Z. & Nebel, L. (1979) : Differences in Concanavalin A - FITC binding to rat spermatozoa during epididymal maturation and capacitation. *Arch. Androl.* 2, 279-281.

Lin, D.C., Tobin, K.D., Grumet, M. & Lin, S. (1980) : Cytochalasins inhibit nuclei-induced actin polymerization by blocking filament elongation. *J. Cell Biol.* 84, 455-460.

Lis, H. & Sharon, N. (1977) : Lectins: their chemistry and application to immunology. In 'The Antigens'. Volume 4. pp.429-529. Ed. M. Sela. (Academic Press: New York.)

Liu, S-K. (1965a) : Pathology of *Nematospiroides dubius*. I Primary infections in C_3H and Webster mice. *Exp. Parasitol.* 16, 123-135.

- (1965b) : Pathology of *Nematospiroides dubius*. II Reinfections in Webster mice. *Exp. Parasitol.* 17, 136-147.

Locke, M., Krishnan, N. & McMahon, J.T. (1971) : A routine method for obtaining high contrast without staining sections. *J. Cell Biol.* 50, 540-544.

Lucker, J.T. (1936) : Preparasitic moults in *Nippostrongylus muris*, with remarks on the structure of the cuticula of trichostrongyles. *Parasitol.* 28, 161-171.

Luft, J.H. (1971a) : Ruthenium Red and Violet. I Chemistry, purification, methods of use for electron microscopy and mechanism of action. *Anat. Rec.* 171, 347-368.

Maeda, T., Harada, R., Nakashima, A., Sadakata, Y., Ando, M., Yonamine, K., Otsuji, Y. & Sato, H. (1970) : Electron microscopic studies on spermatogenesis in *Dirofilaria immitis*. In 'Recent Advances in Researches on Filariasis and Schistosomiasis in Japan.' pp.73-97. Ed. M. Sasa. (Univ. of Tokyo Press & Univ. Park Press.)

Meek, G.A. (1970) : 'Practical Electron Microscopy for Biologists.' (John Wiley & Sons Ltd: London.)

Millette, C.F. (1977) : Distribution and mobility of lectin binding sites on mammalian spermatozoa. In 'Immunobiology of Gametes'. pp.51-71. Eds. M. Edidin and M.H. Johnson. (Cambridge University Press: Cambridge.)

Montal, M. (1974) : Lipid-protein assembly and the reconstitution of biological membranes. In 'Perspectives in Membrane Biology'. pp.591-622. Eds. S. Estrada-O and M. Gilter. (Academic Press: New York.)

Montesano, R., Didier, P. & Orci, L. (1981) : The ciliary junction: a unique membrane specialization in the ciliate, *Glaucoma ferox*. *J. Ultrastruct. Res.* 77, 360-365.

Moy, G.W. & Vacquier, V.D. (1979) : Immunoperoxidase localization of bindin during the adhesion of sperm to sea urchin eggs. *Curr. Top. Dev. Biol.* 13, 31-44.

Myles, D.G., Primakoff, P. & Bellvé, A.R. (1980) : Establishment and maintenance of cell surface domains of the guinea pig sperm. *J. Cell Biol.* 87, 99a.

Neill, B.W. & Wright, K.A. (1973) : Spermatogenesis in the hologonic testes of the trichuroid nematode *Capillaria hepatica* (Bancroft 1893). *J. Ultrastruct. Res.* 44, 210-234.

Nelson, G.A., Roberts, T.M. & Ward, S. (1982) : *Caenorhabditis elegans* spermatozoon locomotion: amoeboid movement with almost no actin. *J. Cell Biol.* 92, 121-131.

Nelson, G.A. & Ward, S. (1980) : Vesicle fusion, pseudopod extension and amoeboid motility are induced in nematode spermatids by the ionophore monensin. *Cell* 19, 457-464.

- (1981) : Amoeboid motility and actin in *Ascaris lumbricoides* sperm. *Exp. Cell Res.* 131, 149-160.

Nevo, A.C., Michaeli, I. & Schindler, H. (1961) : Electrophoretic properties of bull and of rabbit spermatozoa. *Exp. Cell Res.* 23, 69-83.

Nicolson, G.L. (1973) : Neuraminidase 'unmasking' and failure of trypsin to 'unmask' β-D-galactose-like sites on erythrocyte, lymphoma and normal and virus-transformed fibroblast cell membranes. *J. Natl. Cancer Inst.* 50, 1443-1451.

Nicolson, G.L. (1974) : The interactions of lectins with animal cell surfaces. *Int. Rev. Cytol.* 39, 89-190.

Nicolson, G.L., Lacorbiere, M. & Yanagimachi, R. (1972) : Quantitative determination of plant agglutinin membrane sites on mammalian spermatozoa. *Proc. Soc. Exp. Biol. Med.* 141, 661-663.

Nicolson, G.L., Poste, G. & Ji, T.H. (1977) : The dynamics of cell membrane organization. *Cell Surface Reviews* 3, 1-73.

Nicolson, G.L., Usui, N., Yanagimachi, R., Yanagimachi, H. & Smith, J.R. (1977) : Lectin-binding sites on the plasma membranes of rabbit spermatozoa. Changes in surface receptors during epididymal maturation and after ejaculation. *J. Cell Biol.* 74, 950-962.

Nicolson, G.L. & Yanagimachi, R. (1972) : Terminal saccharides on sperm plasma membranes: identification by specific agglutinins. *Science* 177, 276-279.

Nicolson, G.L., Yanagimachi, R. & Yanagimachi, H. (1975) : Ultrastructural localization of lectin-binding sites on the zonae pellucidae and plasma membranes of mammalian eggs. *J. Cell Biol.* 66, 263-274.

Ogilvie, B.M. & Hockley, D.J. (1968) : Effects of immunity on *Nippostrongylus brasiliensis* adult worms: reversible and irreversible changes in infectivity, reproduction and morphology. *J. Parasitol.* 54, 1073-1084.

Ogilvie, B.M. & Jones, V.E. (1971) : *Nippostrongylus brasiliensis*: a review of immunity and the host/parasite relationship in the rat. *Exp. Parasitol.* 29, 138-177.

Ogilvie, B.M. & Love, R.J. (1974) : Co-operation between antibodies and cells in immunity to a nematode parasite. *Transplant. Rev.* 19, 147-168.

Oikawa, T., Yanagimachi, R. & Nicolson, G.L. (1973) : Wheat germ agglutinin blocks mammalian fertilization. *Nature* 241, 256-259.

Olson, G.E. & Danzo, B.J. (1981) : Surface changes in rat spermatozoa during epididymal transit. *Biol. Reprod.* 24, 431-443.

Olson, G.E. & Hamilton, D.W. (1978) : Characterization of the surface glycoproteins of rat spermatozoa. *Biol. Reprod.* 19, 26-35.

Olson, G.E., Lifsics, M., Fawcett, D.W. & Hamilton, D.W. (1977) : Structural specializations in the flagellar plasma membrane of opposum spermatozoa. *J. Ultrastruct. Res.* 59, 207-221.

Olson, G.E. & Linck, R.W. (1980) : Membrane differentiations in spermatozoa of the squid, *Loligo pealeii*. *Gamete Res.* 3, 329-342.

Panter, H.C. (1969) : Host-parasite relationships of *Nematospiroides dubius* in the mouse. *J. Parasitol.* 55, 33-37.

Pasternak, J. & Samoiloff, M.R. (1972) : Cytoplasmic organelles present during spermatogenesis in the free living nematode *Panagrellus silusiae*. *Can. J. Zool.* 50, 147-151.

Pedersen, H. (1972a) : The post acrosomal region of the spermatozoa of man and *Macaca arctoides*. *J. Ultrastruct. Res.* 40, 366-377.

- (1972b) : Further observations on the fine structure of the human spermatozoon. *Z. Zellforsch.* 123, 305-315.

Phillips, D.M. (1974) : 'Spermiogenesis'. (Academic Press: New York.)

Phillipson, R.F. (1969) : Reproduction of *Nippostrongylus brasiliensis* in the rat intestine. *Parasitol.* 59, 961-971.

Phillipson, R.F. (1970) : Experiments on the reproduction of *Nippostrongylus brasiliensis* in the rat intestine. *Parasitol.* 61, 317-322.

- (1973) : Extrinsic factors affecting the reproduction of *Nippostrongylus brasiliensis*. *Parasitol.* 66, 405-413.

Pinto da Silva, P., Kachar, P., Torrisi, M.R., Brown, C. & Parkison, C. (1981) : Freeze-fracture cytochemistry: replicas of critical point dried cells and tissues after fracture label. *Science* 215, 230-233.

Pinto da Silva, P. & Martinez-Palomo, A. (1974) : Induced redistribution of membrane particles, anionic sites and ConA receptors in *Entamoeba histolytica*. *Nature* 249, 170-171.

Pinto da Silva, P. & Nicolson, G.L. (1974) : Freeze-etch localization of concanavalin A receptors to the membrane intercalated particles of human erythrocyte ghost membranes. *Biochim. Biophys. Acta* 363, 313-319.

Pinto da Silva, P., Torrisi, M.R. & Kachar, B. (1981) : Freeze-fracture cytochemistry: localization of wheat germ agglutinin and Concanavalin A binding sites on freeze-fractured pancreatic cells. *J. Cell Biol.* 91, 361-372.

Plattner, H., Miller, F. & Bachmann, L. (1973) : Membrane specializations in the form of regular membrane-to-membrane attachment sites in *Paramecium*. A correlated freeze-etching and ultrathin-sectioning analysis. *J. Cell Sci.* 13, 687-719.

Pollard, T.D., Fujiwara, K., Niederman, R. & Maupin-Szamier, (1976) : Evidence for the role of cytoplasmic actin and myosin in cellular structure and motility. In 'Cell Motility'. Book B. pp.689-724. Eds. R. Goldman, T. Pollard and J. Rosenbaum. (Cold Spring Harbour Laboratory.)

Pollard, T.D. & Maupin, P. (1978) : Electron microscopy of cytoplasmic contractile proteins. *9th Int. Congr. on Elect. Micros.* 3, 606-614.

Porter, D.A. (1935) : Studies on the pathology of *Nippostrongylus muris* in rats and mice. *J. Parasitol.* 21, 226-228.

Prestage, J.J. (1960) : The fine structure of the growth region of the ovary of *Ascaris lumbricoides* var. *suum* with special reference to the rachis. *J. Parasitol.* 46, 69-78.

Prowse, S.J., Ey, P.L. & Jenkin, C.R. (1978) : Immunity to *Nematospiroides dubius*: cell and immunoglobulin changes associated with the onset of immunity in mice. *Ajebak* 56, 237-246.

Pryzwansky, K.B., Schliwa, M. & Porter, K.R. (1981) : Visualization of the three-dimensional organization of human polymorphonuclear leukocytes (PMNL). *J. Cell Biol.* 91, 293a.

Railliet, A. & Henry, A. (1909) : Sur classification des *Strongylidae* et *Metastrongylidae*. *C.R. Soc. Biol.* 66, 85-88.

Ramsey, W.S. (1974) : Leucocyte locomotion and chemotaxis. *Antibiotics & Chemotherapy* 19, 179-190.

Reger, J.F. (1974) : The origin and fine structure of cellular processes in spermatozoa of the tick *Dermacentor andersoni*. *J. Ultrastruct. Res.* 48, 420-434.

Reger, J.F. & Fitzgerald, M.E. (1979) : The fine structure of membrane complexes in spermatozoa of the millipede, *Spirobolus* sp., as seen by thin-section and freeze-fracture techniques. *J. Ultrastruct. Res.* 67, 95-108.

Reger, J.F., Itaya, P.W. & Fitzgerald, M.E. (1979) : A thin section and freeze-fracture study on membrane specializations in spermatozoa of the Isopod *Armadillidium vulgare*. *J. Ultrastruct. Res.* 67, 180-193.

Reynolds, E.S. (1963) : The use of lead citrate at high pH as an electron-opaque stain in electron microscopy. *J. Cell Biol.* 17, 208-212.

Roberts, T.M. & Ward, S. (1982a) : Centripetal flow of pseudopodial surface components could propel the amoeboid movement of *Caenorhabditis elegans* spermatozoa. *J. Cell Biol.* 92, 132-138.

- (1982b) : Membrane flow during nematode spermiogenesis. *J. Cell Biol.* 92, 113-120.

Robertson, J.D. & Vergara, J. (1980) : Analysis of the structure of intramembrane particles of the mammalian urinary bladder. *J. Cell Biol.* 86, 514-528.

Rogers, W.P. & Lazarus, M. (1949) : The uptake of radioactive phosphorus from host tissues and fluids by nematode parasites. *Parasitol.* 39, 245-250.

Roosen-Runge, E.C. (1969) : Comparative aspects of spermatogenesis. *Biol. Reprod.* Supp.1, 24-39.

- (1977) : 'The Process of Spermatogenesis in Animals.' (Camb. Univ. Press: London.)

Rosati, F., de Santis, R. & Monroy, A. (1978) : Studies on fertilization in the Ascidians. II Lectin binding to the gametes of *Ciona intestinalis*. *Exp. Cell Res.* 116, 419-427.

Roth, J. (1978) : The lectins. Molecular probes in cell biology and membrane research. *Exp. Path.* Supp.3, 5-186.

Ryan, G.B., Borysenko, J.Z. & Karnovsky, M.J. (1974) : Factors affecting the redistribution of surface bound concanavalin-A on human polymorphonuclear leukocytes. *J. Cell Biol.* 62, 351-365.

Sabatini, D.D., Kreibich, G., Morimoto, T. & Adesnik, M. (1982) : Mechanisms for the incorporation of proteins in membranes and organelles. *J. Cell Biol.* 92, 1-22.

Sandoz, D., Boisvieux-Ulrich, E. & Chailley, B. (1979) : Relationships between intramembrane particles and glycoconjugates in the ciliary membrane of the quail oviduct. *Biol. Cell.* 36, 267-280.

Schmell, E., Earles, B.J., Breaux, C. & Lennarz, W.J. (1977) : Identification of a sperm receptor on the surface of the eggs of the sea urchin *Arbacia punctulata*. *J. Cell Biol.* 72, 35-46.

Schwartz, B. & Alicata, J. (1934) : The development of the trichostrongyle, *Nippostrongylus muris* in rats following ingestion of larvae. *J. Wash. Acad. Sci.* 24, 334-338.

Schwarz, M.A. & Koehler, J.K. (1979) : Alterations in lectin binding to guinea pig spermatozoa accompanying *in vitro* capacitation and the acrosome reaction. *Biol. Reprod.* 21, 1295-1307.

Scott, T.W., Voglmayr, J.K. & Setchell, B.P. (1967) : Lipid composition and metabolism in testicular and ejaculated ram spermatozoa. *Biochem. J.* 102, 456-461.

Seagull, R.W. & Heath, I.B. (1979) : The effects of tannic acid on the *in vivo* preservation of microfilaments. *Eur. J. Cell Biol.* 20, 184-188.

SeGall, G.K. & Lennarz, W.J. (1979) : Chemical characterization of the component of the jelly coat from sea urchin eggs responsible for induction of the acrosome reaction. *Dev. Biol.* 71, 33-48.

Segrest, J.P., Gulik-Krzywicki, T. & Sardet, C. (1974) : Association of the membrane-penetrating polypeptide segment of the human erythrocyte MN-glycoprotein with phospholipid bilayers. I Formation of freeze-etch intramembranous particles. *Proc. Natl. Acad. Sci.* 71, 3294-3298.

Senda, N., Tamura, H., Shibata, N., Yoshitake, J., Kondo, K. & Tanaka, K. (1975) : Mechanism of movement of leucocytes. *Exp. Cell Res.* 91, 393-407.

Setchell, B.P. (1978) : 'The Mammalian Testis.' (Paul Elek: London.)

Sharon, N. & Lis, H. (1975) : Use of lectins for the study of membranes. In 'Methods in Membrane Biology'. Volume 3. pp.147-200. Ed. E.D. Korn. (Plenum Press: New York.)

Shepherd, A.M. (1981) : Interpretation of sperm development in nematodes. *Nematologica* 27, 122-125.

Shepherd, A.M. & Clark, S.A. (1976) : Spermatogenesis and the ultrastructure of sperm and the male reproductive tract of *Aphelenchoides blastophthorus* (Nematoda : Tylenchida, Aphelenchina). *Nematologica* 22, 1-9.

- (1977) : Sperm and male reproductive tract of *Rhabditis oxycerca*. In 'Report of Rothamsted Experimental Station for 1976'. p.206. Ed. F.G.W. Jones.

- (1979) : Spermatogenesis and sperm structure. In 'Report of the Rothamsted Experimental Station for 1978'. p.183. Ed. F.G.W. Jones.

- (1980) : Ultrastructure of nematode sperm. In 'Report of the Rothamsted Experimental Station for 1979'. p.141. Ed. A.R. Stone.

Shepherd, A.M., Clark, S.A. & Kempton, A. (1974) : Spermatogenesis and sperm ultrastructure in some cyst nematodes, *Heterodera* spp. *Nematologica* 19, 551-560.

Shotton, D., Thompson, K., Wofsy, L. & Branton, D. (1978) : Appearance and distribution of surface proteins of the human erythrocyte membrane. *J. Cell Biol.* 76, 512-531.

Shure, M.S. (1980) : *In vivo* analysis of leukocyte movement in larvae of *Xenopus laevis*. *J. Cell Biol.* 87, 89a.

Simionescu, N. & Simionescu, M. (1976) : Galloylglucoses of low molecular weight as mordant in electron microscopy. I. Procedure and evidence for mordanting effect. *J. Cell Biol.* 70, 608-621.

Skrjabin, K.I. (1952) : 'Key to Parasitic Nematodes.' Vol.III. (Israel Program for Scientific Translations: Jerusalem.)

Sommerville, R.I. (1976) : Personal communication. Zoology Department. University of Adelaide.

Sommerville, R.I. & Bailey, M.A. (1973) : *Nematospiroides dubius*: exsheathment of infective juveniles. *Exp. Parasitol.* 33, 1-9.

Sommerville, R.I. & Weinstein, P.P. (1964) : Reproductive behaviour of *Nematospiroides dubius in vivo* and *in vitro*. *J. Parasitol.* 50, 401-409.

\- (1967) : The *in vitro* cultivation of *Nippostrongylus brasiliensis* from the late fourth stage. *J. Parasitol.* 53, 116-125.

Spurlock, G.M. (1943) : Observations on host-parasite relations between laboratory mice and *Nematospiroides dubius*, Baylis. *J. Parasitol.* 29, 303-311.

Stackpole, C.W. & Devorkin, D. (1974) : Membrane organization in mouse spermatozoa revealed by freeze-fracture. *J. Ultrastruct. Res.* 49, 167-187.

Staehelin, L.A. (1976) : Reversible particle movements associated with unstacking and restacking of chloroplast membranes *in vitro*. *J. Cell Biol.* 71, 136-158.

Stoolman, L.M. & Rosen, S.D. (1981) : The molecular basis of lymphocyte binding to high endothelial venules of lymph nodes. *J. Cell Biol.* 91, 81a.

Stossel, T.P., Hartwig, J.H., Yin, H.L. & Stendahl, O.I. (1980) : The motor of amoeboid leukocytes. In 'The Cell Surface: Mediator of Developmental Processes'. pp.9-21. Eds. S. Subtelny and N.K. Wessells. (Academic Press: New York.)

Subirana, J.A. (1975) : On the biological role of basic proteins in spermatozoa and during spermiogenesis. In 'The Biology of the Male Gamete'. pp.239-244. Eds. J.G. Duckett and P.A. Racey. (Academic Press: London.)

Suzuki, F. & Nagano, T. (1980) : Epididymal maturation of rat spermatozoa studied by thin sectioning and freeze-fracture. *Biol. Reprod.* 22, 1219-1231.

Symons, L.E.A. (1965) : Kinetics of the epithelial cells, and morphology of villi and crypts in the jejunum of the rat infected by the nematode *Nippostrongylus brasiliensis*. *Gastroenterology*. 49, 158-168.

Szubinska, B. & Luft, J.H. (1971) : Ruthenium Red and Violet. III Fine structure of the plasma membrane and extraneous coats in amoebae. *Anat. Rec.* 171, 417-442.

Talbot, P. & Chanmanon, P. (1980) : Morphological features of the acrosome reaction of the lobster (*Homarus*) sperm and the role of the reaction in generating forward sperm movement. *J. Ultrastruct. Res.* 70, 287-297.

Temple-Smith, P.D. & Bedford, J.M. (1976) : The features of sperm maturation in the epididymis of a marsupial, the brushtailed possum *Trichosurus vulpecula*. *Amer. J. Anat.* 147, 471-499.

Terner, C., Maclaughlin, J. & Smith, B.R. (1975) : Changes in lipase and phosphatase activities of rat spermatozoa in transit from the caput to the cauda epididymidis. *J. Reprod. Fert.* 45, 1-8.

Terry, A., Terry, R.J. & Worms, M.J. (1961) : *Dipetalonema witei*, filarial parasites of the jurd, *Meriones libycus*. II The reproductive system, gametogenesis and development of the microfilariae. *J. Parasitol.* 47, 703-711.

Tilney, L.G., Clain, J.G. & Tilney, M.S. (1979) : Membrane events in the acrosomal reaction of *Limulus* sperm. Membrane fusion, filament-membrane particle attachment, and the source and formation of new membrane surface. *J. Cell Biol.* 81, 229-253.

Tilney, L.G. & Mooseker, M.S. (1976) : Actin filament-membrane attachment: are membrane particles involved? *J. Cell Biol.* 71, 402-416.

Torpier, G. & Capron, A. (1980) : Intramembrane particle movements associated with binding of lectins on *Schistosoma mansonii* surface. *J. Ultrastruct. Res.* 72, 325-335.

Tourtellotte, M.E. & Zupnik, J.S. (1973) : Freeze-fractured *Acholeplasma laidlawii* membranes: nature of particles observed. *Science* 179, 84-86.

Travassos, L. & Darriba, A. (1929) : Notas sobre *Heligmosominae*. *Sc. Med.* 7, 432-438.

Ugwanna, S.C. & Foor, W.E. (1977) : Spermatogenesis in *Ancylostoma caninum*. *Proc. 52nd Ann. Meeting, Amer. Soc. Parasitologists* pp.31-32.

Vacquier, V.D. (1980) : The adhesion of sperm to sea urchin eggs. In 'The Cell Surface: Mediator of Developmental Processes'. pp. 151-168. Eds. S. Subtelny and N.K. Wessells. (Academic Press: New York.)

Luft, J.H. (1971b) : Ruthenium Red and Violet. II Fine structural localization in animal tissues. *Anat. Rec.* 171, 369-416.

- (1976) : The structure and properties of the cell surface coat. *Int. Rev. Cytol.* 45, 291-382.

Lumsden, R.D., Oaks, J.A. & Alworth, W.L. (1970) : Cytological studies on the absorptive surfaces of cestodes. IV Localization and cytochemical properties of membrane-fixed cation binding sites. *J. Parasitol.* 56, 736-747.

Lung, B. (1974) : Architecture of mammalian sperm: analysis by quantitative electron microscopy. In 'Advances in Cell and Molecular Biology'. Volume 3. pp.73-133. Ed. E.J. Du Praw. (Academic Press: New York.)

Lunger, P.D. (1971) : Early stages of spermatozoon development in the colonial hydroid *Campanularia flexuosa*. *Z. Zellforsch.* 116, 37-51.

MacLean-Fletcher, S. & Pollard, T.D. (1980) : Mechanism of action of cytochalasin B on actin. *Cell* 20, 329-341.

McLaren, D.J. (1973a) : The structure and development of the spermatozoan of *Dipetalonema viteae* (Nematoda : Filarioidea). *Parasitol.* 66, 447-463.

- (1973b) : Oogenesis and fertilization in *Dipetalonema viteae* (Nematoda : Filarioidea). *Parasitol.* 66, 465-472.

McMahon, J.T. & Foor, W.E. (1977) : The origin of microfilaments and acquisition of motility in *Ascaris* sperm. *J. Cell Biol.* 75, 260a.

McNutt, N.S. (1977) : Freeze-fracture techniques and applications to the structural analysis of the mammalian plasma membrane. *Cell Surface Reviews* 3, 75-126.

Maeda, T., Harada, R., Nakashima, A., Sadakata, Y., Ando, M., Yonamine, K., Otsuji, Y. & Sato, H. (1970) : Electron microscopic studies on spermatogenesis in *Dirofilaria immitis*. In 'Recent Advances in Researches on Filariasis and Schistosomiasis in Japan'. pp.73-97. Ed. M. Sasa. (University of Tokyo Press and University Park Press.)

Marchesi, V.T., Tillack, T.W., Jackson, R.L., Segrest, J.P. & Scott, R.E. (1972) : Chemical characterization and surface orientation of the major glycoprotein of the human erythrocyte membrane. *Proc. Natl. Acad. Sci.* 69, 1445-1449.

Martin, J. & Lee, D.L. (1980a) : Observations on the structure of the male reproductive system and spermatogenesis of *Nematodirus battus*. *Parasitol.* 81, 579-586.

- (1980b) : Changes in the structure of the male reproductive system of *Nematodirus battus* during its rejection from lambs. *Parasitol.* 81, 587-592.

van Beneden, E. (1883) : Recherches sur la fécondation et la maturation. *Archiv. Biol.* 4, 265-641.

Voglmayer, J.K., Fairbanks, G., Jackowitz, M.A. & Colella, J.R. (1980) : Post-testicular developmental changes in the ram sperm cell surface and their relationship to the luminal fluid proteins of the reproductive tract. *Biol. Reprod.* 22, 655-667.

Ward, S., Argon, Y. & Nelson, G.A. (1981) : Sperm morphogenesis in wild-type and fertilization-defective mutants of *Caenorhabditis elegans*. *J. Cell Biol.* 91, 26-44.

Ward, S. & Carrel, J.S. (1979) : Fertilization and sperm competition in the nematode *Caenorhabditis elegans*. *Dev. Biol.* 73, 304-321.

Ward, S., Hogan, E. & Nelson, G.A. : The initiation of *Caenorhabditis elegans* spermiogenesis *in vivo* and *in vitro*. Submitted for publication.

Ward, S. & Klass, M. : The location of the major protein in *C. elegans* sperm and spermatocytes. *Dev. Biol.* in press.

Ward, S., Roberts, T.M., Nelson, G.A. & Argon, Y. (1982) : The development and motility of *Caenorhabditis elegans* spermatozoa. *J. Nematol.* 14, 259-266.

Weinstein, P.P. & Jones, M.F. (1959) : Development *in vitro* of some parasitic nematodes of vertebrates. *Ann. N.Y. Acad. Sci.* 77, 137.

Wharton, D.A. (1979) : Oogenesis and egg-shell formation in *Aspiculuris tetraptera*, Schulz (Nematoda : Oxyuroidea). *Parasitol.* 78, 131-143.

Wickner, W. (1980) : Assembly of proteins into membranes. *Science* 210, 861-868.

Willmer, P.G., Skaer, H.leB. & Treherne, J.E. (1979) : Physiologically induced changes in intramembranous particle frequency in the axons of an osmoconforming bivalve. *Tissue & Cell* 11, 507-516.

Wirth, U. (1974) : Spermatogenesis and sperm ultrastructure in some oxyuroid nematodes. *Proc. 3rd Int. Congr. Parasitol.* 1, 441.

Wolf, N., Hirsh, J.R. & McIntosh, J.R. (1978) : Spermatogenesis in males of the free living nematode *Caenorhabditis elegans*. *J. Ultrastruct. Res.* 63, 155-169.

Wright, E.J. (1974) : Differentiation of the sperm of *Nematospiroides dubius*. Honours Thesis, University of Adelaide.

Wright, E.J. & Sommerville, R.I. (1977) : Movement of a non-flagellate spermatozoon: a study of the male gamete of *Nematospiroides dubius* (Nematoda). *Int. J. Parasitol.* 7, 353-359.

Wright, K.A., Hope, W.D. & Jones, N.O. (1973) : The ultrastructure of the sperm of *Deontostoma californicum*, a free-living marine nematode. *Proc. Helminth. Soc. Wash.* 40, 30-36.

Wu, Y-J. & Foor, W.E. (1980) : *Ascaris* oocytes: ultrastructural and immunocytochemical changes during passage through the oviduct. *J. Parasitol.* 66, 439-447.

Yanagimachi, R. & Nicolson, G.L. (1976) : Lectin-binding properties of hamster egg zona pellucida and plasma membrane during maturation and preimplantation development. *Exp. Cell Res.* 100, 249-257.

Yanagimachi, R., Nicolson, G.L., Noda, Y.D. & Fujimoto, M. (1973) : Electron microscopic observations of the distribution of acid anionic residues on hamster spermatozoa and eggs before and during fertilization. *J. Ultrastruct. Res.* 43, 344-353.

Yanagimachi, R., Noda, Y.D., Fujimoto, M. & Nicolson, G.L. (1972) : The distribution of negative surface charges on mammalian spermatozoa. *Am. J. Anat.* 135, 497-520.

Yanagimachi, R. & Usui, N. (1974) : Calcium dependence of the acrosome reaction and activation of guinea pig spermatozoa. *Exp. Cell Res.* 89, 161-174.

Yokogawa, S. (1920) : A new nematode from the rat. *J. Parasitol.* 7, 29-33.

Young, L.G. & Goodman, S.A. (1980) : Characterization of human sperm cell surface components. *Biol. Reprod.* 23, 826-835.

Yu, J. & Branton, D. (1976) : Reconstitution of intramembrane particles in recombinants of erythrocyte protein Band 3 and lipid: effects of spectrin-actin association. *Proc. Natl. Acad. Sci.* 73, 3891-3895.

Zigmond, S.H. (1978) : Chemotaxis by polymorphonuclear leukocytes. *J. Cell Biol.* 77, 269-287.

Zingsheim, H.P. & Plattner, H. (1976) : Electron microscopic methods in membrane biology. In 'Methods in Membrane Biology'. Volume 7. pp.1-146. Ed. E.D. Korn. (Plenum Press: New York.)

Zuckerman, B.M. & Himmelhoch, S. (1980) : Nematodes as models to study aging. In 'Nematodes as Biological Models'. Volume 2. pp.3-28. Ed. B.M. Zuckerman. (Academic Press: New York.)

Zur Strassen, O. (1896) : Embryonalentwicklung der *Ascaris megalocephala*. *Arch. Entw. Mech. Org.* 3, 27-105.